2011

Structural and functional characterization of E2-25K

Randall Wilson

STRUCTURAL AND FUNCTIONAL CHARACTERIZATION OF E2-25K

by

RANDALL WILSON

A DISSERTATION

Submitted in partial fulfillment of the requirements
for the degree of Doctor of Philosophy
in
The Biotechnology Science & Engineering Program
to
The School of Graduate Studies
of
The University of Alabama in Huntsville

HUNTSVILLE, ALABAMA

2011

In presenting this dissertation in partial fulfillment of the requirements for a doctoral degree from The University of Alabama in Huntsville, I agree that the Library of this University shall make it freely available for inspection. I further agree that permission for extensive copying for scholarly purposes may be granted by my advisor or, in his/her absence, by the Director of the Program or the Dean of the School of Graduate Studies. It is also understood that due recognition shall be given to me and to The University of Alabama in Huntsville in any scholarly use which may be made of any material in this dissertation.

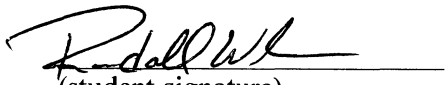

(student signature)

3/28/11

(date)

DISSERTATION APPROVAL FORM

Submitted by Randall Wilson in partial fulfillment of the requirements for the degree of Doctor of Philosophy in the Biotechnology Science & Engineering Program and accepted on behalf of the Faculty of the School of Graduate Studies by the dissertation committee.

We, the undersigned members of the Graduate Faculty of The University of Alabama in Huntsville, certify that we have advised and/or supervised the candidate on the work described in this dissertation. We further certify that we have reviewed the dissertation manuscript and approve it in partial fulfillment of the requirements for the degree of Doctor of Philosophy in the Biotechnology Science & Engineering Program.

3/28/11
Committee Chair
(Date)

Department Chair

College Dean

Graduate Dean

ABSTRACT
The School of Graduate Studies
The University of Alabama in Huntsville

Degree Doctor of Philosophy Program Biotechnology Science & Engineering Program

Name of Candidate Randall Wilson

Title Structural and Functional Characterization of E2-25K

Protein degradation by the ubiquitin-proteasome system (UPS) seems to be implicated in a number of protein misfolding diseases. The ubiquitin-conjugating enzyme E2-25K is a unique E2 that contains an ubiquitin-associated (UBA) domain C-terminal to the catalytic ubiquitin-conjugating (UBC) domain and synthesizes Lys48-linked free polyubiquitin chains *in vitro* in the absence of an E3 ligase. Although the full range of E2-25K functions is not yet known, numerous systems have been identified as targets. In particular, E2-25K interacts with proteins involved in the endoplasmic reticulum-associated response to cellular stress and is known to play a role in mediating cellular toxicity in diseases of protein misfolding such as Alzheimer and Huntington. In order to gain insight into E2-25K, structural and functional characterization studies were conducted. The x-ray crystallographic structure revealed key active site residues along with previously unreported domain-domain interactions. Oligomerization studies revealed E2-25K exists as a monomer in solution and dimerization is not required for polyubiquitin chain formation, as seen with other E2 proteins. NMR spectroscopy was used to map the relevant binding surfaces on E2-25K required for interaction with three RING E3 ubiquitin-ligase partners, ubiquitin, and the Ubl domain of Parkin. NMR spectroscopy was further used to show domain-domain interactions between the catalytic

UBC and the UBA domains do not induce significant structural changes or alter the affinity of the UBA domain for ubiquitin.

As a first step towards determining the role of the UBA domain the protein-protein interfaces involved in the E2-25K UBA/ubiquitin complex were mapped by solution NMR spectroscopy and subsequently used to model the complex structure. Functional studies were used to determine that one of the roles of the E2-25K UBA domain is to increase processivity in Lys48-linked polyubiquitin chain synthesis, possibly through increased binding to the ubiquitinated substrate. Additional evidence elucidated that the UBA domain directs specificity in polyubiquitin chain linkage and contributes to the thermal stability of the full-length protein.

Abstract Approval: Committee Chair 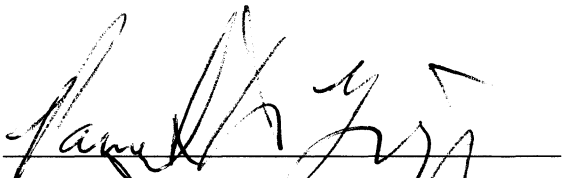

Department Chair 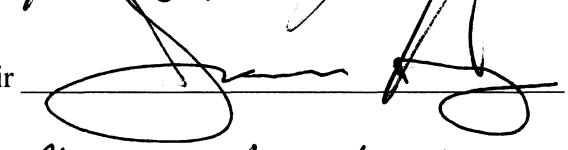

Graduate Dean Rhonda Kay Hardie

ACKNOWLEDGMENTS

The work described in this dissertation would not have been possible without the assistance of a number of people who deserve special mention. First, I would like to thank Dr. Pamela Twigg for her suggestion of the research topic and for her guidance throughout all the stages of the work. Second, the other members of my committee have been very helpful with comments and suggestions. Third, I would like to thank the National Science Foundation EPSCoR Graduate Fellowship program, the National Institute of Health and the Alpha Foundation for the financial support in which they provided.

I would also like to thank my family and friends who encouraged me to begin work on this degree. Without their support, obtaining this degree would not have been possible.

TABLE OF CONTENTS

Page

LIST OF FIGURES

LIST OF TABLES

CHAPTER 1

INTRODUCTION

Protein degradation by the ubiquitin-proteasome system (UPS) seems to be implicated in a number of protein misfolding diseases. Mutations or misregulations of individual UPS components are known causes of numerous pathological conditions, including the E3 ligase parkin (Parkinson disease) [1]; the Nedd-4 E3 ligase (Liddle's syndrome) [2]; and Skp2 a component of multi-subunit E3 ligase (epithelial cancer and lymphomas) [3]. Furthermore, the presence of ubiquitin is noted in intranuclear inclusions in Huntington disease (HD) [4], as well as in fibrillary tangles in Alzheimer disease (AD) and other tauopathies [5, 6]. This may indicate that a malfunction of the ubiquitin-proteasome pathway contributes to the accumulation of misfolded protein aggregates. E2-25K, an ubiquitin-conjugating enzyme, is upregulated in Alzheimer disease, and its presence is required for the toxicity generated by Aβ fragments [7]. This same enzyme is also a binding partner for huntingtin, the key protein mutated in HD [4]. E2-25K is highly expressed in the brain, and co-localizes with neuronal intranuclear inclusions in the brain tissue of patients with the polyglutamine disorders HD and spinocerebellar ataxia 3 [8].

1.1 The Ubiquitin-Proteasome System

The UPS is one of the primary means by which the cell degrades and recycles proteins [9]. The UPS is mediated by the covalent conjugation of ubiquitin, a highly

conserved 76 amino acid residue protein found in all eukaryotes, to the target protein. Multiple ubiquitin additions to this protein targets it for interaction with the 26S proteasome, which in mammalian systems consists of a cylindrical 20S core containing multiple protease activities, capped on both ends by 19S subunits. The function of the proteasome is to recognize and proteolytically degrade these ubiquitin-tagged proteins, while releasing the ubiquitin molecules to be recycled. In addition to this critical function, the UPS is also involved in cell cycle regulation [3, 10], endocytosis, DNA repair [11], transcription [12, 13], signal transduction [14], apoptosis [15] and the immune response [16].

1.1.1 Steps Involved in Ubiquitination

Once a protein has been conjugated to ubiquitin, the destination for that protein is based on the number of ubiquitin molecules and the lysine-linkage used to attach them. Ubiquitin has seven lysine residues that can function as conjugating sites, of which four [Lys6, Lys11, Lys27, and Lys33] have been found to conjugate. The function of these four types of conjugates has yet to be determined [17-20]. Lys29-linked ubiquitin chains have been discovered in the ubiquitin fusion degradation pathway [21]. Lys48-linked chains target proteins for degradation by binding to the 26S proteasome [22]. Mono-ubiquitin and poly-ubiquitin Lys6 and Lys63-linked chains have been shown to produce changes in protein activity and binding, as well as subcellular localization [23]. Lys63-linked chains have also been found to be associated with DNA repair, translation, endocytosis, and vesicle transport [24-26].

Conjugation of a target protein with ubiquitin requires a multi-step, multi-enzyme process. The first step is the ATP-dependent formation of a thioester bond between the

C-terminal Gly76 residue of ubiquitin and the E1 ubiquitin-activating enzyme [27]. The ubiquitin is transferred to a conserved cysteine residue of an E2 ubiquitin-conjugating enzyme, and finally, is covalently linked through an isopeptide bond between the ubiquitin C-terminal carboxylate group and the ε-amino group of a substrate lysine residue of the target protein [11]. This final step is catalyzed by the actions of an E2 and/or E3 (ubiquitin-ligase) enzyme. Subsequent addition of ubiquitin molecules to the lysine residue of the conjugated ubiquitin builds a polyubiquitin chain that is recognized by the destined pathway. Lys48 linked polyubiquitin chains are recognized by the 19S subunit where deubiquitinating enzymes remove and break down the polyubiquitin chain while the target protein is degraded by the proteasome [10, 28]. Figure 1.1 illustrates the steps involved in Lys48 linked conjugating site.

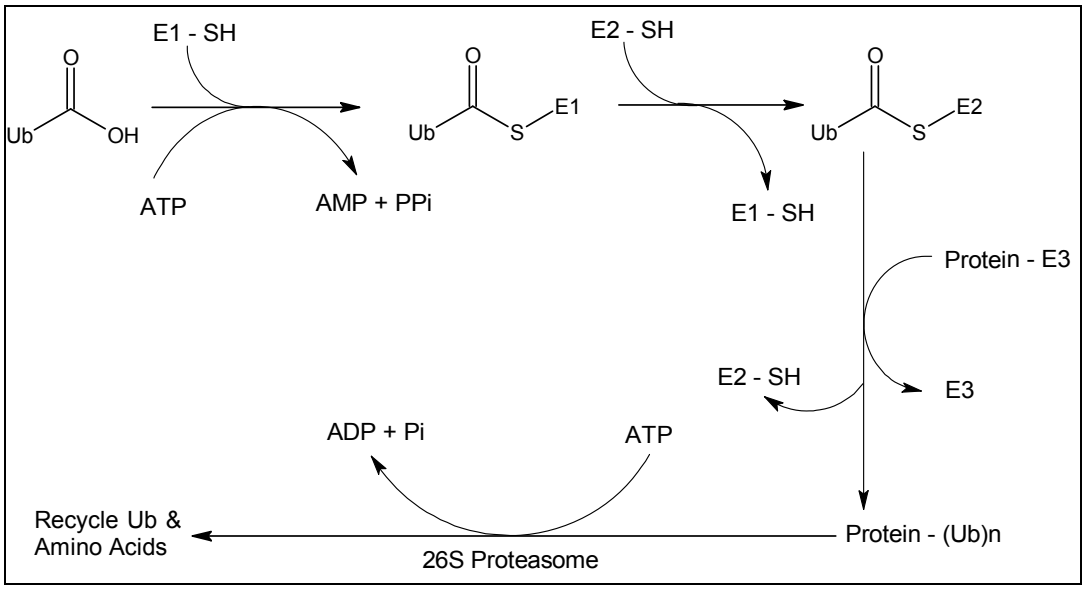

Figure 1.1 The Ubiquitin-Proteasome Pathway

1.1.2 Enzymes Involved in Ubiquitination

It was initially thought that only one E1 (UBE1) was responsible for charging ubiquitin to E2's in *Homo sapiens*. However, a second E1 (UBA6) has recently been

discovered and shown to bind to different E2's [29]. The distinction in E2 selection between the two E1 enzymes is thought to occur in the ubiquitin fold domain within the C-terminus of the E1. The E1 enzyme-ubiquitin complex is a critical component for the initiation of ubiquitin conjugation reactions [30]. The E1 enzyme is responsible for the first step in the ubiquitin protein isopeptide bond formation via a high-energy thioester intermediate between the E1 catalytic cysteine and C-terminus of ubiquitin. Before ubiquitin is transferred to the E2, a second ubiquitin molecule is added to the E1 via adenylation of the ubiquitin C-terminus [31].

The ubiquitin that is bound to the catalytic cysteine of the E1 is directly transferred to the catalytic cysteine of an ubiquitin-conjugating enzyme or E2. The transfer of the ubiquitin from the E1 to the E2 occurs through a transthiolation reaction between the two catalytic cysteines. There are multiple E2 enzymes that have associated families of many E3 ubiquitin-protein ligases. The interactions between the enzymes in the ubiquitin cascade are shown in Figure 1.2. The total number of E2 proteins in *Homo sapiens* is unknown, but there are typically 10 – 30 in most eukaryotes [11]. Research has shown that the simple *S. cerevisiae* genome encodes for 13 E2-like proteins [28]. The structures of E2 proteins contains a conserved ubiquitin-conjugating (UBC) catalytic domain, which consists of a 150 amino acid core with a single active site cysteine that binds the C-terminal tail of the thioester linked ubiquitin. Some E2s contain extensions to the UBC domain, and therefore categories have been assigned based on the location of these extensions (Figure 1.3). Ubc1 & Ubc3 – *S. cerevisiae* [32] and E2-25K – *Homo sapiens* [33] are examples of class II E2 proteins which contain a C-terminal domain. This particular extension is between 20-50 residues and was identified as a UBA

(ubiquitin-associated) domain. The significance of this domain is still not completely understood, but it is believed to play a role in poly-ubiquitin chain formation [32] and will be discussed in detail later.

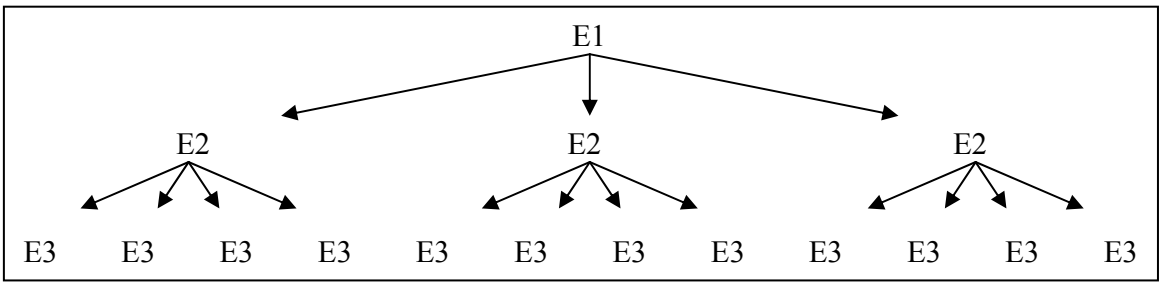

Figure 1.2 The Ubiquitin Cascade - Enzymatic Reactions of the Ubiquitin System

The regulators of the ubiquitin cascade are ubiquitin-protein ligases or E3. They are tasked with bringing the E2-ubiquitin complex and the target protein together. There are three distinct categories of E3s based on the domains they contain and E2 binding partners: the HECT (Homologous to E6-AP carboxy-terminus), the RING (Really Interesting New Gene) finger [11], and a minor category of those not resembling either [31, 34]. Currently, there are two different mechanisms for how the E3 may be involved in the transfer of the ubiquitin from the E2-ubiquitin complex to the substrate. The suggestion is that RING finger E3s position the E2-ubiquitin complex and the substrate in close proximity to facilitate the direct transfer of ubiquitin from the E2 to the substrate. In the HECT domain E3, the ubiquitin is transferred from the E2 to the E3 then subsequently to the substrate via a conserved cysteine that forms a thioester bond with the C-terminus of ubiquitin. The final E3 category is suggested to bind or transfer ubiquitin to the substrate in a composite of both the RING and HECT categories.

1.1.3 Ubiquitin-Conjugating Enzymes

Ubiquitin-conjugating enzymes, E2s, accept ubiquitin or an ubiquitin-like protein (UBL) from the E1 and typically interact with an E3 to promote ubiquitin/UBL transfer to the target [35]. As previously stated, all E2s share a ~150-residue conserved catalytic core (UBC) domain. This catalytic core domain is sufficient for all E2 activities, even though E2s have been found to contain extensions at either or both ends of their core domains (Figure 1.3) and several are regulated by posttranslational modifications.

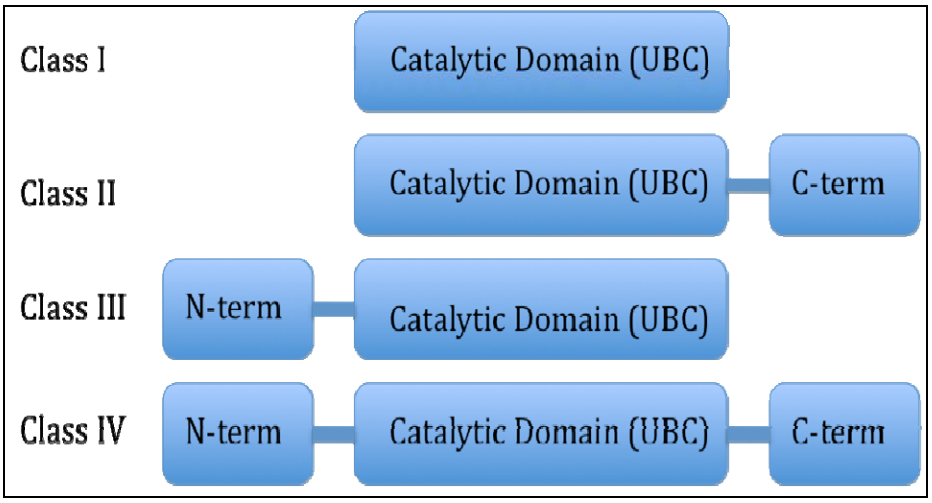

Figure 1.3 The Classes of E2 Ubiquitin-conjugating Enzymes

Recent structural studies have given insight into E2 activity and a further understanding of their interactions with other enzymes in the cascade. The crystal structure of an E1-E2 complex (NEDD8's E1 to Ubc12) revealed that the E1 and E3 binding sites on the E2 partially overlap [36]. Further competitive binding studies, with three different E2s, revealed binding was mutually exclusive between E1s and E3s to E2s [37]. These findings suggest that the cascade is a stepwise process where the E1 interacts with the ubiquitin free E2 and the E3 binds with the ubiquitin-bound E2.

Binding of ubiquitin to the catalytic domain of E2s has been studied for several different E2s. Nuclear magnetic resonance (NMR) studies confirmed the binding surfaces were between the residues around the active site cysteine of the UBC domain and the C-terminal tail residues of ubiquitin [38]. This type of orientation for ubiquitin leaves the binding surface for the E1 and E3 intact on the E2. The exact details of the transfer of ubiquitin to the E2 and subsequently to the substrate are still unknown [11]. However, research suggests that the mechanism for transfer of ubiquitin from the E2 to the substrate protein may be similar to that proposed for other isopeptide bond formations [11], where the isopeptide bond is formed by a lysine sidechain in the substrate attacking the E2 thioester bond to form an oxyanion intermediate. In order for this to occur, a base is required near the active site to stabilize the approaching negative charge or to deprotonate the incoming lysine residue. There are two key residues located N-terminal to the catalytic cysteines that are absolutely conserved among all E2s (Figure 1.4): histidine and asparagine. Recent work has shown that the conserved asparagine, originally thought to be critical for the hydrogen bonding network around the active site, could be involved in stabilizing the oxyanion intermediate [39]. However, structural studies of E2 enzymes still have not elucidated a catalytic group near the active site that could be responsible for the deprotonation of the incoming lysine.

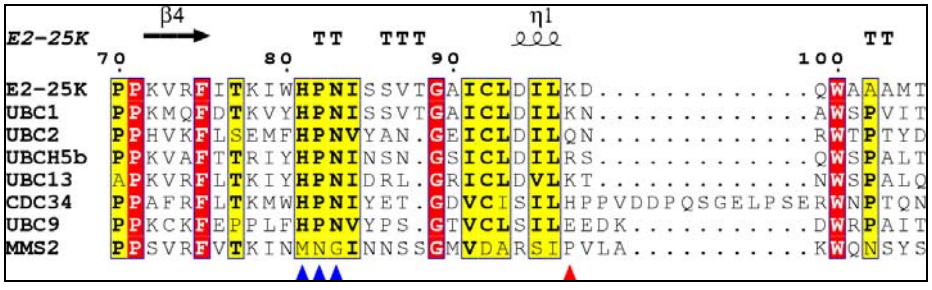

Figure 1.4 E2 active site sequence alignment. [Highly conserved residues are boxed. Triangle, Δ, indicates highly conserved HPN region and position of Lys-97.]

The next function of E2s, which are involved in polyubiquitination, is the attachment of additional ubiquitin molecules to the substrate. The processivity and the attachment sites of ubiquitin during polyubiquitination are influenced by additional factors. Structural studies of the Ubc13/Mms2 ubiquitin complex revealed that both an E2 and a non-catalytic E2 variant (UEV) are required in a heterodimeric complex for synthesis of free Lys63-linked polyubiquitin chains [40]. Further studies have shown that some E2s transfer the ubiquitin to a lysine on a previously monoubiquitinated substrate, as is the case for Ubc3 or Cdc34 [41].

1.1.4 Ubiquitin Ligases

The ubiquitin ligases or E3s are classified by their domains. In eukaryotes, there are two major types of E2 binding domains: the HECT or RING domain. These two major E3 categories also differ in terms of the mechanism by which ubiquitin is attached to the substrate. The HECT E3, like the E2, has a conserved cysteine residue that provides a catalytic contribution to the cascade. However, the RING E3 is primarily used as a scaffold or matchmaker for the E2 and substrate or target protein.

The HECT E3 is a conserved 250 amino acid domain that consists of N and C lobes that either pack to form a “L” or inverted “T” shape. HECT domains have been shown to have three main functions: interaction with an E2, covalent binding to ubiquitin through a thioester intermediate, and recognition of the substrate and subsequent transfer of the ubiquitin molecule [11]. Exactly how ubiquitin is transferred from the E2 to the HECT E3 is still under investigation. However, recent crystallographic structures have given two possible mechanisms for transfer which would both require substantial

mobility of the hinge loop in order for the ubiquitin to be transferred from the cysteine of the E2 to E3 [42, 43].

The RING E3s are highly conserved across eukaryotes and over 600 have been identified by sequence homology [44], but only half are thought to have ligase activity. The domain is primarily made up of eight conserved cysteine and histidine residues that coordinate two Zn^{2+} ions within the core to maintain the overall fold of the domain. The primary function of RING E3s is to serve as a scaffold for the E2 and the substrate. Structural studies of UbcH7-Cbl and UbcH5-Cnot4 revealed a hollow surface between the zinc-binding loops of the RING domain. The hollow surface of the RING domain contains a conserved isoleucine and a hydrophobic residue, typically a leucine or tryptophan, that has been implicated in binding to the E2 [44]. The RING E3 holds the E2 via a hydrophobic interaction with a conserved proline-phenylalanine sequence in the E2 [45, 46]. It is believed that surrounding residues on the E2s are what dictate the specificity of E2-E3 binding. How ubiquitin is transferred from the E2 to the substrate remains somewhat of a mystery. However, it has been hypothesized that the E3 may play a catalytic role in the ubiquitin transfer or the E3 may induce structural changes in the E2-Ub complex that facilitates rapid turnover. Structural studies are leaning toward the latter, but this is still under debate [47, 48].

1.1.5 UBB+1

Ubiquitin is translated in two different ways. The ubiquitin protein can be fused to a ribosomal protein or as a linear repeat of three ubiquitin molecules (UBB). The mutant ubiquitin or UBB+1 is shorthand for Ubiquitin-B +1 and is thought to arise from a molecular misreading of the ubiquitin linear repeat gene. The UBB+1 protein is formed

by a dinucleotide deletion (ΔGT) [49], which leads to a frame shift in the mRNA. This frame shift causes the subsequent translation of the ubiquitin protein to contain a 19 amino acid aberrant C-terminus. These deletions are not present in the genomic DNA and the mechanism of this molecular misreading is not completely understood.

1.1.6 Ubiquitin-like Protein Modifiers

The ubiquitin cascade is ever-expanding. Recent research has discovered a growing family of ubiquitin-like proteins (UBLs). The UBLs function in parallel pathways to ubiquitin and adopt a similar structure. It has been shown that each UBL has its own set of enzymes that conjugate the UBL to a target protein. Several of the known UBLs have been shown to covalently bind to and alter the function of the target protein. The most studied UBLs include neuronal-precursor-cell-expressed developmentally downregulated protein-8 (NEDD8) and small ubiquitin-like modifier (SUMO). One known function of NEDD8 is to activate cullin-RING, which is involved in the cell cycle, signaling, and embryogenesis [50]. SUMO has been show to regulate transcription, DNA repair, nuclear transport, chromosomal function, and signal transduction, and to even block ubiquitin binding sites [51].

Another interesting discovery has been the identification of ubiquitin-like (Ubl) domains within proteins [52]. These domains have sequence and structural homology to ubiquitin and even share the function of interaction with the proteasome [52, 53]. However, the main function of the Ubl domain in most proteins has still not been discovered.

1.2 Neurological Disorders

The UPS of protein degradation seems to be implicated in a number of protein misfolding diseases. In particular, the presence of ubiquitin is noted in intranuclear inclusions in Huntington disease (HD) [4], as well as in fibrillary tangles in Alzheimer disease (AD) and other tauopathies [5, 6]. There is also a direct link to Parkinson disease (PD) through the mutation of UPS component E3 ligase, Parkin [54]. This may indicate that a malfunction of the ubiquitin-proteasome pathway contributes to the accumulation of misfolded protein aggregates and ultimately contributes to these diseases.

Huntington disease (HD) is a neurodegenerative disorder characterized by death of cortical and striatal neurons, and caused by a mutation involving the expansion of a polyglutamine tract in the huntingtin protein. This mutation in the Exon 1 region of the gene results in an increased number of repeating CAG codons and subsequent translated glutamine residues. Patients with HD typically are found to have 40 or more glutamines, with a "normal" huntingtin protein consisting of a 10- to 35-glutamine stretch. A huntingtin protein that contains 36 to 39 glutamines falls into an intermediate range that, depending on other genetic and environmental factors, may or may not produce disease symptoms in the patient's lifetime. The extended number of glutamine repeats in HD huntingtin protein characterizes it as one of nine polyglutamine expansion disorders [55]. The function of huntingtin is unknown but studies have revealed a large array of proteins that bind to huntingtin in the cell. The presence of ubiquitin is noted in intranuclear inclusions in HD patients.

Alzheimer disease (AD), the most common form of dementia, is a neurodegenerative disorder that is thought to be caused by the accumulation of amyloid

beta (Aβ) deposits or plaques [56]. The Aβ deposits arise from the neuronal transmembrane amyloid beta precursor protein. A build up of microtubule-associated protein tau aggregates are also observed in AD patients. These tau protein aggregates are seen in neurofibrillary tangles that cause a disintegration of the microtubules that serve the neurons [57]. AD is linked to the UPS by the presence of ubiquitin in fibrillary tangles in AD patients [5].

Parkinson disease (PD) is a neurodegenerative disorder that is caused by an accumulation of Lewy bodies in the substantia nigra region of the brain. The Lewy bodies are cytoplasmic proteinaceous inclusions that contain a dense core and contain proteins that are ubiquitinated [54]. To date there have been six genetic mutations discovered that have been linked directly to PD patients [58]. The LRRK2 gene (leucine-rich repeat kinase 2 or dardarin protein) is the only gene that has consistently appeared in patients that have a family history of PD; however, this only occurs around 5% of the time. A gene mutation of PARK2, the gene that encodes for the E3 ligase parkin, has also been discovered [58]. The parkin gene is a highly conserved gene which is thought to play a critical and common role in other organisms as well [54].

1.3 Ubiquitin Conjugating Enzyme E2-25K

E2-25K was initially identified by Dr. Cecile Pickart's lab as a 25-kDa mammalian E2 conjugating enzyme with the ability to generate Lys48-linked polyubiquitin chains, independent of the presence of protein substrate or E3 ligase. E2-25K is a Class II E2 protein that has a conserved ubiquitin-conjugating (UBC) domain and a C-terminal ubiquitin-associated (UBA) domain. The UBC domain consists of a 150 amino acid core (~18 kDa) with a single active site cysteine (Cys-92) that binds the

C-terminal tail of the thioester linked ubiquitin. Additionally, E2-25K consists of a 50 amino acid (~5 kDa) C-terminal UBA domain [33] whose function is the key focus of this study. The significance of the C-terminal UBA domain in the context of an E2 is not well understood but was proposed to play a role in polyubiquitin chain formation [32]. Initial examination of the role of the UBA domain indicated that removal of the domain results in a non-functional E2-25K; however, subsequent research revealed that the location of the truncation was of critical importance [59]. Slightly longer constructs (still missing the UBA domain) were able to catalyze polyubiquitin chain formation, although the processivity was impaired relative to full-length E2-25K [59].

The three-dimensional structure of E2-25K has been determined by X-ray crystallography (PDB ID: 3E46) [60]. The UBA domain (blue portion Figure 1.5), while ordered in the crystal structure of E2-25K, shows tremendous mobility and flexibility in the solution structure of the yeast homolog, Ubc1 *Saccharomyces cerevisiae* (Figure 1.6) [61]. Ubc1 is also a Class II E2 enzyme and has 40 percent sequence identity to E2-25K.

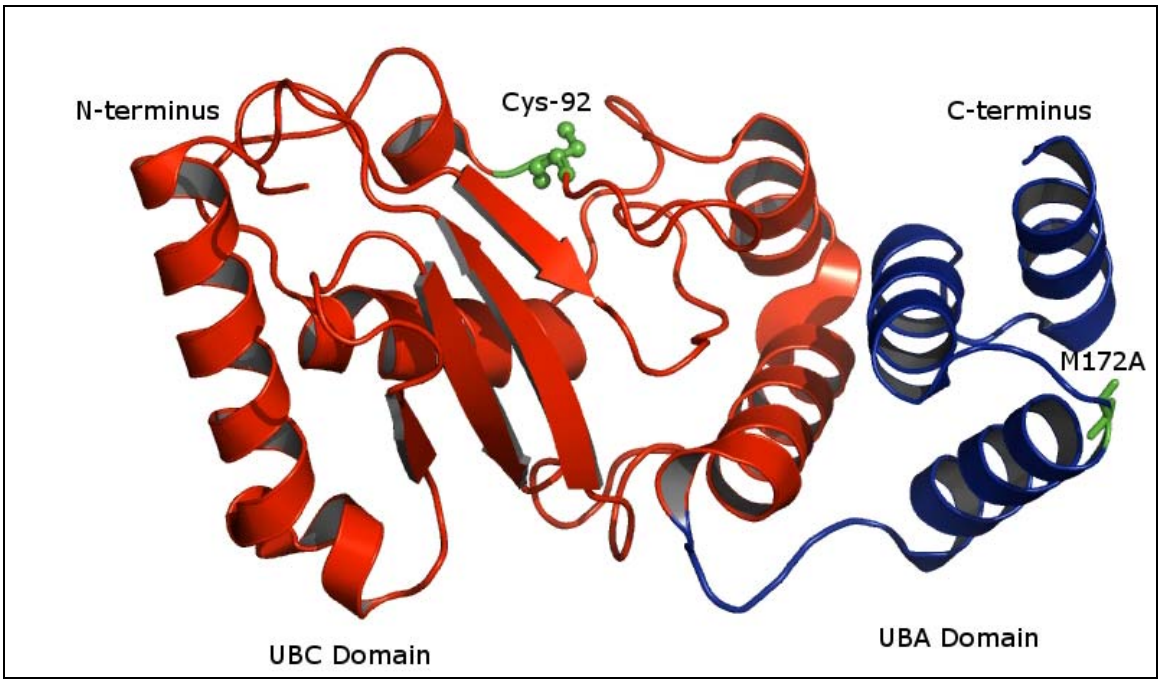

Figure 1.5 X-Ray Crystallographic Structure of E2-25K (PDB ID: 3E46). [62] [The catalytic UBC domain is shown in red and the C-terminal UBA domain is shown in blue.]

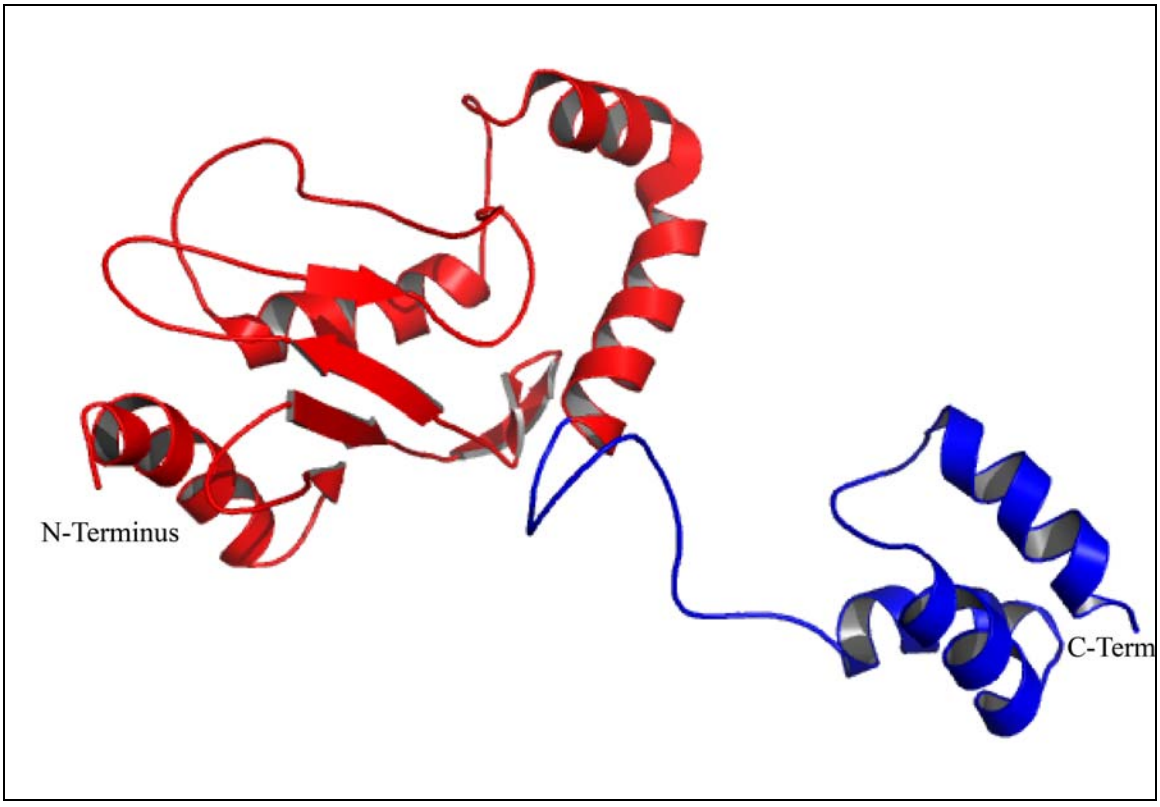

Figure 1.6 NMR Solution Structure of Ubc1 S. cerevisiae (PDB ID: 1TTE) [61]. [The catalytic UBC domain is shown in red and the C-terminal UBA domain is shown in blue.]

1.3.1 Function and Role in Ubiquitin Cascade

E2-25K was not initially identified as a partner E2 for known UPS pathways using functional assays, but was identified by the use of a yeast two-hybrid screen with RING E3 binding partners [63]. The reason that the initial UPS assays were unsuccessful did not become clear until recent studies presented evidence that E2-25K functions as a "second-step" E2. This means E2-25K recognizes protein substrates that have already been monoubiquitinated by another E2 [64, 65]. Unlike other E2s, E2-25K has the ability to synthesize free polyubiquitin chains without the presence of an E3 ligase *in vitro* [33]. However, this has not been definitively shown *in vivo*. There is evidence of an accumulation of Lys48-linked polyubiquitin chains in the cell [66], but the function of these free polyubiquitin chains is not known. It can be speculated that the free Lys48-linked polyubiquitin chains play a role in the rapid turnover of certain protein substrates as well as potentially regulating the activity of the proteasome. Further evidence has shown that E2-25K can catalyze the cyclization of polyubiquitin in the presence of an excess of polyubiquitin chains [67]. These findings suggest that E2-25K may be involved in an additional regulatory mechanism to prevent either inhibition of proteasome activity or to facilitate the rapid degradation of certain substrates under certain cellular conditions. Currently there are ten known E3 binding partners for E2-25K that affect six different cellular pathways, which are listed in Table 1.1. The interaction between three of these Ring E3 proteins and E2-25K, as well as E3 parkin, is another focus of this study. Furthermore, it has recently been shown in mouse models that E2-25K regulates expression and activation of caspase-12 in endoplasmic reticulum stress-mediated Aβ neurotoxicity [68]. E2-25K has been further linked to cell cycle

regulation and apoptosis via interaction with the cell cycle regulators cyclin B1 and Smac/DIABLO [69, 70].

Table 1.1 Identified RING E3 Ubiquitin-Ligase partners of E2-25K and Affected Pathways

E3 Ligase	**Target**
RNF2	Histone 2A [63]
Mdm2/Hdm2	Transcription [71]
APC11	Cell cycle [65]
Parkin*	Unknown – Current Study
gp78	ERAD** [72]
Rhysin2/BBAP	Transcription [63]
RNF138/NARF/HSD4	Transcription [63]
RNF24	Intracellular trafficking [63]
MuRF1	Muscle atrophy [73]
MARCHVII/axotrophin	ERAD* [72]
RNF4/SNURF	Transcription [74]

* UBL/RING Type E3
**Endoplasmic reticulum associated degradation

1.3.2 Function and Role in Neurological Disorders

Many neurological disorders are characterized by aggregates of misfolded proteins [9]. Typically the problem of misfolding is dealt with by the cell through molecular chaperones and the UPS. E2-25K has been identified as a key E2 involved in

the clearance of misfolded proteins as they emerge from the endoplasmic reticulum [65, 72], interacting with such membrane-bound E3s as gp78 and MARCHVII/axotrophin. Consistent with this role, it has been determined that E2-25K is upregulated in AD, and its presence is required for the toxicity generated by Amyloid-β (Aβ) fragments [5, 7]. Studies with E2-25K in AD model systems (neuronal cells and mouse models) have shown that the presence of E2-25K is necessary for the toxic effects of Aβ amyloid protein [7]. Furthermore, overexpression of E2-25K in rat neuroblastoma cells exposed to $A\beta_{1-42}$ resulted in increased cell death, while overexpression of E2-25K mutants lacking the UBA domain (150-200), or with S86Y or C92S mutations, significantly reduced the $A\beta_{1-42}$ neurotoxicity. Reducing the levels of expressed E2-25K using anti-sense DNA also suppressed the toxic effects.

E2-25K was identified as a binding partner for huntingtin, the key protein mutated in HD, and been given the additional name of Huntingtin Interaction Protein-2 (HIP2) [4]. E2-25K is highly expressed in the brain, and it has been found to co-localize with intranuclear neuronal inclusions in the brain tissue of patients with the polyglutamine disorders HD and spinocerebellar ataxia 3 (SCA3) [8]. Similar to the results seen in AD research, overexpression of E2-25K in HD cell models enhanced the toxicity of a polyglutamine construct, while suppression of E2-25K or overexpression of a ΔUBA mutant of E2-25K caused a decrease in toxicity and aggregation and brought cell survival rates back to normal [8]. This suggests that these mutants function in a dominant-negative manner, perhaps by competing with full-length E2-25K for cellular binding partners. Neuronal inclusions have also been found in other diseases such as PD and Lewy body disease [6].

1.3.3 Ubiquitin-associated Domain of E2-25K

The amino acid sequence of the Ubiquitin-associated (UBA) domain of E2-25K is well-conserved among mammalian species, but diverges from the UBA domain sequence found in non-mammalian homologs. The UBA domain is a small (40-50 amino acids) three-helix bundle characterized by a conserved Met-Gly-Phe (MGF) loop connecting helix 1 and helix 2, which is involved in binding to ubiquitin (Figure 1.7). Several key hydrophobic residues form the core of the domain. UBA domains belong to a specific class of ubiquitin binding domains that mediate ubiquitination [75]. To date sixteen domains have been discovered to bind ubiquitin and half are α-helical. The UBA domain is of the α-helical group and has structural homology only with the CUE (couple of ubiquitin conjugation to endoplasmic reticulum degradation) domain. Both the UBA and CUE domains have been found to bind to the hydrophobic patch near Ile44 of ubiquitin [75]. UBA domains are found in a wide range of proteins with diverse functions, including the ubiquitin-proteasome pathway, nuclear excision DNA repair, membrane fusion, signal transduction, etc. [76]. In general they recognize and bind polyubiquitin chains or ubiquitin-like (Ubl) domains, although this has not been widely observed.

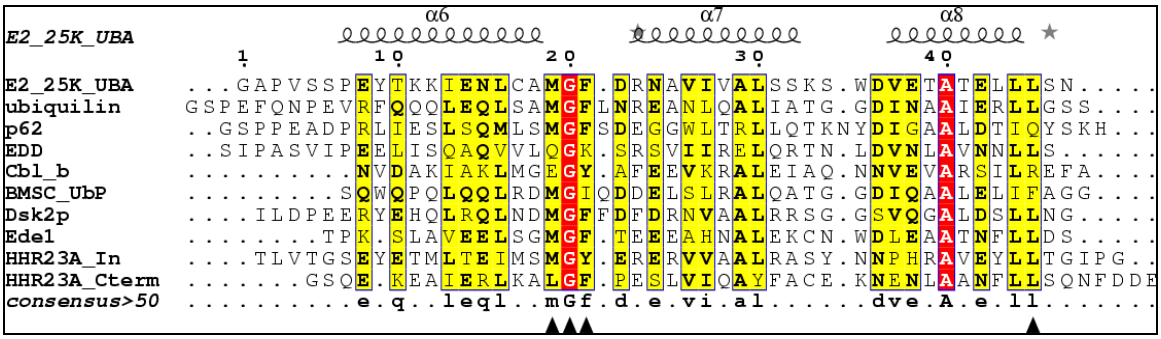

Figure 1.7 Sequence Alignment for UBA Domains. [Highly conserved residues are indicated by a Triangle, Δ.]

Initial work by Haldeman *et al.* with UBA truncation mutants, E2-25K (1-151) and E2-25K (1-153), suggested that the UBA domain was essential for formation of free Lys48-linked polyubiquitin chains but not for conjugation of ubiquitin by the UBC domain [77]. The crystal structure of E2-25K [78] revealed that residues 151 and 153 are located within an α-helix, and that truncation at these residues could cause protein instability or improper folding. Furthermore, a single amino acid mutation of Ser-86 to Tyr (S86Y) also blocked ligase activity [79] indicating that preliminary research of the UBA domain's function may be misleading by demonstrating that unstable or misfolded protein is not functional. The addition of a GST-fusion tag to the truncated E2-25K constructs restored chain synthesis activity, possibly through stabilization of the protein or through dimerization via the GST. Later studies with truncated E2-25K (1-155) contradicted the claims that the UBA domain was required for chain synthesis [59]. Even though the difference in length was only two additional amino acids, this construct may not disrupt the formation of helix 5. The presence of a GST-fusion at the N-terminus of the slightly longer E2-25K (1-153) mutant was an additional difference that produced a functional enzyme. This opens up the possibility that the GST may have conferred some additional solubility or stability of the protein, or perhaps aided in the formation of dimerization in solution.

1.4 Dimerization in Ubiquitin-Conjugating Enzymes

Research has shown that dimerization of E2 enzymes is required to direct chain linkage specificity in other E2s [40, 80]. Li *et al.* demonstrated that homodimerization of Ube2g2 through association with gp78 (a membrane-linked RING domain E3 involved in ER associated degradation of misfolded proteins) is responsible for the building of

polyubiquitin chains by transfer of a conjugated ubiquitin from one E2 molecule to the other [81]. They also concluded that building of polyubiquitin chains on Ube2g2 precedes transfer of the polyubiquitin to the substrate molecule. Dimerization has also been noted for other E2s, including Cdc34 [82] which homodimerizes through interaction with components of the SCF ligase complex, and Ubc13/Uev1a, a heterodimeric complex of a catalytic (Ubc13) and non-catalytic (Uev1a) E2 [83]. An example, in *Homo Sapiens,* is the presence of the non-catalytic E2 in a heterodimeric complex such as Mms2/Ubc13, which synthesizes free Lys63-linked polyubiquitin chains [40]. These interactions require the presence of a conjugated ubiquitin at the active site of the catalytic E2.

1.5 Purpose of Study

As previously stated, E2-25K is a unique E2 ubiquitin-conjugating enzyme that contains an ubiquitin-associated (UBA) domain C-terminal to the catalytic ubiquitin-conjugating (UBC) domain and synthesizes Lys48-linked free polyubiquitin chains *in vitro* in the absence of an E3 ligase. The objectives of this research were to determine the role, if any, the unique UBA domain plays in the function and structural stability of E2-25K. Furthermore, an understanding of the oligomerization state of E2-25K was needed to elucidate the need for dimerization in polyubiquitin chain formation.

Preliminary solution NMR studies suggested conformational flexibility in the E2-25K catalytic domain. Another goal was to determine the X-ray crystallographic structure of E2-25K and NMR assignments to elucidate the key residues within E2-25K involved in binding to ubiquitin and conjugation of polyubiquitin chains. Studying subtle changes in the structure may lead to a better understanding of polyubiquitin chain

synthesis by E2-25K *in vitro* and of the mechanism of ubiquitin transfer by E2s in general.

E2-25K interacts with multiple E3 ligases that determine the specificity of the cellular pathways affected [63, 65, 71-74]. Identifying the E2-25K key residues involved in binding may lead to prediction of other E2 partners through sequence comparison. E2-25K also binds to ubiquitin and polyubiquitin non-covalently through the UBA domain [84]. Because the available binding surfaces are limited by size and the binding partners have minimal sequence homology, it will be useful to examine how E2-25K adapts.

CHAPTER 2

METHODOLOGY

2.1 Materials

The pET30b expression vector encoding full-length E2-25K and RNF2 were obtained as a gift from Dr. Seongman Kang of the Graduate School of Biotechnology, Korea University. The pET15b expression vector encoding ubiquitin was obtained as a gift from Dr. Lynn Boyd of the Department of Biological Sciences, University of Alabama in Huntsville. The pET15b expression vector encoding Parkin was obtained as a gift from Dr. Marie Wooten of the Department of Biological Sciences, Auburn University. Expression vectors for ubiquitin-conjugating enzyme, UbcH5b (plasmid 11475), and ubiquitin-protein ligases, gp78 (plasmid # 11429) and MDM2 (plasmid 11492), were obtained from Addgene. An expression vector for APC11 RING finger was synthesized by iXpressGenes. Primers were obtained from MWG Biotech and Operon. All other expression vectors and host strains were provided by Novagen. Ubiquitin-activating enzyme, Ub K27R-K48R-K63R, Ub K0 (all lysines mutated to arginines), Mg-ATP solution, and energy regeneration solution were obtained from BostonBiochem.

2.2 Plasmid Constructs

2.2.1 E2-25K, UBC and UBA Plasmid Construction

The E2-25K construct from Dr. Kang contains an N-terminal hexa-histidine tag followed by an enterokinase cleavage site. Removal of the tag results in a construct with seven additional, non-native residues at the N-terminus. The UBC (residues M1- S159 of E2-25K) and UBA domains (residues G154-N200 of E2-25K) were both amplified by polymerase chain reaction (PCR) from the E2-25K construct provided by Dr. Kang using synthetic oligonucleotide primers (Table 2.1) that generated NheI and BamHI restriction sites. The presence of PCR products was verified by 1% agarose DNA gel electrophoresis as shown in Figure 2.1. The amplified UBC and UBA domains were purified by PCR purification kit (Qiagen) and setup for overnight restriction digest with NheI and BamHI restriction enzymes (Promega). The overnight digest of both constructs were again purified by PCR purification kit and ligated with a pET28b expression vector that was also cut with the same enzymes. The ligated UBC and UBA domain constructs were transformed into Nova Blue *E. coli* competent cells, a protease deficient strain of used for DNA production, by incubating 5 µL of ligated construct with 100 µL of Nova Blue *E. coli* competent cells. The remainder of the transformation process was followed as described in Section 2.3. Single colonies were inoculated into 5 mL of LB medium containing 35 µg/ml kanamycin and grown at 37 °C with shaking for ~14 hours. To screen for the presence of the cloned insert, plasmids were purified from overnight cultures (HiSpeed Plasmid Mini Prep Kit – Qiagen) and restriction digestion was performed using NheI and BamHI to verify insert. The presence of the inserts was verified by DNA gel electrophoresis as shown in Figure 2.2. The constructs containing

the full-length E2-25K, the UBC and the UBA domains were sent to SeqWright for sequence verification (Table A.1). The resulting proteins contained a hexa-histidine tag followed by a thrombin cleavage site on the N-terminus of the proteins.

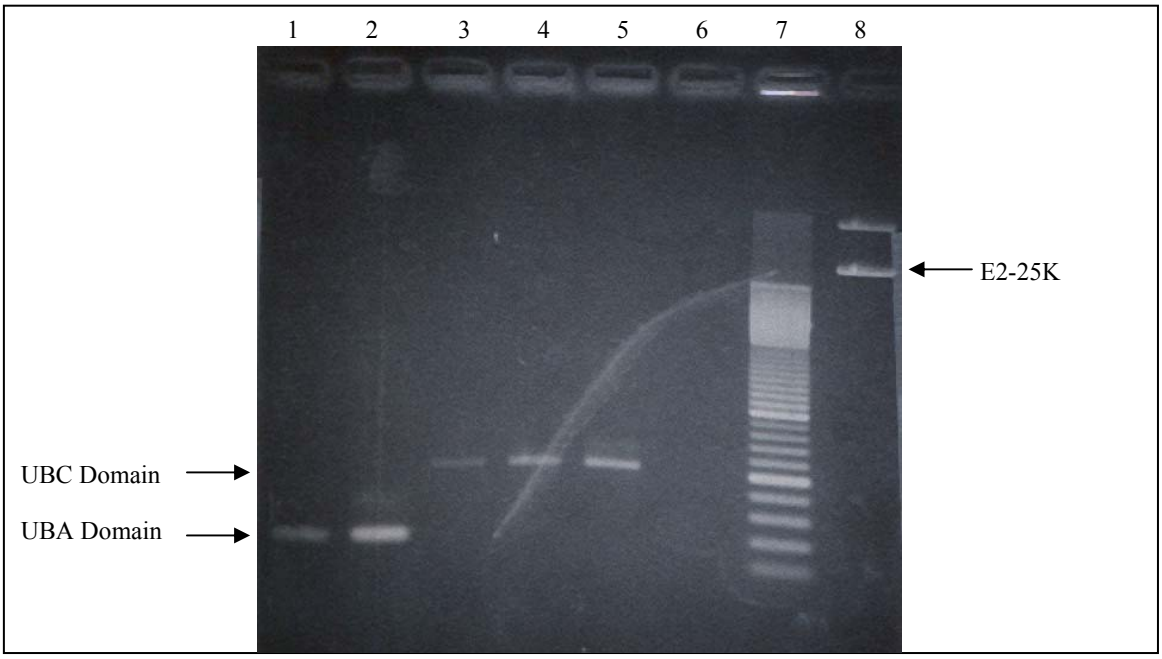

Figure 2.1 DNA Gel of UBC & UBA PCR Product. [PCR product of UBA domain (lanes 1 & 2), PCR Product of UBC domain (lanes 3-5), 100 bp DNA ladder (lane 7), and full-length E2-25K in pET30b (lane 8).]

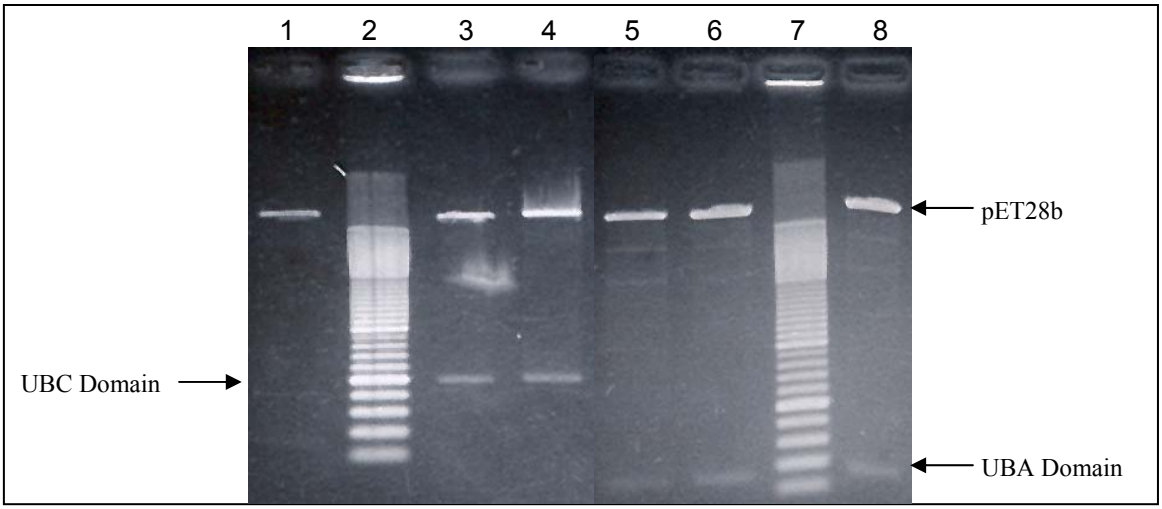

Figure 2.2 DNA Gel of UBC & UBA Insert Verification. [Lane 1 is a negative result, Restriction digest verification of UBC domain in pET28b (lanes 3 & 4), Restriction digest verification of UBA domain in pET28b (lanes 5, 6 & 8), and 100 bp DNA ladder (lanes 2 & 7).]

The E2-25K, UBC and UBA mutants were generated by site-directed mutagenesis using the complementary primers shown in Table 2.1 and PCR amplification. Following the manufacturer's instructions (Stratagene) for site-directed mutagenesis, single colonies of each construct were inoculated into 5 mL of LB medium containing 35 μg/ml kanamycin and grown at 37 °C with shaking for ~14 hours. The plasmids were purified from overnight cultures (HiSpeed Plasmid Mini Prep Kit – Qiagen) and sent to Functional Biosciences, Inc. for sequence verification. Sequence verified (Table A.1) mutant clones were named accordingly for later use: E2-25K K97R, E2-25K C92S, E2-25K M172A, UBA M172A, E2-25K L198A, and UBA L198A.

2.2.2 Ubiquitin and Mutant Plasmid Construction

The wild-type ubiquitin (Ub) was amplified by PCR from the ubiquitin construct supplied by Dr. Boyd using synthetic oligonucleotide primers (Table 2.2) that generated NheI and BamHI restriction sites. Figure 2.3 verifies the presence of the Ub insert. The pET28b expression vector encoding wild-type Ub contains an N-terminal hexa-histidine tag followed by a thrombin cleavage site. The ubiquitin D77 mutant was PCR amplified using the above expression vector as a template with Ub Forward and Ub-D77 Reverse primers (Table 2.2) to generate the addition of the aspartic acid. The insert verification is shown in Figure 2.3. The Ub- K48C, K63C, and K48C-K63C mutants were generated by site-directed mutagenesis following the manufacturer's instructions (Stratagene). The complementary primers shown in Table 2.2 were used to generate the Ub- K48C, K63C, and K48C-K63C mutants. Mutant clones were sequence verified by Functional Biosciences, Inc. (Table A.1) and named Ub-D77, Ub-K48C, Ub-K63C, and Ub-K48C-K63C, respectively. The resulting proteins contained an N-terminal histidine tag

followed by a thrombin cleavage site with the sequence MGSSHHHHHHSSGLVPRGSHM.

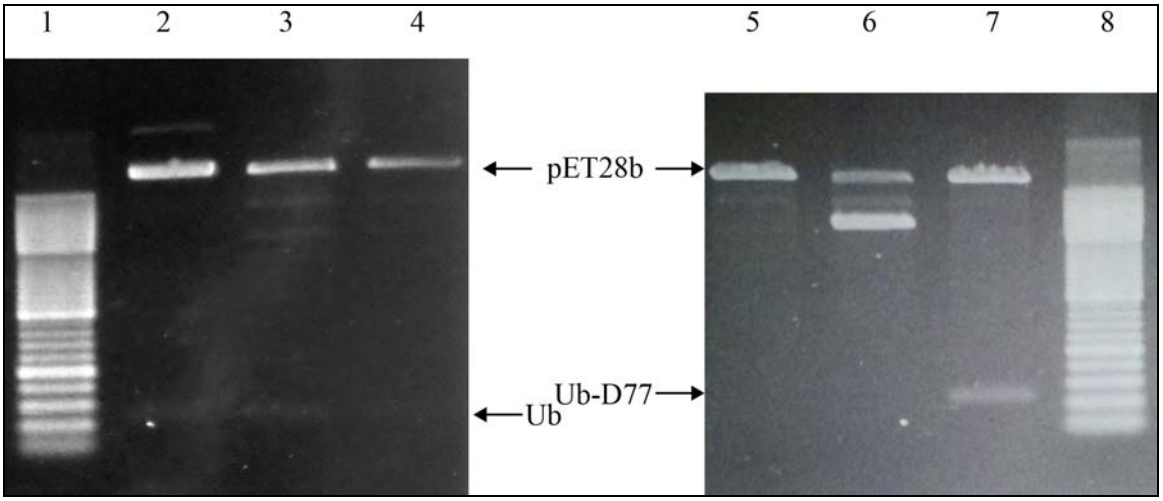

Figure 2.3 DNA Gels of Ub Wild-Type and Ub-D77 Insert Verification. [Lanes 1 & 8 are 100 bp DNA ladder, Restriction digest verification of Ub in pET28b (lanes 2 & 3), Restriction digest verification of Ub-D77 in pET28b (lane 7), Lanes 4, 5, & 6 are negative results.]

The frame-shifted mutant arising from the Ubiquitin-B gene (UBB+1), was generated with three consecutive PCR amplifications. The pET28b expression vector encoding wild-type Ub was used as a template with Ubb1 Forward 1 and Ubb1 Reverse 1 primers (Table 2.3) to generate the addition of the N-terminal hexa-histidine tag and the first thirty-four bases of the mutation. The addition of the last twenty-six bases was generated by using the previous PCR product as the template with Ubb1 Forward 1 and Ubb1 Reverse 2 primers (Table 2.3). The third PCR amplification used the second PCR product as the template with Ubb1 Forward 2 and Ubb1 Reverse 3 primers (Table 2.3) to generate the stop codon and the pET3a (Novagen) 3' and 5'vector specific sequences in order to facilitate directional cloning via *in vivo* homologous recombination. The resulting product was mixed with a previously double-digested pET3a vector prior to transformation into competent DH5α *E. coli* cells. The expression plasmid was obtained

using a standard plasmid mini-prep procedure (Qiagen). The UBB+1 construct was sequence verified by Functional Biosciences, Inc. (Table A.1).

2.2.3 Parkin Plasmid Construction

The Parkin ubiquitin-like-domain (Ubl) was amplified by PCR from the full-length Parkin construct supplied by Dr. Wooten using synthetic oligonucleotide primers (Forward 5'-GGT ATC CTC ATA TGA TAG TGT TTG TCA GGT TCA ACT -3' AND Reverse 5'-CCA GGA TCC TCA CGG TCT CTG CAC AAT GTG AAC AAT -3') that generated NheI and BamHI restriction sites. The pET28b expression vector encoding Parkin Ubl contains an N-terminal hexa-histidine tag followed by a thrombin cleavage site. The presence of the Parkin insert was verified as with Ub. The construct containing the appropriately sized insert was sent to SeqWright for sequence verification.

Table 2.1 E2-25K, UBC, and UBA Domain PCR Synthetic Oligonucleotide Primers

Primer Target	Primer Sequence*
UBA Domain Forward	GAG AGC TAG CGG AGC ACC AGT TTC TAG TCC AGA ATA
UBA Domain Reverse	CGC GGA TCC TCA GTT ACT CAG TAG CAA TTC TGT TG
UBC Domain Forward	GAG AGC TAG CAT GGC CAA CAT CGC GGT GCA
UBC Domain Reverse	GCG GAT CCT CAA CTA GAA ACT GGT GCT CCA
E2-25K & UBC K97A Forward	GTT TGG ATA TCC TGG CAG ATC AAT GGG CAG CTG
E2-25K & UBC K97A Reverse	CAG CTG CCC ATT GAT CTG CCA GGA TAT CCA AAC
E2-25K & UBC K97R Forward	GTT TGG ATA TCC TGA GAG ATC AAT GGG CAG CTG
E2-25K & UBC K97R Reverse	CAG CTG CCC ATT GAT CTC TCA GGA TAT CCA AAC
E2-25K C92S Forward	GTT CCG TCA CAG GGG CTA TTA GCT TGG ATA TCC T GA AAG ATC
E2-25K C92S Reverse	GAT CTT TCA GGA TAT CCA AGC TAA TAG CCC CTG TGA CGG AAC
E2-25K & UBA M172A Forward	GAA AAC CTA TGT GCT GCG GGC TTT GAT AGG AAT GC
E2-25K & UBA M172A Reverse	CTG CAT TCC TAT CAA AGC CCG CAG CAC ATA GGT TTT CTG
E2-25K L198A Forward	CAA CAG AAT TGC TTG CGA GTA ACT GAG GCA TAG AGA GCT G
E2-25K L198A Reverse	CAG CTC TCT ATG CCT CAG TTA CTC GCA AGC AAT TCT GTT G
UBA L198A Forward	CAA CAG AAT TGC TTG CGA GTA ACT GAG GAT CCG AAT TC
UBA L198A Reverse	GAA TTC GGA TCC TCA GTT ACT CGC AAG CAA TTC TGT TG

*Red text denotes Nhe1 or Nde1 restriction sites and blue text denotes BamH1 restriction site. Green T indicates mutated A to T to reduce stem loop structure formation in the synthetic primer. Underlined text denotes site directed mutation site.

Table 2.2 Ubiquitin and Ubiquitin Mutants PCR Synthetic Oligonucleotide Primers

Primer Target	Primer Sequence*
Ub Forward	GGT ATC CTC ATA TGC AGA TCT TCG TGA AAA CCC TTA CCG G
Ub Reverse	CCA GGA TCC TCA ACC ACC TCT CAG GAC C
Ub-D77 Reverse	CCA GGA TCC TCA ATC ACC ACC TCT CAG ACG CAG GAC C
Ub-K48C Forward	G TTG ATC TTT GCT GGG TGT CAG CTG GAA GAT GGA CG
Ub-K48C Reverse	CG TCC ATC TTC CAG CTG ACA CCC AGC AAA GAT CAA C
Ub-K63C Forward	GAC TAC AAC ATC CAG TGT GAG TCC ACC CTG CAC
Ub-K63C Reverse	GTG CAG GGT GGA CTC ACA CTG GAT GTT GTA GTC

*Red text denotes Nhe1 or Nde1 restriction sites and blue text denotes BamH1 restriction site. Underlined text denotes site directed mutation site.

Table 2.3 Ubiquitin+1 Mutant PCR Synthetic Oligonucleotide Primers

Primer Target	Primer Sequence*
Ubb1 Forward Primer 1 (UBPFPH1)	ATG AAG CAT CAT CAT CAT CAT CAT CAG ATG CAG ATC TTC GTG AAA ACC C
Ubb1 Reverse Primer 1 (UBRPCB1)	CCT GGC GAT CCG GAT CTT CGC GCA GAT CCG CAT AAC CTC TCA GAC GCA GGA CCA GG
Ubb1 Reverse Primer 2 (UBRPADD1)	CTG CGC GCC GCT GCC CGG ATG ATG ATC CTG GCG ATC CGG ATC TTC G
Ubb1 Forward Primer 2 (MFPVH1)	TTT GTT TAA CTT TAA GAA GGA GAT ATA CAT ATG AAG CAT CAT CAT CAT CAT CAT CAG
Ubb1 Reverse Primer 3 (UBRPVH1)	CTT CCT TTC GGG CTT TGT TAG CAG CCG GAT CCT CAC TGC GCG CCG CTG CCC GGA TGA TGA T

* Underlined text denotes pET3a vector overlap sequence and red text denotes N-terminal hexa-histidine tag and stop codon. Blue text denotes first half of mutant and green text denotes second half of mutant.

2.3 Protein Expression

All constructs were transformed into competent BL21(DE3) *E. coli* cells (a protease deficient strain of *E. coli*) by incubating 1 µL of purified plasmid construct

(~ 1 μg/μL) with 100 μL of competent cells on ice for 15 minutes. The cells were heat-shocked at 42 °C for 30 seconds and put back on ice, where 400 μL of SOC medium 2% (w/v) tryptone, 0.5 % (w/v) yeast extract, 10 mM NaCl, 2.5mM KCl, 10 mM $MgCl_2$, 20 mM $MgSO_4$, and 20 mM glucose) was immediately added. The cells were then incubated at 37 °C with shaking for 30 minutes and 100 μL were plated onto LB plates (tryptone – 10 g/L, yeast extract – 5 g/L, NaCl - 10 g/L and agar – 15 g/L) with the appropriate antibiotic (35 μg/ml kanamycin or 50 μg/ml ampicillin (Table 2.4)) and grown overnight at 37 °C. Single colonies were inoculated into 5mL of LB medium (Tryptone – 10 g/L, Yeast Extract – 5 g/L and NaCl - 10 g/L) containing similar antibiotic and grown at 37°C with shaking for ~14 hours. The overnight cultures were used to inoculate two litters of fresh LB media with similar antibiotic concentration and grown at 37°C with shaking to an OD_{600} of ~0.6. RING finger E3 proteins (RNF2, APC11, and MDM2) were grown in the additional presence of 100 μM $ZnSO_4$.

Protein expression was induced by the addition of isopropyl-β-D-thiogalactopyranoside (IPTG) to a final concentration of 0.5 mM. Cultures were grown for 4 hours after induction at 37 ºC or were grown overnight at 18 ºC (see Table 2.4), then cooled to 4 ºC. The cells were harvested by centrifuging for 25 minutes at 6000 x g (Beckman JLA-9.1 rotor). The pellets were collected and stored at -20 or -80 ºC until purification.

Table 2.4 Plasmid Construct Specific Details

Target Protein	Vector	Antibiotic	Induction Temperature & Time
E2-25K	pET30a	kanamycin	37 ºC for 4 hours
E2-25K M172A	pET30a	kanamycin	37 ºC for 4 hours
E2-25K L198A	pET30a	kanamycin	37 ºC for 4 hours
E2-25K K97R	pET30a	kanamycin	37 ºC for 4 hours
E2-25K K97A	pET30a	kanamycin	37 ºC for 4 hours
E2-25K C92S	pET30a	kanamycin	37 ºC for 4 hours
UBC Domain	pET28b	kanamycin	37 ºC for 4 hours
UBC K97R	pET28b	kanamycin	37 ºC for 4 hours
UBC K97A	pET28b	kanamycin	37 ºC for 4 hours
UBA Domain	pET28b	kanamycin	18 ºC overnight
UBA M172A	pET28b	kanamycin	18 ºC overnight
UBA L198A	pET28b	kanamycin	18 ºC overnight
Ub	pET28b	kanamycin	37 ºC for 4 hours
Ub K48C	pET28b	kanamycin	37 ºC for 4 hours
Ub K63C	pET28b	kanamycin	37 ºC for 4 hours
Ub K48C K63C	pET28b	kanamycin	37 ºC for 4 hours
Ub D77	pET28b	kanamycin	37 ºC for 4 hours
UBB+1	pET3a	ampicillin	18 ºC overnight
RNF2	pET30a	kanamycin	37 ºC for 4 hours
MDM2	pGEX	ampicillin	18 ºC overnight
Parkin	pET28b	kanamycin	37 ºC for 4 hours
APC11	pET3a	ampicillin	37 ºC for 4 hours
UbcH5b	pET15b	ampicillin	37 ºC for 4 hours

2.3.1 Uniformly Enriched Protein Expression

As with standard expression, ^{13}C, ^{15}N-labeled full-length E2-25K and the UBA domain protein expression were performed by transforming the construct into BL21(DE3) *E. coli* cells. Single colonies were inoculated into 5mL LB media containing 35 µg/ml kanamycin and grown at 37 °C for ~9 hours. The LB growth was used to inoculate 10 mL of M9 medium (Na_2HPO_4•$7H_2O$ - 12.8 g/L, KH_2PO_4 – 3 g/L, NaCl – 0.5 g/L, $MgSO_4$ (anhydrous) – 0.24 g/L, $CaCl_2$ – 15 mg/L, pH 7.0 with addition of

$FeCl_3 \cdot 6H_2O$ – 5 mg/L and Thiamine – 1 mg/L) containing 2 g/L U-$^{13}C_6$-glucose, 1 g/L ^{15}N-NH_4Cl and 35 μg/ml kanamycin for overnight growth at 37°C with shaking. The overnight cultures were inoculated into one litter fresh ^{13}C, ^{15}N-enriched M-9 media with similar kanamycin concentration and grown at 37 °C with shaking to an OD_{600} of ~0.6. The protein expression and harvesting of cells were performed as described in Section 2.3.

Expression of ^{15}N-labeled full-length E2-25K, UBC domain, UBA domain and Ub were performed as with ^{13}C, ^{15}N-labeled E2-25K UBA domain except 2 g/L of D-glucose was added instead of 2 g/L U-$^{13}C_6$-glucose. Similarly, expression of ^{13}C, ^{15}N-labeled deuterated full-length E2-25K was performed as with ^{13}C, ^{15}N-labeled full-length E2-25K except D_2O was added instead of distilled H_2O and the cells were grown for 6 hours before harvesting.

2.4 Protein Purification

In order to express protein, the verified construct of interest was transformed into BL21(DE3) *E. coli* competent cells as described in detail in Section 2.3. The full-length E2-25K, the UBC and UBA domains, UBA domain mutants and Ub were expressed in labeled (as described in Section 2.3.1) as well as unlabeled medium. All other constructs were only expressed in unlabeled medium. The purification of all proteins will be discussed in detail in the sections to follow.

2.4.1 Purification of full-length E2-25K or E2-25K Mutants

The purification of both labeled and unlabeled full-length E2-25K and mutant proteins were conducted in a similar manner. The full-length E2-25K or mutant was

resuspended in Ni^{2+} binding buffer (20 mM Tris-HCL, 5 mM Imidazole, and 500 mM NaCL, pH 8.0) and lysed by sonication. Total crude lysate (TCL) was centrifuged at 20,000 x g (Beckman JA-25.5 rotor) for 15 minutes. The soluble crude lysate (SCL) supernatant was filtered (0.45 μm filter) and chromatographed onto a Ni^{2+}-chelating sepharose column (GE Biosciences). E2-25K or mutant was washed with 11% Ni^{2+} elution buffer and then eluted with 70% Ni^{2+} elution buffer (20 mM Tris-HCL, 400 mM Imidazole, and 500 mM NaCL, pH 8.0). The fractions containing E2-25K or mutant (lanes 5-11 shown in Figure 2.4) were pooled and dialyzed against enterokinase buffer (20 mM Tris-HCl, pH 7.4, 50 mM NaCl, 2 mM $CaCl_2$).

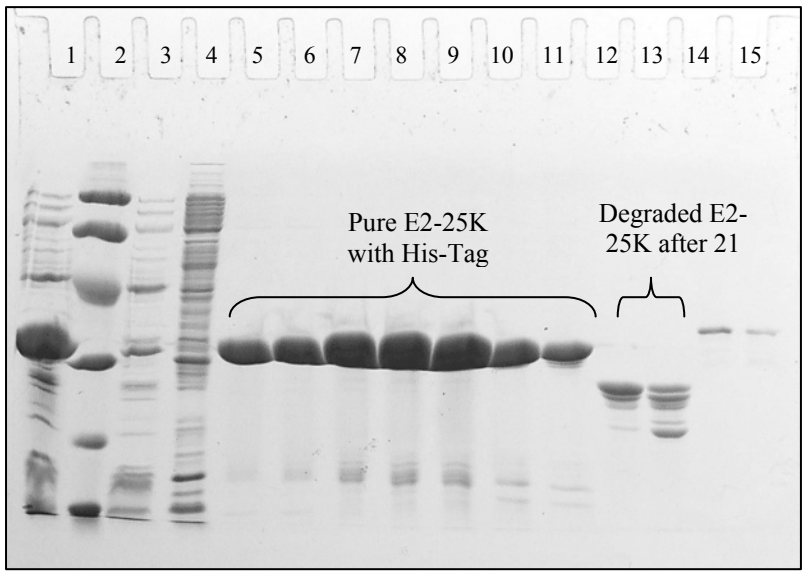

Figure 2.4 SDS PAGE Gel for Ni^{2+}-chelating column of Full-length E2-25K. [Lane 1 – SCL, Lane 2 – LMWM, Lane 3 - Ni^{2+} column flow-through, Lane 4 – 11% Ni^{2+} elution buffer wash, Lanes 5-11 – Pure E2-25K, Lanes 12-13 – Degraded E2-25K after 21 days at 4°C.]

Digestion with 0.5 units of enterokinase per milligram of E2-25K was allowed to proceed for 6 hours at room temperature and separation of digested from undigested was by ion-exchange chromatography on a HiTrap Q column (GE Biosciences) via FPLC

with 1 M NaCl gradient, chromatograph shown in Figure 2.5. Fractions containing digested E2-25K or mutant were verified by SDS PAGE electrophoresis, (lanes 4-7 in Figure 2.6) and were pooled and dialyzed against the NMR buffer (50 mM NaH_2PO_4/Na_2HPO_4, pH 6.5) if labeled protein, or chain assay buffer (20 mM Tris-HCl, pH 8.0, 50 mM NaCl) if unlabeled protein. The E2-25K or mutant protein was then concentrated by ultra-filtration (Amicon 10,000 MWCO) to 4 - 12 mg/mL for further analysis or storage at -20 °C. The final NMR sample buffer for full-length E2-25K was 50 mM NaH_2PO_4/Na_2HPO_4, pH 6.5, and 0.12 mM DSS in 90% H_2O/10% D_2O.

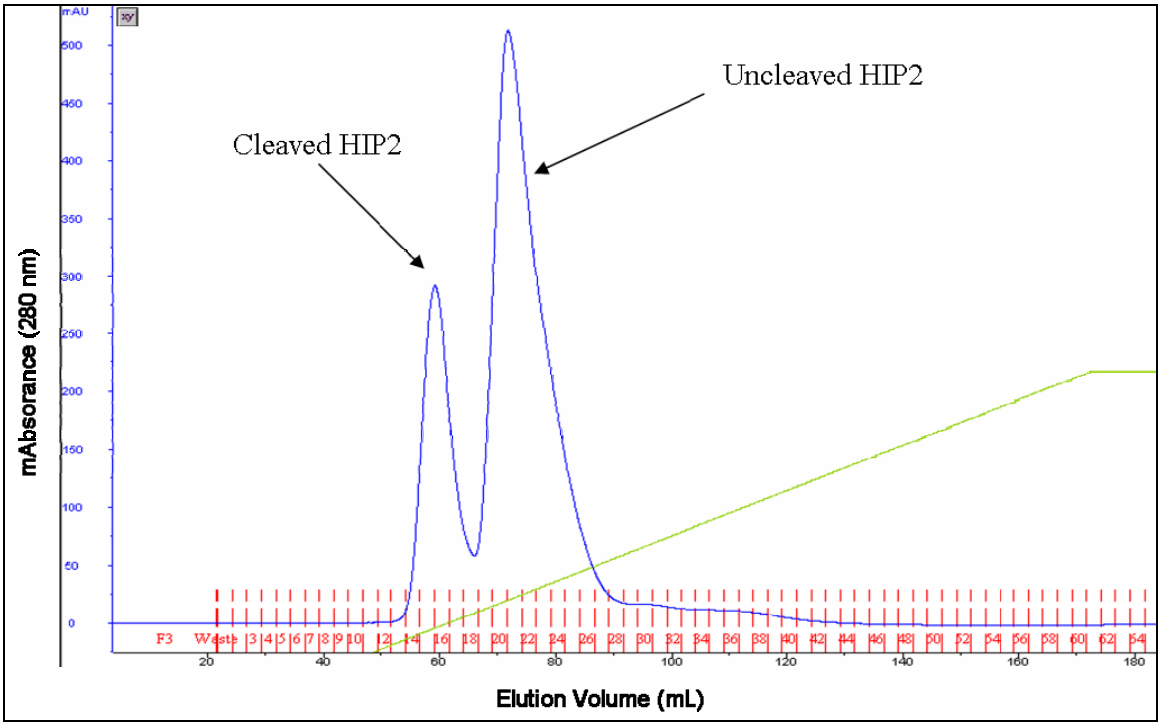

Figure 2.5 Ion-exchange Chromatograph of Full-length E2-25K. [First peak is cleaved E2-25K and second peak is uncleaved E2-25K.]

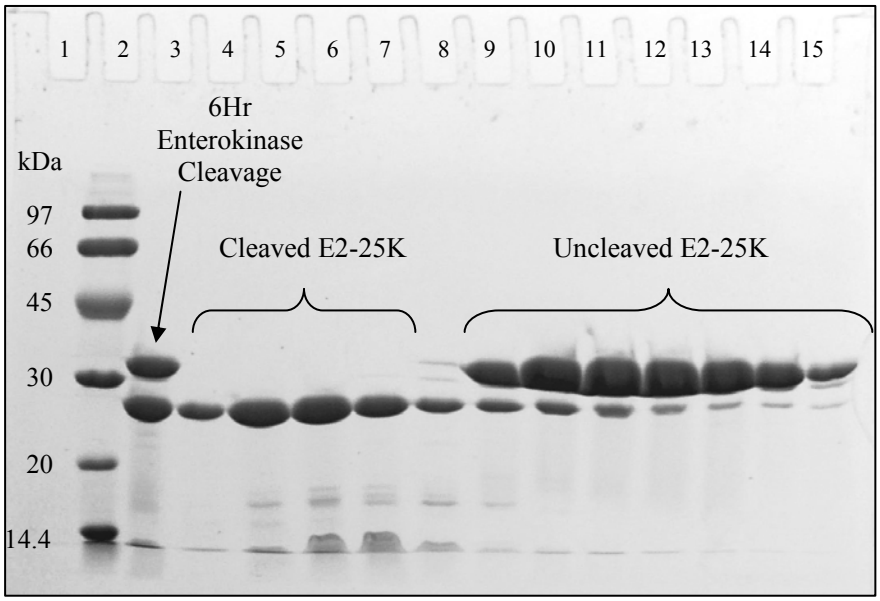

Figure 2.6 SDS PAGE Gel for Ion-exchange column of Full-length E2-25K. [Lane 2 – Low Molecular Weight Marker (LMWM), Lane 3 – 6 hour enterokinase cleavage, Lanes 4-7 – Pure Cleaved E2-25K, Lanes 9-15 – Pure Uncleaved E2-25K.]

2.4.2 Purification of E2-25K UBA Domain or Mutants

As with full-length E2-25K, the purification of E2-25K UBA domain or mutant were performed in the same manner for both labeled and unlabeled protein. The cell pellets, containing the protein of interest, were resuspended in Ni^{2+} binding buffer and lysed by sonication. The SCL supernatant was filtered (0.45 μm filter) and chromatographed onto a Ni^{2+}-chelating sepharose column (GE Biosciences). The E2-25K UBA domain or mutant was washed with 11% Ni^{2+} elution buffer and then eluted with Ni^{2+} elution buffer. The fractions containing E2-25K UBA domain or mutant were pooled and dialyzed against QA buffer (20 mM Tris-HCl, pH 8.0, 50 mM NaCl). The E2-25K UBA domain or mutant sample was then applied to a HiTrap Q and SP column series (5 ml each, GE Biosciences) and eluted with QB buffer (20 mM Tris-HCl, pH 8.0, 1 M NaCl). The fractions containing E2-25K UBA domain or mutant were verified by SDS PAGE electrophoresis as shown in Figure 2.7.

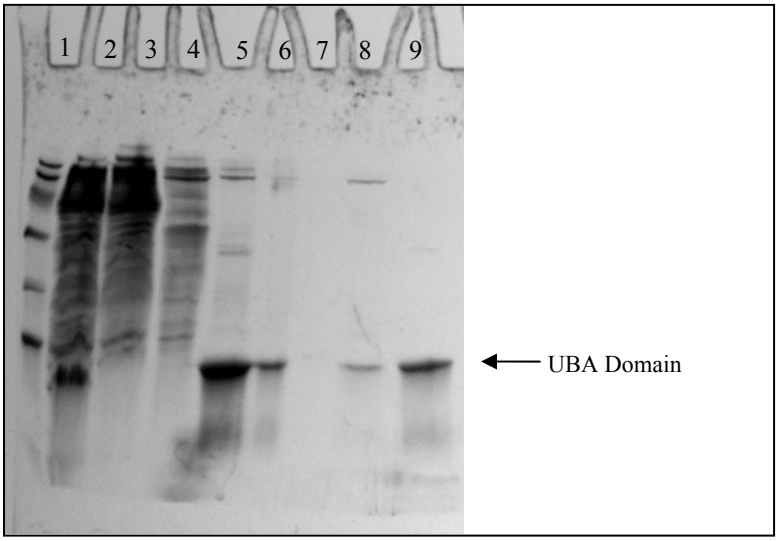

Figure 2.7 SDS PAGE Gel of E2-25K UBA Domain. [Lane 1 – LMWM, Lane 2 – SCL, Lane 3 – Ni^{2+} column flow-through, Lane 4 – 11% Ni^{2+} column elution buffer wash, Lane 5 – Ni^{2+} column 500 mM Imidazole elution fraction, Lane 6 – UBA domain dialyzed sample loaded onto Q & SP column series, Lane 7 – Q & SP column series flow-through, Lane 8 – Q column 1M NaCl elution fraction, Lane 9 – SP column 1M NaCl elution fraction.]

The E2-25K UBA domain or mutant sample was then dialyzed against the NMR buffer (50 mM NaH_2PO_4/Na_2HPO_4, 100 mM NaCl, 0.1 mM BME, pH 7.0) if labeled protein or chain assay buffer if unlabeled protein. The UBA domain or mutant protein was concentrated by ultra-filtration (Amicon 5000 MWCO) to 4 - 8 mg/mL for further analysis or storage at -20 °C.

2.4.3 Purification of E2-25K UBC Domain or Mutant

As with full-length E2-25K, the purification of E2-25K UBC domain or mutant were performed in the same manner for both labeled and unlabeled protein. The UBC domain or mutant cell pellet was resuspended in Ni^{2+} binding buffer and lysed by sonication. The supernatant was chromatographed onto a Ni^{2+}-chelating sepharose column. UBC domain or mutant was washed with 11% Ni^{2+} elution buffer and then eluted with 400 mM Imidizole. Fractions containing UBC domain or mutant were pooled and dialyzed against NMR buffer (50 mM NaH_2PO_4/Na_2HPO_4, 100 mM NaCl, 0.1 mM

BME, pH 7.0) or chain assay buffer and concentrated by ultra-filtration (Amicon 5000 MWCO) to 4 - 12 mg/mL.

2.4.4 Purification of Ubiquitin and Mutant Proteins

As with full-length E2-25K, the purification of Ub or mutants was performed in the same manner for both labeled and unlabeled protein. The Ub or mutant cell pellets were resuspended in Ni^{2+} binding buffer and lysed by sonication. The supernatant was chromatographed onto a Ni^{2+}-chelating sepharose column, washed with 11% Ni^{2+} elution buffer and then eluted with 400 mM Imidazole. The fractions containing Ub or mutant were verified by SDS PAGE electrophoresis and dialyzed against the NMR buffer (50 mM NaH_2PO_4/Na_2HPO_4, 50 mM NaCl, pH 7.2) if labeled protein or chain assay buffer (50 mM Tris-HCl, pH 8.0, 0.1 mM EDTA, 0.5 mM DTT) if unlabeled protein. The Ub or mutant protein was then concentrated by ultra-filtration (Amicon 5000 MWCO) to 4 – 14.2 mg/mL for further analysis or storage at -20 °C.

As with wild-type Ub, UBB+1 were resuspended in Ni^{2+} binding buffer and lysed by sonication. The supernatant was chromatographed onto a Ni^{2+}-chelating sepharose column, washed with 11% Ni^{2+} elution buffer and eluted with 400 mM Imidizole. The fractions containing UBB+1 were pooled, concentrated by ultra-filtration (Amicon 5000 MWCO), injected onto a HiPrep 16/60 Sephacryl S-100 column (GE Biosciences) and chromatographed via FPLC in 50 mM Tris-HCl, pH 8.0, 25 mM NaCl, 1.0 mM EDTA buffer. The fractions containing UBB+1 were pooled and concentrated by ultra-filtration to 30 to 40 mg/mL.

2.4.5 Purification of E3 and Additional E2 Proteins

The cells containing the MDM2 protein were resuspended in PBS binding buffer (10 mM Na_2HPO_4, 1.8mM KH_2PO_4, 140 mM NaCl, 2.7 mM KCl, pH 7.3) and lysed by sonication. The supernatant was chromatographed onto a Glutathione S-transferase (GST) HiTrap column (GE Biosciences). MDM2 was eluted with GST elution buffer (50 mM Tris-HCl, 10mM reduced glutathione, pH 8.0) and fractions containing MDM2 were pooled and dialyzed against QA buffer and concentrated by ultra-filtration (Amico 10,000 MWCO) to ~6.7 mg/mL.

The cells containing the APC11 protein were resuspended in Ni^{2+} binding buffer (pH 9.0) and lysed by sonication. The supernatant was chromatographed onto a Ni^{2+}-chelating sepharose column and washed with 11% Ni^{2+} elution buffer (pH 9.0). APC11 was then eluted with 400 mM Imidizole and fractions containing APC11 were pooled and dialyzed against QA buffer and concentrated by ultra-filtration (Amico 5000 MWCO) to ~6.7 mg/mL.

The cells containing the RNF2 protein were resuspended in Ni^{2+} binding buffer and lysed by sonication. The supernatant was chromatographed onto a Ni^{2+}-chelating sepharose column and washed with 11% Ni^{2+} elution buffer. RNF2 was then eluted with 400 mM Imidizole and fractions containing RNF2 were pooled and concentrated by ultra-filtration to a final volume of 2 mL. The RNF2 sample was injected onto a HiPrep 16/60 Sephacryl S-200 column (GE Biosciences) and chromatography via FPLC in 20 mM Tris-HCl, pH 8.0, and 150 mM NaCl buffer. The fractions containing RNF2 were pooled and concentrated by ultra-filtration (Amicon 10,000 MWCO) to ~13.5 mg/mL.

The cells containing the Parkin protein were resuspended in Ni^{2+} binding buffer (pH 8.0) and lysed by sonication. The supernatant was chromatographed onto a Ni^{2+}-chelating sepharose column and washed with 11% Ni^{2+} elution buffer. Parkin was then eluted with 400 mM Imidizole and fractions containing Parkin were pooled and dialyzed against QA buffer and concentrated by ultra-filtration (Amicon 5000 MWCO) to ~12.8 mg/mL.

The cells containing the UbcH5b protein were resuspended in QA binding buffer and lysed by sonication. The supernatant was applied to a HiTrap Q and SP column series and the flow-through fractions containing UbcH5b were pooled and concentrated by ultra-filtration (Amicon 5000 MWCO) to a final volume of 2 mL. The UbcH5b sample was injected onto a HiPrep 16/60 Sephacryl S-200 column and chromatographed via FPLC in 20 mM Tris-HCl, pH 8.0, and 50 mM NaCl buffer. The fractions containing UbcH5b were verified by SDS PAGE electrophoresis (Figure 2.8, Lanes 10 and 11), pooled and concentrated by ultra-filtration (Amicon 5000 MWCO) to ~ 4.5 mg/mL.

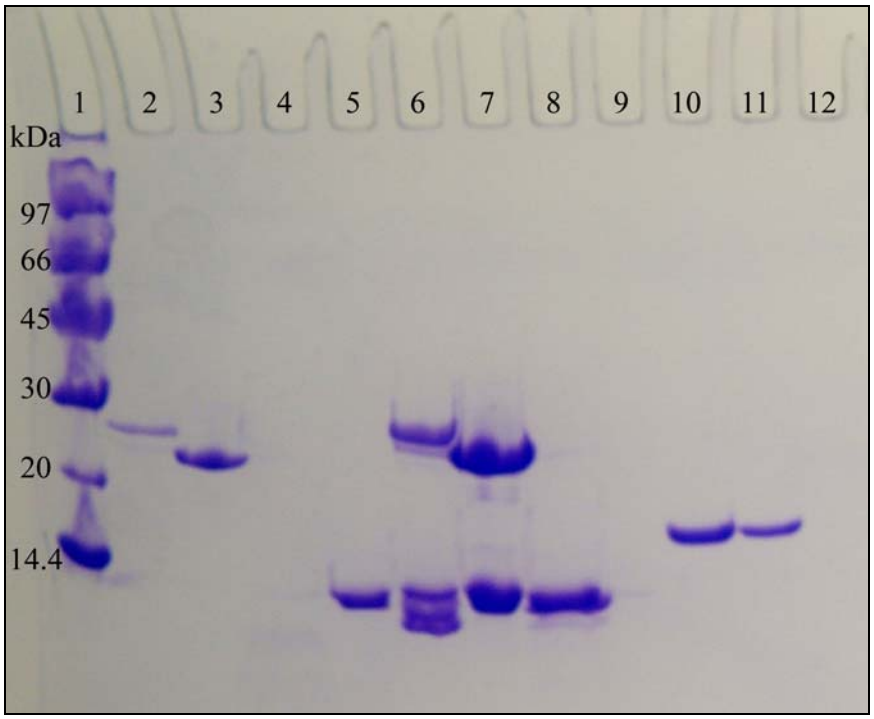

Figure 2.8 SDS PAGE Gel of UbcH5b. [SDS PAGE of UbcH5b Purification. Lane 1 – LMW Marker, Lane 10 – UbcH5b FPLC fraction 4, Lane 11 – UbcH5b FPLC fraction 5, Lane 12 – UbcH5b FPLC fraction 6.]

2.5 Crystallization

Initial crystallization trials with E2-25K, E2-25K M172A, UBC and UBB+1 were performed with commercially available reagents using the sitting-drop vapor diffusion method in a 96-well Intelliplate (Art Robbins). Hampton Screen I (1-48) and Hampton Screen II (1-48) (Hampton Research, Laguna Hills, CA) were used as reservoir solutions (100μL) in the initial trial. Protein to precipitant ratios of 1:1 (2μL:2μL) and 2:1 (2μL:1μL) were placed in sample wells. Crystal trays were monitored for the appearance of precipitation and/or crystalline morphology.

Several crystals were screened in-house using the RU-300 (Rigaku, Japan) rotating anode generator operating at 50 kV and 100 mA. The X-ray diffraction data was collected with a Rigaku R-AXIS IV image plate detector.

2.6 Fluorescence Titration Ubiquitin Binding

Fluorescence spectra were acquired at 20 °C on a Jobin Yvon FluoroMax-3 spectrofluorimeter. The 2.5 mL samples were placed in a semi-micro quartz cuvette (Wilmad) with a 1-cm excitation light path that was stirred continuously with an internal cylindrical Teflon-coated magnetic stirrer using a magnetic drive mounted below the cuvette holder. Tryptophan titration measurements utilized an excitation wavelength of 295 nm (slit width, 4 nm) and an emission wavelength range of 315 to 355 nm [85] (slit width, 4 nm). The data were collected over a range of 310 - 450 nm using the Fluoromax software. Tryptophan quenching data were collected by adding 5 μL aliquots of 0.37 mM Ub-K48C to the 2.5 mL sample of 0.5 uM E2-25K, UBC or UBA domain. After mixing, fluorescence emission at the respective maximum emission wavelength for the E2-25K, UBC domain or UBA domain complex was recorded. The emission intensities were subsequently corrected for the sample dilution by using Wavemetrics IGOR Pro and in-house scripts.

2.7 Fluorescence ANS Binding Assay

E2-25K C92S samples were prepared with 100:1 molar ratio of 1-anilino naphthalene-8-sulfonic acid (ANS) to protein. Purified protein samples (as described in Section 2.4.1) were diluted to a 5 uM solution with sterile-filtered dH_2O to a final volume of 1 mL which also contained 500 uM ANS. Samples were compared to a control which consisted of the same buffer as the protein samples and ANS diluted in sterile-filtered dH_2O. Emission spectra were collected on a Jobin Yvon FluoroMax-3 fluorimeter over a range from 380 nm to 600 nm with an excitation wavelength of

365 nm (slit width, 4 nm). The temperature was maintained at 20 °C by a thermostatted cell holder.

2.8 Nuclear Magnetic Resonance

NMR spectra were collected at 22º and 25 °C on a Varian (Palo Alto, CA) 800 MHz (18.7 Tesla field) INOVA NMR spectrometer using a triple resonance probe with triaxial pulsed field capability. Pulse sequences were those provided by Varian BioPack. ^{1}H chemical shifts were referenced using sodium 4,4-dimethyl-4-silapentane-1-sulfonate (DSS) as an internal reference. ^{13}C and ^{15}N chemical shifts were referenced indirectly to DSS and liquid ammonia, respectively, using the appropriate frequency ratios [86]. NMR spectra were processed using NMRpipe [87]. NMRView [88] was used for visualization and chemical shift assignments of NMR data.

2.8.1 Residual Dipolar Coupling Measurements of the E2-25K UBA Domain

The model of the E2-25K UBA domain was calculated using residual dipolar coupling (RDC) measurements. A ^{15}N-labeled E2-25K UBA domain sample was aligned in the magnetic field (Varian 800 MHz) with a nonionic liquid crystalline medium made up of 5% C12E6 [n-dodecyl hexa(ethylene glycol)] and 5% n-hexanol [89] and gave a ^{2}H splitting of 18 Hz at 30° C. Alignment was verified using the quadrupolar splitting of the ^{2}H spectrum. RDCs were determined from aligned and unaligned samples using gNHSQCS3 (Varian Biopack) experiments with the phase cycling adjusted to observe the two proton components individually. Couplings were measured using in-house scripts written for NMRView [88] and the RDC values were analyzed using MODULE [90].

2.8.2 Titration of ^{15}N-labeled full-length E2-25K and UBA Domain with Ubiquitin

Binding of full-length E2-25K and UBA domain to monoubiquitin (Ub) was examined by solution NMR using a series of two-dimensional ^{1}H-^{15}N-filtered Heteronuclear Single Quantum Coherence Spectrum (HSQC) experiments. A 0.5 mM solution of ^{15}N-labeled E2-25K UBA domain was prepared in 50 mM NaH_2PO_4/Na_2HPO_4, 100 mM NaCl, 0.1 mM BME, 0.12 mM DSS, pH 7.0 in 90% H_2O/10% D_2O as previously described. Increasing amounts of unlabeled Ub (34.8 mM) to a maximum molar ratio of 3.5:1 Ub:UBA were titrated into the sample. Specific changes in chemical shift values were used to identify amino acids in the UBA domain whose chemical environment was altered upon binding.

Titration of full-length E2-25K with Ub was performed in the same manner as the UBA domain, except that only molar ratios of 2.0:1 Ub:E2-25K were reached before significant broadening of peaks led to loss of signal.

2.8.3 Titration of ^{15}N-labeled Ubiquitin with UBA Domain and full-length E2-25K

Titration of ^{15}N-Ub (0.6 mM) was performed as with the UBA domain except that the buffer pH was 7.2 and unlabeled UBA domain (2.5 mM) was added to a final molar ratio of 1.5:1 UBA:Ub. Titration of ^{15}N-Ub (0.85 mM) with full-length E2-25K was performed in the same manner as with the UBA domain, except unlabeled full-length E2-25K (71 μM) was added to a final molar ratio of 0.03:1 E2-25K:Ub.

2.8.4 Titration of ^{15}N-labeled full-length E2-25K with E3 proteins

Titration of full-length E2-25K with E3 proteins was performed in the same manner as with Ub, except only molar ratios of 0.14:1 RNF2:E2-25K, 0.16:1 APC11:E2-

25K, 0.21:1 MDM2:E2-25K and 0.54:1 Parkin:E2-25K were reached before significant broadening of peaks led to loss of signal.

2.9 Polyubiquitin Chain Assay

The polyubiquitin chain synthesis assays were adapted from work performed by Piotrowski et al. [91]. The assays contained 20 μM E2-25K (or E2-25K mutant of interest or E2-25K UBC domain) along with 4 mM Mg-ATP solution, 0.2 μM E1 activating enzyme (BostonBiochem), 10 mM phosphocreatine, 0.6 unit/ml of inorganic phosphokinase, 0.6 unit/ml of creatine phosphokinase, 10 mM phosphocreatine and 0.5 mM DTT. Modifications to the adapted protocol were in the type of ubiquitin added: wild-type only, constructs Ub-K48C and Ub-D77 at equal molar concentrations, Ub-K48C only, Ub-K48C-K63C only, or Ub-D77 only. Assays were incubated at 37 °C for 3 to 4 hours, and analyzed by SDS-PAGE.

CHAPTER 3

CRYSTALLIZATION

To better understand the functional role of the UBA domain in the context of E2-25K, a M172A mutant protein was prepared for comparison with the wild-type. UBB+1 was also prepared in an attempt to understand the aberrant C-terminus that is produced from molecular misreading of the ubiquitin linear repeat gene. The X-ray crystallographic structures of E2-25K M172A mutant protein were determined for two different conditions. The crystal structures were determined to 1.9 Å resolution (~ pH 6.5) and to 2.2 Å resolution (~ pH 8.5). Comparison of these structures with that of the wild-type E2-25K revealed few structural differences overall, but showed some significant changes in the positions of catalytic active site residue sidechains. Crystal trials for UBB+1 were unsuccessful and abandoned after the structure was determined and deposited by another lab [92].

Initial crystallization trials with E2-25K, E2-25K M172A, and UBB+1 were performed with commercially available reagents using the sitting-drop vapor diffusion method in a 96-well Intelliplate (Art Robbins). Hampton Screen I (1-48) and Hampton Screen II (1-48) (Hampton Research, Laguna Hills, CA) were used as reservoir solutions (100µL) in the initial trial. Protein to precipitant ratios of 1:1 (2µL:2µL) and 2:1 (2µL:1µL) were placed in sample wells. Crystal trays were monitored for the appearance of precipitation and/or crystalline morphology. Several conditions produced crystals for

all three proteins, however, all UBB+1 trials ended unproductive, producing salt crystals or non-diffracting crystals.

3.1 Crystallization of Wild-type E2-25K

While crystal conditions were being optimized for the wild-type E2-25K, the crystal structure (PDB code 1YLA) [93] was deposited into the Molecular Modeling Database (MMDB) [94] by Structural Genomics Consortium. Interestingly enough, the conditions used in the published crystal structure (PDB code 1YLA) [93] are the same as components used to produce the small crystals shown in Figures 3.1.

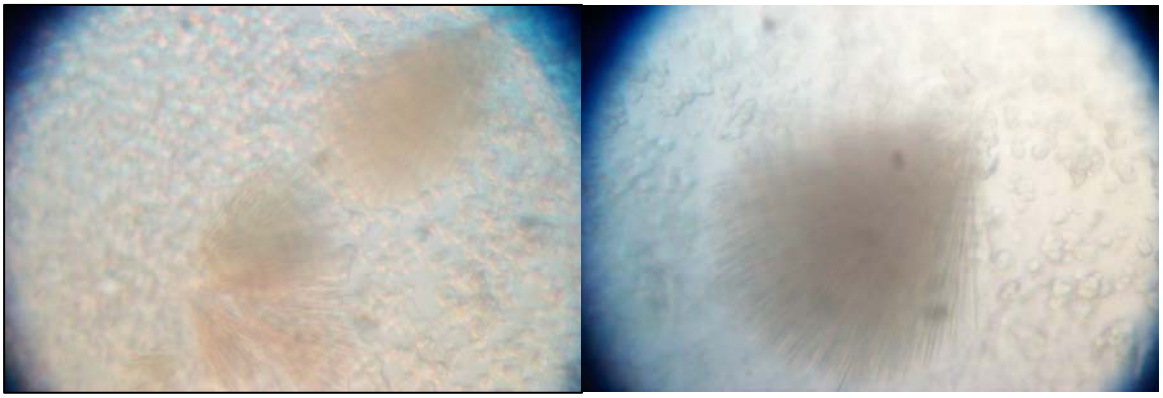

Figure 3.1 E2-25K Crystals with 18% PEG 8000, 0.1 M Na Cacodylate pH 6.5, 0.2 M Calcium Acetate at 4 °C.

3.2 Crystallization of E2-25K M172A

The 96 well-plate containing E2-25K M172A was allowed to equilibrate undisturbed for one week at 21 ºC in a temperature-controlled incubator. After one week two sets of conditions 0.1 M sodium cacodylate trihydrate pH 6.5, 0.2 M calcium acetate hydrate, 18% (w/v) polyethylene glycol 8,000 (low pH condition) and 0.1 M sodium HEPES pH 7.5, 0.2 M calcium chloride dihydrate, 28% PEG 400 (high pH condition) produced poorly formed needle-like E2-25K M172A protein crystals similar to the wild-type E2-25K (Figure 3.1). Optimization screens around both conditions were performed

with ionic strength and pH as the target screening parameters. Stock buffers with optimal buffering capacity at pH 4.6, 6.0, and 9.0 were mixed with the original reservoir solutions in order to produce two optimal conditions that produced well-diffracting E2-25K M172A protein crystals. The final optimal condition for the E2-25K M172A low pH condition was formulated by supplementing 50 μL reservoir solution of 0.1 M sodium cacodylate trihydrate pH 6.5, 0.2 M calcium acetate hydrate, 18% (w/v) polyethylene glycol 8,000 (Hampton Research) with 10 μL of stock buffer containing 500 mM NaCl, 500 mM sodium acetate pH 4.6 (measured), and 10 mM EDTA. The final optimal condition for the E2-25K M172A high pH condition was formulated by supplementing 50 μL reservoir solution of 0.1 M HEPES sodium pH 7.5, 0.2 M calcium chloride dihydrate, 28% PEG 400 (Hampton Research) with 10 μL of stock buffer containing 500 mM NaCl, 500 mM bicine pH 9.0 (measured), and 10 mM EDTA. E2-25K M172A crystals were first observed after one week for the low pH condition (Figure 3.2) and after one month for the high pH condition. The initial conditions that produced the low pH crystals after optimization were similar to those reported for the wild-type E2-25K crystals (PDB code 1yla).

Figure 3.2 E2-25K M172A Crystal for Low pH Condition. [Crystal that produced 1.9 Å structure PDB code 3e46]

3.3 E2-25K M172A Data Collection and Structure Determination

E2-25K M172A protein crystals suitable for X-ray analysis as described in Section 2.4.1 were soaked in a cryogenic solution consisting of the reservoir solution and 28% (v/v) glycerol prior to mounting in an appropriately sized nylon loop (Figure 3.2). Data collection was performed at Southeast Regional Collaborative Access Team beam line ID22 (Argonne National Lab, Chicago, IL). The crystals diffracted to 1.9 Å (low pH condition) and 2.2 Å (high pH condition). A 125-frame data set was collected for the low pH crystal form and a 75-frame data set was collected for the high pH crystal form, using 0.97Å and 1.0 Å X-ray radiation, respectively, with 1º oscillation and 1 second per frame exposure time. X-ray diffraction was recorded with a MAR300 CCD (charge coupled device) detector. The data was processed with the DENZO and SCALEPACK program packages from within HKL2000 [95]. The data collection statistics are recorded in Table 3.1. Both crystal forms indexed and scaled as I-centered tetragonal with unit cell dimensions of a=b=134.5 Å, c=38.4 Å, for the low pH condition and a=b=134.8 Å, c=38.2 Å, for the high pH condition. The asymmetric units contain one molecule, and the crystals have a Matthew's coefficient of 3.1 corresponding to a solvent content of 60 percent.

The structure of each crystal form was solved by the molecular replacement method using the program MOLREP [96] from the CCP4 program suite (Collaborative Computational Project, Number 4, 1994): Wild-type E2-25K (PDB code 1yla) [93] was used as the search model for the low pH crystal structure. Subsequently the low pH structure (PDB code 3e46) [62] was used as the search model for the high pH data set (PDB code 3f92) [97]. Refinement was carried out using the program REFMAC5 [98].

The structure was visualized and modified with the program COOT [99]. Modifications were made to the protein molecule by manually fitting the calculated model against 2 $|F_o|$ - $|F_c|$ and $|F_o|$ - $|F_c|$ electron density maps using cut-offs of 1.0σ and 3.5σ, respectively, followed by subsequent iterative cycles of restrained refinement. An initial set of solvent atoms was added to each structure using ARP/wARP [100]. Additional water molecules and ligands were added to the model manually after each round of fitting and refinement. Figure 3.3 is a representation of the $2|F_o|$ - $|F_c|$ electron density map showing a close-up view of the Ca^{2+} ion-coordination geometry that represents a crystal contact between symmetry-related molecules that is present in both crystallization conditions. The low pH structure contained 207 water molecules and one ligand (Ca^{2+}), and refined with final R_{work} and R_{free} factors of 17.4 and 21.0 %, respectively. The high pH structure contained 89 water molecules, one Ca^{2+}, two PEG 400 molecules, one TRIS molecule, and one BME molecule. The high pH structure refined with final R_{work} and R_{free} factors of 17.4 and 21.3 %, respectively. The refinement statistics are summarized in Table 3.1.

The low pH final structure contained one ligand (Ca^{2+}) and the high pH final structure one Ca^{2+}, two PEG 400 molecules, one TRIS molecule, and one BME molecule. The calcium ion in both crystal structures forms crystal contacts by coordinating Asp-0 with Glu-20 and Glu-99 of symmetry-related molecules (Figure 3.3). In order to identify the ligand type, the calcium ion was initially modeled as a water molecule. However, the temperature factor of the water was calculated to be 8.2, which was significantly lower than either temperature factors of the surrounding water molecules or the surrounding protein atoms. Positive density was observed in the $|F_o|$ - $|F_c|$ electron density map suggesting that the oxygen could not account for the observed density. The possibility of

a sodium ion was also ruled out based upon the same criteria. The coordination shell surrounding the atom contains six oxygen atoms with distances of less than 2.5 Å and angles characteristic of an octahedrally-coordinated calcium ion. Furthermore, the crystallization of the protein was later shown to be dependent upon the presence of calcium and the optimized condition contained a final concentration of 0.1 M calcium chloride. The two PEG 400 molecules, TRIS, and the BME in the high pH final structure were identified based on best fit of the density using molecules known to be present in the crystallization solvent.

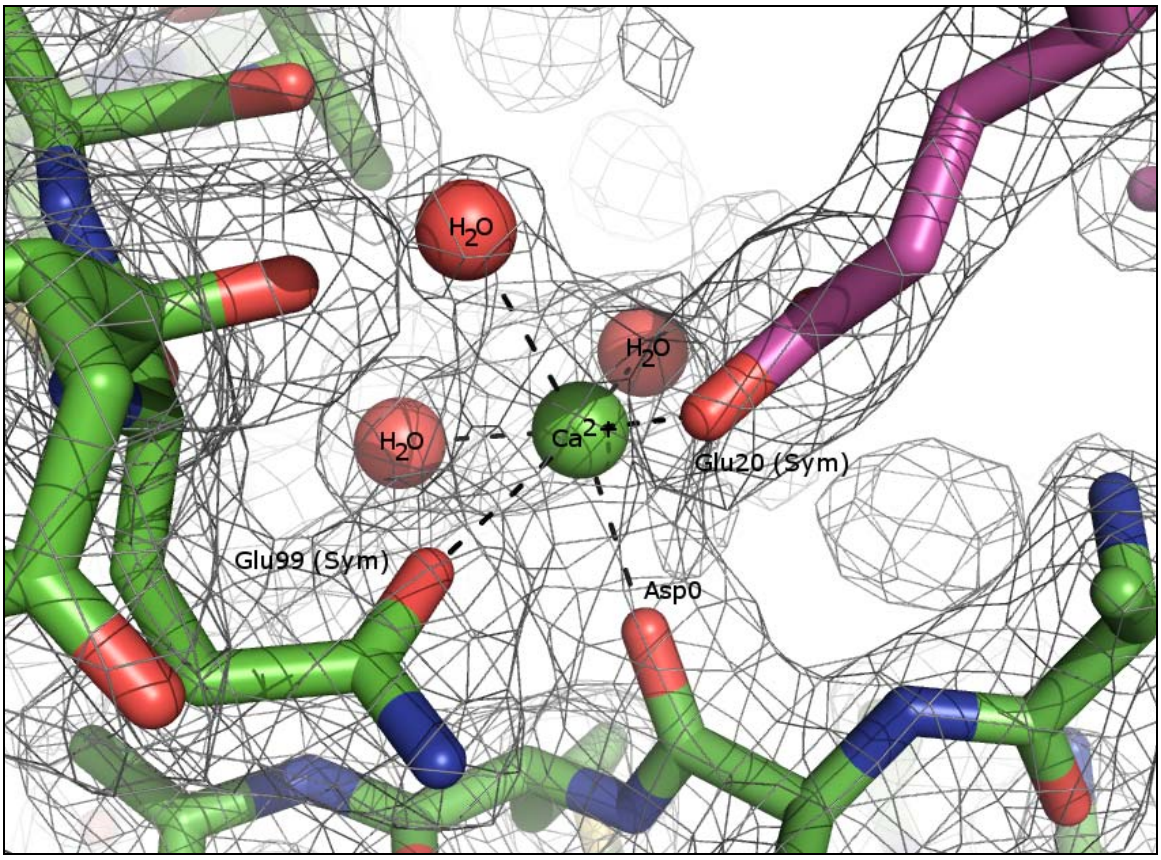

Figure 3.3 Close-up View of the Ca^{2+} Ion-coordination Geometry of E2-25K M172A.

Table 3.1 Data-collection and refinement statistics for E2-25K M172A mutant structures.

Data collection (SERCAT ID22)	Low pH crystal (PDB code 3e46)	High pH crystal (PDB code 3f92)
Wavelength (Å)	1.0	0.97
Space group	I_4	I_4
Molecules per AU	1	1
Unit-cell parameters (Å, º)	a =b =134.5	a =b= 134.8
	c=38.4	c=38.2
	α=β=γ=90	α=β=γ=90
Resolution (Å)	50.0-1.86 (1.91-1.86)	50.0-2.23 (2.31-2.23)
R_{symm}[a] % (outer shell)	8.1 (37.4)	6.9 (37.7)
$<I/\sigma_I>$ (outer shell)	19.65 (1.98)	11.95 (2.39)
Completeness (%)	93.4 (52.4)	98.2 (88.8)
No. of reflections (unique)	109109 (27414)	48847 (16794)
Redundancy (outer shell)	4.0 (1.4)	2.9 (1.9)
Number of Frames	125	75
Matthews Coefficient	3.1	3.1
Refinement		
Resolution (Å)	32.38-1.86	42.64-2.23
No. of reflections	27404	15939
R_{work}[b]/R_{free}[c] (%)	17.4/21.0	17.4/21.3
No. of atoms/molecules		
Protein	1597	1599
Non H_2O molecules	1	5
Water molecules	207	89
R.m.s.d. bonds (Å)	0.018	0.024
R.m.s.d. angles (º)	1.5	1.85
Ramachandran plot		
Most favoured region (%)	99.0	99.0
Additional allowed region (%)	1.0	1.0

[a] $R_{symm} = \sum_{hkl}\sum_i \left| I_i(hkl) - \langle I(hkl)\rangle \right| / \sum_{hkl}\sum_i I_i(hkl)$, where $I_i(hkl)$ is the observed intensity of reflection *i* and $\langle I(hkl)\rangle$ is the average intensity of multiple observations.

[b] R_{work} and [c] $R_{free} = \sum_{hkl} \left| |F_{obs}| - k|F_{calc}| \right| / \sum_{hkl} |F_{obs}|$, where R_{free} was calculated using 5% of the total reflections chosen at random and not used in the refinement.

3.4 Structure of the E2-25K Mutant Protein

The E2-25K M172A structure consists of a conserved 150 amino acid N-terminal UBC domain and a 50 amino acid C-terminal UBA domain (Figure 1.5). Superposition of the M172A mutant structures and the wild-type enzyme structures resulted in an overall Cα r.m.s.d. of 0.34 Å. The UBC domain is comprised of an N-terminal α-helix followed by four anti-parallel β-strands, then by an additional three α-helixes. Additionally, the C-terminal UBA domain is made up of a three-helix bundle.

A Ramachandran plot calculated using MolProbity [101] shows 99.0% (198/200) of the residues in most favoured regions and the remaining residues in additionally allowed regions. The two residues that fall outside the most favoured regions are Lys-97 and Ala-119. Ala-119 is located at the end of helix 3, N-terminal to a flexible 8-amino acid loop. Lys-97 is located at the end of helix 2, C-terminal to the catalytic cysteine (Cys-92). In Ubc1, the E2-25K homolog in *Saccharomyces cerevisiae*, mutation of this lysine to arginine eliminated Lys-48 linked poly-Ub chain synthesis [102]. Comparing both M172A structures with the wild-type structure reveals that most side chains in the active site are conformationally similar (Figure 3.4). The exception is the sidechain of Lys-97, which exhibits multiple rotamer conformations as a function of differing crystallization conditions.

The UBA domain is stabilized primarily by hydrophobic residues in the core of the domain. These residues include Leu-169, Val-179, Leu-183, Val-190, and Leu-197. The relative positioning of the helices of the UBA domain of E2-25K is determined by ring stacking between the sidechains of residues Tyr-162 in helix 6 and Trp-188 in the loop between helices 7 and 8. The UBC/UBA domain-domain interface consists of

hydrophobic interactions between residues Met-140, Leu-147, and Val-151 (helix 5) of the UBC domain and residues Ile-166 (helix 6) and Ile-180 (helix 7) of the UBA domain. Additionally, three hydrogen bonds exist between the side-chains of Thr-144 and Trp-188, Trp-148 and Ser-184, and Tyr-152 and Asn-177 (Figure 3.5).

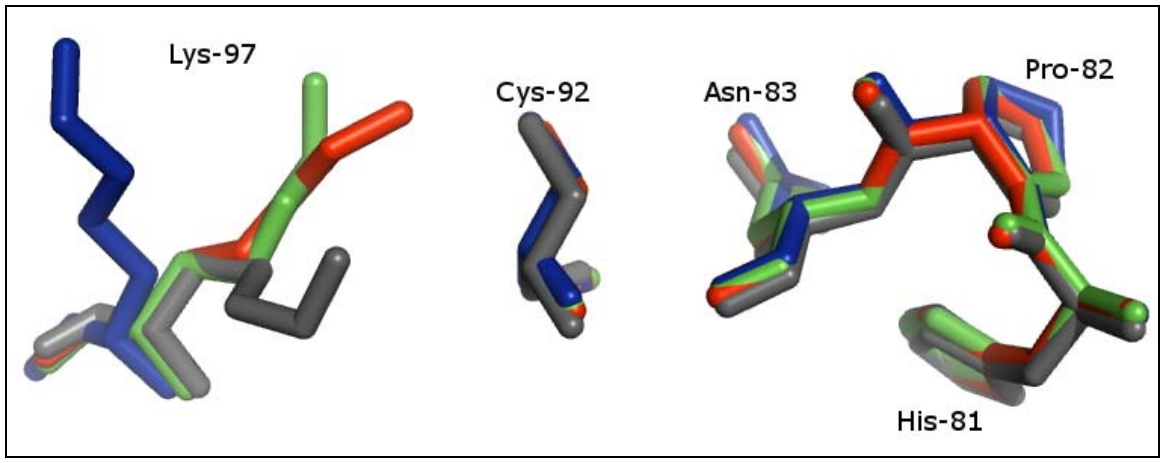

Figure 3.4 E2-25K Active-site superposition. [The M172A mutant protein structures superimposed with wild-type E2-25K and catalytic domain structures -- Red - 3E46 (M172A at pH 6.5), Green - 3F92 (M172A at pH 8.5), Grey - 1YLA (wt at pH 6.5), Blue - 2BEP (UBC domain at pH 8.5).]

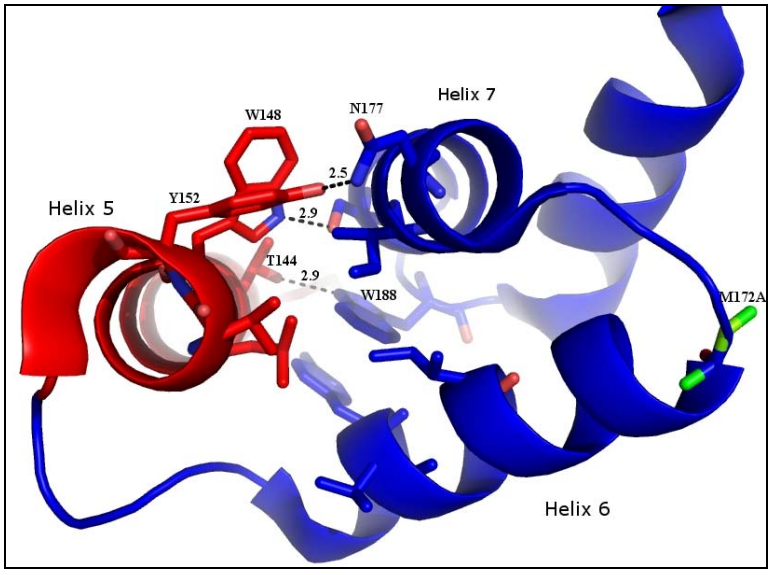

Figure 3.5 UBC/UBA Domain-Domain Interactions. [UBC/UBA crystal structure domain interactions between helix 5 (red) of the UBC domain and helix 6 and 7 (blue) of the UBA domain. Three hydrogen bonds between the two domains are shown with dashed lines and bond length in Ångstroms. M172A mutation site shown in green.]

Met-172 is located in the loop between helices 6 and 7 of the UBA domain and forms part of the primary contact surface with ubiquitin [103]. The M172A mutant, when compared to the wild-type structure, has a slight rotation (~ 10°) of the UBA domain relative to the UBC domain with the axis of rotation along helix 7. However, this rotation did not impose structural changes on either the domain or the ubiquitin binding surface. Furthermore, the M172A mutation did not significantly alter the primary contacts between the UBC and UBA domain but did slightly decrease the length of the 3 inter-domain hydrogen bonds (from 3.0, 3.0, and 2.6 Å in the wild-type to 2.9, 2.9, and 2.5 Å in M172A).

3.5 Conclusions

Two crystal structures of the ubiquitin conjugating enzyme E2-25K M172A have been reported and published [78]. The high pH (PDB code 3F92) and the low pH (PDB code 3E36) structures have been solved to 1.9 Å and 2.2 Å, respectively, and subsequently compared to the wild-type structure (PDB code 1YLA). It was shown that the E2-25K M172A mutant is structural homologous to the wild-type enzyme, demonstrating that the mutation does not disrupt the overall fold of the protein. The interactions between the UBC and UBA domains have been discussed and shown not to be significantly altered by the M172A mutation. These observations will be crucial in further exploration of the effects of the mutation on the catalytic activity of the enzyme. It was also shown that the active site of E2-25K M172A mutant compares extremely well with the wild type with only notable differences seen in Lys-97. Based on these observations, a further examination of the functional role of Lys-97 in E2-25K could be helpful in understanding the catalytic mechanism of E2-25K.

CHAPTER 4

PHYSICAL CHARACTERIZATIONS OF E2-25K

In order to gain a better understanding of the ubiquitin conjugating enzyme E2-25K a series of biophysical studies were conducted on the wild-type protein, the domains that constitute it, and strategic mutants. One of the research objectives was to determine the role, if any, the unique UBA domain plays in the structural stability of E2-25K. This objective was achieved by performing thermal denaturation experiments using circular dichroism and differential scanning calorimetry. Fluorescence ANS binding studies along with size-exclusion chromatography of E2-25K bound and unbound to Ub were used to determine the oligomerization state of E2-25K. These results will be used to elucidate the potential for dimerization of E2-25K in polyubiquitin chain formation, as required by other E2 proteins.

4.1 Circular Dichroism

To determine the relative secondary structure and the melting temperature of full-length E2-25K, UBC and UBA domains circular dichroism (CD) analysis was performed. The protein was purified as described in Section 2.4 and was diluted with sterile dH_2O to a concentration of 0.02 mg/mL. CD measurements were performed on an OLIS rapid scanning monochromator in a 1 mm path length quartz cylindrical cell cuvette over a range of wavelengths from 190 to 260 nm. Temperature studies were performed in 5 °C

increments from 5 °C to 85 °C using a 10 mm cylindrical cell cuvette. Raw CD data (difference in absorbance for left- and right-circularly polarized light) was converted to molar circular dichroism [$\varepsilon_L - \varepsilon_R$] using equation 4.1, with path length (l) equal to 1 cm and C equal to the molar concentration of protein molecules for each sample. Results of these calculations are presented in the figures to follow.

$$\varepsilon_L - \varepsilon_R = \frac{\Delta A}{Cl} \tag{4.1}$$

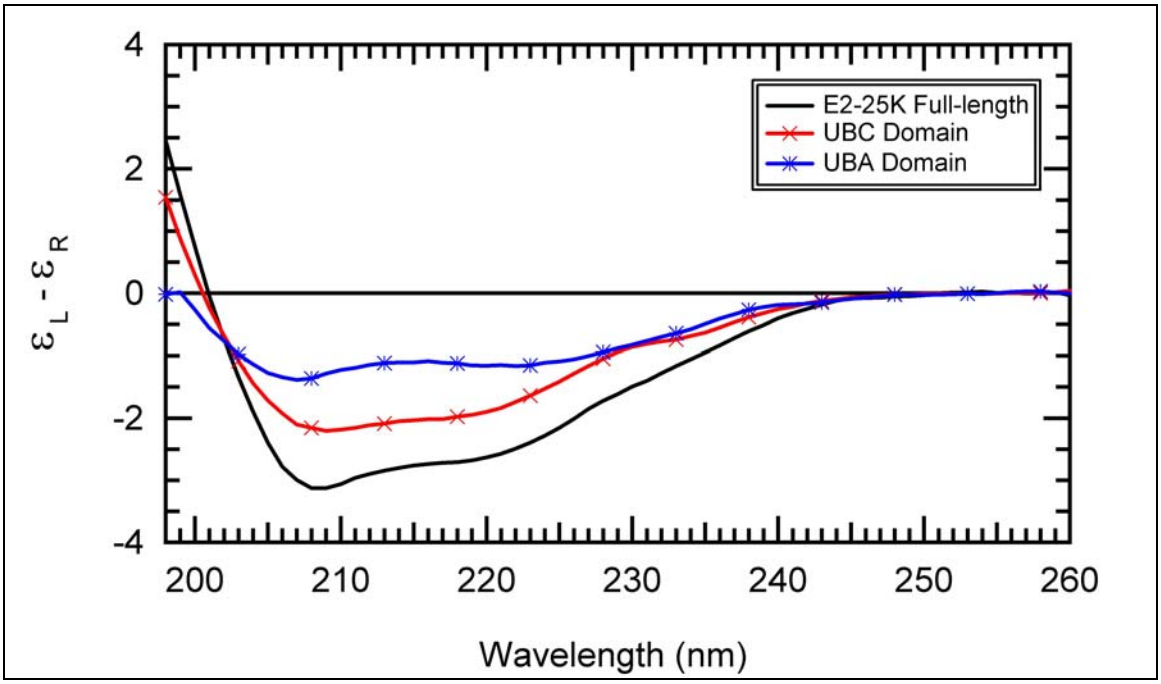

Figure 4.1 Overlay of CD Spectra of Full-length E2-25K, UBC and UBA Domains.

The overlayed CD spectra (Figure 4.1) for the full-length E2-25K, UBC and UBA domains confirmed that all constructs were independently folded. The CD spectrum for the full-length E2-25K and the UBC domain construct revealed a combination of beta sheet and alpha helix, whereas the UBA domain spectrum demonstrated only alpha

helical tendencies (Figure 4.1). Two E2-25K mutants, M172A and L198A, were also analyzed and compared with the wild-type E2-25K and the UBC domain (Figure 4.2). The comparison of the mutant proteins was made to the wild-type with and without the fifty amino acid expression tag. These comparisons were made to confirm that the overall fold of the protein is not altered by the presence of the expression tag. This can be seen by the similarities in the shape of the curves shown in Figure 4.2.

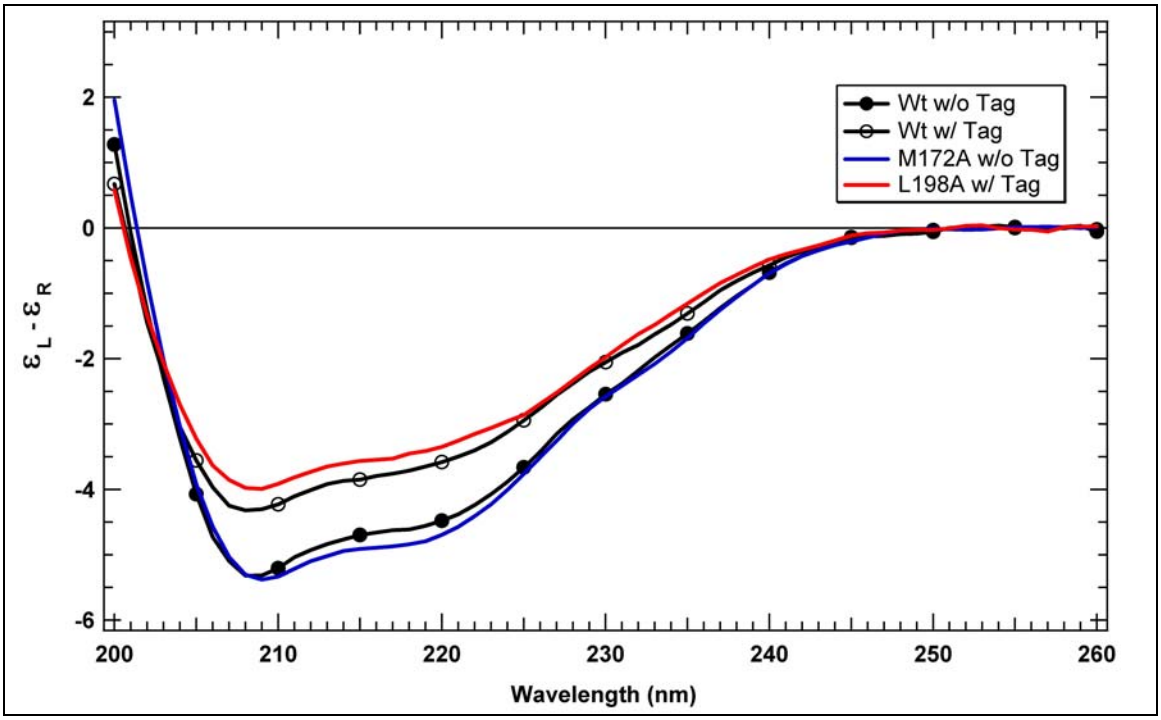

Figure 4.2 Overlay CD Spectra of Wild-type E2-25K, E2-25K L198A and E2-25K M172A.

Two E2-25K UBA domain mutants, M172A and L198A, were also tested and compared with the wild-type E2-25K UBA domain (Figure 4.3). The comparison revealed that the mutant proteins do not have the same fold as the wild-type UBA domain, unlike the same mutants of the full-length E2-25K (Figure 4.2). This overall change in conformation was later confirmed by NMR spectroscopy (discussed in a later chapter).

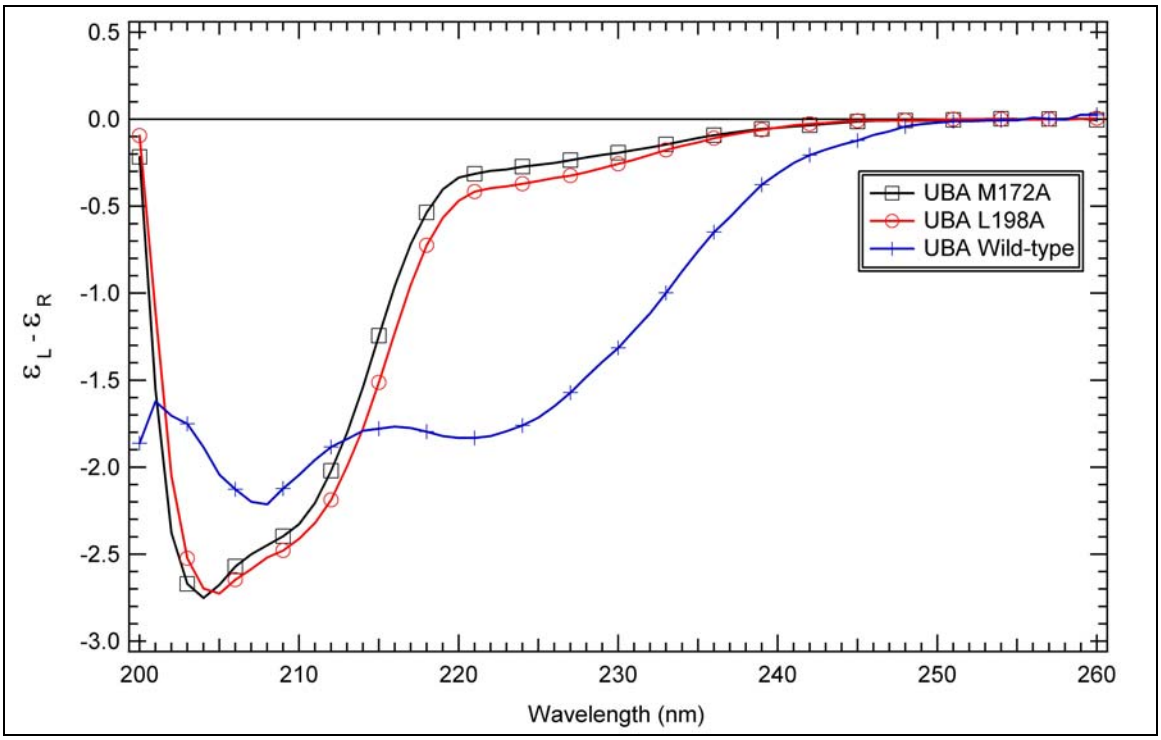

Figure 4.3 Overlay CD Spectra of E2-25K UBA Domain, UBA L198A, and UBA M172A.

4.1.1 Thermal Denaturation Studies by CD

A thermal denaturation assay was also explored for both the full-length E2-25K and the UBC domain. As can be seen in the figures to follow, the results are well defined. The CD data was fitted with a simple two-state folded to unfolded model with accurate determination of the melting temperature (T_m) aided by the appearance of sigmoidicity in the UBC domain melting curve, as monitored at a wavelength of 216 nm. The overlay of the UBC domain CD spectra from 5 °C to 80 °C, in 5 °C increments is shown in Figure 4.4 and the melting curve at 216 nm (Figure 4.5) indicated a T_m for the UBC domain of ~ 47 °C.

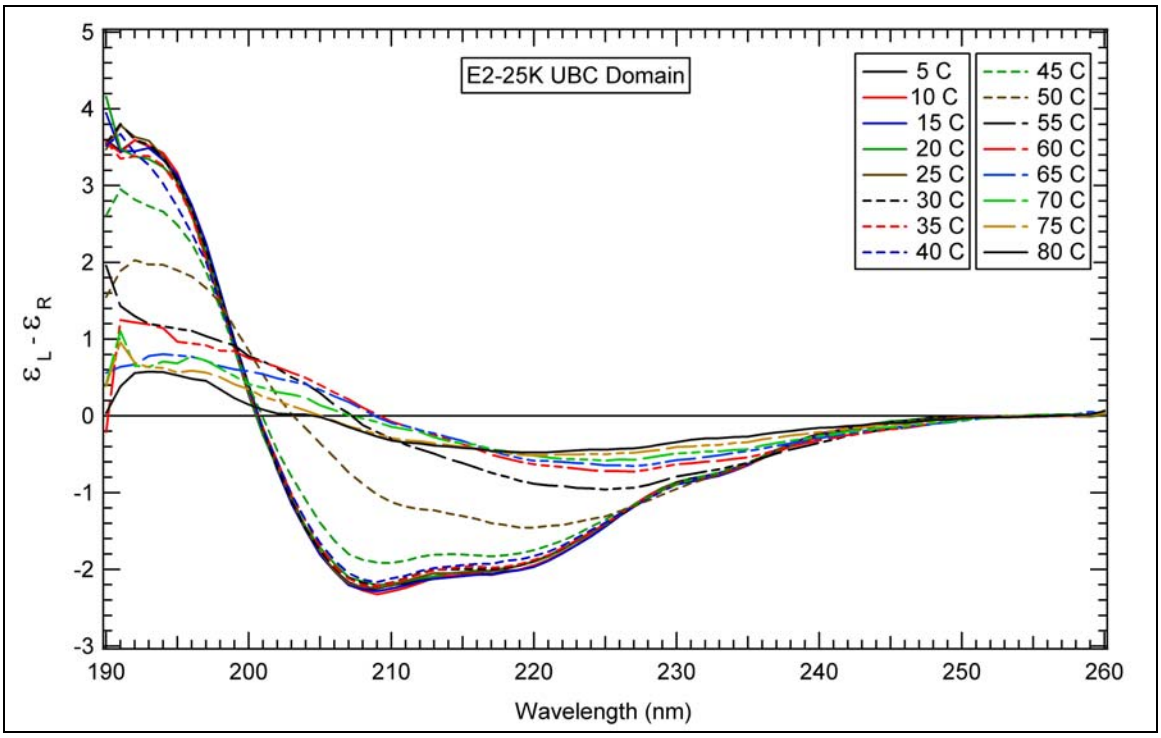

Figure 4.4 Thermal Denaturation of E2-25K UBC Domain. [The CD spectra of E2-25K UBC domain over a range of temperature from 5 °C - 80 °C.]

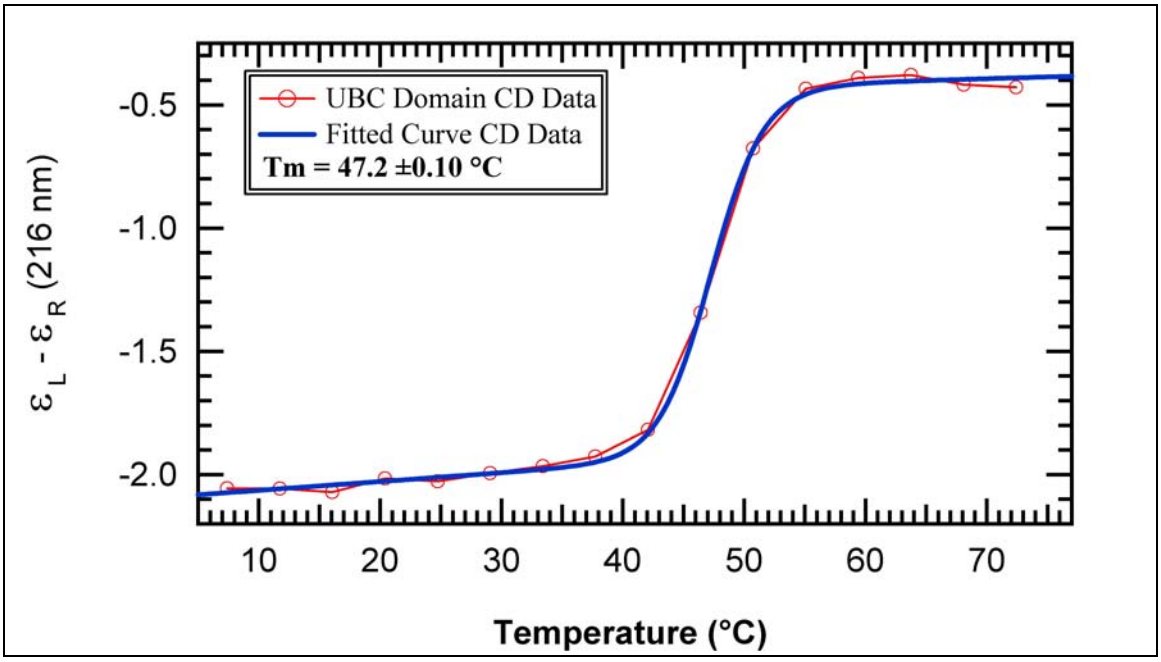

Figure 4.5 E2-25K UBC Domain Melting Curve. [The CD of E2-25K UBC domain over a range of temperature from 5 °C - 80 °C extracted at 216 nm shows a melting temperature of 47°C. The data was fitted with a simple two-state folded to unfolded model and the van't Hoff ΔH of the fit was 95.1 ± 4.1 kJ/mol]

The overlay of full-length E2-25K M172A CD spectra from 20 °C to 85 °C, in 5 °C increments is shown in Figure 4.6. The CD data was also fitted with a simple two-state folded to unfolded model with accurate determination of the melting temperature for the full-length E2-25K aided by the appearance of sigmoidicity in the E2-25K M172A melting curve (Figure 4.7), as monitored at a wavelength of 210 nm. These thermal denaturation studies of E2-25K M172A demonstrate that E2-25K is stable up to a temperature of 60.3 °C (Figure 4.7). Whereas, the thermal denaturation studies of the UBC domain (Figure 4.5) revealed a melting temperature (T_m) of only 47.3 °C. This indicates that the presence of the UBA domain is contributing to thermal stability of the full-length protein.

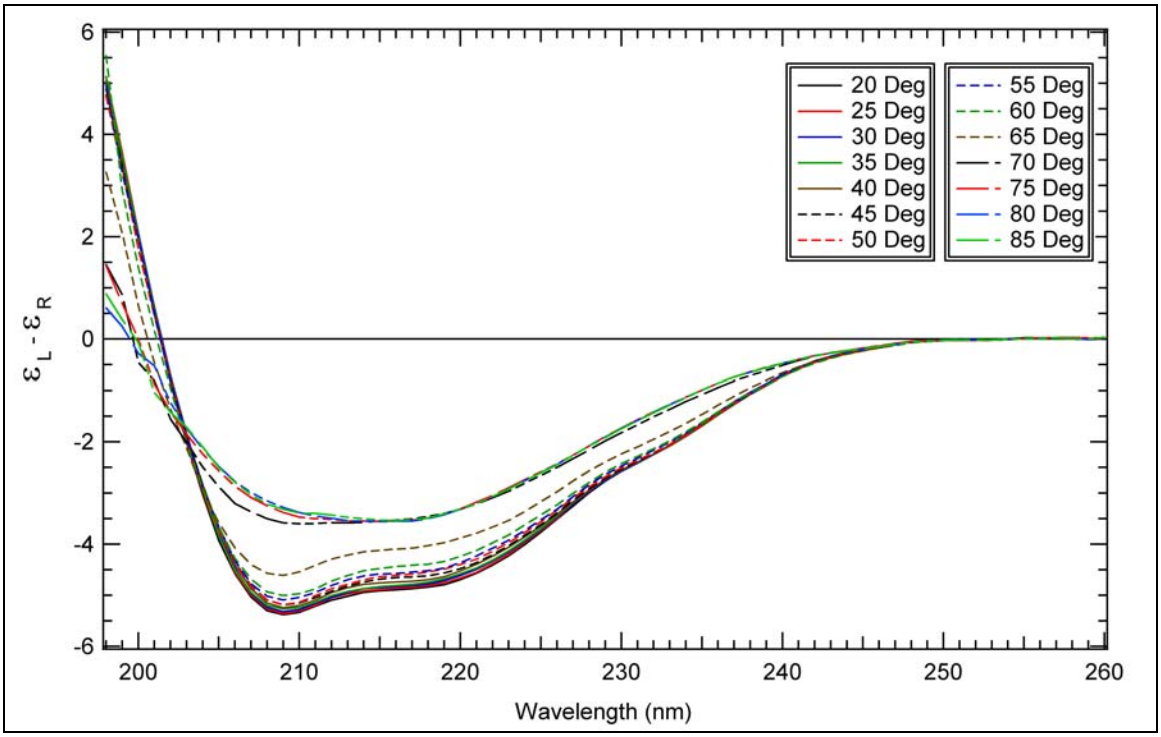

Figure 4.6 Thermal Denaturation of E2-25K M172A. [The CD spectra of E2-25K M172A over a range of temperature from 20 °C – 85 °C.]

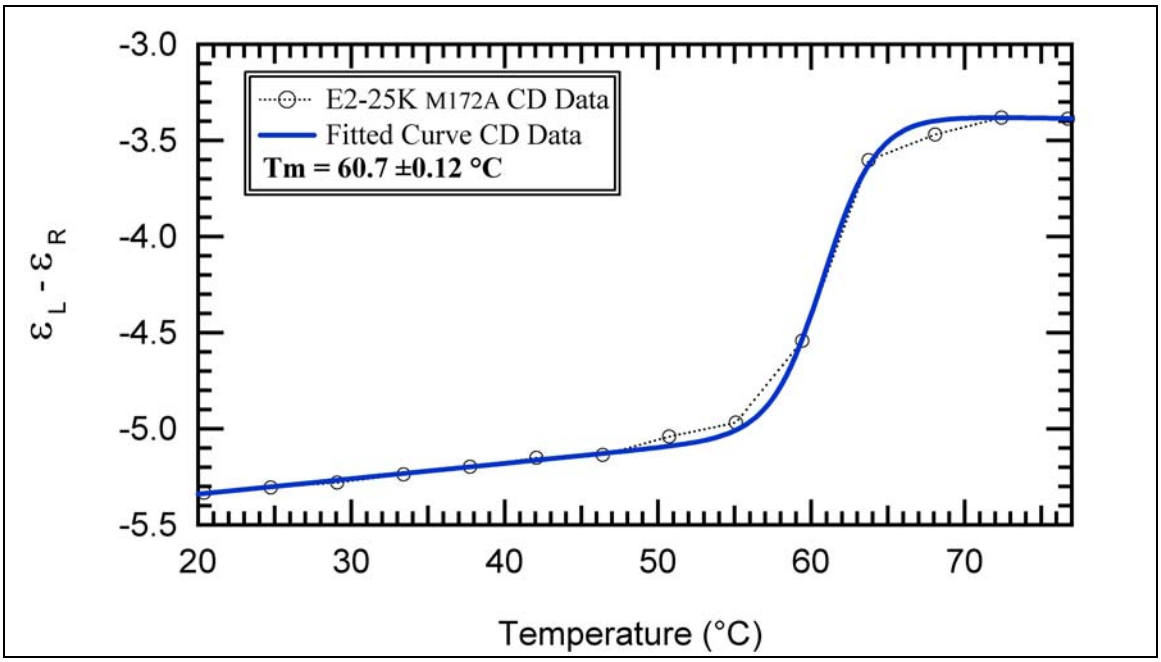

Figure 4.7 E2-25K M172A Melting Curve. [The CD of E2-25K M172A over a range of temperature from 20 °C – 85 °C extracted at 210 nm shows a melting temperature of 60 °C. The data was fitted with a simple two-state folded to unfolded model and the van't Hoff ΔH of the fit was 128.1 ± 7.3 kJ/mol]

4.2 Differential Scanning Calorimetry

Differential scanning calorimetry (DSC) was used as a second technique to confirm the melting temperature of E2-25K. DSC analyses were performed on a MicroCal (Northampton, MA) Extended Range VP-DSC with a cell volume of 1.0 mL. Purified protein as described in Section 2.4 was diluted in chain assay buffer to a concentration of 1.23 mg/mL. Baseline buffer scans were subtracted from the sample data and converted to molar heat capacity per protein monomer by using Wavemetrics IGOR Pro and in house scripts, by Dr. Steve Edmondson, as shown in Figure 4.8. The melting temperature for wild-type E2-25K by DSC was shown to be 334K or 60.9 °C, which is in excellent agreement with CD thermal denaturation data (Figure 4.7).

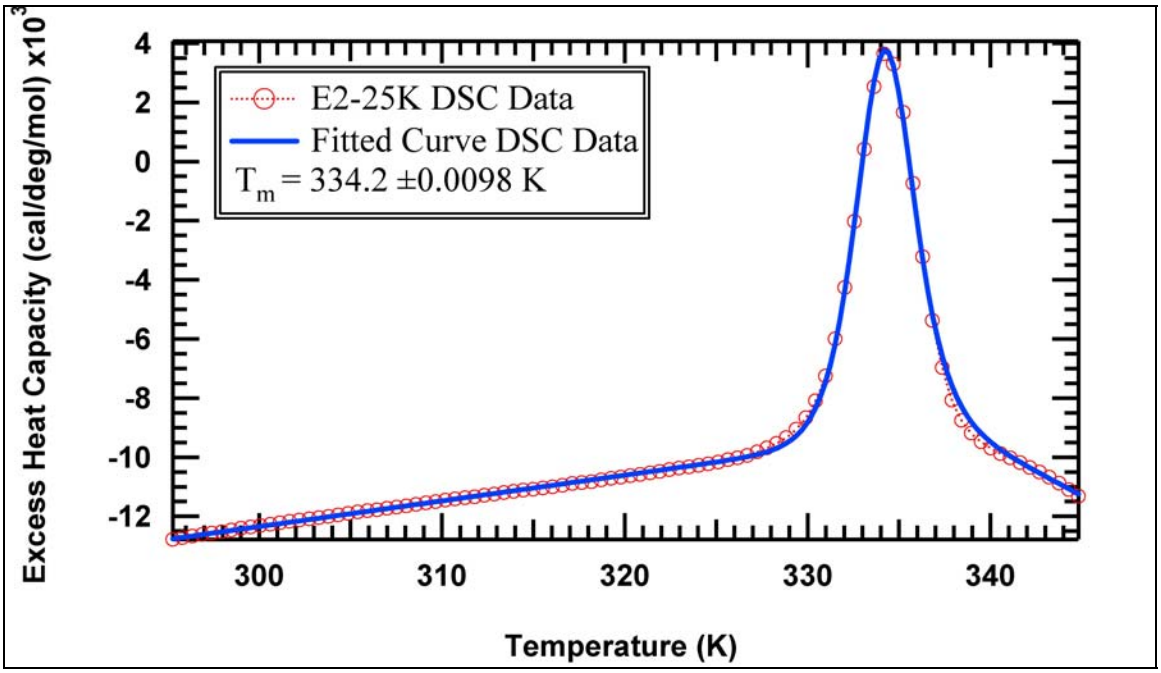

Figure 4.8 DSC of Wild-type E2-25K at pH 8.0. [The DSC of wild-type E2-25K shows a melting temperature of 334K or 60.9 °C which is in excellent agreement with CD data for E2-25K M172A. The van't Hoff ΔH of the fit was 211.5 ± 1.4 kJ/mol]

4.3 Fluorescence ANS Binding Assay

1-anilino naphthalene-8-sulfonic acid (ANS) is often used to identify the molten globule state of proteins because its protein interaction occurs primarily at a solvent exposed hydrophobic region of the protein. Upon binding of ANS to a protein, an observed blue shift of fluorescence emission maxima and an increase of fluorescence intensity are generally attributed to the hydrophobicity of a binding site and the restricted mobility of ANS [104]. Samples of E2-25K C92S were prepared with 100:1 molar ratio of ANS to protein and emission spectra for ANS were collected as described in Section 2.7. The E2-25K construct with and without the presence of the expression tag both presented an increase in fluorescence with the ANS and a minor blue shift, which suggests hydrophobic sections are exposed for ANS binding. However, as can be seen from Figure 4.9 a considerable increase in fluorescence intensity is seen for the construct

with the expression tag intact. These data suggest that the expression tag has secondary structure unlike previously suggested by the crystal structure data because there would be no change in fluorescence intensity if the expression tag was unordered and ANS was unable to bind. The results shown in Figure 4.9 are a buffer-only sample compared to a similar ANS ratios as the E2-25K protein with and without the expression tag.

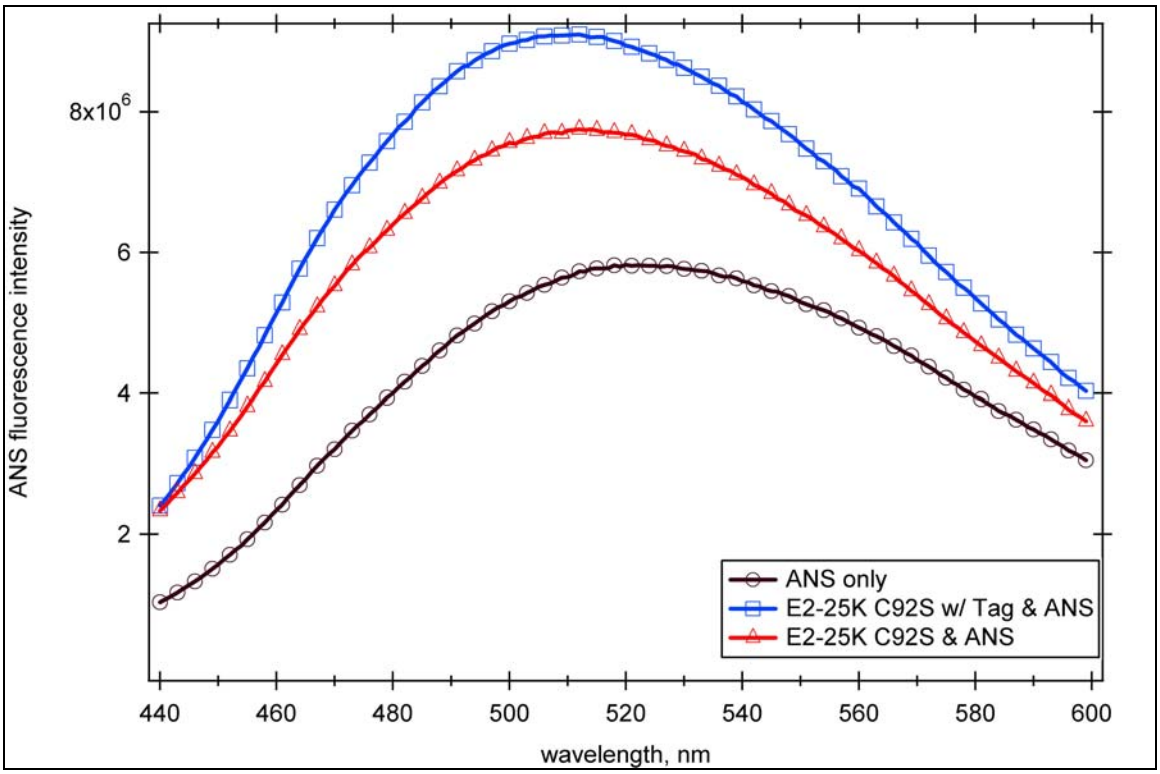

Figure 4.9 ANS Fluorescence Spectra of E2-25K C92S.

4.4 Oligomerization of E2-25K in the Presence of Ubiquitin

It was previously determined that full-length E2-25K does not dimerize in solution in the absence of binding partners or covalent modifications [103]. Other members of the E2 ubiquitin-conjugating enzyme family are known to dimerize as a consequence of interactions through E3 ligase partners [82] or the presence of a Ub covalently bound to the active-site cysteine [105]. Therefore, it was important to

investigate the effects of multiple conditions on the dimerization of E2-25K. The labile nature of the thioester bond between Ub and the catalytic cysteine side-chain of E2-25K makes it difficult to isolate the covalent complex. Therefore, in order to examine the oligomerization state of E2-25K a C92S mutant was generated as described in Section 2.2. This amino acid mutation choice was based on work by Eddins *et al.* [40], which demonstrated that mutation from cysteine to serine functions in a similar manner for conjugation of Ub and the resulting ester intermediate is more stabile and approximates the native covalent linkage. The complex assays used to determine the oligomerization of E2-25K in the presence of Ub contained a 2:1 molar ratio of Ub-K48C to E2-25K C92S. The complex assays also contained a 4 mM Mg-ATP solution, 0.2 μM E1 activating enzyme (BostonBiochem), 10 mM phosphocreatine, 0.6 unit/ml of inorganic phosphokinase and creatine phosphokinase, 10 mM phosphocreatine and 0.5 mM beta mercaptoethanol. Complex assays were mixed with either Ub-K48C or both Ub-K48C and Ub-D77 then incubated at 37 °C for 3 to 4 hours before being analyzed by SDS-PAGE gel (Figure 4.10).

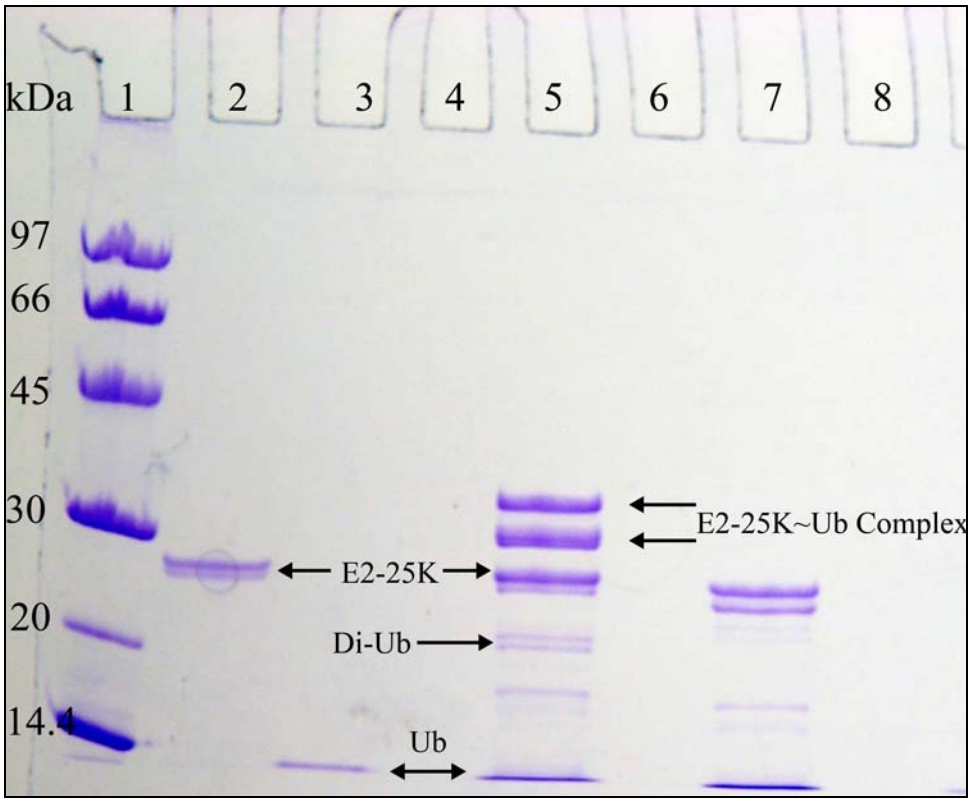

Figure 4.10 E2-25K – Ubiquitin Complex Assay SDS PAGE Gel. [SDS page of E2-25K C92S – Ub Complex Assays. Lane 1 – LMW Marker, Lane 2 – E2-25K C92S, Lane 3 – Ub-K48C, Lane 4 – Empty, Lane 5 – E2-25K C92S – Ub-K48C complex assay, Lane 6 – Empty, Lane 7 – E2-25K C92S – Ub-K48C & Ub-D77 mixture, Lane 8 – Empty, Lanes 9-10 – OPTN 550 experiment.]

The complex assays were then injected onto a HiPrep 16/60 Sephacryl S-300 column (GE Biosciences) and chromatographed via FPLC in 20 mM Tris-HCl, pH 8.0, 150 mM NaCl buffer. The chromatographic overlay of the complex samples with gel filtration standards is shown in Figure 4.11. Only two peaks are present for either the complex assay or the mixture of E2-25K and Ub. However, the complex assay containing only E2-25K and Ub-K48C has a much broader peak that is consistent with the SDS gel (Figure 4.10, Lane 5) that multiple size proteins are present between 25 and 40 kDa. Based on these results, it can be concluded that E2-25K exists as a monomer in complex with Ub because only two peaks are present and both occur at the appropriate sizes.

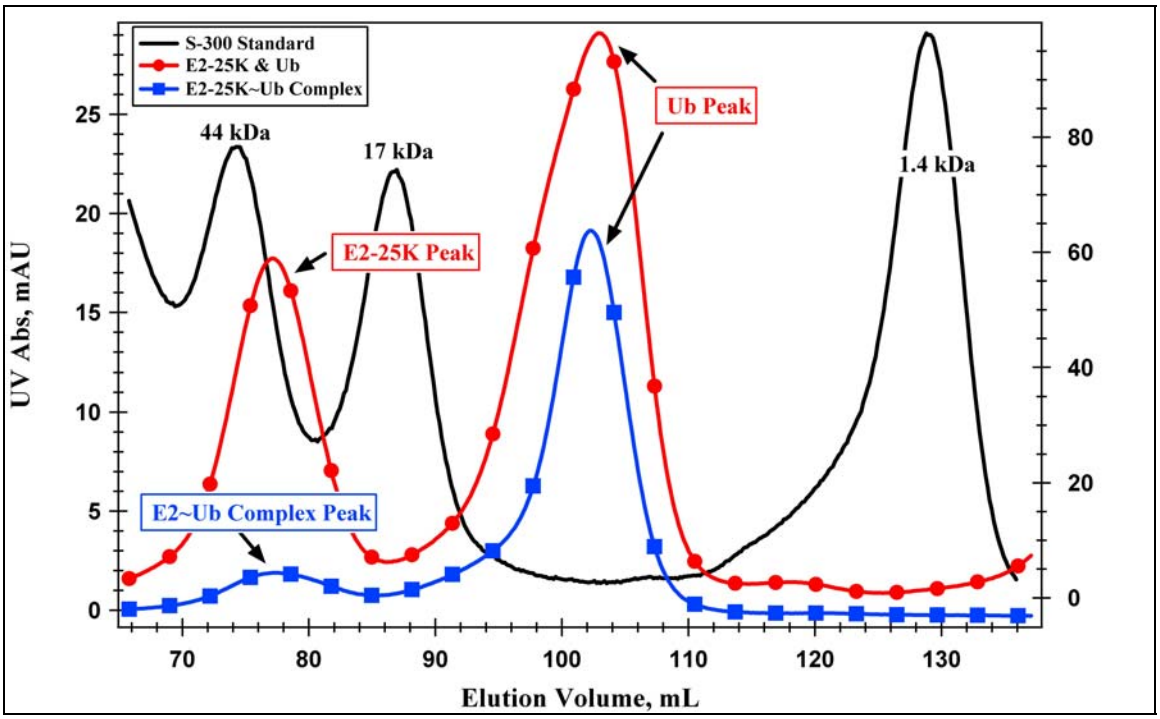

Figure 4.11 Gel Filtration Chromatograph of E2-25K – Ub Complex Assays. [S-300 gel filtration column of E2-25K C92S & Ub-K48C mixture (shown in red), E2-25K C92S ~ Ub-K48C complex (shown in blue) overlaid with standard (shown in black).]

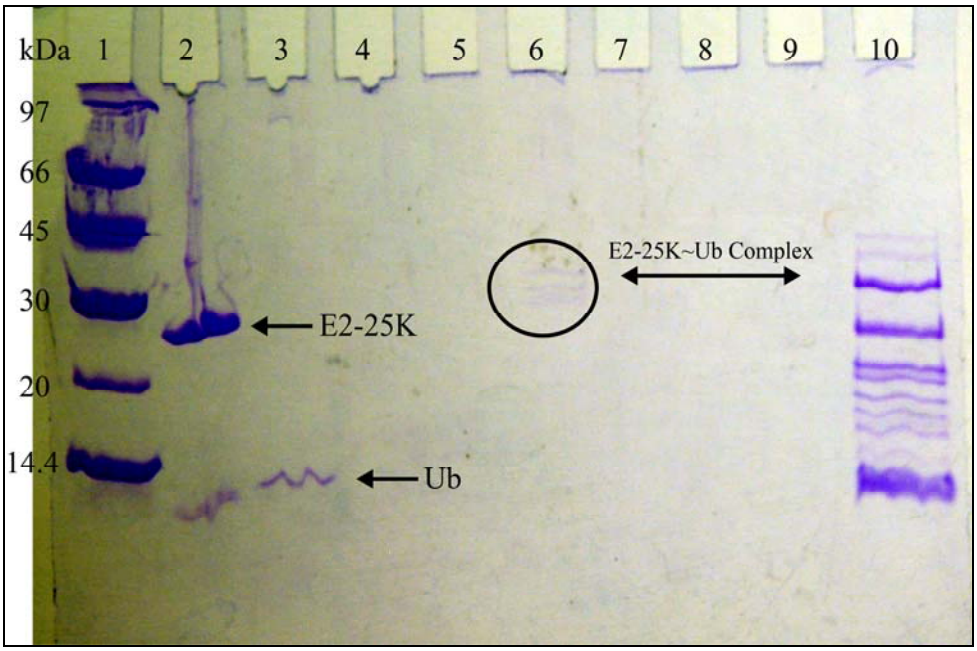

Figure 4.12 E2-25K – Ubiquitin Complex Gel Filtration SDS PAGE Analysis. [SDS page of E2-25K C92S – Ub Complex Gel Filtration. Lane 1 – LMW Marker, Lane 2 – E2-25K C92S, Lane 3 – Ub-K48C, Lane 4 – Fraction 21, Lane 5 – Fraction 24, Lane 6 – Fraction 27, Lane 7 – Fraction 33, Lane 8 – Fraction 39, Lane 9 – Fraction 49, Lane 10 – Gel Filtration Load (E2-25K C92S – Ub-K48C complex assay).]

The size of the E2-25K~Ub complex sample from gel filtration was confirmed by SDS gel electrophoresis, Figure 4.12 and comparison to gel filtration molecular weight standards, Figure 4.13. Where the red solid line from Figure 4.11 is the E2-25K peak (Figure 4.10, lane 7) eluted at ~77 mL and red dash line is the E2-25K peak from previous reported work [103]. Blue solid line from Figure 4.11 is E2-25K~Ub complex peak (Figure 4.10, lane 5) confirmed by SDS gel electrophoresis (Figure 4.12, lane 6) eluted at ~78 mL. The conflict in size of the unbound E2-25K to the E2-25K~Ub complex in both electrophoresis and chromatography can be explained by decreased mobility of the unbound state. This decrease in mobility in is likely due to the elongated shape of the molecule, which is consistent with ANS binding studies that demonstrated E2-25K has exposure of the hydrophobic regions instead of tightly packed arrangement.

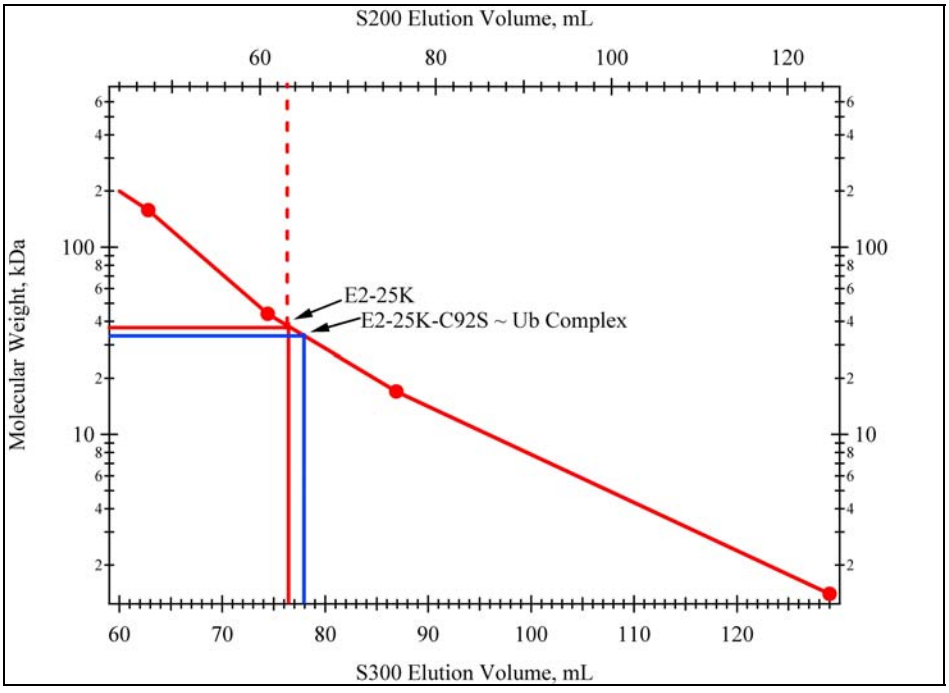

Figure 4.13 E2-25K ~ Ub Complex Size Determination from Gel Filtration Column. [S-300 & S-200 gel filtration column standards compared to the maximum of the E2-25K~Ub complex. Red solid line is E2-25K peak from Figure 4.11 eluted at ~77 mL and blue line is E2-25K~Ub complex peak from Figure 4.11 eluted at ~78 mL]

4.5 Conclusions

In order to gain a better understanding of the ubiquitin conjugating enzyme E2-25K, a series of biophysical studies was conducted on the wild-type protein, the UBC domain, the UBA domain, and two E2-25K mutants (M172A and L198A). These comparisons confirmed the overall fold of the protein is not altered by the presence of the mutants and the domains are independently folded. The thermal denaturation studies of E2-25K M172A demonstrate that E2-25K has a T_m of 60.7 °C. This is consistent with a melting temperature for wild-type E2-25K of 60.9 °C, determined by DSC. The thermal denaturation studies of the UBC domain revealed a T_m of only 47.2 °C, demonstrating that the UBA domain contributes to the thermal stability of the full-length protein.

In order to determine whether oligomerization of E2-25K occurs through the interaction between E2-25K and Ub a C92S mutant was generated and subsequently used to form a covalently linked ubiquitin to the active site cysteine. The E2-25K~Ub complex was compared with E2-25K by size exclusion chromatography. These results, under these conditions, indicate that E2-25K exists as a monomer in solution regardless of the presence of ubiquitin. Furthermore, it was shown that E2-25K likely exists in an elongated shape or open conformation that causes decreased mobility and exposure of the hydrophobic regions to ANS binding. These results imply that dimerization of E2-25K is not required in polyubiquitin chain formation, as required by other E2 proteins.

CHAPTER 5

BINDING STUDIES OF E2-25K AND UBIQUITIN

In order to gain a better understanding of the ubiquitin conjugating enzyme E2-25K a series of binding studies was conducted to study the interaction of Ub the wild-type protein, the UBC domain and UBA domain. One of the research objectives was to determine the E2-25K to ubiquitin binding constant and non-covalent binding surfaces. The binding was examined by fluorescence and Nuclear Magnetic Resonance (NMR) spectroscopy. Furthermore, examination of the X-ray crystallographic structure revealed interactions between the UBC and UBA domains [78]. These interactions were closely examined by NMR spectroscopy to determine structural significance.

5.1 Fluorescence Titration

The interaction of E2-25K UBA domain with Ub was studied by steady-state fluorescence of the sole tryptophan (Trp) residue in the UBA domain and in the respective complex with Ub. The Trp maximum emission wavelength was at 352 nm (Figure 5.1) for the free UBA Domain, which indicates a full exposure of the Trp indole ring to an aqueous environment. Upon binding to Ub, the maximum wavelength of the Trp shifted slightly to around 355 nm (Figure A.9), which suggested that the Trp side chain environment was relatively unchanged [85].

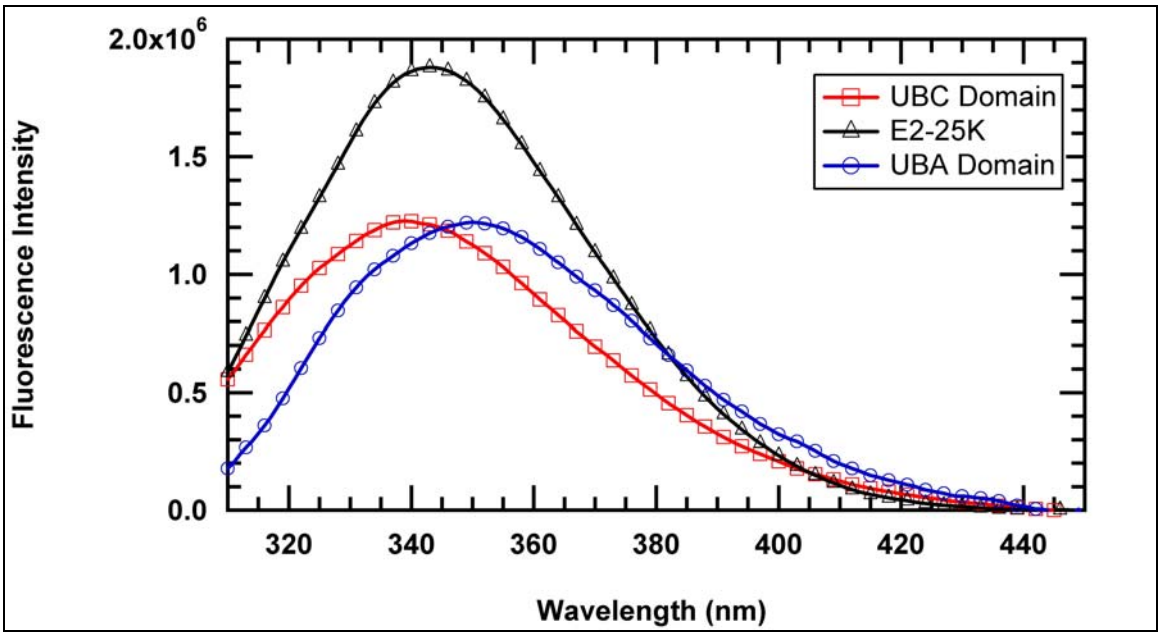

Figure 5.1 Overlay of Tryptophan Fluorescence Spectra of full-length E2-25K, UBC and UBA Domains. [The Trp maximum emission wavelength was 343 nm for full-length E2-25K, 339 nm for the UBC domain, and 352 nm for the UBA domain.]

The interaction of the full-length E2-25K and the UBC domain with Ub was also studied by steady-state fluorescence. The major difference from the UBA domain is the presence of two Trp residues in the UBC domain. The Trp maximum emission wavelength was at 343 nm for the full-length E2-25K and slightly blue shifted to 339 nm for the free UBC Domain (Figure 5.1). The blue shift in the maximums, as compared to the UBA domain, indicates only partial exposure of the additional Trp indole rings to the aqueous environment [85], which is consistent with structural data. Upon titration with Ub, the maximum emission wavelength of the full-length E2-25K and UBC domain did not change, which suggests that the Trp side chain environments were unchanged for E2-25K and no binding occurred for the UBC domain.

Fluorescence titrations experiments were performed as described in Section 2.6. Trp titration data were collected by adding 5 μL aliquots of 373 μM uncleaved Ub-K48C

or 10 μL aliquots of 410 μM cleaved Ub-K48C to a 2.5 mL sample of 0.5 μM E2-25K, UBC or UBA domain. The Trp emission intensities were corrected for sample dilution by using equation 5.1, where F_{obs} is the observed fluorescence value multiplied by the ratio of the initial sample concentration, c_o, and the current concentration, c_i.

$$F_i = F_{obs}\left(\frac{c_o}{c_i}\right) \tag{5.1}$$

In order to compare the E2-25K, UBC or UBA domain sample titration experiments to one another the corrected samples were normalized. Figures 5.2 and 5.3 show the comparisons of the E2-25K, UBC or UBA domain sample titration experiments with cleaved and uncleaved Ub. Uncleaved Ub has twenty additional tag affinity residues as a product of the cloning vector. The normalized values were calculated by using equation 5.2, where, the corrected normalized value is denoted by F_{cor}, the initial Trp fluorescence value before the addition of Ub is shown by F_o, and F_i is obtained from equation 5.1 as previously described. The data was subsequently fit with a single site-binding model, equation 5.3, to determine the dissociation constant, K_D.

$$F_{cor} = \frac{F_i - F_o}{F_o} \tag{5.2}$$

$$f(ligand) = \frac{ligand}{ligand + K_D} \tag{5.3}$$

As seen in Figures 5.3 and 5.4, both full-length E2-25K and the UBA domain bind to both Ub, whereas the UBC domain shows little or no specific binding or

conformational change of the Trp residue indole rings. The noticeable difference between the binding affinities of the full-length E2-25K and the UBA domain to cleaved and uncleaved Ub can be explained by the similarities of the tag residues to linear diubiquitin (Figure 5.2). It has been demonstrated by other groups that the UBA domain has a higher affinity to Lys63 linked polyubiquitin chains [84], which are similar in conformation to linear diubiquitin [106]. However, the slight difference in affinity between full-length E2-25K and the UBA can be said to be not statistically significant.

```
                                 1         10        20
MonoUb_with_expression_tag       MGSSHHHHHHSSGLVPRGSHMQIFVKTL
Linear_diubiquitin               .ESTLHLV.....LRLRGG.MQIFVKTL
```

Figure 5.2 Sequence Alignment of Uncleaved Ubiquitin with Linear Di-Ubiquitin. [Conserved residues are boxed and colored.]

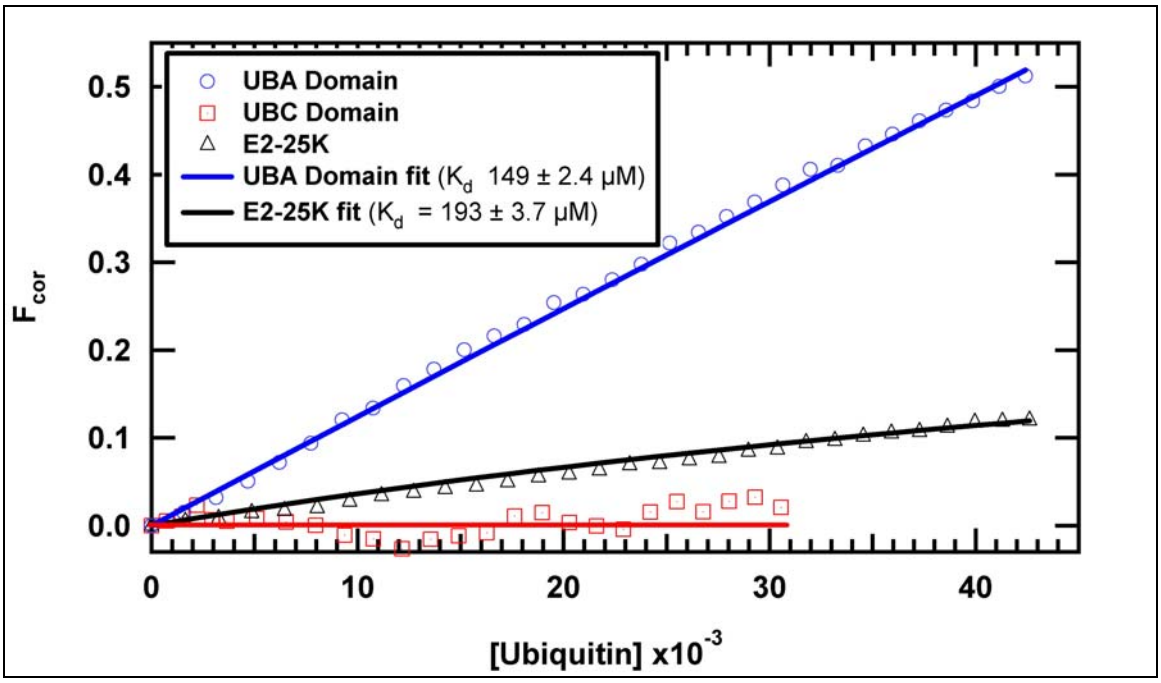

Figure 5.3 Fluorescence Titration Binding Spectra of full-length E2-25K, UBC and UBA Domains to Cleaved Ubiquitin. [Plots of F_{cor} versus the total concentration of cleaved Ub to full-length E2-25K and UBA domains are fitted with the single site binding model (equation 5.3) and are indicative of a single binding site. The data shows an affinity for Ub similar to binding studies by NMR. The UBC domain plot however, indicated no specific binding or conformational change of the Trp residues.]

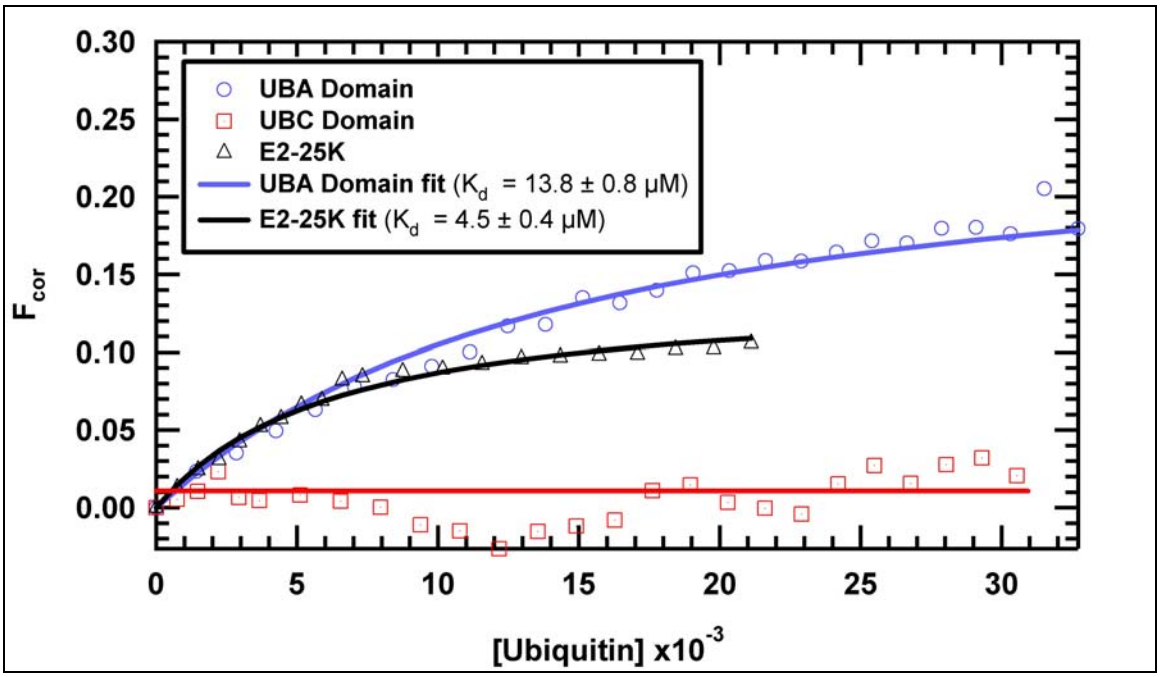

Figure 5.4 Fluorescence Titration Binding Spectra of Full-length E2-25K, UBC and UBA Domains to Uncleaved Ub. [Plots of F_{cor} versus the total concentration of uncleaved Ub to full-length E2-25K and UBA domains are fitted with the single site binding model (equation 5.3) and are indicative of a single binding site. The UBC domain plot again indicated no specific binding or conformational change of the Trp residues.]

5.2 Nuclear Magnetic Resonance

NMR spectra of the full-length E2-25K, the UBC and UBA domains, as well as Ub were collected at 22 º (full-length E2-25K) and 25 °C on a Varian (Palo Alto, CA) 800 MHz (18.7 Tesla field) INOVA NMR spectrometer using a triple resonance probe with triaxial pulsed field capability. Pulse sequences were those provided in the Varian BioPack. ^{1}H chemical shifts were referenced using sodium 4,4-dimethyl-4-silapentane-1-sulfonate (DSS) as an internal reference. ^{13}C and ^{15}N chemical shifts were referenced indirectly to DSS and liquid ammonia, respectively, using the appropriate frequency ratios [107]. NMR spectra were processed using NMRPipe [87]. NMRView [88] was used for visualization and chemical shift assignments of NMR data. The NMR spectra were used to determine backbone resonance assignments of full-length E2-25K, its

corresponding UBA domain, and Ub. The spectra were also used to determine the binding interface of the full-length E2-25K and its UBA domain to Ub, binding interface of full-length E2-25K to E3 proteins, UBC domain to UBA domain, and Ub to the full-length E2-25K and its UBA domain.

5.2.1 NMR Backbone Resonance Assignments of Full-length E2-25K

Samples of ^{13}C, ^{15}N-labeled deuterated full-length E2-25K protein were brought to 0.3-0.5 mM in NMR sample buffer (50 mM NaH_2PO_4/Na_2HPO_4, pH 6.5). These samples were used for the collection of two-dimensional ^{1}H-^{15}N HSQC spectrum and three-dimensional HNCACB, HNCA, HNCO, and HN(CO)CACB [108] spectra for the chemical shift assignments of backbone ^{1}H, ^{13}C, and ^{15}N resonances. Samples of ^{13}C, ^{15}N-labeled full-length E2-25K protein were brought to ~0.6 mM in NMR sample buffer. These samples were used for collection of CBCA(CO)NH [108] and ^{15}N-edited NOESY [108] spectra.

The chemical shifts present in the two-dimensional ^{1}H-^{15}N HSQC TROSY spectrum of full-length E2-25K (Figure 5.5) exhibit signal dispersion consistent with an ordered structure. Assignments of the backbone ^{1}H, ^{13}C, and ^{15}N resonances are 95.3% (731/767) complete (Table A.2) and have been published in the Biological Magnetic Resonance Data Bank (BMRB) (BMRB ID: 17362) [109]. The missing resonances primarily result from the presence of thirteen proline residues in the sequence and from overall conformational flexibility of the N-terminus and several loop regions. Certain regions of the spectra displayed spectral resonance overlap as seen in Figures 5.5 and 5.6.

Analysis of the chemical shift index (CSI) of certain nuclei in a protein structure has been used successfully as an indicator of secondary structure [110]. Using the $^{13}C\alpha$,

$^{13}C\beta$, and ^{13}CO resonance assignments the consensus CSI values were calculated. Figure 5.7 shows the comparison of the predicted secondary structure with those reported in the crystal structure of E2-25K (PDB code 3F92). As can be seen, there was excellent agreement between the two, which indicated that the E2-25K is folded and maintains an overall structure in solution similar to that found in the context of the full-length protein crystal structure.

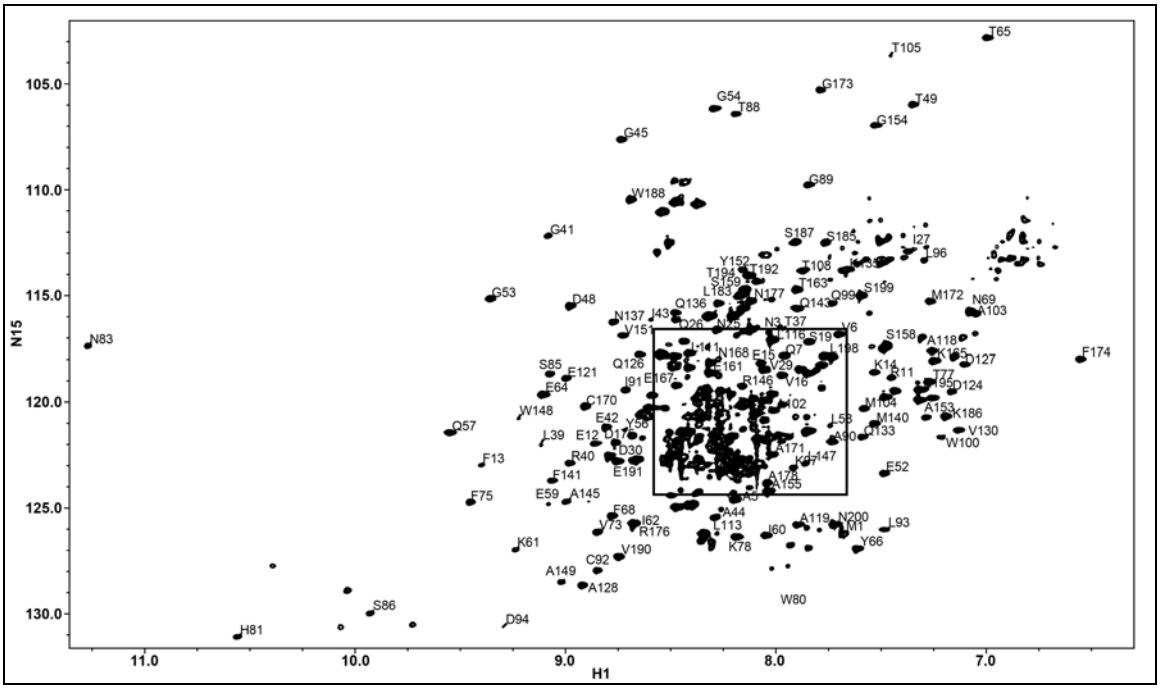

Figure 5.5 ^{1}H, ^{15}N-HSQC-TROSY Spectrum of E2-25K. [The spectrum, peaks are labeled with the assigned amino acid residue, demonstrates the chemical shift dispersion. Boxed region is shown in Figure 5.6.]

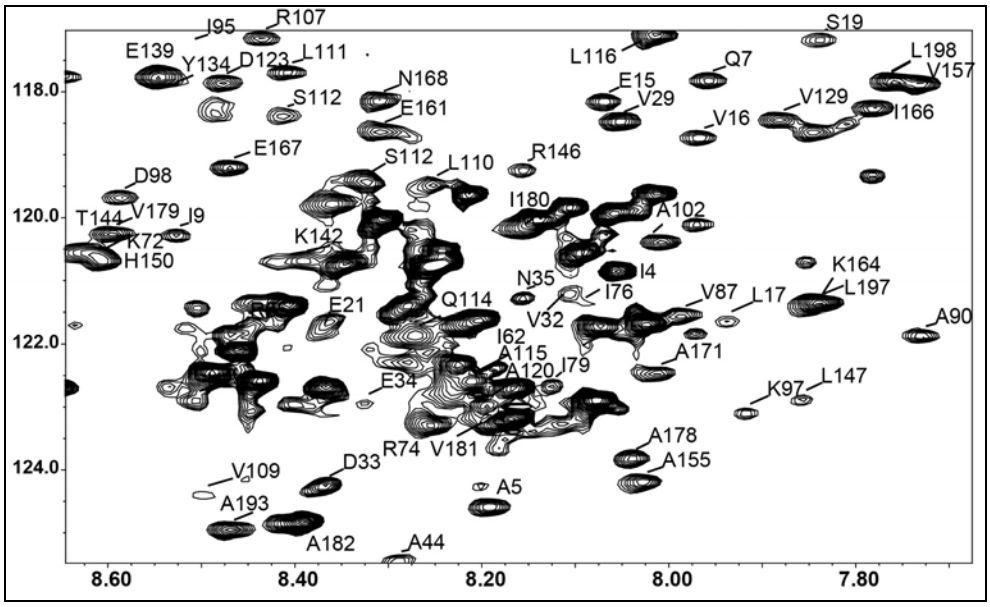

Figure 5.6 Boxed Region of ^{1}H, ^{15}N-HSQC-TROSY Spectrum of E2-25K. [The boxed region of the full-length spectrum, Figure 5.5. Peaks are labeled with the assigned amino acid residue.]

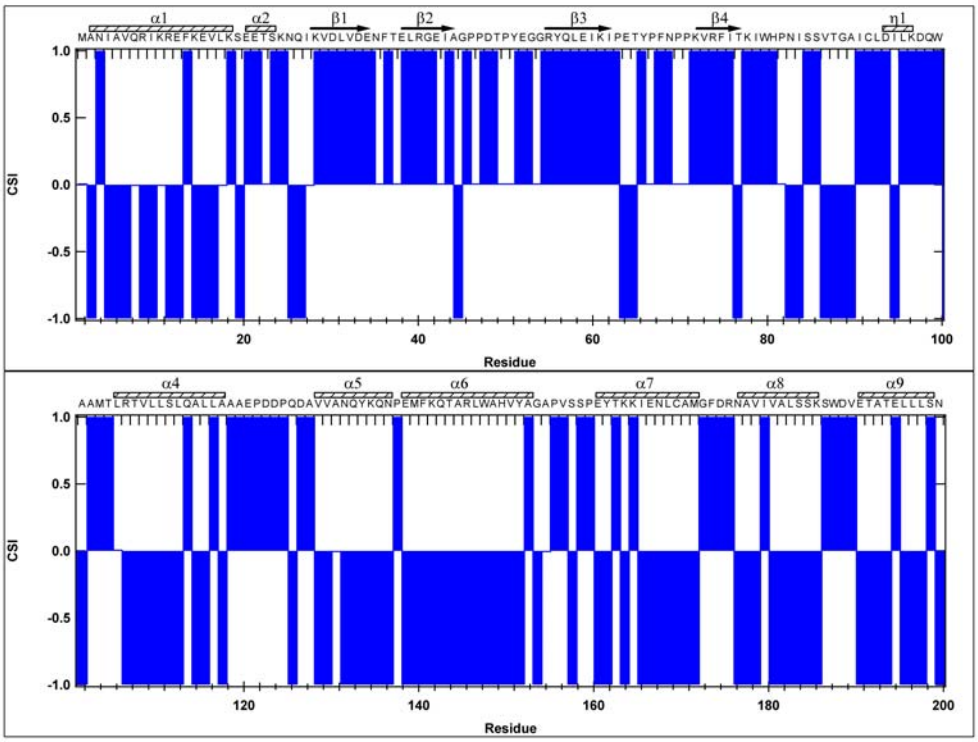

Figure 5.7 Consensus Chemical Shift Index Prediction of Secondary Structure Elements for Full-length E2-25K. [Graph of consensus chemical shift index (CSI) values calculated for ^{13}Cα, ^{13}Cβ, and ^{13}CO resonance assignments as a function of amino acid residue number. Negative indexes correlate with alpha-helix formation, while positive indexes correlate with beta-strand formation. Clusters of contiguous negative or positive indexes indicate regions of continuous secondary structure within the folded protein.]

5.2.2 NMR Backbone Resonance Assignments of the UBC Domain of E2-25K

Samples of ^{13}C, ^{15}N-labeled UBC domain of E2-25K protein were concentrated to 0.7 mM in NMR sample buffer. These samples were used for the collection of two-dimensional ^{1}H-^{15}N HSQC spectrum and three-dimensional HNCACB, CBCA(CO)NH, and HNCO [108] spectra for the chemical shift assignments of backbone ^{1}H, ^{13}C, and ^{15}N resonances. The chemical shifts present in the two-dimensional ^{1}H-^{15}N HSQC spectrum of UBC domain of E2-25K (Figure 5.8) exhibit signal dispersion consistent with an ordered structure. However, assignments of the backbone ^{1}H, ^{13}C, and ^{15}N resonances of the UBC domain of E2-25K were not completed because of the shifting, broadening, and splitting of peaks that indicate that there are subtle differences in structure because of the absence of the UBA domain.

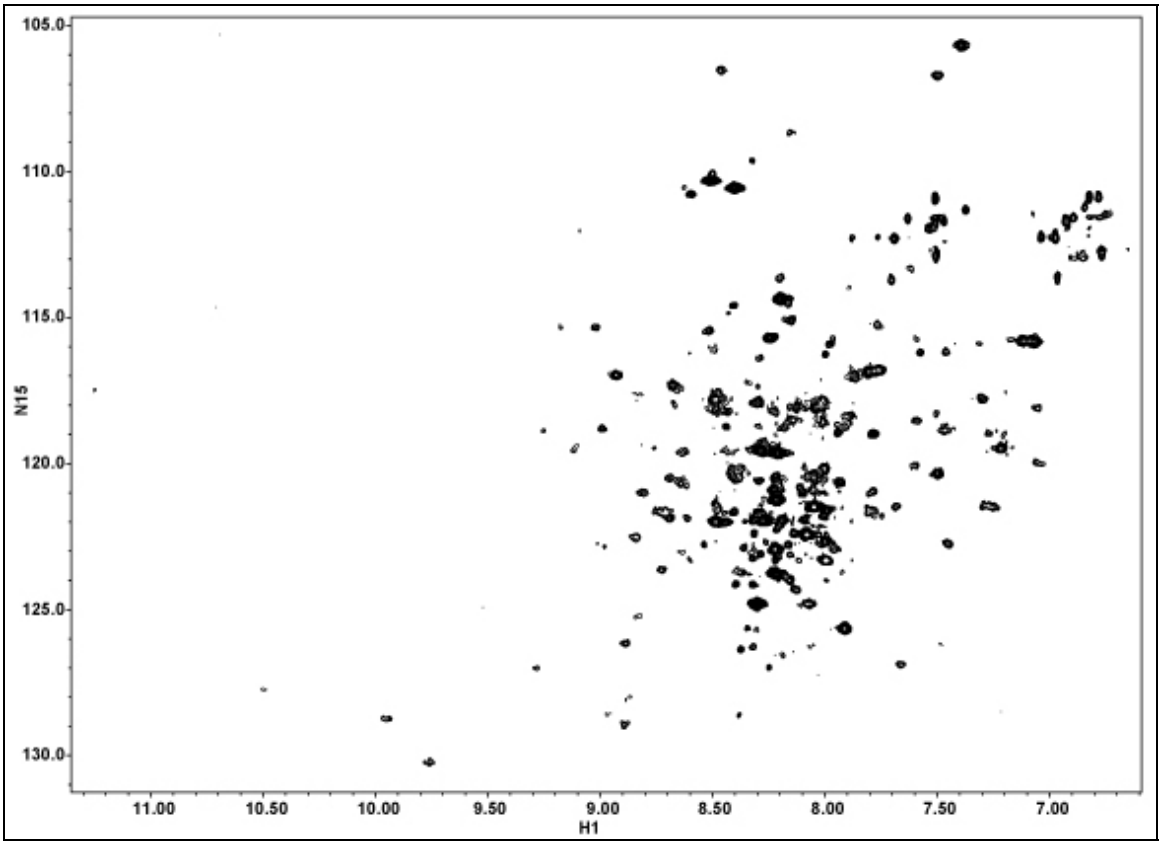

Figure 5.8 ^{1}H, ^{15}N-HSQC Spectrum of E2-25K UBC Domain.

5.2.3 Comparison of UBC and UBA Domain NMR Spectra to E2-25K NMR Spectra

Two-dimensional ^{1}H-^{15}N HSQC spectra collected on full-length E2-25K and the UBC and UBA domains, as previously described, were compared to determine whether significant structural differences existed in the UBC and UBA domains expressed alone. While the resonances for the UBC domain alone and in the full-length protein were generally similar in chemical shift, there were differences seen across the domain. The differences in the context of the full-length, including shifting, broadening, and splitting of peaks (Figure 5.9) which indicate that there are subtle differences in structure as a result of the absence of the UBA domain. The differences in chemical shifts, which result from variations in the chemical environment around certain amino acids in the interaction between the UBC and UBA domains, might suggest that the UBA domain contributes to the stability of the full-length protein by stabilizing the UBC domain.

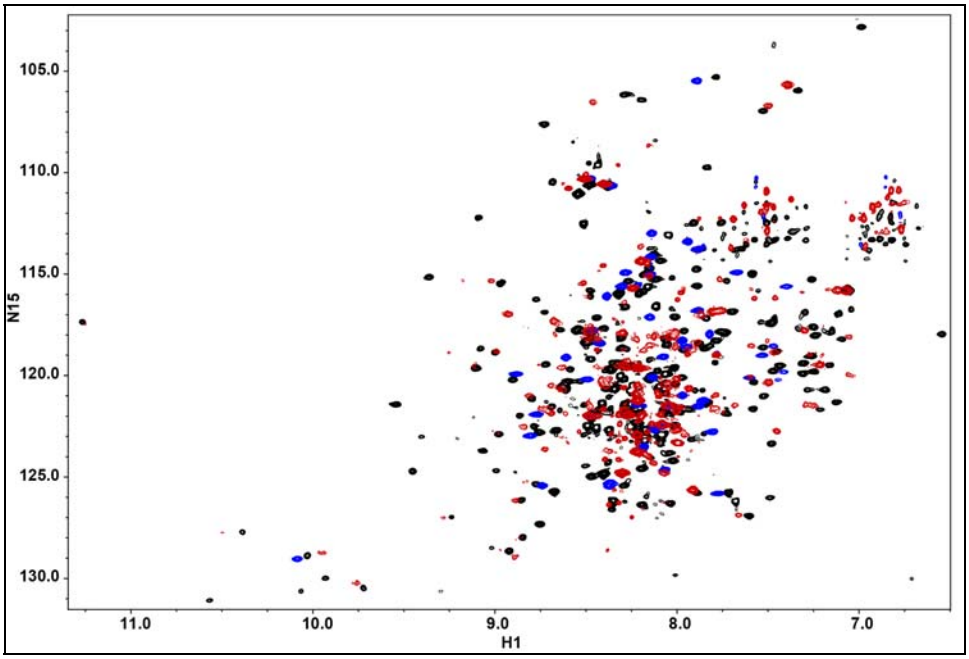

Figure 5.9 ^{1}H, ^{15}N-HSQC Overlay Spectra of E2-25K, UBC and UBA Domains. [The full-length spectrum is represented by the black contours; the UBC domain is represented by the red contours, and the UBA domain is represented by blue contours.]

5.2.4 NMR Backbone Resonance Assignments of Ubiquitin

Samples of ^{15}N-labeled Ub were brought to 1.3 mM in NMR sample buffer. These samples were used for the collection of two-dimensional ^{1}H-^{15}N HSQC spectrum [108] spectra for the chemical shift assignments of backbone ^{1}H and ^{15}N resonances. Backbone assignments of Ub at pH 7.2 were completed by comparing published assignments at pH 6.0 and 7.4 [111, 112]. The chemical shifts present in the two-dimensional ^{1}H-^{15}N HSQC spectrum of Ub (Figure 5.10) exhibit signal dispersion consistent with an ordered structure.

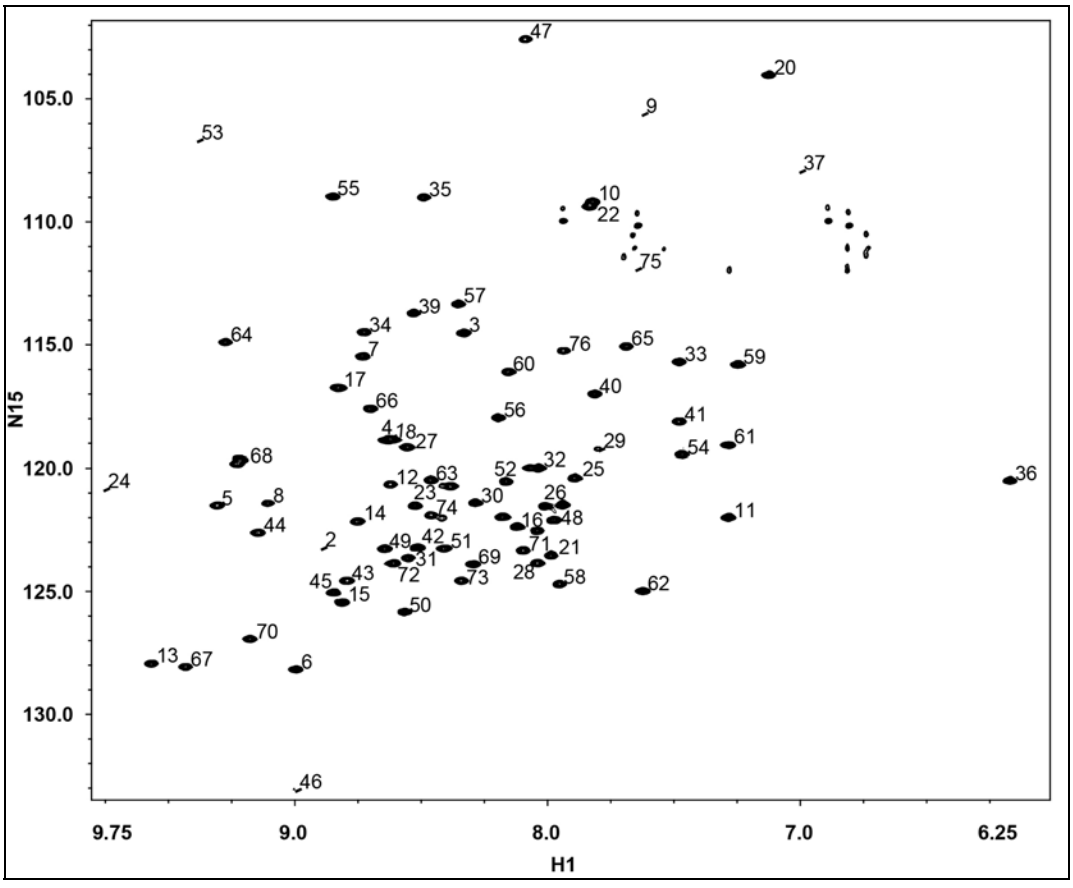

Figure 5.10 ^{1}H, ^{15}N-HSQC Spectrum of Ubiquitin at pH 7.2. [The spectrum, with peaks labeled with the assigned amino acid residue, demonstrates the chemical shift dispersion.]

5.2.5 Temperature-dependent NMR spectroscopy of Ubiquitin

In order to determine amino acid chemical shifts at 37 º C, a two-dimensional ^{1}H-^{15}N HSQC at four different temperatures was performed. A ^{15}N-labeled sample of Ub was expressed as described in section 2.3.1 and purified as detailed in section 2.4.4 to 1.3 mM in NMR sample buffer. The sample was examined by a two-dimensional ^{1}H-^{15}N-filtered HSQC at 25 ºC, 30 º C, 35 ºC, and 37 ºC. No additional peaks appeared at higher temperatures, as shown in Figure 5.11.

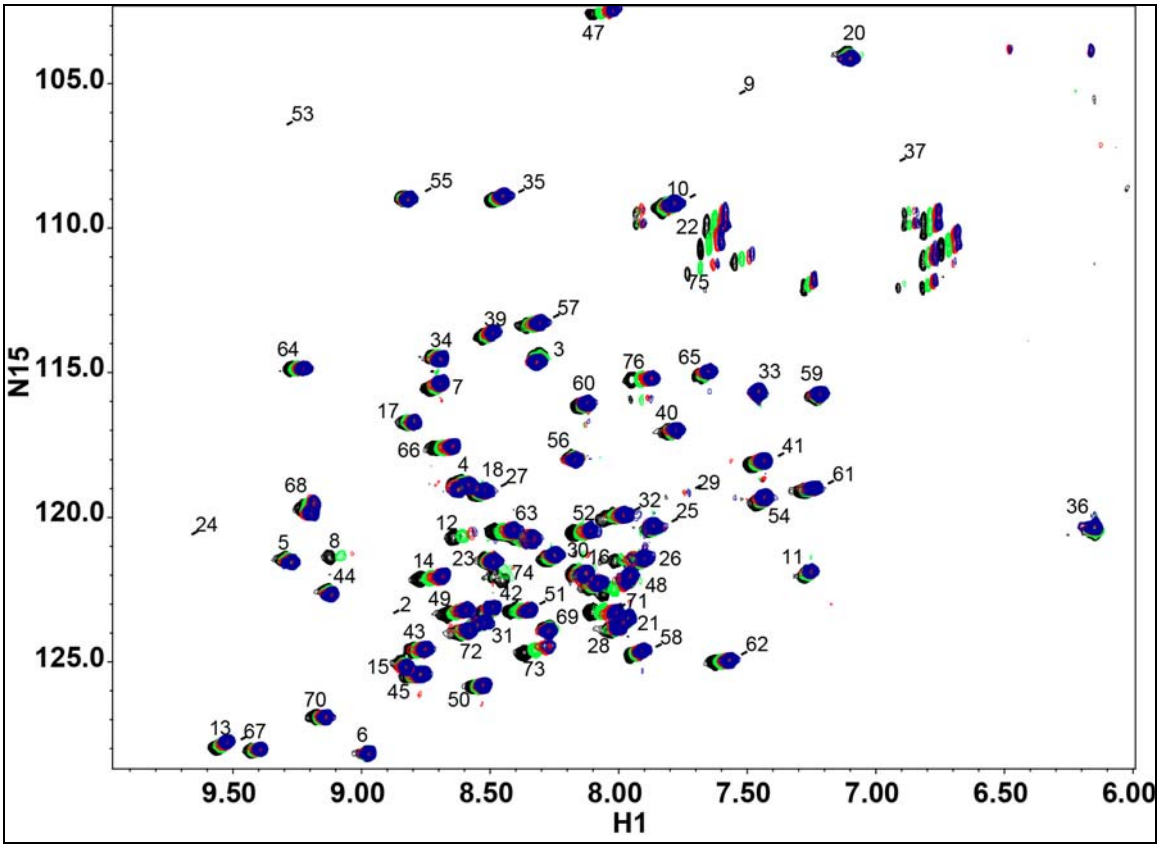

Figure 5.11 Overlay of ^{1}H, ^{15}N-HSQC Ubiquitin Spectra at 25ºC, 30ºC, 35ºC and 37ºC. [Black contours represent 25 ºC, green contours represent 30 ºC, red contours represent 35 ºC, and blue contours represent 37 ºC.]

5.2.6 Identification of UBA/Ub Binding Surfaces by Solution NMR

Binding of E2-25K UBA domain to Ub was examined by solution NMR from a series of two-dimensional ^{1}H-^{15}N HSQC experiments [103]. Increasing amounts of

unlabeled Ub (34.8 mM) to a maximum of 3.5 Ub/UBA were titrated into the sample, Figure 5.12. Specific changes in chemical shift values were used to identify amino acids in the UBA domain whose chemical environment was altered upon binding.

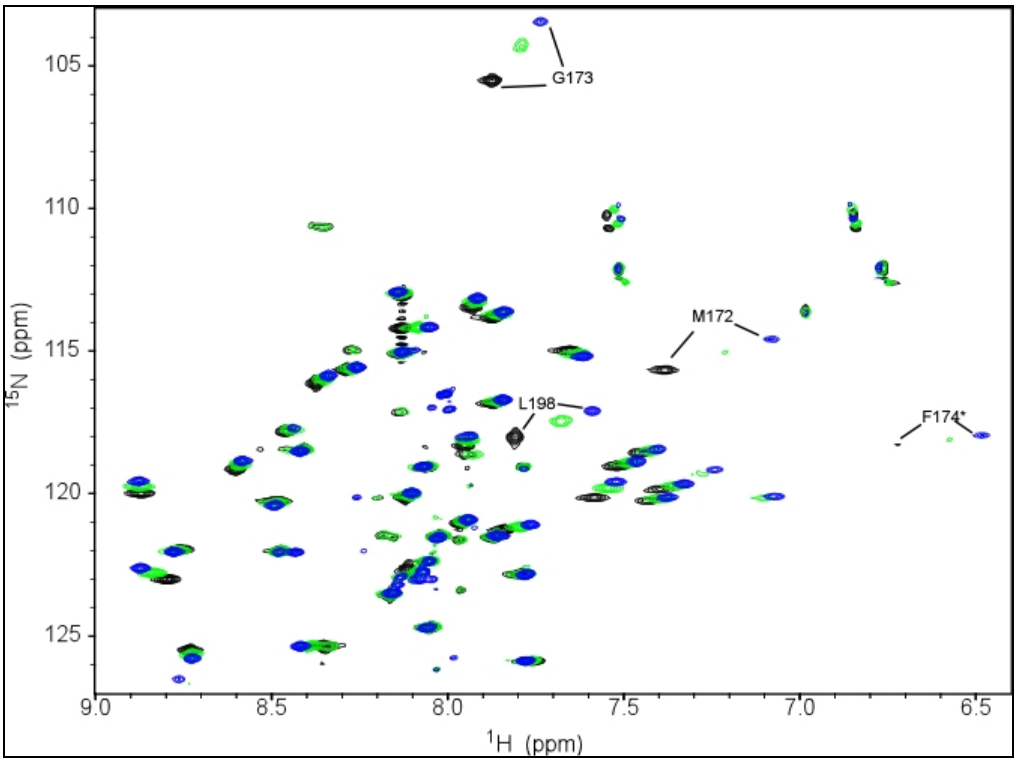

Figure 5.12 Specific Interaction of Ubiquitin with the UBA Domain from E2-25K. [Titration of ^{15}N-labeled UBA domain with unlabeled ubiquitin was followed by solution NMR spectroscopy. Overlay of the ^{1}H-^{15}N HSQC spectra of the UBA domain where black contours represent 0 equivalents of ubiquitin added. Blue contours represent 3.5 equivalents of ubiquitin added.]

The binding of the UBA domain of E2-25K to Ub was initially reported by [33, 84] with a K_d of approximately 300-500 μM. Because chemical shifts are extremely sensitive reporters of the local magnetic environment, ligand binding generally changes the chemical shifts of nearby backbone and sidechain resonances. This approach is sensitive to weak binding [113] and has been used previously to characterize binding of other UBA domains with ubiquitin [32, 114, 115]. When stoichiometric amounts of unlabeled ubiquitin were added to ^{15}N-labeled UBA domain, a limited number of protein

^{1}H and ^{15}N resonances exhibited large frequency changes in 2D HSQC spectra (residues M172, G173, L198), and a few additional peaks appeared (one of which was identified as F174) (Figure 5.13). The chemical shift perturbation data (Figure 5.14) demonstrate weak binding of Ub by the UBA domain (Figure 5.15), in fast exchange on the NMR time scale. The perturbed residues fall primarily in the MGF loop between helices 1 and 2 of the UBA domain and in the adjacent face of helix 3 (Figure 6.5). Using the existing NMR data, the estimated K_d for binding of Ub is approximately 1.2 mM (Figure 5.15), which is consistent with the value determined by surface plasmon resonance [84] and fluorescence (Figure 5.2).

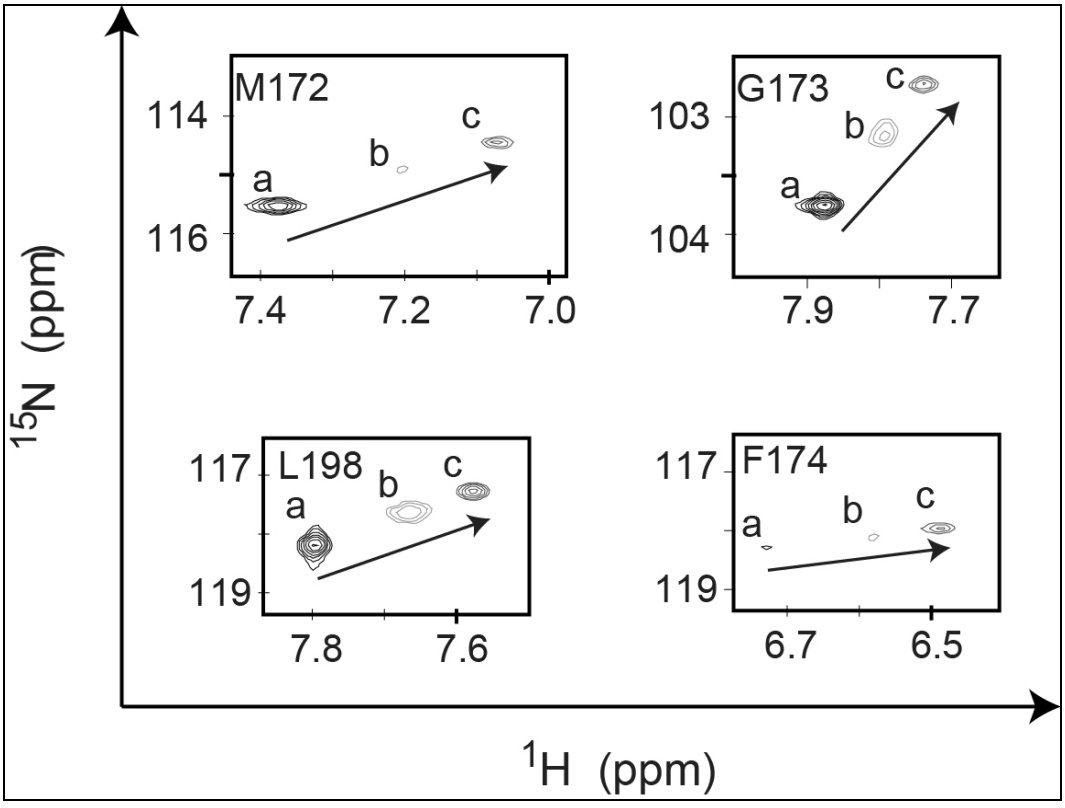

Figure 5.13 Chemical Shift Perturbation for UBA Domain with Ubiquitin. [Overlay of the ^{1}H-^{15}N HSQC spectra for residues M172, G173, F174, and L198 in the UBA domain, where *contours* labeled (a) represent 0 equivalents, *contours* labeled (b) represent 2.0 equivalents and *contours* labeled (c) represent 3.5 equivalents of Ub added. Arrows indicate direction of shift as Ub concentration is increased.]

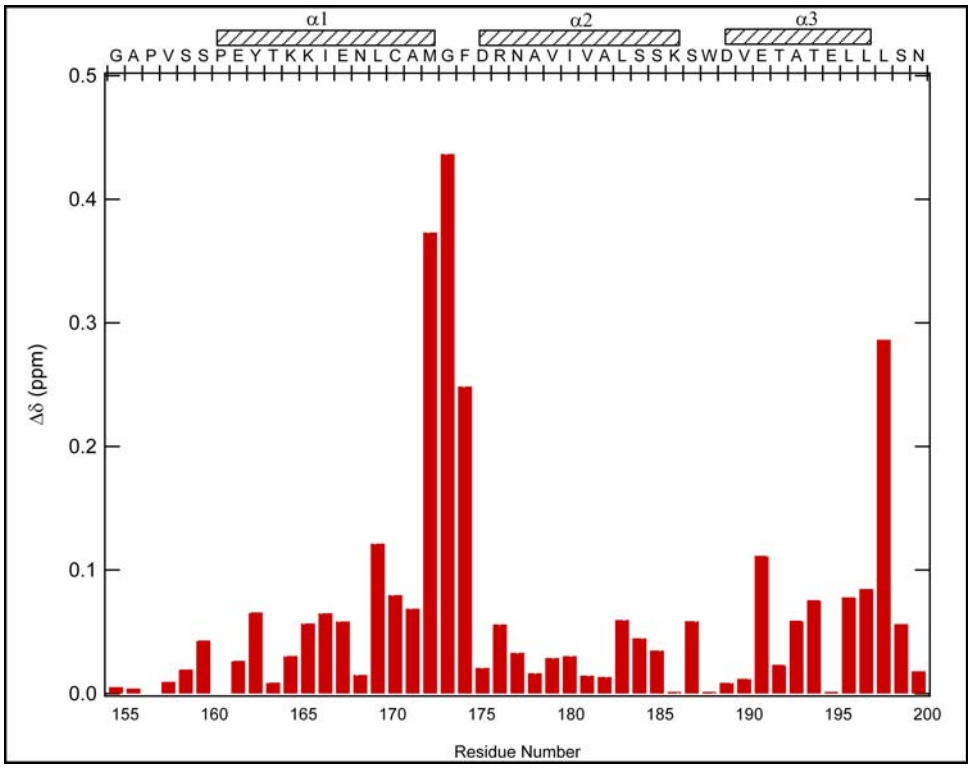

Figure 5.14 Chemical Shift Perturbation for UBA Domain with Ubiquitin. [The chemical shift perturbations were determined using chemical shift changes from the ubiquitin titration. Chemical shift changes were calculated as $\Delta\delta = \mathrm{sqrt}[(\Delta\delta(^{15}N)/5)^2 + (\Delta\delta(^{1}H)^2)]$.]

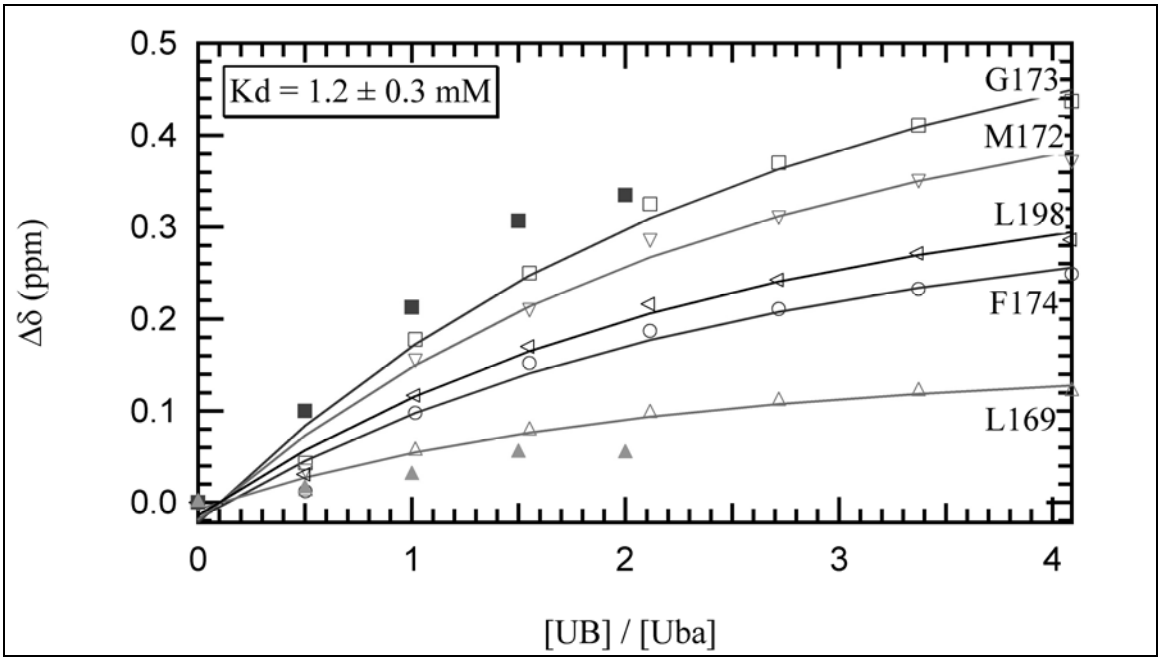

Figure 5.15 Binding Curves for UBA Domain with Ubiquitin. [Plots of chemical shift differences versus the total concentration of unlabeled Ub to the UBA domain are global fitted using the single site binding model (equation 5.3) to achieve an overall K_d and are indicative of a single binding site.]

Titration of ^{15}N-Ubiquitin (0.6 mM) was performed using a series of two-dimensional ^{1}H-^{15}N HSQC experiments as with the UBA domain of E2-25K, except the buffer pH was 7.2. The unlabeled UBA domain (2.5 mM) was added to a final molar ratio of 1.5 UBA/Ub (Figure 5.16). Chemical shift resonances in ubiquitin which were perturbed upon binding belonged to residues L8, R42, I44, A46, K48, Q49, H68, L71, and R72 (Figures 5.16, 5.17, and 5.18), which is consistent with binding studies involving other UBA domains and Ub [116]. The titration experiments yielded an average K_d of approximately 0.5 mM (Figure 5.19) which is consistent with the reverse experiment (Figure 5.15). Both titration experiments provided information on the residues involved in binding which were used later in calculating the UBA domain/Ub complex model.

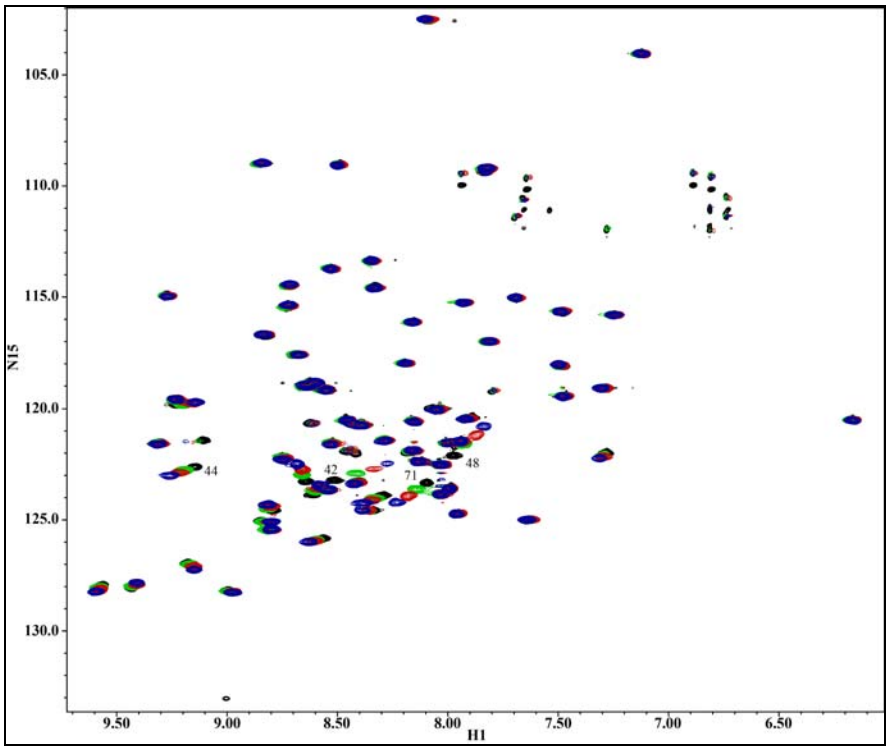

Figure 5.16 NMR Titration of Ubiquitin with E2-25K UBA Domain. [Titration of ^{15}N-labeled ubiquitin with unlabeled UBA domain was followed by NMR spectroscopy. Overlay of the ^{1}H-^{15}N HSQC spectra of the Ub, where black contours represent 0 equivalents of UBA Domain added. Blue contours represent 1.5 equivalents of UBA added.]

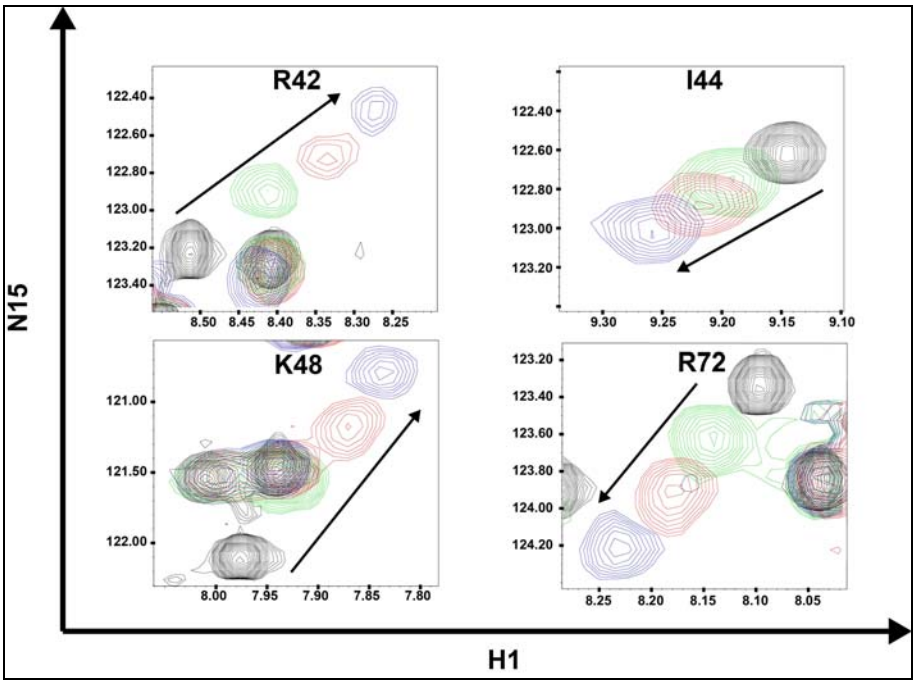

Figure 5.17 Specific Chemical Shift Changes for Ubiquitin Titrated with UBA Domain. [Overlay of the ^{1}H-^{15}N HSQC spectra for residues R42, I44, K48 and R72 of Ub, where black *contours* represent 0 equivalents, green c*ontours* represent 0.5 equivalents, red *contours* represent 1.0 equivalents, and blue contours represent 1.5 equivalents of UBA added. Arrows indicate direction of shift as UBA domain concentration is increased.]

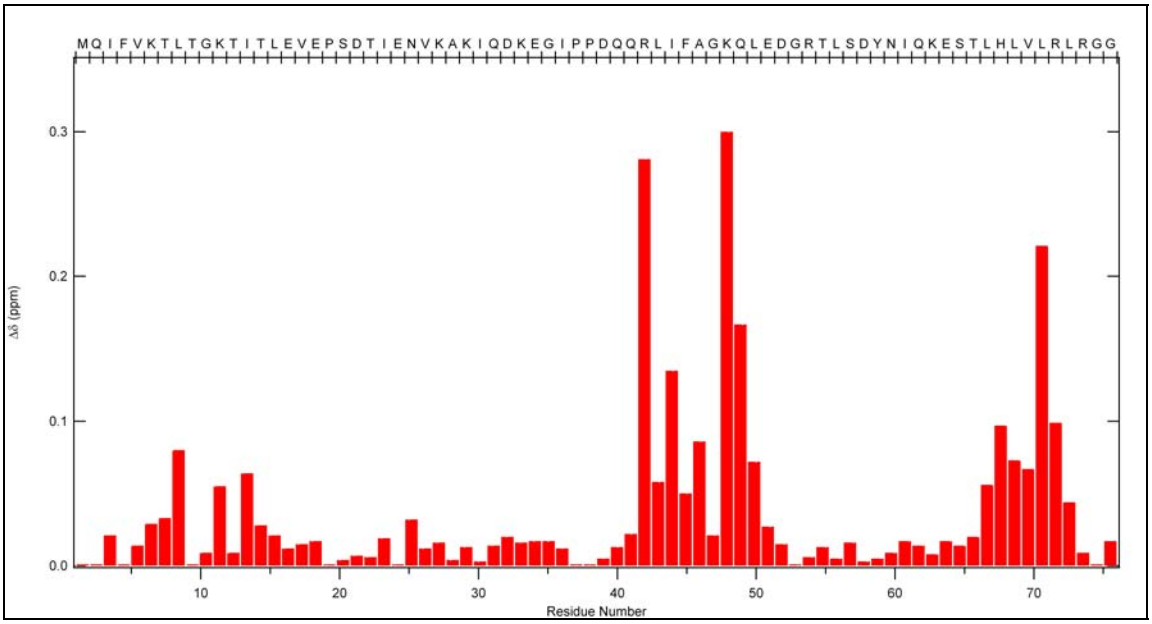

Figure 5.18 Chemical Shift Perturbation for Ubiquitin Titrated with UBA Domain. [The chemical shift perturbations were determined using chemical shift changes from the UBA Domain titration. Chemical shift changes were calculated as $\Delta\delta = \mathrm{sqrt}[(\Delta\delta(^{15}N)/5)^2 + (\Delta\delta(^{1}H)^2)]$.]

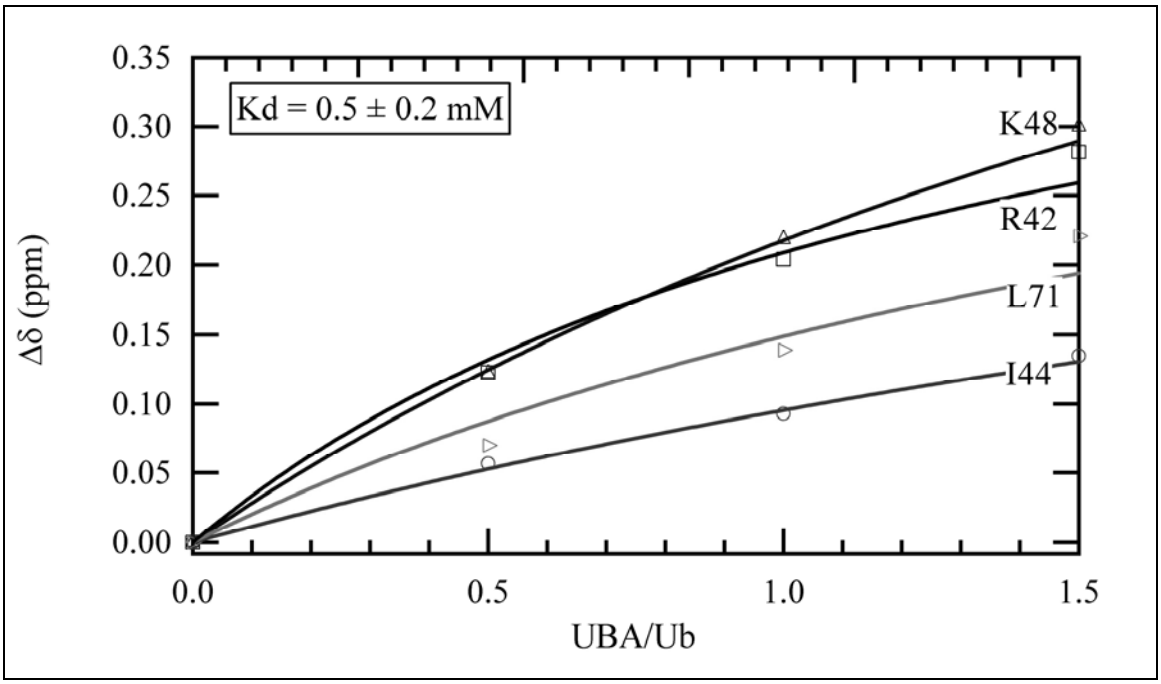

Figure 5.19 Binding Curves for Ubiquitin with UBA Domain. [Plots of chemical shift differences versus the total concentration of unlabeled UBA domain to Ub are global fitted using the single site binding model (equation 5.3) to achieve an overall K_d and are indicative of a single binding site.]

5.2.7 Identification of E2-25K/Ub Binding Surfaces by Solution NMR

As with the UBA domain, binding of E2-25K to Ub was examined by solution NMR from a series of two-dimensional ^{1}H-^{15}N HSQC experiments. Titration of full-length E2-25K (0.5 mM) with Ub (34.8 mM) was performed as with the UBA domain, except only molar ratios of 2:1 Ub/E2-25K (Figure 5.20) were reached before significant broadening of peaks led to loss of signal. Chemical shift changes were noted only for a small subset of resonances within the UBA domain (Figure 5.21), indicating specific regional binding. Broadening of many peaks also occurred as a result of titration, which confirms formation of a Ub:E2-25K complex. The titration experiments yielded an average K_d of approximately 0.34 mM (Figure 5.22) which is consistent with fluorescence data (Figure 5.2) and with NMR titration experiments using the UBA domain only (Figures 5.15 and 5.19).

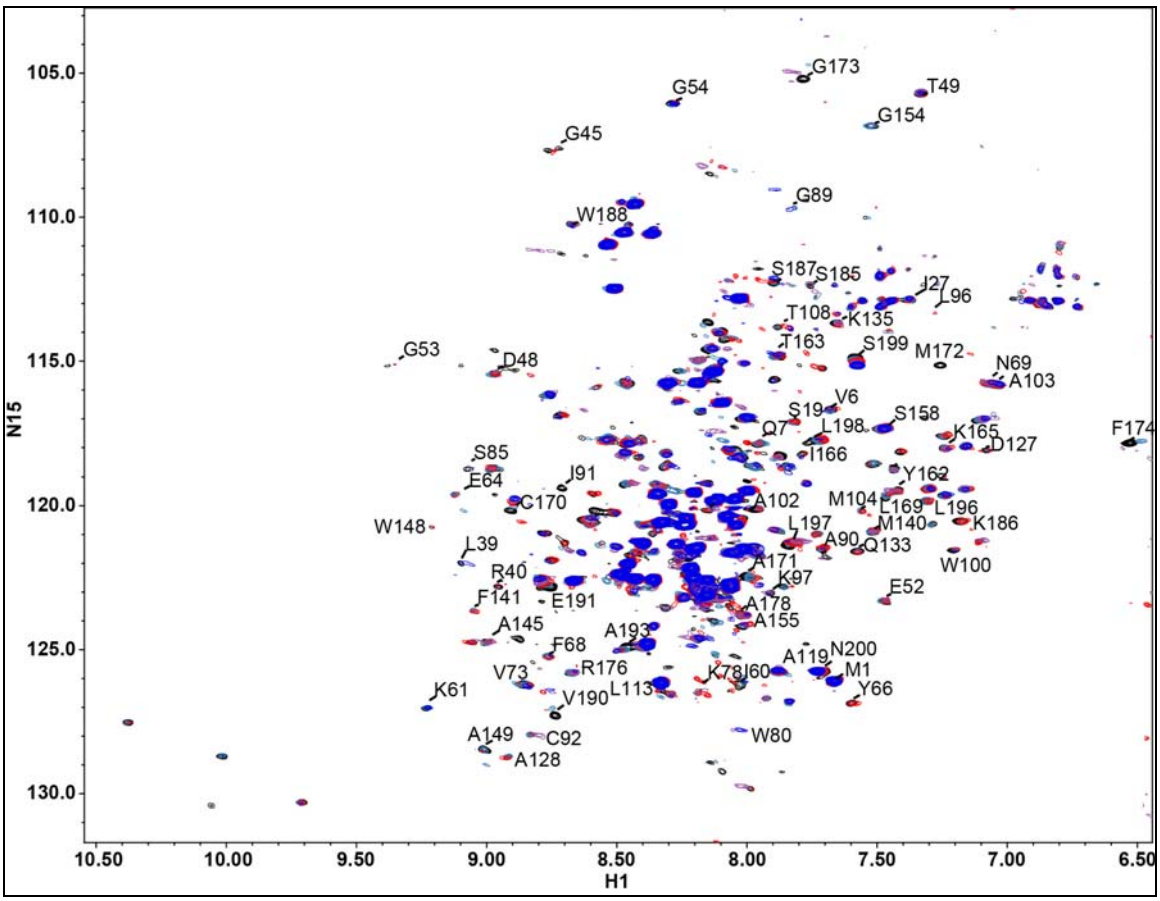

Figure 5.20 NMR Titration of Ubiquitin with E2-25K. [Titration of ^{15}N-labeled E2-25K with unlabeled ubiquitin was followed by solution NMR spectroscopy. Overlay of the ^{1}H-^{15}N HSQC spectra of the E2-25K where *black contours* represent 0 equivalents of Ub added. B*lue contours* represent 2.0 equivalents of Ub added.]

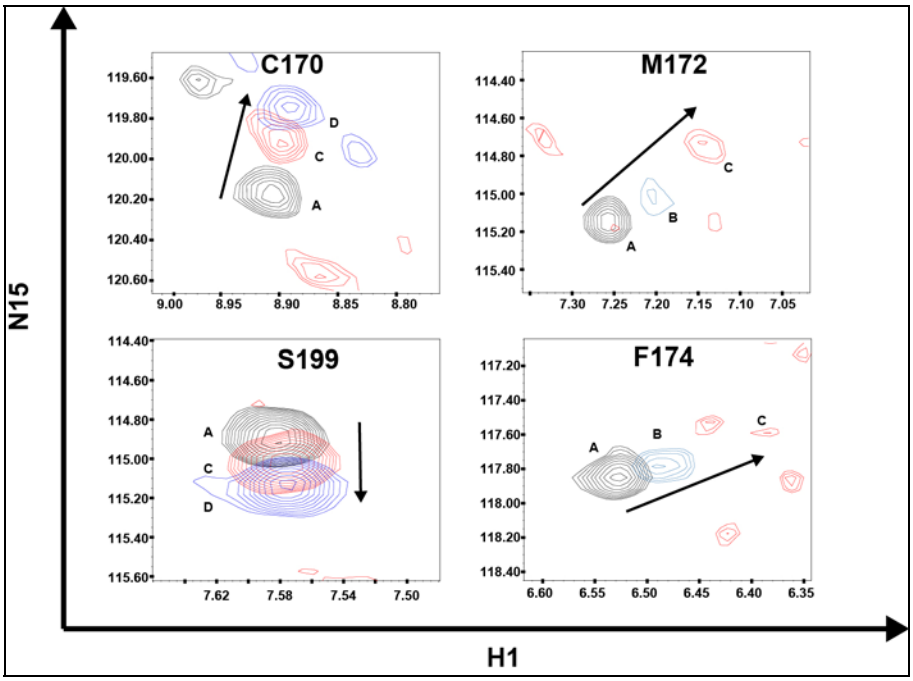

Figure 5.21 Chemical Shift Perturbations for E2-25K with Ubiquitin. [Overlay of the ^{1}H-^{15}N HSQC spectra for residues C170, M172, F174, and S199 in the UBA domain of the full-length E2-25K, where *contours* labeled (A) represent 0 equivalents, *contours* labeled (B) represent 0.5 equivalents, *contours* labeled (C) represent 1.0 equivalents, and contours labeled (D) represent 2.0 equivalents of Ub added. Arrows indicate direction of shift as Ub concentration is increased.]

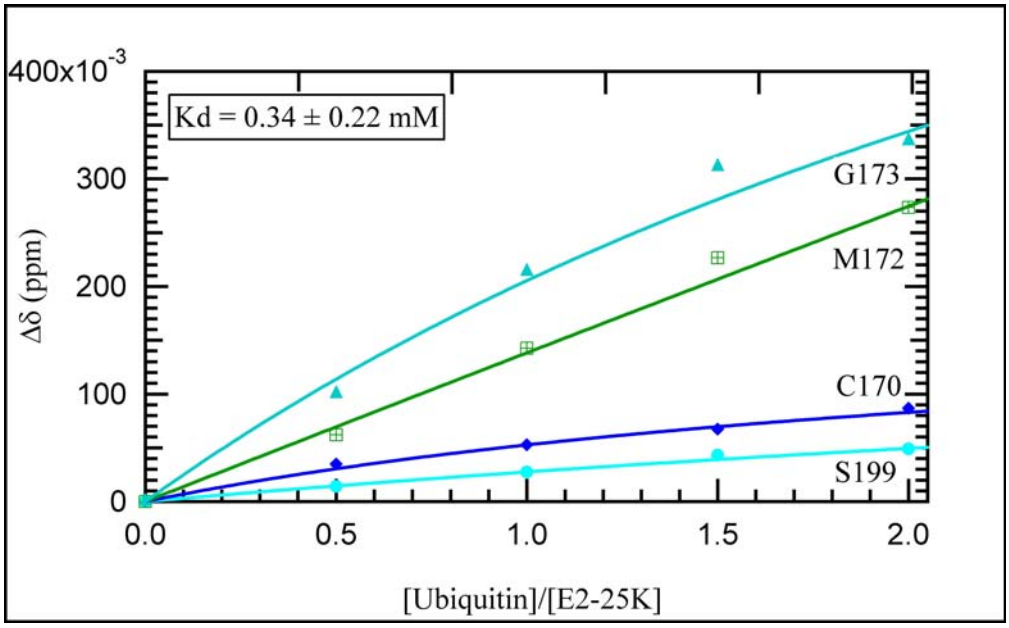

Figure 5.22 Binding Curves for E2-25K with Ubiquitin. [Plots of chemical shift differences versus the total concentration of unlabeled Ub to E2-25K are global fitted using the single site binding model (equation 5.3) to achieve an overall K_d and are indicative of a single binding site.]

Titration of ^{15}N-Ubiquitin (0.85 mM) was performed using a series of two-dimensional ^{1}H-^{15}N HSQC experiments, as with the UBA domain of E2-25 K, except the buffer pH was 7.2. The unlabeled E2-25K (71 μM) was added to a final molar ratio of 0.03:1.0 E2-25K/Ub. The titration experiments yielded an average K_d of approximately 0.87 mM (Figure 5.26) which is consistent with the reverse experiment (Figure 5.22). Chemical shift resonances in ubiquitin that were perturbed on binding belonged to residues L8, R42, I44, A46, K48, Q49, H68, L71, and R72 (Figures 5.23, 5.24, and 5.25). This binding is consistent with binding studies involving just the UBA domain (Figure 5.27). Titration studies at 37 °C, activity of E2-25K assays, did not reveal any additional residues involved in binding initially (Figures A.1 and A.2) or after 15 hours (Figure A.3).

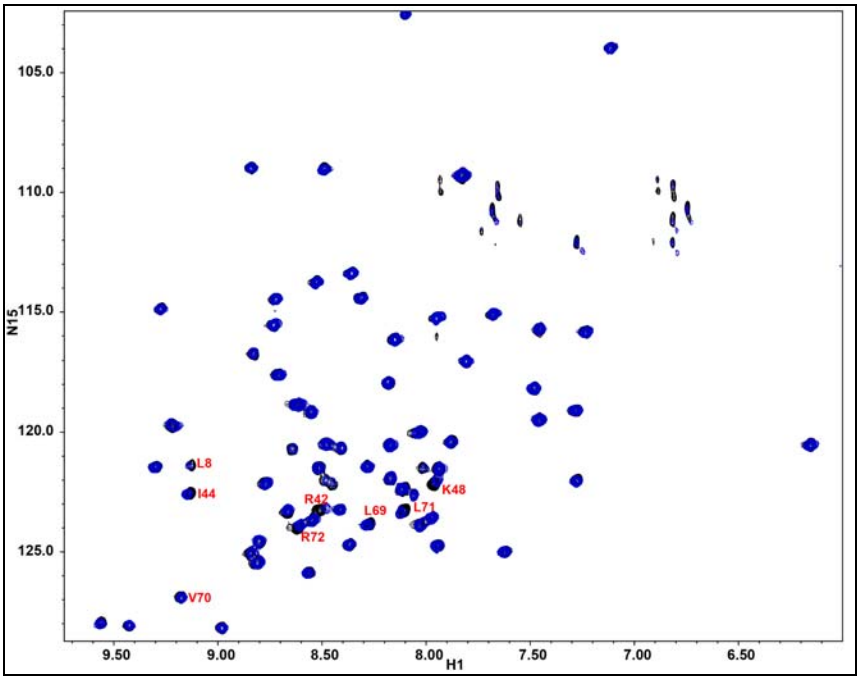

Figure 5.23 Specific Interaction of E2-25K with Ubiquitin. [Titration of ^{15}N-labeled Ub domain with unlabeled E2-25K was followed by solution NMR spectroscopy. Overlay of the ^{1}H-^{15}N HSQC spectra of the Ub where black contours represent 0 equivalents of E2-25K added. Blue contours represent 0.03 equivalents of E2-25K added.]

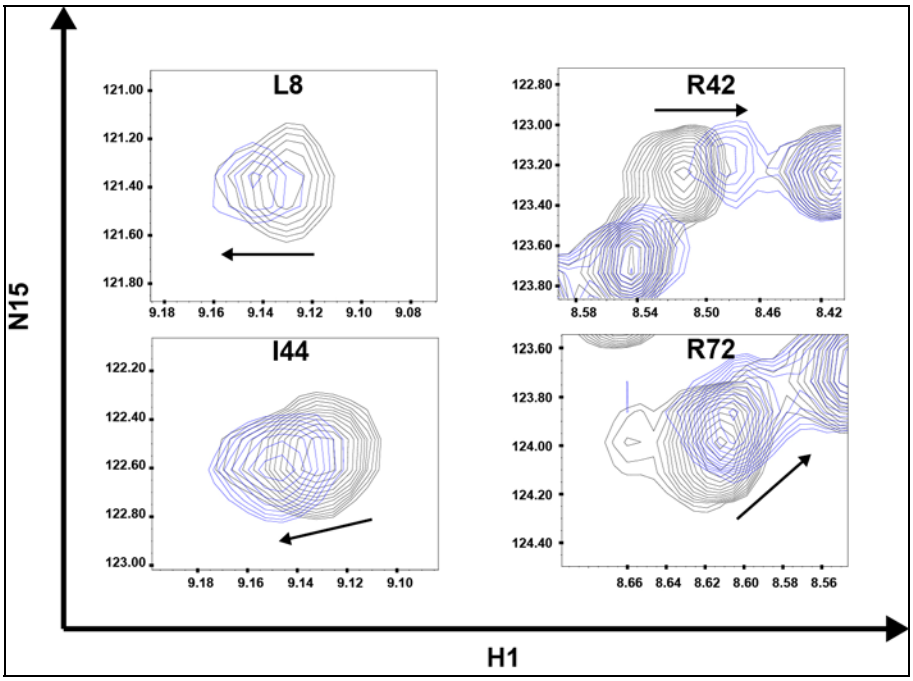

Figure 5.24 Specific Chemical Shift Changes for Ubiquitin Titrated with E2-25K. [Overlay of the ^{1}H-^{15}N HSQC spectra for residues L8, R42, I44, and R72 in Ub, where *black contours* represent 0 equivalents and *blue contours* represent 0.03 equivalents of E2-25K added. Arrows indicate direction of shift as E2-25K concentration is increased.]

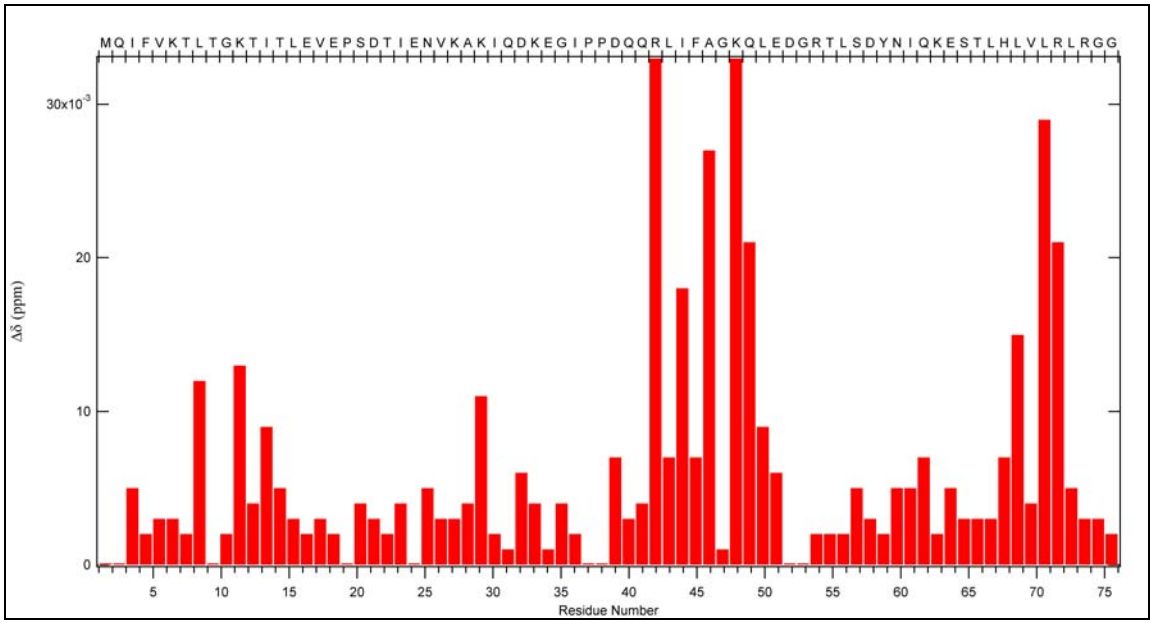

Figure 5.25 Chemical Shift Perturbation for Ubiquitin Titrated with E2-25K. [The chemical shift perturbations were determined using chemical shift changes from the Ub titration. Chemical shift changes were calculated as $\Delta\delta = \mathrm{sqrt}[(\Delta\delta(^{15}N)/5)^2 + (\Delta\delta(^{1}H)^2)]$.]

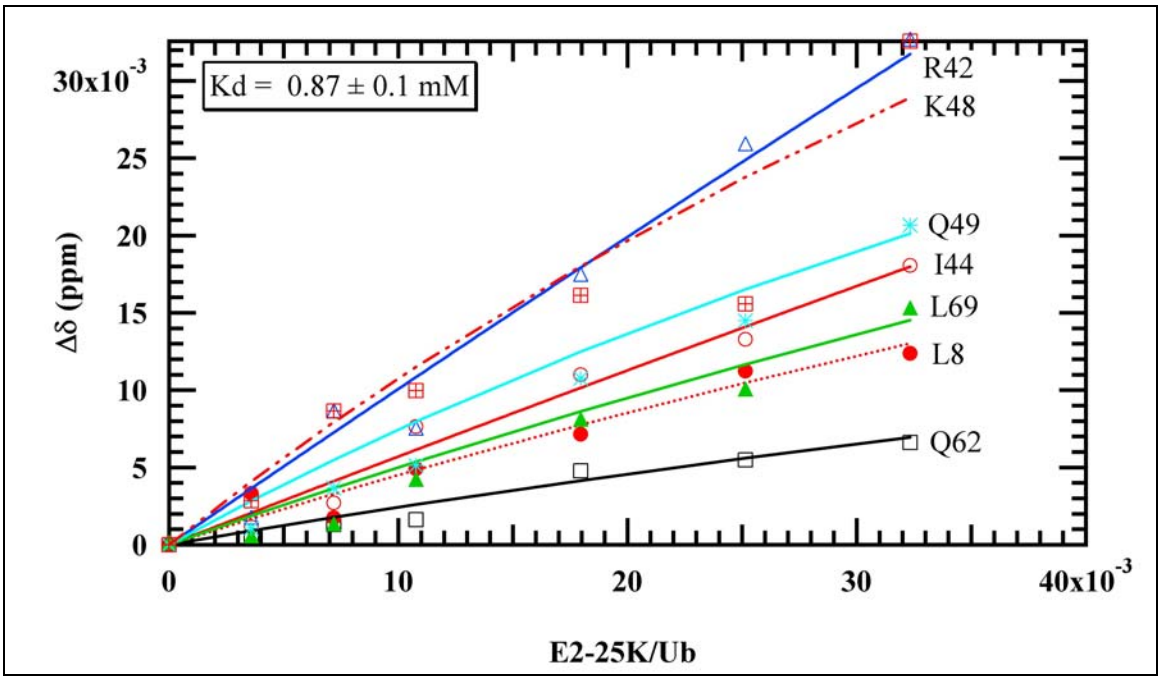

Figure 5.26 Binding Curves for Ubiquitin Titration with E2-25K. [Plots of chemical shift differences versus the molar ratio of unlabeled E2-25K to Ub are global fitted using the single site binding model (equation 5.3) to achieve an overall K_d and are indicative of a single binding site.]

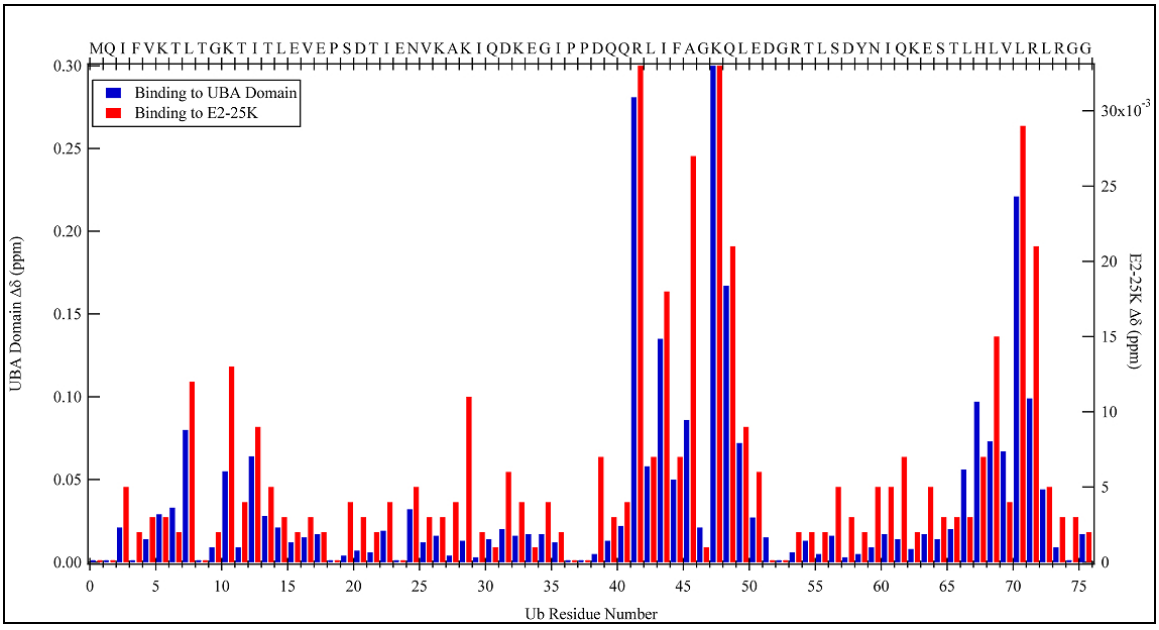

Figure 5.27 Ubiquitin Chemical Shift Perturbation Comparison of E2-25K and the UBA Domain. [The chemical shift perturbations were determined using chemical shift changes from the ubiquitin titrations. Red bars indicate chemical shift perturbations of Ub upon titration with full-length E2-25K whereas; blue bars indicate titration with UBA domain only.]

5.2.8 Identification of UBC/UBA Domain Binding Interface by Solution NMR

In order to determine if the domain-domain interactions between the UBC and the UBA domains of E2-25K seen in the crystal structure are crystallographically induced, binding was examined by solution NMR using a series of two-dimensional ^{1}H-^{15}N HSQC experiments. The UBC/UBA domain-domain interface noted in the crystal structure consists of hydrophobic interactions between residues M140, L147, and V151 (helix 5) of the UBC domain and residues I166 (helix 6) and I180 (helix 7) of the UBA domain [78]. Further interactions include three hydrogen bonds between the side-chains of T144 and W188, W148 and W184, and Y152 and N177 (Figure 3.5). Titration of ^{15}N-UBC domain (0.53 mM) of E2-25K was titrated with unlabeled UBA domain (0.86 mM) to a final UBA:UBC molar ratio of 1:1. The titration experiments yielded a slight loss of signal due to decreased mobility of the UBC domain or dilution of the sample and similar domain-domain interactions as the crystal structure (Figure 5.28). Slight chemical shift changes were noted for two of the residues in the UBC domain involved in hydrophobic interactions, M140 and V151. These residues were identified by overlaying the full-length E2-25K and UBC domain NMR spectra, whereas the interaction of L147 could not be confirmed. However, it can not be definitively stated that the domain-domain interactions seen here are exactly the same as those seen in the crystal structure without the completion of the reverse experiment and a side-chain interactions comparison.

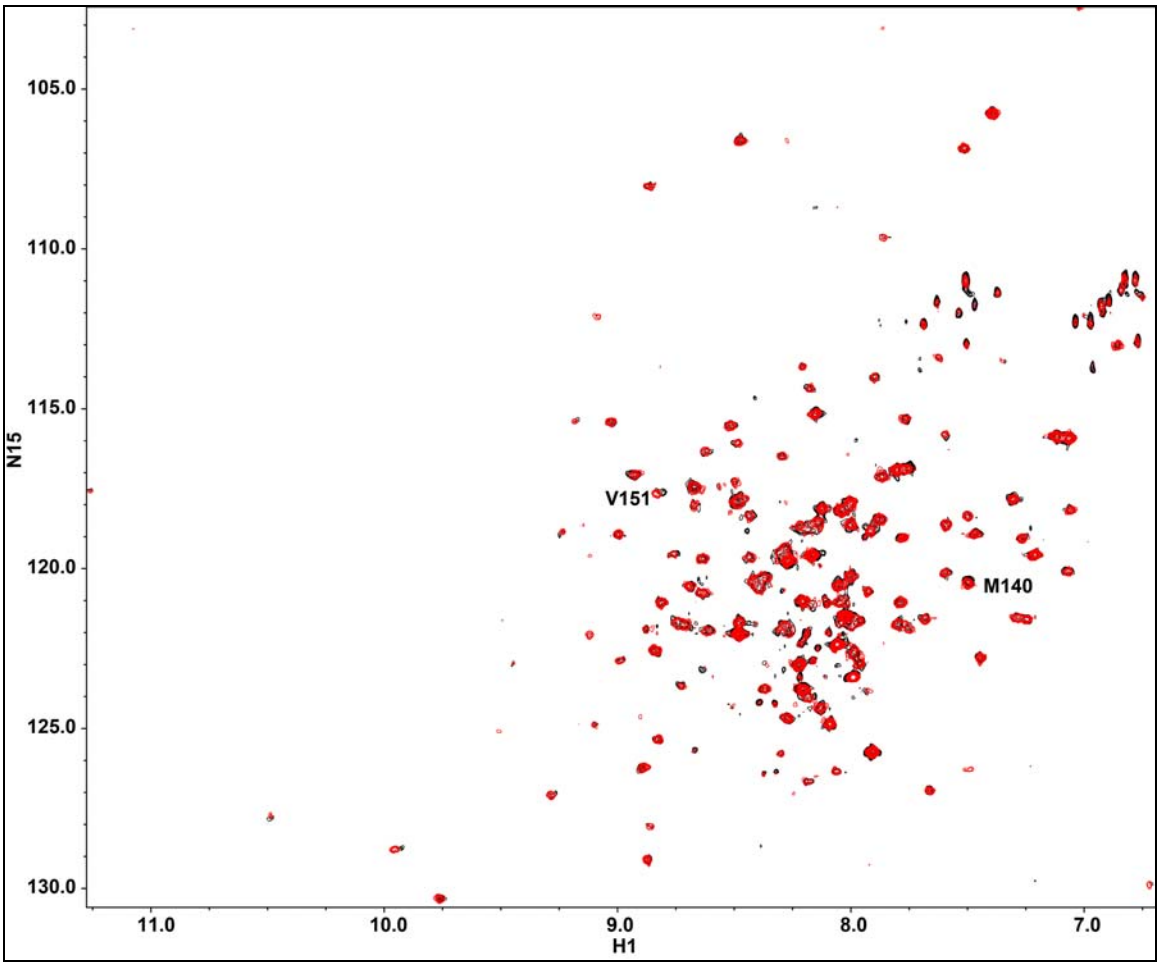

Figure 5.28 Specific Interactions of UBC/UBA Domain-Domain Interactions. [Titration of ^{15}N-labeled UBC domain with unlabeled UBA domain was followed by solution NMR spectroscopy. Overlay of the ^{1}H-^{15}N HSQC spectra of the UBC domain where black contours represent 0 equivalents of UBA domain added. Red contours represent 1 equivalents of UBA domain added.]

5.3 Conclusions

A series of binding studies with the ubiquitin conjugating enzyme E2-25K and Ub were conducted. The series of experiments involved binding to Ub with the wild-type protein, the UBC domain and the UBA domain. The NMR backbone assignments of full-length E2-25K and Ub at pH 7.4 have been completed. The binding constants for E2-25K/Ub and UBA domain/Ub interaction which have been determined by fluorescence and NMR spectroscopy revealed weak binding (Table 5.1), on the millimolar scale,

which is consistent with the value determined by surface plasmon resonance [84]. An interesting finding was the noticeable difference in binding of the full-length E2-25K and the UBA domain to uncleaved Ub.

NMR titration experiments of the full-length E2-25K and UBA domain with Ub and the reverse experiments were conducted to determine the non-covalent binding surfaces on each protein. The binding interfaces on the UBA domain and ubiquitin were used in calculating a UBA domain/Ub complex model (Chapter 6). The subsequent NMR binding experiments of full-length E2-25K and ubiquitin did not elucidate any additional binding surfaces within either protein. NMR titration studies of Ub with E2-25K at various temperatures including physiological conditions also did not reveal any additional residues within ubiquitin involved in binding to E2-25K. Furthermore, the interactions between the UBC and UBA domains were examined by NMR spectroscopy. The titration experiments revealed domain-domain interactions for M140 and V151, two of the residues in the UBC domain of the crystal structure believed to be involved in hydrophobic interactions with the UBA domain.

Table 5.1 Binding Constant Summary for E2-25K and UBA Domain with Ubiquitin

Method	**E2-25K**	**UBA Domain**
Fluorescence with cleaved Ub	193 ± 3.7 μM	149 ± 2.4 μM
Fluorescence with uncleaved Ub	4.5 ± 0.4 μM	13.8 ± 0.8 μM
NMR with unlabeled Ub	0.34 ± 0.22 mM	1.2 ± 0.3 mM
NMR with labeled Ub*	0.87 ± 0.1 mM	0.5 ± 0.2 mM

* Reverse titration experiments with labeled Ub and unlabeled E2-25K or UBA domain.

CHAPTER 6

E2-25K UBA STRUCTURE AND FUNCTION

One of the main goals of this research was to explore key aspects of the ubiquitin-conjugating enzyme E2-25K as it relates to synthesis of Lys48-linked polyubiquitin chains. As previously stated, E2-25K is a unique E2 ubiquitin-conjugating enzyme which contains an UBA domain C-terminal to the catalytic UBC domain and synthesizes Lys48-linked free polyubiquitin chains *in vitro* in the absence of an E3 ligase. In order to gain insight into E2-25K, the role of the unique C-terminal UBA domain as it relates to function and structural stability of E2-25K has been determined. In an attempt to further understand the UBA domain of E2-25K and the non-covalent binding to ubiquitin, the solution NMR structure of the UBA domain was calculated along with the subsequent modeling of the E2-25K UBA domain/Ub complex using HADDOCK.

6.1 NMR Studies of E2-25K UBA Domain

Chemical shift assignments for the backbone ^{1}H, ^{13}C, and ^{15}N resonances of the UBA domain were completed using a two-dimensional ^{1}H-^{15}N HSQC [117] spectrum and three-dimensional HNCACB, CBCACONH, and HNCO [108] spectra collected on $^{15}N/^{13}C$-uniformly labeled protein (Figure 6.1) (BMRB ID: 17195) [103, 118]. The chemical shifts were well resolved with the exception of F174, K186, W188, and Q195 in the HSQC spectrum.

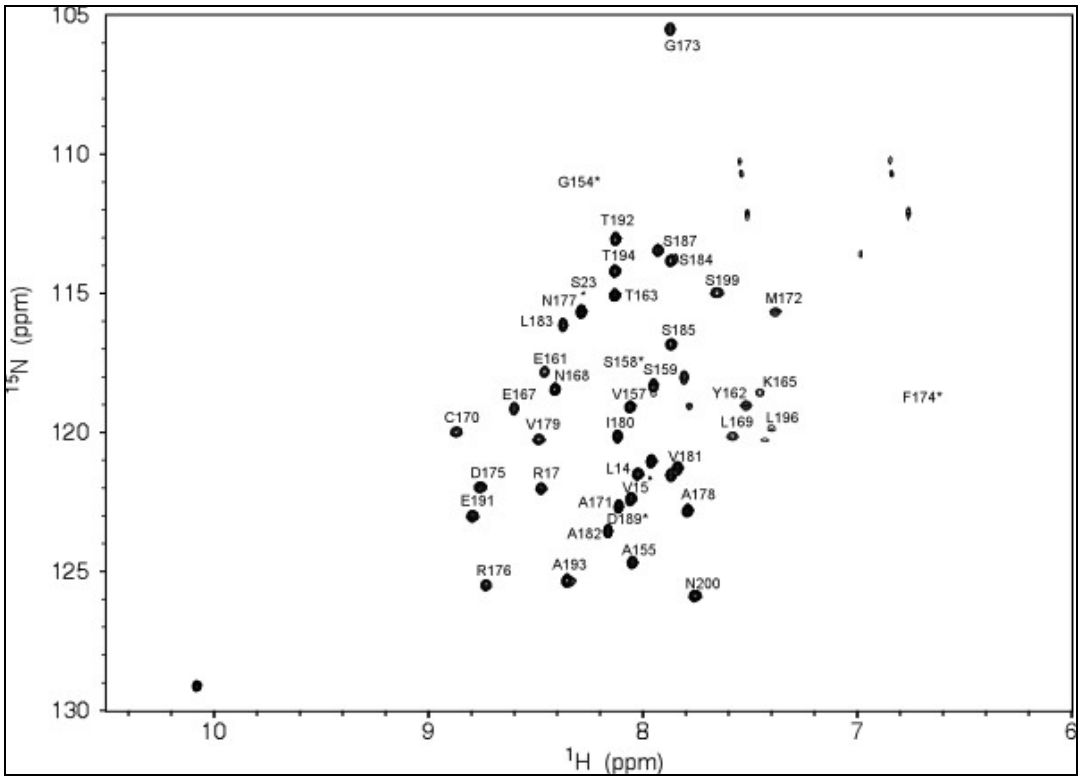

Figure 6.1 ^{1}H, ^{15}N-HSQC Spectrum of E2-25K UBA Domain. [The spectrum, with peaks labeled with the assigned amino acid residue, demonstrates the chemical shift dispersion and minimal overlap. Identified tag residues are labeled with number sign (#).]

Samples of two ^{15}N-labeled E2-25K UBA domain mutants, M172A and L198A, were expressed and concentrated to 0.4 mM in NMR sample buffer. These samples were used for the collection of two-dimensional ^{1}H-^{15}N HSQC spectrum [108] spectra and comparison with the wild-type E2-25K UBA domain, as shown in Figure 6.2. The NMR comparison was consistent with CD data (Figure 4.3) demonstrating that the mutant proteins do not have the same fold as the wild-type. This is in contrast to results from the same mutants in the full-length E2-25K (Figure 4.2). Furthermore, titration of UBA M172A (0.5 mM) with Ub (34.8 mM) was performed as with the UBA domain, with no noticeable changes in the chemical shifts or the structure, indicating binding did not occur between the mutant and Ub.

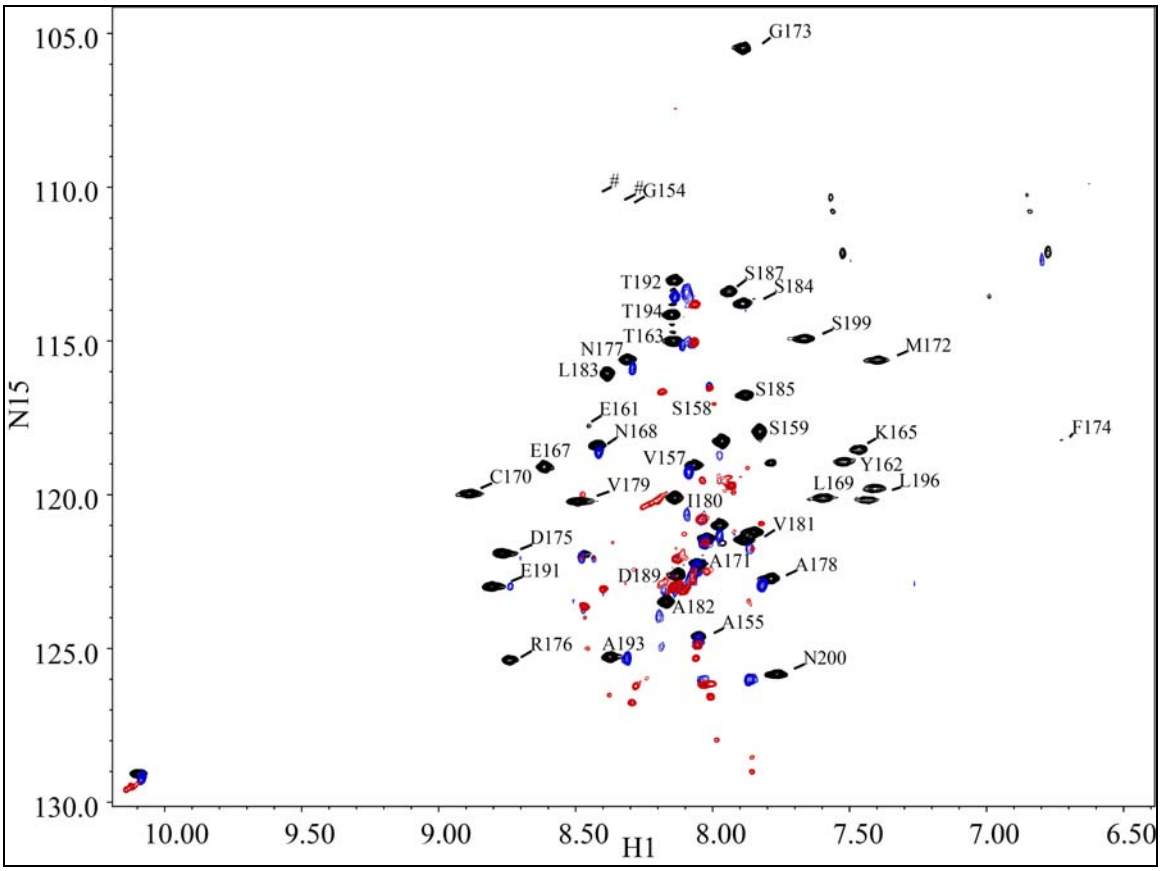

Figure 6.2 ^{1}H, ^{15}N-HSQC Overlay Spectra of the UBA Domain and UBA Domain Mutants, M172A and L198A. [The wild-type UBA domain spectrum is represented by the black contours; the UBA domain M172A mutant is represented by the red contours, and the UBA domain L198A mutant is represented by blue contours.]

6.2 Residual Dipolar Structure of the E2-25K UBA Domain

A model for the solution structure was calculated from the N-H residual dipolar couplings (RDC) (Section 2.8.1) and aligned with coordinates from the crystal structure of E2-25K M172A [78]. The domain was aligned to a local coordinate system for each of the three helices and then the independent helices were aligned to a common coordinate system [90]. The resulting structure was validated using *MolProbity* [40]. A Ramachandran plot calculated using *MolProbity* showed 92.9% (39/42) residues in the allowed regions. The three residues that fall outside the allowable regions are P156, V157, and F174, all of which are in flexible loop regions. These results, along with the

comparison of the experimental and back-calculated N-H RDC's (Figure 6.3), indicate that the UBA domain is independently folded and maintains an overall structure in solution similar to that found in the context of the full-length protein crystal structure (RMSD = 1.56 Å). The most marked differences occur in the third helix of the domain (Figure 6.4).

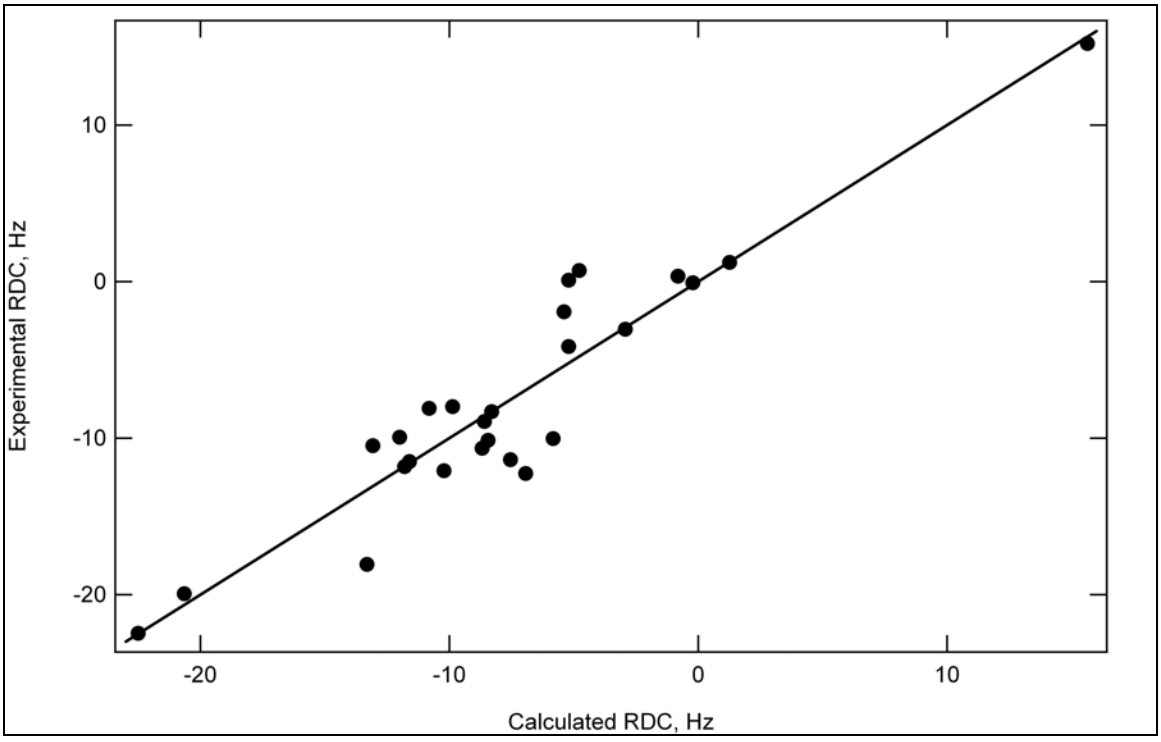

Figure 6.3 Plot of the Experimental vs. Back-calculated N-H RDCs from the E2-25K UBA Domain.

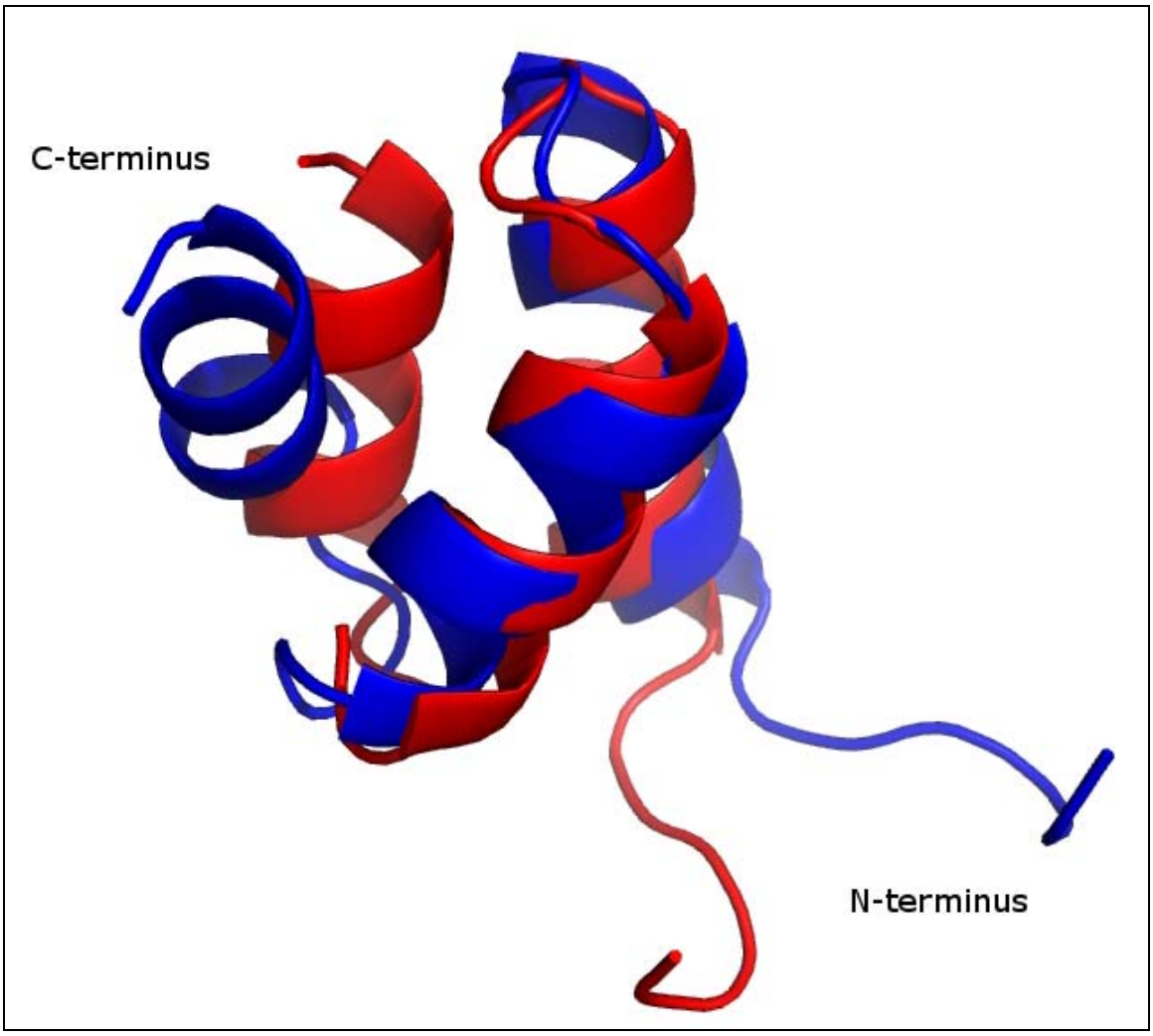

Figure 6.4 Comparison of the Calculated NMR and X-ray Crystallographic Structures of the E2-25K UBA Domain. [NMR model is shown in red, crystal structure (PDB code 3E46) in blue. The RMSD value of 1.56 Å reflects primarily differences in the position of the third helix.]

6.3 Modeling the UBA Domain and Ubiquitin Complex

The UBA domain/Ub complex structure model, shown in Figure 6.5, was calculated using the protein-protein docking approach, incorporating the chemical shift perturbation data from NMR titration analysis (Chapter 5). The program HADDOCK [119] was used to complete the docking using the UBA domain solution structure (Figure 6.4) and ubiquitin (PDB code 1UBQ [120]) proteins as the inputs.

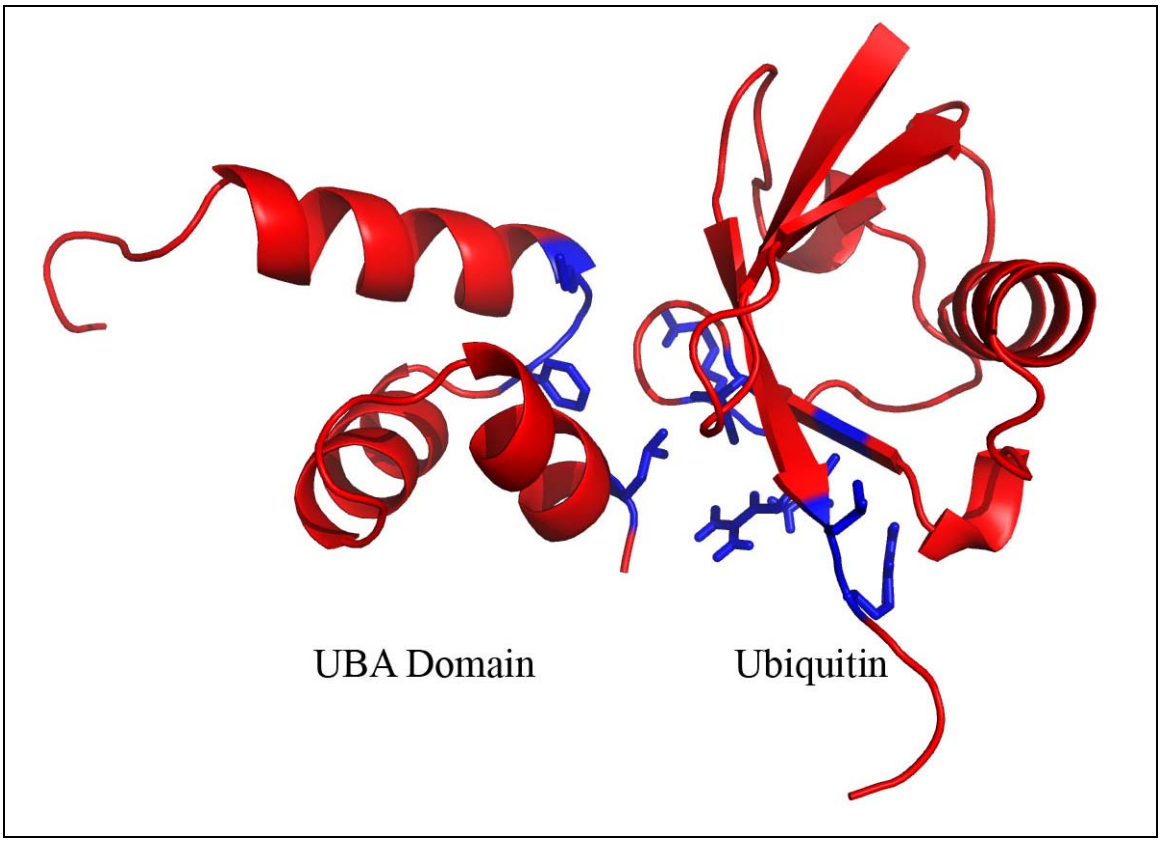

Figure 6.5 Modeled Complex Structure of E2-25K UBA Domain and Ubiquitin. [The active residues involved in binding are shown in blue.]

Active residues for each protein were selected based on similar criteria, which included relative positioning as related to the solvent and/or a $\Delta\delta$ greater than 0.15 ppm. The active residues involved in binding for the UBA domain included M172, G173, F174 and L198 (Figures 5.14 and 6.6) and residues L8, I44, A46, Q49, and L71 (Figures 5.18 and 6.7) were selected from the ubiquitin molecule. HADDOCK initially calculated one thousand structures by rigid body minimization. The lowest 200 energy level structures were selected for torsion angle dynamics and cartesian molecular dynamic calculations in water solvent. Three clusters were generated, but only one contained the majority of the structures. The 10 lowest energy UBA/Ub complex were selected (Figure 6.8) and validated using MolProbity [101]. A Ramachandran plot calculated

using MolProbity showed 94.9% (112/118) residues in the most favored regions and 98.3% (116/118) residues in the allowed regions. The two residues that fall outside the allowable regions are P156 and V157 of the UBA domain, both of which are in the flexible loop region at the N-terminal end of the domain.

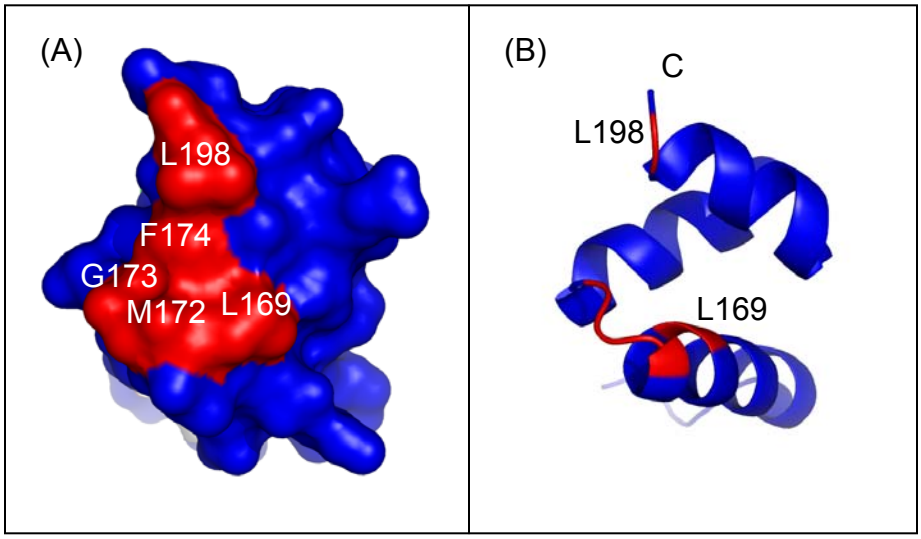

Figure 6.6 Surface Representation Showing the Ubiquitin Binding Site on the UBA Domain of E2-25K. [(*A*), surface representation of the UBA domain where *red regions* indicate surface residues having a significant chemical shift change upon ubiquitin binding. (*B*), ribbon diagram of the UBA domain with affected residues also *highlighted in red*.]

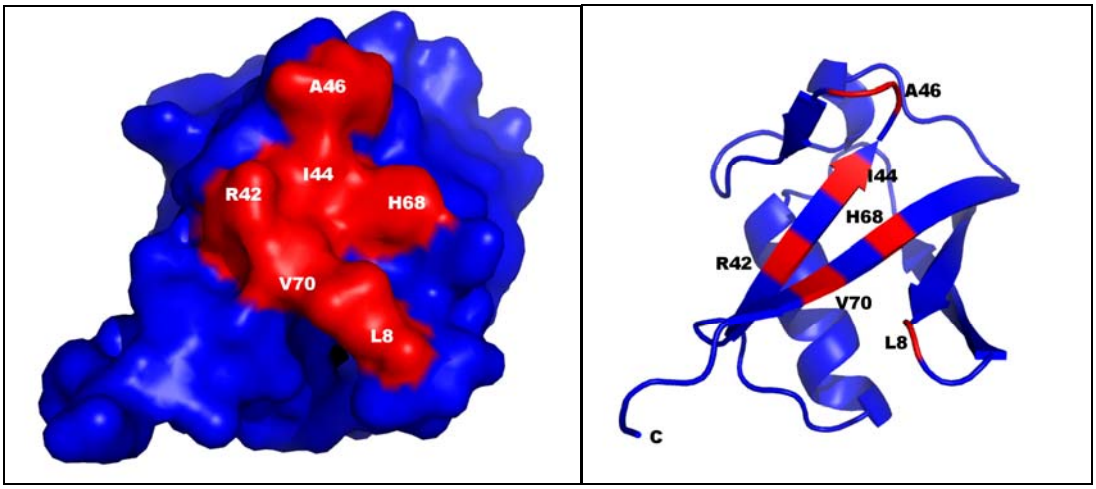

Figure 6.7 Surface Representation Showing the UBA Domain Binding Site on Ubiquitin. [(*Left*), surface representation of Ubiquitin where *red regions* indicate surface residues having a significant chemical shift change upon UBA domain binding. (*Right*), ribbon diagram of Ubiquitin with affected residues also *highlighted in red*.]

Figure 6.8 Complex Structure of E2-25K UBA Domain with Ubiquitin. [Backbone Cα traces for the ten refined UBA Domain (left) and Ub (Right) complex structures.]

6.4 Polyubiquitin Chain Assay

The polyubiquitin chain synthesis assays adapted from work performed by Piotrowski *et al.* [91] and described in Section 2.9 were used to determine the activity of E2-25K and its mutants, and to evaluate the function of the UBA domain. The assays contained no E3 ligase and no substrate other than ubiquitin itself. Assays comparing the abilities of the full-length E2-25K and the UBC domain to synthesize polyubiquitin chains from wild-type ubiquitin revealed that the UBA domain is required for efficient manufacture of chains larger than Ub_4 (Figure 6.9, Top gel Lanes 4 & 7, Bottom gel Lanes 5 & 8). The additional assays utilized two modified ubiquitin proteins Ub-K48C and Ub-D77 in equimolar ratios to restrict the chain length to diubiquitin, if only Lys48-

linked chains are formed [19]. With these restrictions, chain synthesis analysis by SDS page demonstrated that both full-length E2-25K and the UBC domain efficiently synthesized diubiquitin (Figure 6.9, Top gel Lanes 5 & 8, Bottom gel Lanes 6 & 9). However, chains larger than diubiquitin were also observed for the UBC domain, suggesting that in the absence of the UBA domain, alternative linkages may be used. Polyubiquitin chain assays in the presence of Ub-K48C alone confirmed that chains formed by full-length E2-25K are Lys48-linked (no chain synthesis is present), whereas UBC domain synthesizes polyubiquitin with alternative linkages (Figure 6.9, Top gel Lanes 6 & 9, Bottom gel Lanes 7 & 10), which is noted by the presence of diubiquitin and higher molecular weight proteins. In an attempt to clarify the exact polyubiquitin chain linkage, assays were conducted in the presence of Ub-K48C-K63C double mutant, and under these conditions alternative linkages were still produced (Figure A.8, Lanes 6 & 9). These results suggest that under these conditions the alternative linkages are not Lys-63 linked. These results further indicate a possible role for the UBA domain in positioning the acceptor ubiquitin in the correct orientation for specific Lys-48 chain synthesis.

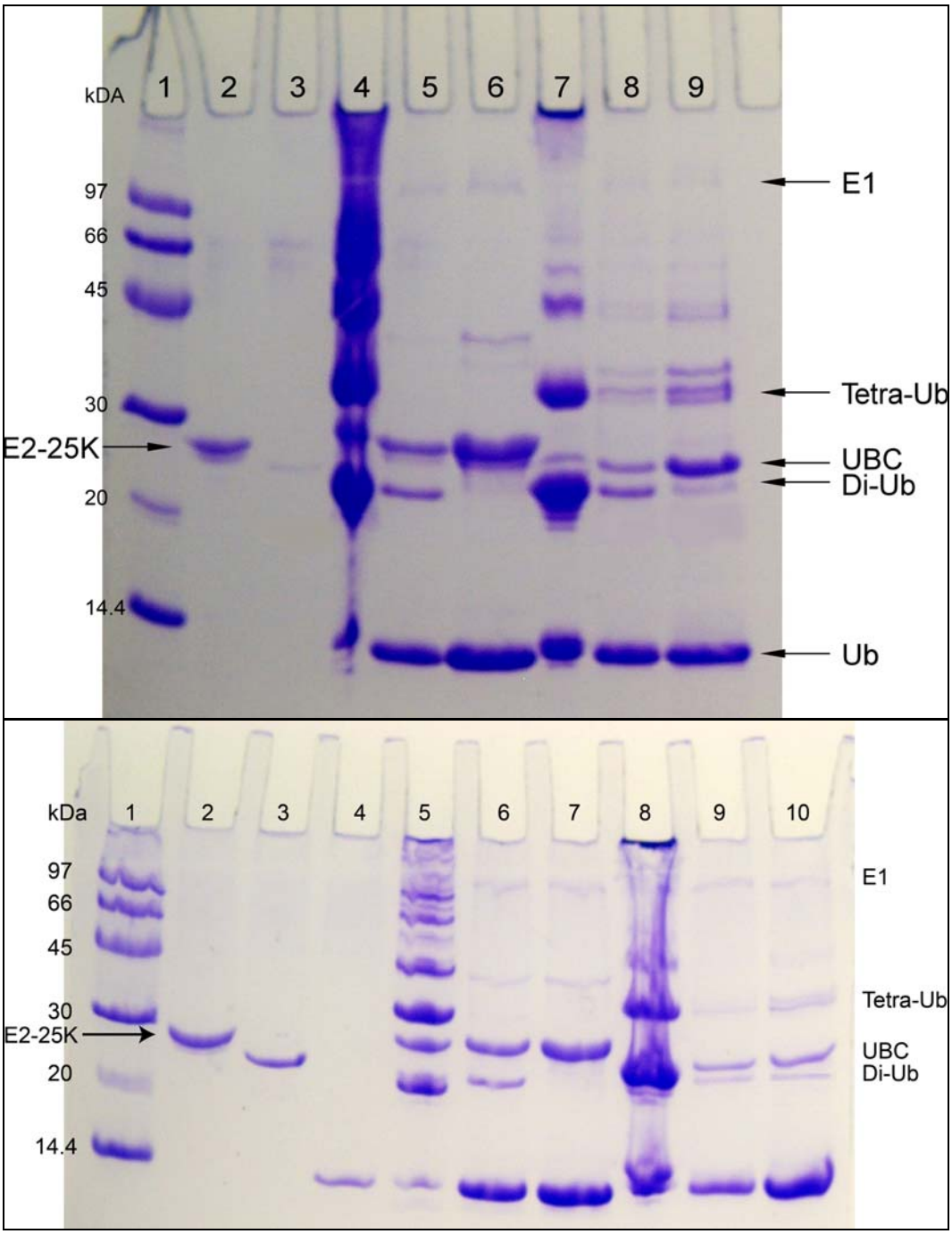

Figure 6.9 E2-25K/UBC Polyubiquitin Chain Assay. [SDS page of Polyubiquitin Chain Assays. **Top Gel** Lane 1 – LMW Marker, Lane 2 – E2-25K, Lane 3 – E2-25K UBC Domain, Lane 4 –E2-25K and wt Ub, Lane 5 –E2-25K and equimolar ratios of Ub-K48C and Ub-D77, Lane 6 –E2-25K and Ub-K48C only, Lane 7 –E2-25K UBC Domain and wt Ub, Lane 8 –E2-25K UBC Domain and equimolar ratios of Ub-K48C and Ub-D77, Lane 9 –E2-25K UBC Domain and Ub-K48C only. **Bottom Gel** Lane 1 – LMW Marker, Lane 2 – E2-25K, Lane 3 – E2-25K UBC Domain, Lane 4 –Ub, Lane 5 –E2-25K and wt Ub, Lane 6 –E2-25K and equimolar ratios of Ub-K48C and Ub-D77, Lane 7 –E2-25K and Ub-K48C only, Lane 8 –E2-25K UBC Domain and wt Ub, Lane 9 –E2-25K UBC Domain and equimolar ratios of Ub-K48C and Ub-D77, Lane 10 –E2-25K UBC Domain and Ub-K48C only.]

The polyubiquitin chain assays with equimolar ratios of Ub-K48C and Ub-D77 were also performed on the E2-25K mutants (C92S, K97R, and M172A) and compared to the wild-type E2-25K, UBC domain, and control E2 (UbcH5b) by SDS page analysis. The assays demonstrated that the E2-25K M172A and K97R mutants are still efficient in synthesizing diubiquitin (Figure 6.10, Lanes 7 & 8), whereas, the E2-25K C92S mutant (Figure 3.58, Lane 6) is significantly less efficient; however, this is to be expected due to the formation of the E2-25K~Ub complex (Chapter 4). The control E2 UbcH5b (Figure 6.10, Lane 10) is deficient as compared to the wild-type, UBC domain and other two mutants.

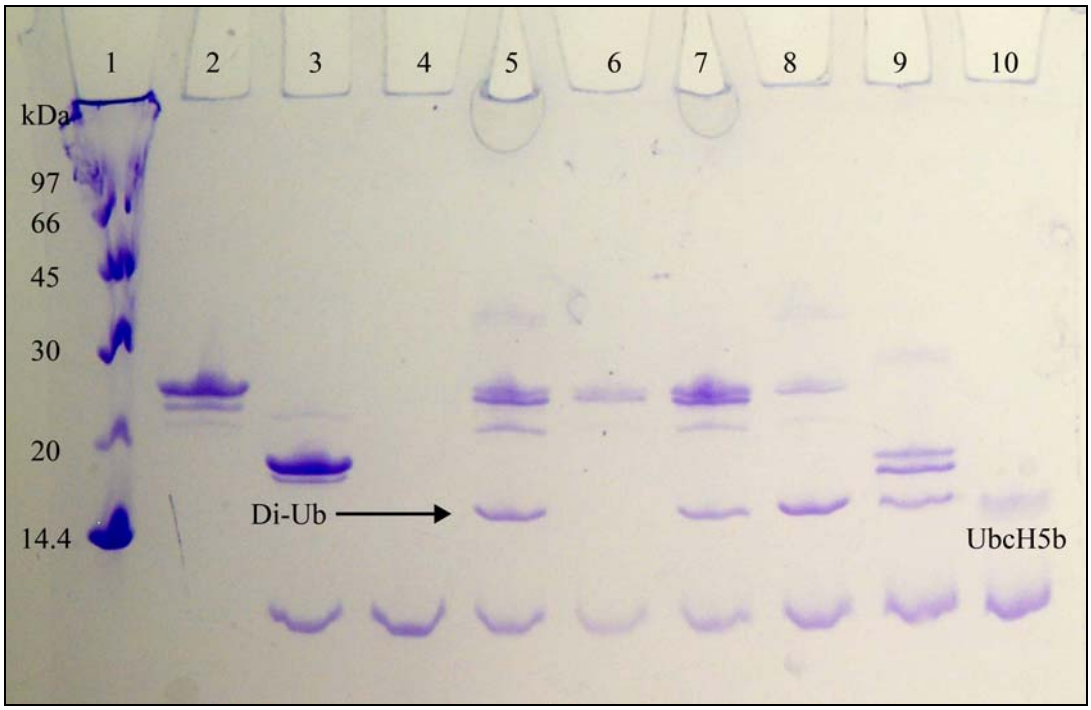

Figure 6.10 E2-25K Mutant Polyubiquitin Chain Assay. [SDS page of Polyubiquitin Chain Assays. Lane 1 – LMW Marker, Lane 2 – E2-25K, Lane 3 – E2-25K UBC Domain, Lane 4 – Ub-K48C, Lane 5 – Assay with wild-type E2-25K, Lane 6 – Assay with E2-25K C92S, Lane 7 – Assay with E2-25K K97R, Lane 8 – Assay with Assay with E2-25K M172A, Lane 9 – Assay with E2-25K UBC Domain, Lane 10 – Assay with UbcH5b.]

6.5 Conclusions

Comparison of the protein-protein interface of E2-25K's UBA domain in complex with ubiquitin reveals similarities seen in several other UBA/Ub complexes [115, 116, 121-123]. NMR data previously reported did not provide evidence for additional binding surfaces in E2-25K (Figures 5.20 and 5.21). Recently, the structures of E2-25K in complex with Ub and Ubb^{+1}, were reported [92] and are consistent with the complex presented here. These findings suggest that the E2-25K ubiquitin non-covalent interaction occurs primarily through the UBA domain in the absence of an E3 ligase or substrate.

Polyubiquitin chain synthesis assays of E2-25K in the absence of an E3 ligase (Figure 6.9) revealed deletion of the UBA domain does allow for the inefficient formation of alternative polyubiquitin chain linkages and decreased processivity. This indicates that the UBA domain may help direct Lys48-linked chain synthesis and chain length in the absence of an E3 partner. These data are consistent with a requirement for dimerization to direct chain linkage specificity in other E2 enzymes [40, 80]. It was previously reported that E2-25K exists as a monomer in solution and dimerization is not required for polyubiquitin chain formation (Chapter 5). These data suggest that the UBA domain of E2-25K mimics the presence of the non-catalytic E2 in a heterodimeric complex such as Mms2/Ubc13, which synthesizes free Lys63-linked polyubiquitin chains. The above structure and function of the UBA domain of E2-25K has been reported and published [124].

Other polyubiquitin chain synthesis assays of key E2-25K mutants, K97R within the active site of the UBC domain and M172A within the conserved MGF loop of the

UBA domain were also examined. Both mutants showed no decrease in Lys48-linked chain synthesis or alteration of polyubiquitin chain linkages. The M172A mutant findings are of interest because another key ubiquitin binding residue of the UBA domain, F174, was also shown not to interfere with Lys48-linked chain synthesis [91]. These findings suggest that even though M172 and F174 are key residues in binding Ub they are not essential for the function of the UBA domain. The K97R mutant findings are also of interest due to research on Ubc1, homolog in *S. cerevisiae*, where mutation of the equivalent lysine to an arginine eliminated Lys-48 linked polyubiquitin chain synthesis [102]. Further studies with Ubc1 alluded to a possible role for the UBA domain of limiting polyubiquitin chain length [32]. The contrasts in findings suggest that even though homologous functional differences are possible between E2-25K and Ubc1 without the presence of cooperating enzymes.

CHAPTER 7

E3 RECOGNITION SITE ON E2-25K

E2-25K interacts with multiple E3 ligases that determine the specificity of the cellular pathways affected (Table 1.1) [63, 65, 71-74]. The remaining goal of this research was to identify the key E2-25K residues involved in binding to three known RING E3 binding partners, RNF2, MDM2, and APC11. These three E3 ligases are well defined in the literature as E2-25K binding partners and represent multiple pathways of regulation. RNF2 (also called Ring1B) plays a role in histone H2A ubiquitination [125], Mdm2 regulates transcription through ubiquitination of p53 [126], and APC11 is involved in cell cycle regulation [127]. RING E3 ligases consist of a conserved region of Zn^{2+}-coordinating residues which are required for interaction with E2 ubiquitin-conjugating enzymes [128]. Sequence alignment of the RING domains of four known RING E3 binding partners for E2-25K yields very little similarity outside the Zn^{2+} coordinating residues (Figure 7.1). Therefore, investigating the binding of these three E3s should give insight into the specificity of E2-E3 binding. The interaction between E2-25K and the Ubl domain of Parkin was also examined, even though there has been no previous indication of binding between E2-25K and Parkin. The Ubl domain of Parkin was initially chosen as the control binding protein for Ub to E2-25K.

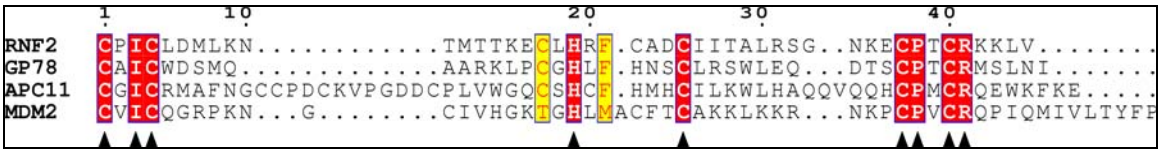

Figure 7.1 Sequence Alignment for RING E3 Ligases. [Highly conserved residues are indicated by a Triangle, Δ.]

7.1 Identification of E2-25K/E3 Binding Interface by Solution NMR

Binding of E2-25K to the three different E3s was examined by solution NMR using a series of two-dimensional ^{1}H-^{15}N HSQC experiments. Titration of full-length E2-25K (0.6 mM) with RNF2 (0.31 mM), APC11 (0.18 mM), and MDM2 (0.2 mM) were performed as with the ubiquitin (section 5.2.7), except only molar ratios of 0.14:1 RNF2/E2-25K, 0.16:1 APC11/E2-25K, and 0.21:1 MDM2/E2-25K (Figures 7.2 and A.4-A.6) were attainable. Although the binding constant could not be calculated, the amino acids that demonstrated chemical shift changes upon binding were identified and depicted by red bars in Figure 7.3. A consensus site, residues perturbed upon binding to all three E3s, was determined for the three E3 ring finger proteins (Figure 7.3, bottom) to demonstrate the consistent ring finger binding interface.

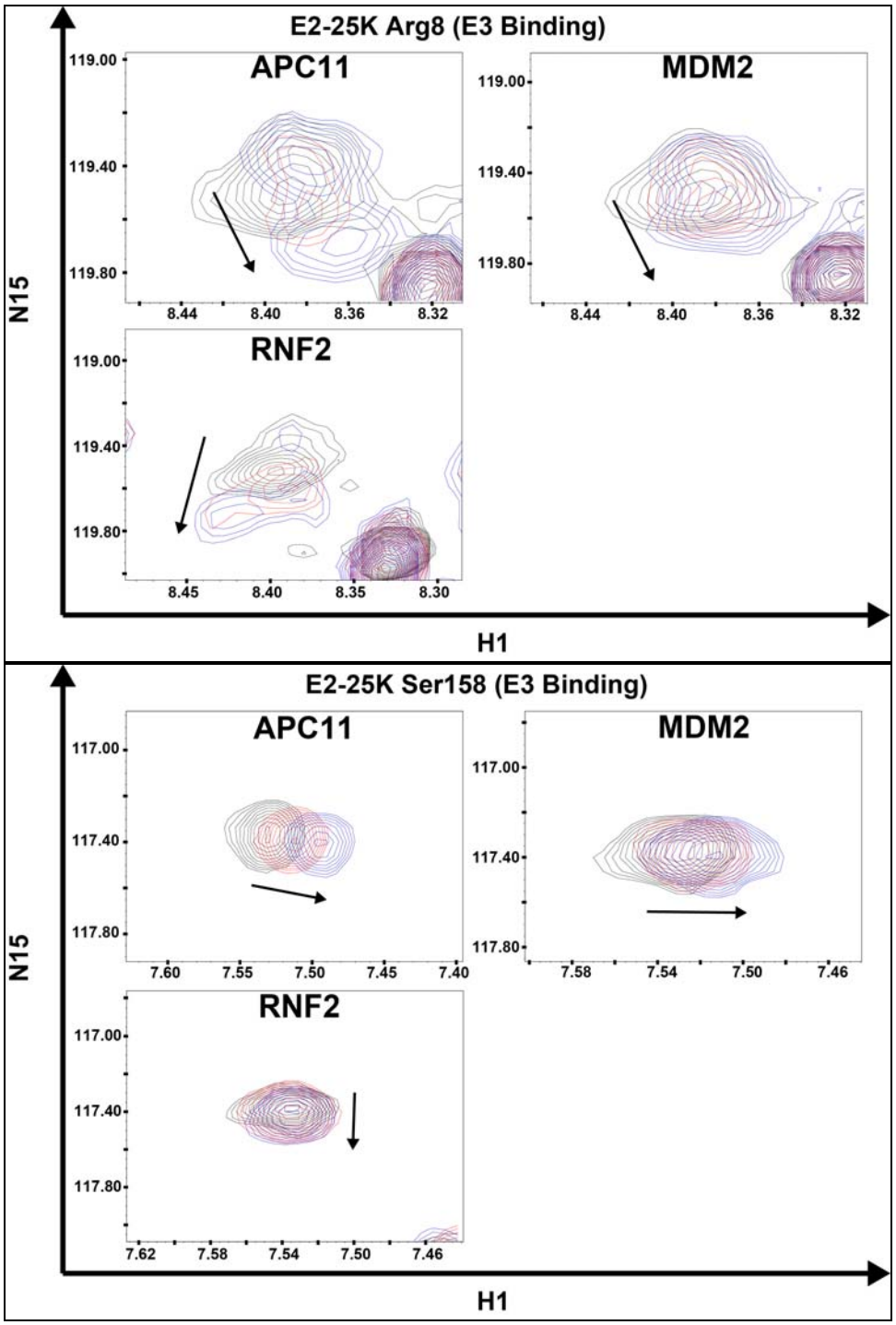

Figure 7.2 Chemical Shift Perturbations for E2-25K with RNF2, MDM2, and APC11. [Overlay of the ^{1}H-^{15}N HSQC spectra for residues R8 and S158 of the full-length E2-25K, where Black *contours* represent 0 equivalents, Red *contours* represent 0.07-0.08 equivalents, and Blue *contours* represent 0.14-0.21 equivalents of E3 added (See Figures A.4-A.6 for appropriate equivalents). Arrows indicate direction of shift as E3 concentration is increased.]

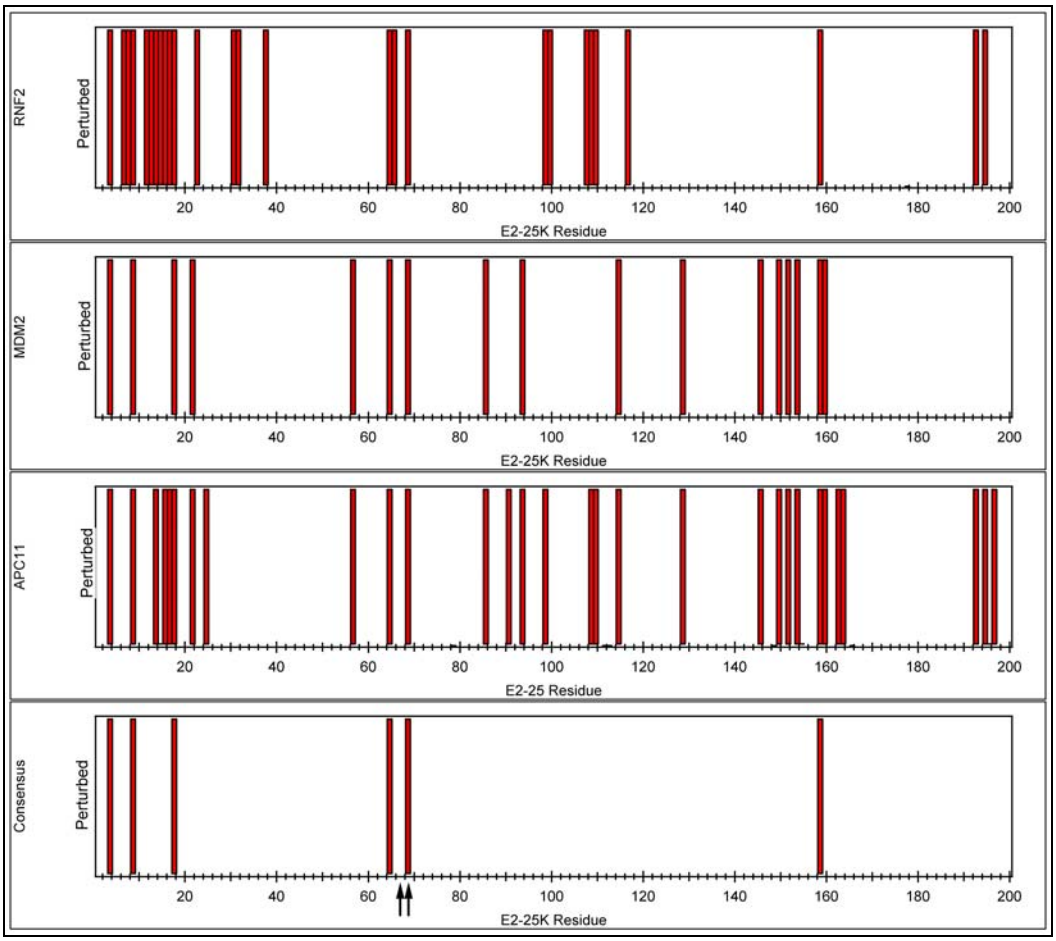

Figure 7.3 Interaction of E2-25K with RNF2, MDM2, and APC11. [Titration of ^{15}N-labeled E2-25K with unlabeled RNF2, MDM2, and APC11 was followed by solution NMR spectroscopy. Consensus plot are residues that are involved in binding to all three RNF2, MDM2 and APC11. Residues that demonstrated chemical shift changes upon binding are indicated by red bars. Arrows indicate conserved E3 binding residues.]

7.2 Identification of E2-25K/Parkin Binding Interface by Solution NMR

Binding of E2-25K to Parkin UBL was examined by solution NMR using a series of two-dimensional ^{1}H-^{15}N HSQC experiments. Titration of full-length E2-25K (0.62 mM) with Parkin Ubl domain (0.96 mM) was performed as with the ubiquitin, except that only molar ratio of 0.54:1 Parkin Ubl/E2-25K was reached before significant broadening of peaks led to loss of signal. The binding of E2-25K to Parkin UBL domain was unexpected and is similar to binding to Ub (Figure 7.4).

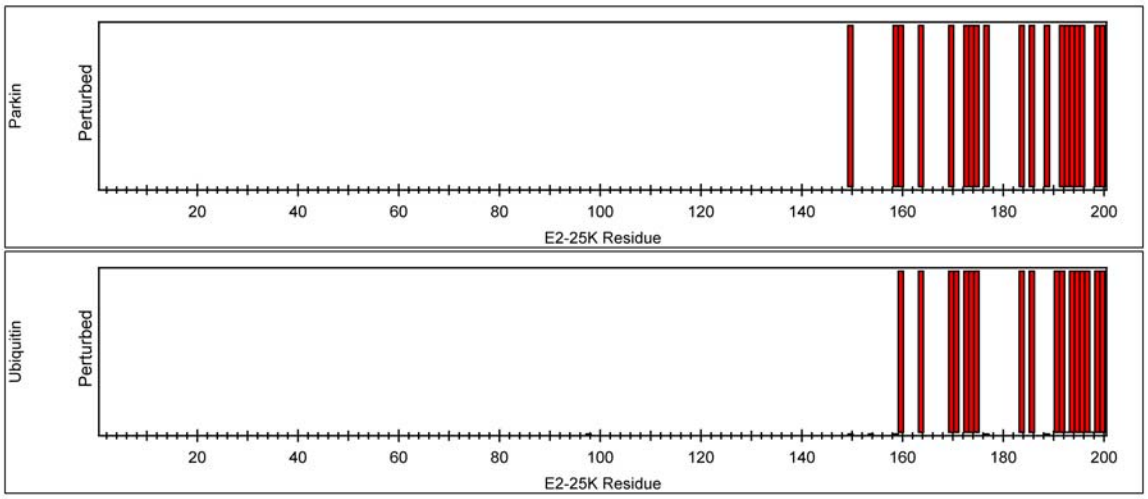

Figure 7.4 Interaction of E2-25K with Parkin Ubl Domain and Ubiquitin. [Titration of ^{15}N-labeled E2-25K with unlabeled Parkin Ubl domain and Ub was followed by solution NMR spectroscopy. Residues that demonstrated chemical shift changes upon binding are indicated by red bars.]

The binding of the UBA domain to Parkin Ubl domain was confirmed by analyzing the sample on 15% native gel electrophoresis. The presence of additional bands on the native gel (Figure 7.5 lanes 7, 9, & 11) and the slight disappearance of the major Parkin Ubl domain band (Figure 7.5 lanes 7 & 9) confirms the binding of Parkin Ubl domain to the UBA domain. Chemical shift changes for E2-25K upon binding to Parkin Ubl domain were noted only for a small subset of resonances within the UBA domain (Figures 7.4 & A.7), indicating specific regional binding. Broadening of many peaks also occurred as a result of titration, which confirms formation of a Parkin:E2-25K complex. Plots of chemical shift differences versus the molar ratio of unlabeled Parkin Ubl domain to E2-25K (Figure 7.7) are indicative of a single weak binding site. The perturbed residues fall primarily in the MGF loop between helices 1 and 2 of the UBA domain and in the adjacent face of helix 3, which is similar to the Ub binding site. Using the existing NMR data, the estimated K_d for binding of Parkin Ubl domain is

approximately 1.5 mM (Figure 7.7), which is the same as the K_d for binding to Ub, 1.2 mM (Figure 5.15), within the error of the experiment.

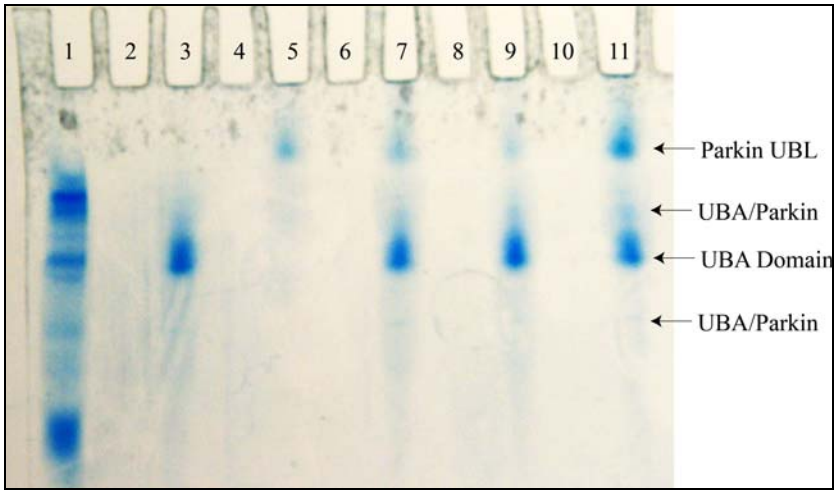

Figure 7.5 Native Gel for UBA Domain and Parkin Binding. [15% native gel - Lane 1 – LMWM, Lanes 2,4,6,8,10 – empty, Lane 3 – Pure UBA domain, Lane 5 – Parkin, Lane 7 – UBA domain plus Parkin (1 to 1 ratio), Lane 9 – UBA domain plus Parkin (1 to 0.5 ratio), Lane 11 – UBA domain plus Parkin (1 to 2 ratio).]

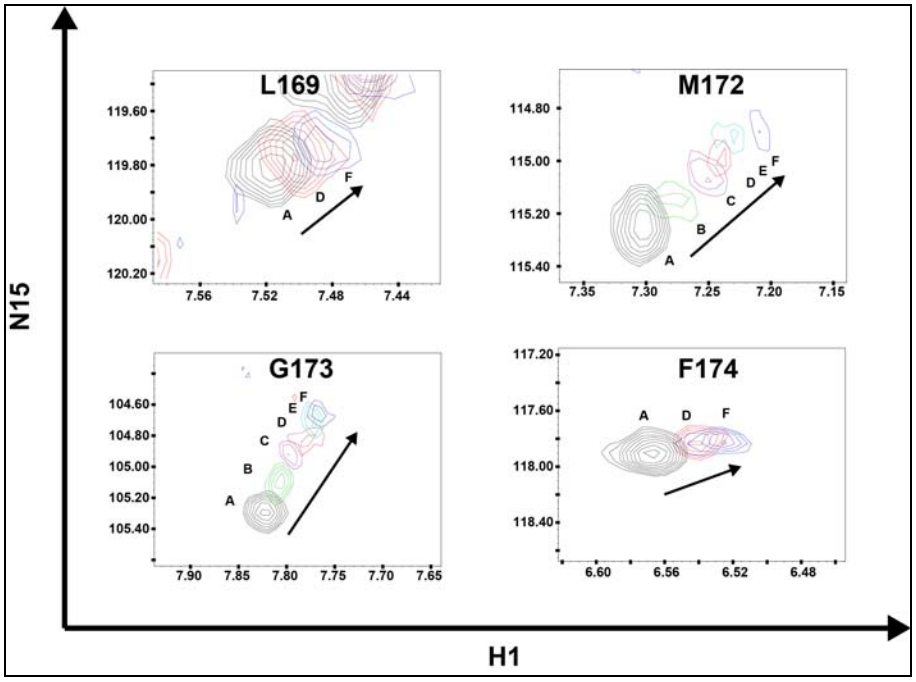

Figure 7.6 Chemical Shift Perturbations for E2-25K with Parkin. [Overlay of the ^{1}H-^{15}N HSQC spectra for residues L169, M172, G173, and F174 in the UBA domain of the full-length E2-25K, where *contours* labeled (A) represent 0 equivalents, (B) represent 0.11 equivalents, (C) represent 0.22 equivalents, (D) represent 0.32 equivalents, (E) represent 0.43, and (F) represent 0.54 equivalents of Parkin added. Arrows indicate direction of shift as Parkin concentration is increased.]

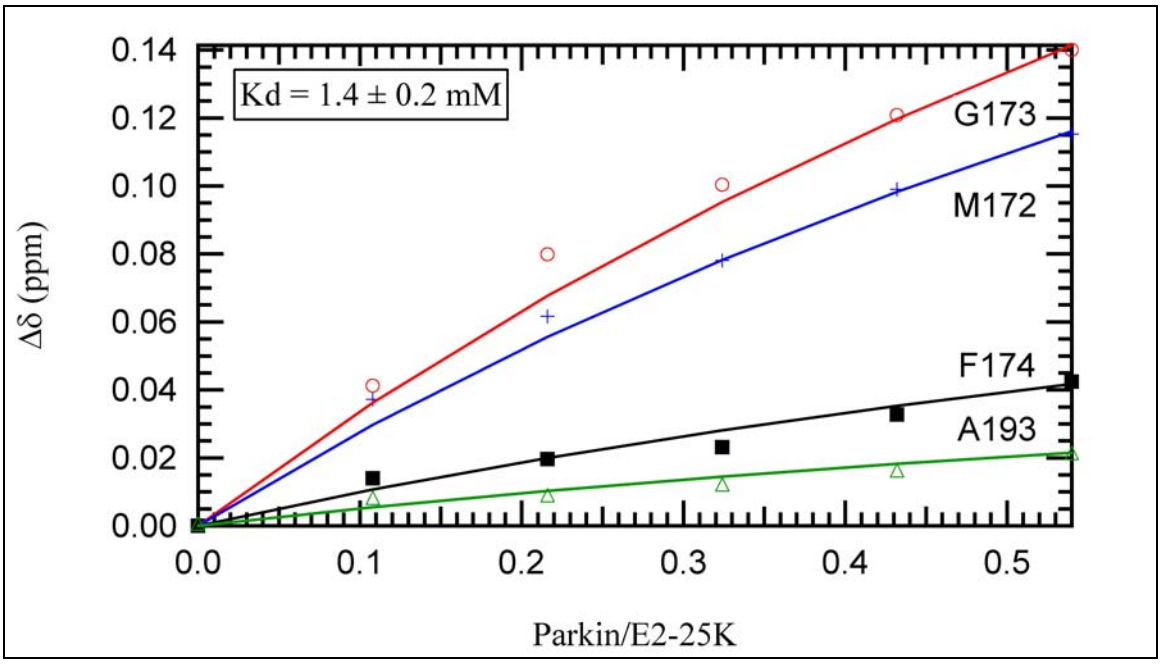

Figure 7.7 Binding Curves for E2-25K to Parkin Ubl Domain. [Plots of chemical shift differences versus the molar ratio of unlabeled Parkin Ubl domain to E2-25K are global fitted using the single site binding model (equation 5.3) to achieve an overall K_d and are indicative of a single binding site.]

7.3 Conclusions

Comparison of the protein-protein interface of E2-25K in complex with three different RING E3s revealed similarities seen in several other E2-E3 complexes [45, 46]. E2s bind to RING E3s through a hydrophobic interaction via a conserved proline-phenylalanine (P67 and F68 in E2-25K) sequence [45, 46]. Titration experiments revealed that only six perturbed residues were common to binding by all three RING E3s (Figure 7.3), N3, R8, L17, E64, F68, and S158. Of the six residues perturbed upon binding only S158 falls outside the N-terminal region (Figure 7.8). Further examination of the local environment of S158 and its surrounding residues revealed that S158 resides in the flexible loop region between the UBC and UBA domains. Therefore it can be speculated that upon binding to RING E3s, the interaction between the UBC and UBA

domains are perturbed or undergo structural changes. These conclusions can be confirmed by the chemical shift perturbations noticed in other residues involved in domain-domain interactions that are perturbed upon binding to the three different E3s. Furthermore, it is believed that residues surrounding the conserved Pro-Phe sequence on the E2s are what dictate the specificity of E2-E3 binding. This hypothesis is supported by the divergence in residues seen upon titration of the three different RING E3s, where patterns are noticed but not always consistent.

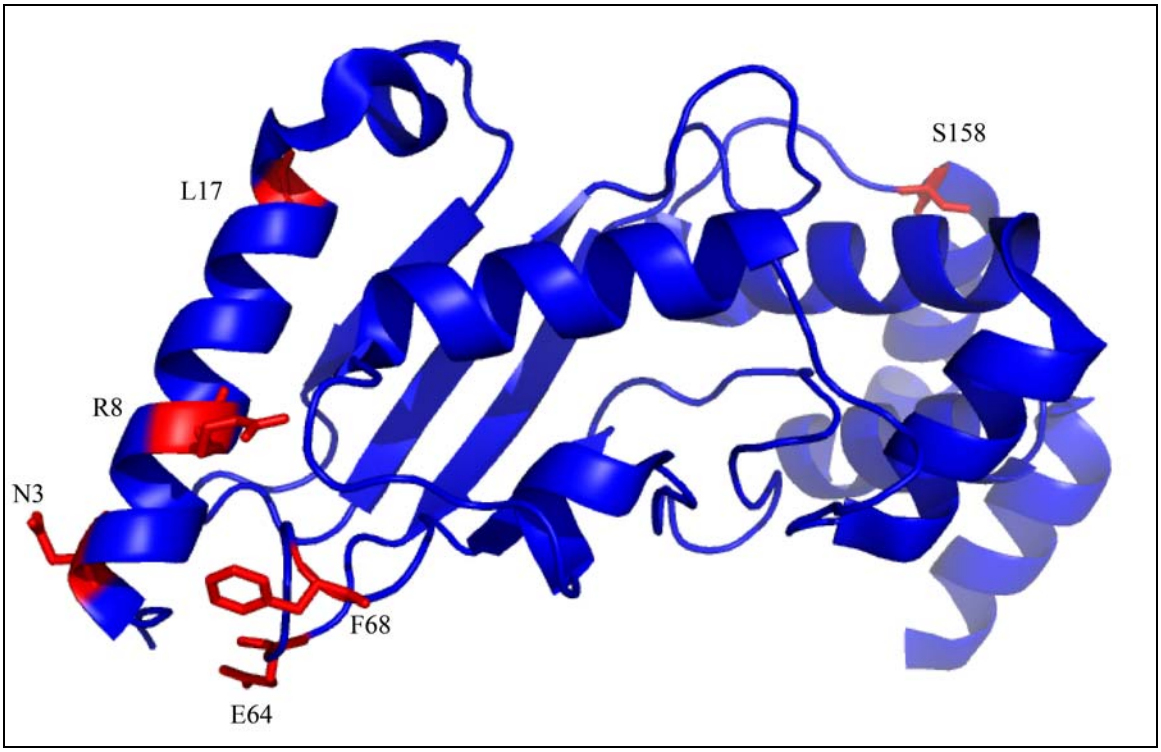

Figure 7.8 Ribbon Diagram of the RING E3 Binding Residues on E2-25K. [Six residues perturbed upon binding to all three RING E3s are labeled and *highlighted in red*.]

The interaction between E2-25K and the Ubl domain of Parkin was also examined to serve as a control protein for binding of Ub. Unexpectedly, binding was observed similar to ubiquitin even though there have been no previous interactions reported between the two. It was generally thought that UBA domains recognize and bind to

ubiquitin-like (Ubl) domains, but these interactions have not been widely observed. The interaction between a UBA and Ubl domain has only been observed in Dsk2 and Rad23, where both domains within the same protein interact to form a homodimer [129, 130]. The results reported here show a K_d 1.4 mM to the Ubl domain of Parkin that is consistent with ubiquitin, 1.2 mM. These results, along with the recent discovered interaction with SUMO [59], open up other possible functions and pathways for E2-25K and its UBA domain.

CHAPTER 8

DISCUSSION AND CONCLUSIONS

E2-25K is a unique ubiquitin-conjugating enzyme that contains an additional C-terminal ubiquitin binding domain along with the conserved catalytic UBC domain. E2-25K has been identified as a key E2 in the ubiquitin proteasome system that interacts with proteins involved in the endoplasmic reticulum-associated response to cellular stress, cell cycle regulation and apoptosis. E2-25K has also been shown to play a role in mediating cellular toxicity in diseases of protein misfolding such as Alzheimer and Huntington. E2-25K also has the unique ability to synthesize Lys48-linked free polyubiquitin chains *in vitro* in the absence of an E3 ligase or helper E2.

The presence of a UBA domain in E2-25K is unique among E2s and its function has not previously been determined. There are several possible functions for the UBA domain of E2-25K. It may serve as an additional protein-protein interaction site for selecting previously monoubiquitinated substrates for polyubiquitin chain elongation/transfer, it may function as a scaffold to position acceptor ubiquitin molecules for chain building or it may function to mediate dimerization through contact with a covalently-linked ubiquitin on an adjacent molecule. These are all definite possibilities because it has been shown that the E2-25K UBA domain preferentially binds Lys63-linked polyubiquitin chains with a K_d of 27 μM [84]. Numerous other studies have also

examined binding of various UBA domains with ubiquitin [114, 115, 122, 131-135] and have shown a range of binding affinities along with diversity in the mode of interaction.

The goals of this research were to characterize the three-dimensional structure of E2-25K using X-ray crystallography and solution NMR spectroscopy. NMR spectroscopy was further used to map the relevant binding surfaces of E2-25K required for interaction with three RING E3 ubiquitin-ligase partners, ubiquitin, and the Ubl domain of Parkin. The unique C-terminal UBA domain was examined for function and contribution to structural stability of E2-25K. Furthermore, the oligomerization state of E2-25K was examined in order to elucidate the need for dimerization in polyubiquitin chain formation. These results will be used to help define the manner in which E2-25K adapts to multiple pathways and ultimately in determining the mechanism of polyubiquitin chain formation.

Much work has been done towards characterizing the thioester bond formation of E2s. However, because of the instability of the thioester bond, the exact details of the transfer of ubiquitin to the E2 and subsequently to the substrate are still unknown [11]. Research also suggests that the mechanism for transfer of ubiquitin from the E2 to the substrate protein may be like that proposed in the formation of other isopeptide bonds [11] where the isopeptide bond is formed by a lysine sidechain in the substrate attacking the E2 thioester. However, in order for this to occur, a base is required near the active site to stabilize the approaching negative charge or deprotonate the incoming lysine residue. Structural studies of E2-25K and E2 enzymes in general have not elucidated a catalytic group, typically a histidine or glutamine, which could be responsible for the deprotonation of the catalytic cysteine. Furthermore, comparing both M172A crystal

structures with the wild-type structure reveals that most side chains in the active site of E2-25K are conformationally similar. The exception is the sidechain of Lys-97, which exhibits multiple rotamer conformations as a function of differing crystallization conditions. The pH dependent differences in the position of Lys-97 relative to the catalytic cysteine (Cys-92) suggest that it may play a role in catalysis. Studies with Ubc1, the E2-25K homolog in *Saccharomyces cerevisiae,* have shown that Lys-93 (homologous to Lys-97) is critical for *in vitro* synthesis of polyubiquitin chains [102]. Hodgins et al. demonstrated that mutating this lysine residue to an arginine eliminated polyubiquitin chain formation, which is in contrast to evidence reported here. This is of interest because there are other E2s (UbcH5 family) that contain arginine in this position [64, 136]; however, these E2s are deficient in the synthesis of polyubiquitin chains *in vitro*. Lys-97 has also been shown to serve as an ubiquitin acceptor site and/or auto-ubiquitination site [102], which would suggest that E2-25K is capable of self-regulation. Additionally, research on three different E2s (UbcH10, Ubc2, Ubc13) has shown that the catalytic cysteines have a unusually high intrinsic pK value (~10) that is due to their surrounding residues [137]. Therefore, based on these data and observations in the crystal structures, Lys-97 could be acting as an acceptor site for the transfer of a conjugated ubiquitin and/or involved in stabilizing the local pH environment around the active site. Additionally, there are a few key residues located N-terminal to the catalytic cysteine that are absolutely conserved among all E2s: His-81, Pro-82, and Asn-83. Of these residues it was originally hypothesized that Asn-83 was critical for the E2 catalytic site fold because of hydrogen bond formation, however recent work has shown that Asn-

83 is not critical for the hydrogen bonding network, but could be involved in stabilizing the oxyanion intermediate [39].

The X-ray crystal structures further revealed a domain-domain interface between the UBC and UBA domains that consists of hydrophobic interactions involving residues Met-140, Leu-147, and Val-151 (helix 5) of the UBC domain and residues Ile-166 (helix 6) and Ile-180 (helix 7) of the UBA domain. These domain-domain interactions were further examined by NMR spectroscopy to determine if the interactions observed in the crystal structures were crystallographically induced. NMR titration experiments confirmed interactions for Met-140 and Val-151. These domain-domain interactions suggest cooperativity between the two domains that was not previously reported.

Biophysical studies confirmed the overall fold of E2-25K was not altered by the presence of the specific mutants, M172A and L198A, and that both domains are independently folded. Thermal denaturation studies demonstrate that the presence of the UBA domain is thermally stabilizing to the full-length protein. These findings, in conjunction with the structural flexibility observed in the UBC domain NMR spectrum, are of biological relevance because noticeable differences were also observed in the functional efficiency assays of the UBC Domain. The decreased processivity of polyubiquitin chain synthesis by the UBC domain leads to one hypothesis that thermal stability, in the presence of the UBA domain, could be a contributing factor in the increased efficiency of the full-length protein, in term of decreased mobility of the protein. This hypothesis is further confirmed by the conformational stability observed in the NMR spectrum for the full-length E2-25K protein as compared to the UBC domain.

Of further interest was the observation in the DSC experiment that indicated the melting of the full-length E2-25K protein occurred as a single unit instead of two independent domains. These data would indicate that there is a cooperativity between the two domains suggesting that the two domains are not independent. However, CD and structural analysis confirm that both the UBC and UBA domains to have similar folds independent of each other. Functional analysis confirms that both domains exhibit the same functions independently as they exhibit in the full-length protein. These findings, taken with the ability of the UBA domain to direct chain linkage specificity in the full-length protein, would further support the argument for cooperativity between two independent domains that are tethered or linked together. It remains unclear if these two independent domains would function cooperatively without the presence of or with a longer inter-domain linker. Evidence for the latter case may be seen in Ubc1, an E2-25K homolog, which exhibits similar functionality, in terms of chain processivity, to the UBC domain alone.

The NMR backbone assignments of full-length E2-25K and ubiquitin were used in surface and binding constant determinations. The titration experiments of full-length E2-25K and UBA domain to ubiquitin revealed weak binding, on the millimolar scale, which is consistent with the value determined by surface plasmon resonance [84]. NMR titration experiments also confirmed that the non-covalent ubiquitin binding surfaces in E2-25K occur primarily through the UBA domain in the absence of an E3 ligase or substrate. In other words, no additional binding surfaces within full-length E2-25K or ubiquitin were elucidated from NMR experiments. Examination of the protein-protein interface of E2-25K's UBA domain in complex with ubiquitin reveals similarities seen in

several other UBA/Ub complexes [115, 116, 121-123]. These findings, along with the subsequent UBA/Ub model, are also consistent with the recent X-ray crystal structure complex of E2-25K with Ub and Ubb^{+1} [92].

The noticeable difference between binding of the full-length E2-25K and the UBA domain to uncleaved ubiquitin was of particular interest due to structural similarities of uncleaved ubiquitin to linear diubiquitin and Lys63-linked polyubiquitin chains. The E2-25K UBA domain has been shown to preferentially bind Lys63-linked polyubiquitin chains [84], which is notable because of E2-25K's propensity to make Lys48-linked polyubiquitin chains. The difference in binding affinity can be explained by examining the recent structural work on Lys48-linked and Lys63-linked polyubiquitin chains [138, 139]. Close examination of the two polyubiquitin chain species demonstrated an open or elongated configuration for Lys63-linked chains (Figure A.10, bottom), whereas the configuration of the Lys48-linked chains are more closed or compact (Figure A.10, top). Therefore, the preferential binding of the UBA domain to Lys63-linked polyubiquitin chains is potentially a case of accessibility to the preferred binding site on Ub, rather than a preference for these types of polyubiquitin chains. However, it cannot be definitively stated that this preference is seen *in vivo.* It can be stated that the UBA domain has a higher propensity to bind polyubiquitin chains than monoubiquitin. This suggests a potential function for the UBA domain of binding to previously conjugated ubiquitin chains.

Several studies look at the potential for E2-25K to function normally in the absence of the UBA domain. Initial studies suggested that the UBA domain was

essential for the polyubiquitin chain synthesizing activity [77]. Removal of the UBA domain resulted in a non-functional E2-25K; however, subsequent research indicated that the location of the truncation was of critical importance. Slightly longer constructs (still missing the UBA domain) were able to catalyze polyubiquitin formation [59], although the processivity was impaired relative to full-length E2-25K. Polyubiquitin chain synthesis assays of E2-25K in the absence of an E3 ligase conducted here showed that deletion of the UBA domain does allow for the inefficient formation of alternative polyubiquitin chain linkages and decreased processivity [140]. This indicates that the UBA domain may help direct Lys48-linked chain synthesis and increase chain lengths in the absence of an E3 partner by binding to or positioning previously conjugated ubiquitin chains. These data are also consistent with a requirement for dimerization to direct chain linkage specificity in other E2 enzymes [40, 80]. Other E2s have been noted to function in dimer complexes [82, 141], and initially it was thought that the function of the UBA domain of E2-25K was to assist in dimer formation. Complex assays in conjunction with size-exclusion chromatography were used to determine that E2-25K exists as a monomer in solution and that dimerization is not required for polyubiquitin chain formation. These findings might suggest that dimerization is not required for E2-25K because its unique UBA domain mimics the presence of the non-catalytic E2 by positioning the acceptor Ub. This mechanism is seen in the heterodimeric complex requirement of Mms2/Ubc13 that synthesizes free Lys63-linked polyubiquitin chains.

Studies of enzymatic activity with Ubc1, an E2-25K homolog in *Saccharomyces cerevisiae*, alluded to a possible role for the UBA domain in limiting ubiquitin chain length [32]. Truncated constructs of Ubc1 missing the UBA domain demonstrated

synthesis of longer polyubiquitin chains than the full-length Ubc1. This is in contrast to the evidence presented here for enhancement of processivity in the presence of the UBA domain. However, unlike this work, the experiments with Ubc1 were conducted in the presence of both an E3 ligase and a substrate. These conditions may alter the effect of UBA/Ub binding. Alternatively, the Ubc1 protein, which has a much longer, flexible linker connecting the UBC and UBA domains, may function in a different manner from E2-25K, as seen by the differences on the K97R mutation. Future studies with E2-25K will explore the effect of E3 ligase partners on processivity.

Other polyubiquitin chain synthesis assays of key E2-25K mutants; C92S and M172A were also examined. The M172A mutant showed no decrease in Lys48-linked chain synthesis or alteration of polyubiquitin chain linkages. These M172A mutant findings are of interest because another key ubiquitin binding residue of the UBA domain, F174, was also shown not to interfere with Lys48-linked chain synthesis [91]. These findings suggest that even though M172 and F174 are key residues in binding Ub, alone they are not essential for the function of the UBA domain. The function of the E2-25K L198A mutant was not verified due to structural instability. Although CD experiments verified that the secondary structure of the L198A was similar to the wild-type protein, these experiments were conducted with the expression tag still attached. In order for the protein to be functional, the expression tag must be removed to allow access to the apparent E1 binding surface. Cleavage of the expression tag from the E2-25K L198A mutant resulted in protein aggregation or misfolding, which was similar to what was observed in the same mutation in UBA domain alone. These data would further support the argument for cooperativity between the two domains by demonstrating a

single mutation destabilizes the entire protein, but structural examination did not reveal an immediate explanation for this phenomenon.

Since E2-25K RING E3 binding partners were identified by the use of a yeast two-hybrid screen instead of using functional assays [63], a understanding of the interactions with RING E3s is crucial for understanding the function of E2-25K. Recent studies indicated that E2-25K functions as a "second-step" E2 by recognizing protein substrates that have already been monoubiquitinated by another E2 [64, 65]. A comparison of the protein-protein interface of E2-25K in complex with three different RING E3s, RNF2, MDM2, and APC11, revealed E2-25K binds to RING E3s through a hydrophobic interaction via a conserved proline-phenylalanine (P67 and F68 in E2-25K) sequence as seen in other E2-E3 complexes [45, 46]. These observations suggest that *in vitro* E2-25K has the same preference of binding to RING E3s as other E2s. However, examination of the one consensus residue not in the N-terminal region location, Ser-158, revealed that the flexible loop region between the UBC and UBA domains is also affected. Further examination of the NMR titration experiments showed additional regions within the UBA domain that were perturbed upon binding to the different RING E3s. These findings suggest that upon binding to RING E3s either the interactions between the UBC and UBA domains are disrupted or structural changes in UBA domain positioning could occur. Structural changes could be explained if the UBA domain is being repositioned to potentially bind or recognize the monoubiquitinated substrate. This repositioning would further strengthen the argument that E2-25K serves as a "second-step" E2, but does not explain its ability to bind RING E3s *in vitro* in the absence of the substrate or Ub. Furthermore, divergence in residues that are perturbed in the titration

experiments is consistent with the theory that the residues surrounding the conserved Pro-Phe sequence on E2s are what dictate the specificity of E2-E3 binding.

There has been no prior evidence to suggest that E2-25K interacts with the RING E3 Parkin, which consists of two separate RING domains and an N-terminal Ubl domain. In theory, UBA domains should bind to Ubl domains in a manner similar to Ub, but UBA/Ubl binding has not been widely observed. The only interactions between a UBA and Ubl domain that has been observed is found in Dsk2 and Rad23, where both domains, within the same protein, interact to form a homodimer [129, 130]. In this study, the NMR titration experiments show the binding surface between the UBA domain of E2-25K and the Ubl domain of Parkin similar to binding with ubiquitin. The titration experiments between E2-25K and the Parkin Ubl domain further showed a binding constant consistent with binding to monoubiquitin. This interaction between the UBA domain of E2-25K and the Ubl domain of Parkin suggests that E2-25K may be involved in additional regulatory mechanisms or pathways.

Studies with E2-25K in Alzheimer Disease model systems (neuronal cells and mouse models) show that the presence of a full-length, active E2-25K is necessary for the toxic effects of Aβ amyloid protein [5]. Overexpression of E2-25K in rat neuroblastoma cells exposed to $A\beta_{1-42}$ resulted in increased cell death, while overexpression of E2-25K mutants lacking the UBA domain (Δ150-200), or with mutations of residues S86Y or C92S, significantly reduced the $A\beta_{1-42}$ neurotoxicity. Reducing the levels of expressed E2-25K using anti-sense DNA also suppressed the toxic effects. Studies with E2-25K and expanded polyglutamine tracts (such as those seen in Huntington Disease) mirrored the results seen with $A\beta_{1-42}$ [8]. Overexpression of E2-25K in cell models enhanced the

toxicity of a polyglutamine construct, while suppression of E2-25K or overexpression of a UBC domain-only mutant caused a decrease in toxicity and aggregation and brought cell survival rates back to normal. This suggests that these mutants function in a dominant-negative manner, perhaps by competing with full-length E2-25K for cellular binding partners or tagging proteins with alternate polyubiquitin chain linkages. This in turn would free the proteasome from over-accumulation of E2-25K targets and allow for degradation of other misfolded proteins.

Polyubiquitination studies of the anaphase promoting complex (APC) targets by Rodrigo-Brenni *et al*. also gives insight into the function of the UBA domain [65]. They concluded that a UBA truncation mutant of E2-25K or its yeast homolog Ubc1 was defective in binding to the APC-substrate complex (resulting in decreased processivity) but was not defective in catalysis or linkage specificity. This suggests that the UBA domain functions to increase specificity for monoubiquitinated or di-ubiquitinated targets and argues against the theory that it serves to position an acceptor ubiquitin in polyubiquitin chain synthesis in the presence of the E3-substrate complex. The results presented here are consistent with this idea, demonstrating that the UBA domain increases processivity through binding to the substrates (in this case ubiquitin and polyubiquitin).

8.1 Suggestions for Future Research

Determining the binding site of the UBA domain to the Ubl domain of Parkin leads to several new avenues of potential exploration. The most obvious is screening the UBA domain for other potential binding partners or pathways and determining the associated binding sites by NMR spectroscopy. Due to the continued emphasis in the

research regarding E2-25K's likely link to Parkinson disease, other work with various combinations of the RING domains and the Ubl domain of Parkin would be helpful in determining if E2-25K interacts with both domains. Identification of the residues of the Ubl domain of Parkin would give greater insight into E2-25K/Parkin Ubl domain complex formation.

The NMR backbone resonance assignments for the full-length E2-25K and ubiquitin are valuable assets. The completion of the assignments may allow potential breakthroughs in the research of E2-25K: screening of potential inhibitors and E2-25K/ubiquitin/E3 complexes. The E2-25K NMR assignments can be used in conjunction with activity assays to determine critical residues involved in the conjugation of ubiquitin, the complex with the E1 and other future determined binding partners. The E2-25K to RING E3 binding data will help identify the critical E2-E3 binding residues and may lead to prediction of other E3 partners through sequence comparison. These results can be used to help define the manner in which E2-25K adapts to multiple pathways, and ultimately to determine the mechanism of polyubiquitin chain formation.

Future studies with E2-25K are also needed to explore the effect of E3 ligase partners on processivity. This will help determine if the UBA domain is mimicking the presence of an E3 ligase. Future polyubiquitin chain-assay studies, with different ubiquitin mutants, could be used to determine if a specific chain linkage is constructed in the absence of the UBA domain. Furthermore, such data, in conjunction with results presented here, will be used to determine if the function of the UBA domain is to position an acceptor ubiquitin for building polyubiquitin chains that can then be added to the

substrate or to provide an additional recognition surface for binding of monoubiquitinated substrates.

APPENDIX

Supporting Material

Table A.1 Construct Sequence Verification in FASTA Format

> **UBA Domain**

NNNNNNNNNNNNNNNNTCCCCTCTNGAATAATTTTGTTTAACTTTAAGA
AGGAGATATACCATGGGCAGCAGCCATNATCATCATCATCACAGCAGCGG
CCTGGTGCCGCGCGGCAGCCATATGGCTAGCGGAGCACCAGTTTCTAGTC
CAGAATACACCAAAAAAATAGAAAACCTATGTGCTATGGGCTTTGATAGG
AATGCAGTAATAGTGGCCTTGTCTTCAAAATCATGGGATGTAGAGACTGC
AACAGAATTGCTACTGAGTAACTGAGGATCCGAATTCGAGCTCCGTCGAC
AAGCTTGCGGCCGCACTCGAGCACCACCACCACCACCACTGAGATCCGGC
TGCTAACAAAGCCCGAAAGGAAGCTGAGTTGGCTGCTGCCACCGCTGAGC
AATAACTAGCATAACCCCTTGGGGCCTCTAAACGGGTCTTGAGGGGTTTT
TTGCTGAAAGGAGGAACTATATCCGGATTGGCGAATGGGACGCGCCCTGT
AGCGGCGCATTAAGCGCGGCGGGTGTGGTGGTTACGCGCAGCGTGACCGC
TACACTTGCCAGCGCCCTAGCGCCCGCTCCTTTCGCTTTCTTCCCTTCCT
TTCTCGCCACGTTCGCCGGCTTTCCCCGTCAAGCTCTAAATCGGGGGCTC
CCTTTAGGGTTCCGATTTAGTGCTTTACGGCACCTCGACCCCAAAAAACT
TGATTAGGGTGATGGTTCACGTAGTGGGCCATCGCCCTGATAGACGGTTT
TTCGCCCTTTGACGTTGGAGTCCACGTTCTTTAATAGTGGACTCTTGTTC
CAAACTGGAACAACACTCAACCCTATCTCGGTCTATTCTTTTGANTTATA
AGGGATTTTGCCNATTTCGGNCTATTGGNTAAAAAATGAGCTGANTTAAC
AAAAATTTAACGCGAATTTTAACAAAATATTAACGCTTN

> **UBC Domain**

NNNNNNNNNNNNNNNNCCNNNCTANNATAATTTTGTTTAACTTTAAGAA
GGAGATATACCATGGGCAGCAGCCNNNATCATCATCATCACAGCAGCGGC
CTGGTGCCGCGCGGCAGCCATATGGCTAGCATGGCCAACATCGCGGTGCA
GCGAATCAAGCGGGAGTTCAAGGAGGTGCTGAAGAGCGAGGAGACGAGCA
AAAATCAAATTAAAGTAGATCTTGTAGATGAGAATTTTACAGAATTAAGA
GGAGAAATAGCAGGACCTCCAGACACACCATATGAAGGAGGAAGATACCA
ACTAGAGATAAAAATACCAGAAACATACCCATTTAATCCCCCTAAGGTCC
GGTTTATCACTAAAATATGGCATCCTAATATTAGTTCCGTCACAGGGGCT
ATTTGTTTGGATATCCTGAAAGATCAATGGGCAGCTGCAATGACTCTCCG
CACGGTATTATTGTCATTGCAAGCACTATTGGCAGCTGCAGAGCCAGATG
ATCCACAGGATGCTGTAGTAGCAAATCAGTACAAACAAAATCCCGAAATG
TTCAAACAGACAGCTCGACTTTGGGCACATGTGTATGCTGGAGCACCAGT
TTCTAGTTGAGGATCCGAATTCGAGCTCCGTCGACAAGCTTGCGGCCGCA
CTCGAGCACCACCACCACCACCACTGAGATCCGGCTGCTAACAAAGCCCG
AAAGGAAGCTGAGTTGGCTGCTGCCACCGCTGAGCAATAACTAGCATAAC
CCCTTGGGGCCTCTAAACGGGTCTTGAGGGGTTTTTTGCTGAAAGGAGGA
ACTATATCCGGATTGNCGAATGGGACGCGCCCTGTAGCGGCGCATTAAGC
GCGGCGGGTGTGGTGGTTACGCGCAGCGTGACCGCTACACTTGCCAGCGC
CCTAGCGCCCGCTCCTTTCGCTTTCTTNCCTTNCTTTCTCN

Table A.1 (Continued)

> E2-25K

NNNNNNNNNNNNNNANTTCCCNNNTNGNNNAATTTTGTTTAACTTTAAG
AAGGAGATATACATATGCACCATCATCATCATCATTCTTCTGGTCTGGTG
CCACGCGGTTCTGGTATGAAAGAAACCGCTGCTGCTAAATTCGAACGCCA
GCACATGGACAGCCCAGATCTGGGTACCGACGACGACGACAAGGCCATGG
CTGATATCGGATCCGAATTCGACATGGCCAACATCGCGGTGCAGCGAATC
AAGCGGGAGTTCAAGGAGGTGCTGAAGAGCGAGGAGACGAGCAAAAATCA
AATTAAAGTAGATCTTGTAGATGAGAATTTTACAGAATTAAGAGGAGAAA
TAGCAGGACCTCCAGACACACCATATGAAGGAGGAAGATACCAACTAGAG
ATAAAAATACCAGAAACATACCCATTTAATCCCCCTAAGGTCCGGTTTAT
CACTAAAATATGGCATCCTAATATTAGTTCCGTCACAGGGGCTATTTGTT
TGGATATCCTGAAAGATCAATGGGCAGCTGCAATGACTCTCCGCACGGTA
TTATTGTCATTGCAAGCACTATTGGCAGCTGCAGAGCCAGATGATCCACA
GGATGCTGTAGTAGCAAATCAGTACAAACAAAATCCCGAAATGTTCAAAC
AGACAGCTCGACTTTGGGCACATGTGTATGCTGGAGCACCAGTTTCTAGT
CCAGAATACACCAAAAAAATAGAAAACCTATGTGCTATGGGCTTTGATAG
GAATGCAGTAATAGTGGCCTTGTCTTCAAAATCATGGGATGTAGAGACTG
CAACAGANTTGCTTCTGAGTAACTGAGGCATAGAGAGCTGCTGACGGATC
CTCTAGAGTCGAGCACCACCACCACCACCACTGAGATCCGGCTGCTAACA
AAGCCCGAAAGGAAGCTGAGTTGGCTGCTGCCACCGCNN

> **E2-25K K97R**

TCCCTCTAGAAATAATTTTGTTTAACTTTAAGAAGGAGATATACATATGC
ACCATCATCATCATCCCTCTTCTGGTCTGGTGCCACGCGNGTTCTGGTAT
GAAAGAAACCGCTTGCTGCTAAATTCGAACGCCAGCACATGGGACAGCCC
ANGATCTGGGTACCNGACGACGACGACAAGGCCATGGCTGATATCGGATC
CGAATTCGACATGGCCAACATCGCGGTGCAGCGAATCAAGCGGGAGTTCA
AGGAGGTGCTGAAGAGCGAGGAGACGAGCAAAAATCAAATTAAAGTAGAT
CTTGTAGATGAGAATTTTACAGAATTAAGAGGAGAAATAGCAGGACCTCC
AGACACACCATATGAAGGAGGAAGATACCAACTAGAGATAAAAATACCAG
AAACATACCCATTTAATCCCCCTAAGGTCCGGTTTATCACTAAAATATGG
CATCCTAATATTAGTTCCGTCACAGGGGCTATTTGTTTGGATATCCTGAG
AGATCAATGGGCAGCTGCAATGACTCTCCGCACGGTATTATTGTCATTGC
AAGCACTATTGGCAGCTGCAGAGCCAGATGATCCACAGGATGCTGTAGTA
GCAAATCAGTACAAACAAAATCCCGAAATGTTCAAACAGACAGCTCGACT
TTGGGCACATGTGTATGCTGGAGCACCAGTTTCTAGTCCAGAATACACCA
AAAAAATAGAAAACCTATGTGCTATGGGCTTTGATAGGAATGCAGTAATA
GTGGCCTTGTCTTCAAAATCATGGGATGTAGAGACTGCAACAGAATTGCT
TCTGAGTAACTGAGGCATAGAGAGCTGCTGACGGATCCTCTAGAGTCGAG
CACCACCACCACCACCACTGAGATCCGGCTG

Table A.1 (Continued)

> **E2-25K C92S**

AAAGAAACCGCTGCTGCTAAATTCGAACGCCAGCACATGGACAGCCCAGA
TCTGGGTACCGACCACGACCACAAGGCCATGGCTGATATCGGATCCGAAT
TCGACATGGCCAACATCGCGGTGCAGCGAATCAAGCGGGAGTTCAAGGAG
GTGCTGAAGAGCGAGGAGACGAGCAAAAATCAAATTAAAGTAGATCTTGT
AGATGAGAATTTTACAGAATTAAGAGGAGAAATAGCAGGACCTCCAGACA
CACCATATGAAGGAGGAAGATACCAACTAGAGATAAAAATACCAGAAACA
TACCCATTTAATCCCCCTAAGGTCCGGTTTATCACTAAAATATGGCATCC
TAATATTAGTTCCGTCACAGGGGCTATTAGCTTGGATATCCTGAAAGATC
AATGGGCAGCTGCAATGACTCTCCGCACGGTATTATTGTCATTGCAAGCA
CTATTGGCAGCTGCAGAGCCAGATGATCCACAGGATGCTGTAGTAGCAAA
TCAGTACAAACAAAATCCCGAAATGTTCAAACAGACAGCTCGACTTTGGG
CACATGTGTATGCTGGAGCACCAGTTTCTAGTCCAGAATACACCAAAAAA
ATAGAAAACCTATGTGCTATGGGCTTTGATAGGAATGCAGTAATAGTGGC
CTTGTCTTCAAAATCATGGGATGTAGAGACTGCAACAGAATTGCTTCTGA
GTAACTGAGGCATAGAGAGCTGCTGACGGATCCTCTAGAGTCGAGCACCA
CCACCACCACCACTGAGAT

> **E2-25K M172A**

TTTTAAGTTGACGAATTCCCTCTGAATATTTTGTTAACTTTAGAAGGAGA
TATACATATGCACCATCATCATCATCATTCTTCTGGTCTGGTGCCACGCG
GTTCTGGTATGAAAGAAACCGCTGCTGCTAAATTCGAACGCCAGCACATG
GACAGCCCAGATCTGGGTACCGACGACGACGACAAGGCCATGGCTGATAT
CGGATCCGAATTCGACATGGCCAACATCGCGGTGCAGCGAATCAAGCGGG
AGTTCAAGGAGGTGCTGAAGAGCGAGGAGACGAGCAAAAATCAAATTAAA
GTAGATCTTGTAGATGAGAATTTTACAGAATTAAGAGGAGAAATAGCAGG
ACCTCCAGACACACCATATGAAGGAGGAAGATACCAACTAGAGATAAAAA
TACCAGAAACATACCCATTTAATCCCCCTAAGGTCCGGTTTATCACTAAA
ATATGGCATCCTAATATTAGTTCCGTCACAGGGGCTATTTGTTTGGATAT
CCTGAAAGATCAATGGGCAGCTGCAATGACTCTCCGCACGGTATTATTGT
CATTGCAAGCACTATTGGCAGCTGCAGAGCCAGATGATCCACAGGATGCT
GTAGTAGCAAATCAGTACAAACAAAATCCCGAAATGTTCAAACAGACAGC
TCGACTTTGGGCACATGTGTATGCTGGAGCACCAGTTTCTAGTCCAGAAT
ACACCAAAAAAATAGAAAACCTATGTGCTGCGGGCTTTGATAGGAATGCA
GTAATAGTGGCCTTGTCTTCAAAATCATGGGATGTAGAGACTGCAACAGA
ATTGCTTCTGAGTAACTGAGGCATAGAGAGCTGCTGACGGATCCTCTAGA
GTCGAGCACCACCACCACCACCACTGAGATCCGGCTGCNTACAAGCCCCG
AAGGAAGCTGAAGTGGCTGCTGCCACCCGCTGAGCATACTAGCATAACCC
CTGGGGGCTCTAAACGGGTCTTGAGGGGTTTTTTGCTGAAAGGAGAACTA
TATCCCGGATGGCGAATGGGACGCGCCTGTAGCGCGCATTAGCGCGGCGG
GTGTGGTGGTACGCGAGCGTGACGCTACACTTGCAGCGCCTAGCGCCGTC

Table A.1 (Continued)

> E2-25K UBA M172A

NNNNNGGAGACGATATTCCTCTGAATAATTTTGTTAACTTTAGAAGGAGA
TATACCATGGGCAGCAGCCATCATCATCATCATCACAGCAGCGGCCTGGT
GCCGCGCGGCAGCCATATGGCTAGCGGAGCACCAGTTTCTAGTCCAGAAT
ACACCAAAAAAATAGAAAACCTATGTGCTGCGGGCTTTGATAGGAATGCA
GTAATAGTGGCCTTGTCTTCAAAATCATGGGATGTAGAGACTGCAACAGA
ATTGCTACTGAGTAACTGAGGATCCGAATTCGAGCTCCGTCGACAAGCTT
GCGGCCGCACTCGAGCACCACCACCACCACCACTGAGATCCGGCTGCTAA
CAAAGCCCGAAAGGAAGCTGAGTTGGCTGCTGCCACCGCTGAGCAATAAC
TAGCATAACCCCTTGGGGCCTCTAAACGGGTCTTGAGGGGTTTTTTGCTG
AAAGGAGGAACTATATCCGGATTGGCGAATGGGACGCGCCCTGTAGCGGC

> **E2-25K L198A**

NNNCCAGACGCCTTCNNNGTGAGAATCCCTCTGAATATTTTGTTAACTTT
AGAAGGAGATATACATATGCACCATCATCATCATCATTCTTCTGGTCTGG
TGCCACGCGGTTCTGGTATGAAAGAAACCGCTGCTGCTAAATTCGAACGC
CAGCACATGGACAGCCCAGATCTGGGTACCGACGACGACGACAAGGCCAT
GGCTGATATCGGATCCGAATTCGACATGGCCAACATCGCGGTGCAGCGAA
TCAAGCGGGAGTTCAAGGAGGTGCTGAAGAGCGAGGAGACGAGCAAAAAT
CAAATTAAAGTAGATCTTGTAGATGAGAATTTTACAGAATTAAGAGGAGA
AATAGCAGGACCTCCAGACACACCATATGAAGGAGGAAGATACCAACTAG
AGATAAAAATACCAGAAACATACCCATTTAATCCCCCTAAGGTCCGGTTT
ATCACTAAAATATGGCATCCTAATATTAGTTCCGTCACAGGGGCTATTTG
TTTGGATATCCTGAAAGATCAATGGGCAGCTGCAATGACTCTCCGCACGG
TATTATTGTCATTGCAAGCACTATTGGCAGCTGCAGAGCCAGATGATCCA
CAGGATGCTGTAGTAGCAAATCAGTACAAACAAAATCCCGAAATGTTCAA
ACAGACAGCTCGACTTTGGGCACATGTGTATGCTGGAGCACCAGTTTCTA
GTCCAGAATACACCAAAAAAATAGAAAACCTATGTGCTATGGGCTTTGAT
AGGAATGCAGTAATAGTGGCCTTGTCTTCAAAATCATGGGATGTAGAGAC
TGCAACAGAATTGCTTGCGAGTAACTGAGGCATAGAGAGCTGCTGACCGG
ATCTCTAGAGTCGAGCACCACCACCCCACCCCTGAGATCCGGCTGCTAAC
CAACCCCAAAGAAACTGAATTGGCTGCTGCCCCCGCTGAACAATAACTAG
CATAACCCCTGGGGGCCCTAAACGGGCCTGAGGGGGTTTTTGCTGAAGGG
AGGAACATATTCCGATTGGCCAATGGGAACCCCCCTGTAACGCCCCTTAA
ACCCCGGGGGGTGGTGGTTACCCCCAACGGGACCCCTTACTTGGCCAGGC
CTTAAGGCCCC

Table A.1 (Continued)

> E2-25K UBA L198A

NNAAAAGGGTGAGAATTCCCTCTGAATATTTTGTTTAACTTTAGAAGGAG
ATATACCATGGGCAGCAGCCATCATCATCATCATCACAGCAGCGGCCTGG
TGCCGCGCGGCAGCCATATGGCTAGCGGAGCACCAGTTTCTAGTCCAGAA
TACACCAAAAAAATAGAAAACCTATGTGCTATGGGCTTTGATAGGAATGC
AGTAATAGTGGCCTTGTCTTCAAAATCATGGGATGTAGAGACTGCAACAG
AATTGCTTGCGAGTAACTGAGGATCCGAATTCGAGCTCCGTCGACAAGCT
TGCGGCCGCACTCGAGCACCACCACCACCACCACTGAGATCCGGCTGCTA
ACAAAGCCCGAAAGGAAGCTGAGTTGGCTGCTGCCACCGCTGAGCAATAA
CTAGCATAACCCCTTGGGGCCTCTAAACGGGTCTTGAGGGGTTTTTTGCT
GAAAGGAGGAACTATATCCGGATTGGCGAATGGGACGCGCCCTGTAGCGG
CGCATTAAGCGCGGCGGGTGTGGTGGTTACGCGCAGCGTGACCGCTACAC
TTGCCAGCGCCCTAGCGCCCGCTCCTTTCGCTTTCTTCCCTTCCTTTCTC
GCCACGTTCGCCGGCTTTCCCCGTCAAGCTCTAAATCGGGGGCTCCCTTT
AGGGTTCCGATTTAGTGCTTTACGGCACCTCGACCCCAAAAAACTTGATT

> Ubiquitin

NNNNNNNNGNNNNNNNCNCCTCTAGANNAATTTTGTTTAACTTTAAGAAGGA
GATATACCATGGGCAGNNNNNATNATCATCATCATCACAGCAGCGGCCTGGT
GCCGCGCGGCAGCCATATGCAGATCTTCGTGAAAACCCTTACCGGTAAGACC
ATCACTCTCGAAGTGGAGCCGAGTGACACCATTGAGAATGTCAAGGCAAAGA
TCCAAGACAAGGAAGGCATCCCTCCTGACCAGCAGAGGTTGATCTTTGCTGG
GAAACAGCTGGAAGATGGACGCACCCTGTCTGACTACAACATCCAGAAGGA
GTCCACCCTGCACCTGGTCCTGCGTCTGAGAGGTGGTTGAGGATCCGAATTCG
AGCTCCGTCGACAAGCTTGCGGCCGCACTCGAGCACCACCACCACCACCACT
GAGATCCGGCTGCTAACAAAGCCCGAAAGGAAGCTGAGTTNNCTGCTGCCNC
CGCTGAGCAATAACTAGCATAACCCCTTGGGGCCTCTAAACGGGTCTTGAGG
GGTTTTTTGCTGAAAGGAGGAACTATATCCGGATTGGCGAATGGGACGCGCC
CTGTAGCGGCNCATTAAGCGCGGCGGGTGTGGTGGTTACGCGCAGCGTGACC
GCTACACTTGCCAGCGCCCTAGCGCCCGCTCCTTTCGCTTTCTTCCCTTCCTTT
CTCGCCACGNTCGCCNGNTTTCCCCGTCAAGCTCTAAATCGGGGGCTCCNNTT
AGGGTTCCNATTTAGTGNTTTANNNNNCCTCNACCCCNAAAAACTTGATTAG
GGTGANGGTTCACGTANNGGGCCATCNCCNTGANANANGGTTTTTCNCCNTT
GACGTTGGAGNCNCGTTCTTTAATANNGNNTNTTGTNNAAANNGAACAACNN
TCAACCCTANCTCGGNNNNTTNNTTTGATNTATAAGGGATTTTNNCNN

Table A.1 (Continued)

> Ubiquitin D77

NNNNCCAGATCACCTTCTCTGAAGAATCCCTCTGAATATTTTGTTAACTT
TAGAAGGAGATATACCATGGGCAGCAGCCATCATCATCATCATCACAGCA
GCGGCCTGGTGCCGCGCGGCAGCCATATGCAGATCTTCGTGAAAACCCTT
ACCGGTAAGACCATCACTCTCGAAGTGGAGCCGAGTGACACCATTGAGAA
TGTCAAGGCAAAGATCCAAGACAAGGAAGGCATCCCTCCTGACCAGCAGA
GGTTGATCTTTGCTGGGAAACAGCTGGAAGATGGACGCACCCTGTCTGAC
TACAACATCCAGAAGGAGTCCACCCTGCACCTGGTCCTGCGTCTGAGAGG
TGGTGATTGAGGATCCGAATTCGAGCTCCGTCGACAAGCTTGCGGCCGCA
CTCGAGCACCACCACCACCACCACTGAGATCCGGCTGCTAACAAAGCCCG
AAAGGAAGCTGAGTTGGCTGCTGCCACCGCTGAGCAATAACTAGCATAAC
CCCTTGGGGCCTCTAAACGGGTCTTGAGGGGTTTTTTGCTGAAAGGAGGA
ACTATATCCGGATTGGCGAATGGGACGCGCCCTGTAGCGGCGCATTAAGC

> Ubiquitin K48C

NNNNGGGTGCGACATCCCTCTGAATATTTTGTTTACTTTAGAAGGAGATA
TACCATGGGCAGCAGCCATCATCATCATCATCACAGCAGCGGCCTGGTGC
CGCGCGGCAGCCATATGCAGATCTTCGTGAAAACCCTTACCGGTAAGACC
ATCACTCTCGAAGTGGAGCCGAGTGACACCATTGAGAATGTCAAGGCAAA
GATCCAAGACAAGGAAGGCATCCCTCCTGACCAGCAGAGGTTGATCTTTG
CTGGGTGTCAGCTGGAAGATGGACGCACCCTGTCTGACTACAACATCCAG
AAGGAGTCCACCCTGCACCTGGTCCTGCGTCTGAGAGGTGGTTGAGGATC
CGAATTCGAGCTCCGTCGACAAGCTTGCGGCCGCACTCGAGCACCACCAC
CACCACCACTGAGATCCGGCTGCTAACAAAGCCCGAAAGGAAGCTGAGTT
GGCTGCTGCCACCGCTGAGCAATAACTAGCATAACCCCTTGGGGCCTCTA
AACGGGTCTTGAGGGGTTTTTTGCTGAAAGGAGGAACTATATCCGGATTG
GCGAATGGGACGCGCCCTGTAGCGGCGCATTAAGCGCGGCGGGTGTGGTG
GTTACGCGCAGCGTGACCGCTACACTTGCCAGCGCCCTAGCGCCCGCTCC
TTTCGCTTTCTTCCCTTCCTTTCTCGCCACGTTCGCCGGCTTTCCCCGTC
AAGCTCTAAATCGGGGGCTCCCTTTAGGGTTCCGATTTAGTGCTTTACGG
CACCTCGACCCCAAAAAACTTGATTAGGGTGATGGTTCACGTAGTGGGCC
ATCGCCCTGATAGACGGTTTTTCGCCCTTTGACGTTGGAGTCCACGTTCT
TTAATAGTGGACTCTTGTTCCAAACTGGAAACACACTCAACCCTATCTCG
GTCTATTCTTTTGATTTATAAGGGATTTTGCCGATTTCGGCCTATTGGTT
AAAAAATGAGCTGATTTAACAAAAATTTAACGCAATTTTAACAAAATATT
AACGCTTACAATTTAGGTGGCACTTTTCGGGGAAATGTGCGCGGACCCCC
TATTGTTTATTTTCTAATACATTCAA

Table A.1 (Continued)

> Ubiquitin K63C

NNNNGGCTGCGGAATCCCTCTAGATATTTTGTTTACTTTAGAAGGAGATA
TACCATGGGCAGCAGCCATCATCATCATCATCACAGCAGCGGCCTGGTGC
CGCGCGGCAGCCATATGCAGATCTTCGTGAAAACCCTTACCGGTAAGACC
ATCACTCTCGAAGTGGAGCCGAGTGACACCATTGAGAATGTCAAGGCAAA
GATCCAAGACAAGGAAGGCATCCCTCCTGACCAGCAGAGGTTGATCTTTG
CTGGGAAACAGCTGGAAGATGGACGCACCCTGTCTGACTACAACATCCAG
TGTGAGTCCACCCTGCACCTGGTCCTGCGTCTGAGAGGTGGTTGAGGATC
CGAATTCGAGCTCCGTCGACAAGCTTGCGGCCGCACTCGAGCACCACCAC
CACCACCACTGAGATCCGGCTGCTAACAAAGCCCGAAAGGAAGCTGAGTT
GGCTGCTGCCACCGCTGAGCAATAACTAGCATAACCCCTTGGGGCCTCTA
AACGGGTCTTGAGGGGTTTTTTGCTGAAAGGAGGAACTATATCCGGATTG
GCGAATGGGACGCGCCCTGTAGCGGCGCATTAAGCGCGGCGGGTGTGGTG
GTTACGCGCAGCGTGACCGCTACACTTGCCAGCGCCCTAGCGCCCGCTCC
TTTCGCTTTCTTCCCTTCCTTTCTCGCCACGTTCGCCGGCTTTCCCCGTC
AAGCTCTAAATCGGGGGCTCCCTTTAGGGTTCCGATTTAGTGCTTTACGG
CACCTCGACCCCAAAAAACTTGATTAGGGTGATGGTTCACGTAGTGGGCC
ATCGCCCTGATAGACGGTTTTTCGCCCTTTGACGTTGGAGTCCACGTTCT
TTAATAGTGGACTCTTGTTCCAAACTGGAACAACACTCAACCCTATCTCG
GTCTATTCTTTTGATTTATAAGGGATTTTTGCGATTTCNGCCTNATGGTT
AAAAAATGAGCTGATTTTAACAAAATTTAACGCGAATTTTTAACAAATAT
AAACGCTTACATTTTANGTGGCACTTTTCGGGGAAATGTGCCGCGAACCC
CTATTTGTTTATTTTTCTAAATACCATCCAATATGTATCCGCC

> Ubiquitin K48C K63C

NGGGGGGTGCGACATCCCTCTGAATATTTTGTTTACTTTAGAAGGAGATA
TCCATGGGCAGCAGCCCTCTAAGCATCATCACAGCAGCGGCCTGGTGCCG
CGCGGCCCTTATATGCAGATCTTCGTGAAAACCCTTACCGGTAAGACCAT
CACTCTCGAAGTGGAGCCGAGTGACACCATTGAGAATGTCAAGGCAAAGA
TCCAAGACAAGGAAGGCATCCCTCCTGACCAGCAGAGGTTGATCTTTGCT
GGGTGTCAGCTGGAAGATGGACGCACCCTGTCTGACTACAACATCCAGTG
TGAGTCCACCCTGCACCTGGTCCTGCGTCTGAGAGGTGGTTGAGGATCCG
AATTCGAGCTCCGTCGACAAGCTTGCGGCCGCACTCGAGCACCACCACCA
CCACCACTGAGATCCGGCTGCTAACAAAGCCCGAAAGGAAGCTGAGTTGG
CTGCTGCCACCGCTGAGCAATAACTAGCATAACCCCTTGGGGCCTCTAAA
CGGGTCTTGAGGGGTTTTTTGCTGAAAGGAGGAACTATATCCGGATTGGC
GAATGGGACGCGCCCTGTAGCGGCGCATTAAGCGCGGCGGGTGTGGTGGT
TACGCGCAGCGTGACCGCTACACTTGCCAGCGCCCTAGCGCCCGCTCCTT
TCGCTTTCTTCCCTTCCTTTCTCGCCACGTTCGCCGGCTTTCCCCGTCAA
GCTCTAAATCGGGGGCTCCCTTTAGGGTTCCGATTTAGTGCTTTACGGCA
CCTCGACCCCAAAAAACTTGATTAGGGTGATGGTTCACGTAGTGGGCCAT

Table A.1 (Continued)

> Ubiquitin +1

NNNNNTCGAGTCCCTAATATTTTGTTTACTTTAGAAGGAGATATACATAT
GAAGCATCATCATCATCATCATCAGATGCAGATCTTCGTGAAAACCCTTA
CCGGTAAGACCATCACTCTCGAAGTGGAGCCGAGTGACACCATTGAGAAT
GTCAAGGCAAAGATCCAAGACAAGGAAGGCATCCCTCCTGACCAGCAGAG
GTTGATCTTTGCTGGGAAACAGCTGGAAGATGGACGCACCCTGTCTGACT
ACAACATCCAGAAGGAGTCCACCCTGCACCTGGTCCTGCGTCTGAGAGGT
TATGCGGATCTGCGCGAAGATCCGGATCGCCAGGATCATCATCCGGGCAG
CGGCGCGCAGTGAGGATCCGGCTGCTAACAAAGCCCGAAAGGAAGCTGAG
TTGGCTGCTGCCACCGCTGAGCAATAACTAGCATAACCCCTTGGGGCCTC
TAAACGGGTCTTGAGGGGTTTTTTGCTGAAAGGAGGAACTATATCCGGAT
ATCCACAGGACGGGTGTGGTCGCCATGATCGCGTAGTCGATAGTGGCTCC
AAGTAGCGAAGCGAGCAGGACTGGGCGGCGGCCAAAGCGGTCGGACAGTG
CTCCGAGAACGGGTGCGCATAGAAATTGCATCAACGCATATAGCGCTAGC
AGCACGCCATAGTGACTGGCGATGCTGTCGGAATGGACGATATCCCGCAA
GAGGCCCGGCAGTACCGGCATAACCAAGCCTATGCCTACAGCATCCAGGG
TGACGGTGCCGAGGATGACGATGAGCGCATTGTTAGATTTCATACACGGT
GCCTGACTGCGTTAGCAATTTAACTGTGATAAACTACCGCATTAAAGCTT
ATCGATGATAAGCTGTNCAACATGAGAATTCTTGAAGACGAAAGGGCCTC
GTGATACGCCTATTTTTATAGGTTAATGTCATGATAATAATGGTTTCTTA
GACGTCAGGTGGCACTTTTCGGGGAAATGTGCGCCGGACCCCTATTTGTT
TATTTTTTCTAATACATTCAAATATGTATCCGCTCATGAAGACAATAACC
CTGATAAATGCTTCAATAATATGAAAAAT

Table A.2 Chemical Shifts of HN, ^{15}N, ^{13}CO, $^{13}C\alpha$ and $^{13}C\beta$ for Full-length E2-25K.
All the chemical shifts are referenced relative to the frequency of the methyl proton resonance of DSS (units: ppm).

Residue		HN	N	CO	CA	CB	Residue		HN	N	CO	CA	CB
1	M	7.68	126.21	ND	56.9	32.6	46	P	ND	ND	ND	ND	ND
2	A	ND	ND	177.8	52.7	17.4	47	P	ND	ND	176.0	62.0	30.9
3	N	8.03	116.73	175.7	53.1	37.9	48	D	8.97	115.48	174.7	55.2	38.4
4	I	8.04	121.24	176.9	63.0	36.8	49	T	7.34	105.97	ND	59.0	70.5
5	A	8.19	124.59	179.2	55.5	18.2	50	P	ND	ND	ND	ND	ND
6	V	7.70	116.82	177.3	65.3	30.7	51	Y	ND	ND	176.6	55.5	37.6
7	Q	7.96	117.82	177.8	58.3	27.4	52	E	7.48	123.36	175.4	57.4	29.1
8	R	8.32	119.43	175.9	57.6	32.5	53	G	9.36	115.14	173.9	44.0	-
9	I	8.53	120.29	ND	60.0	40.6	54	G	8.29	106.17	172.9	42.7	-
10	K	ND	ND	179.5	60.3	30.9	55	R	8.47	121.85	173.9	54.6	31.3
11	R	7.45	118.84	179.4	58.7	29.0	56	Y	8.72	121.32	174.1	57.1	39.4
12	E	8.86	121.96	179.9	59.0	29.4	57	Q	9.55	121.44	180.0	54.1	29.6
13	F	9.40	122.99	174.6	60.9	38.9	58	L	ND	ND	174.7	52.8	44.6
14	K	7.53	118.59	178.1	58.8	31.0	59	E	9.08	124.82	173.9	54.5	32.4
15	E	8.07	118.16	179.4	58.3	28.6	60	I	8.04	126.29	173.6	59.58	38.92
16	V	7.97	118.73	178.8	66.2	30.2	61	K	9.24	126.97	173.5	53.93	33.38
17	L	7.94	121.65	ND	57.2	40.8	62	I	8.67	125.47	ND	60.3	35.5
18	K	ND	ND	176.5	55.2	31.1	63	P	ND	ND	176.9	61.6	31.7
19	S	7.84	117.18	ND	59.0	64.1	64	E	9.10	119.63	176.5	58.3	28.3
20	E	ND	ND	176.5	56.3	29.2	65	T	6.99	102.82	174.6	59.9	67.9
21	E	8.37	121.83	177.2	56.2	29.5	66	Y	7.61	126.91	ND	57.5	39.5
22	T	8.11	115.11	ND	60.8	69.4	67	P	ND	ND	174.6	62.7	31.6
23	S	ND	ND	174.5	57.9	63.3	68	F	8.78	125.36	175.2	59.8	37.1
24	K	8.51	122.90	175.9	55.9	29.3	69	N	7.07	115.73	ND	49.7	40.1
25	N	8.28	116.61	178.3	53.6	36.9	70	P	ND	ND	ND	ND	ND
26	Q	8.48	116.13	178.4	56.6	30.2	71	P	ND	ND	174.6	61.1	31.1
27	I	7.37	112.92	ND	61.4	39.6	72	K	8.61	120.65	176.7	54.4	31.1
28	K	ND	ND	173.8	55.2	35.3	73	V	8.85	126.13	175.9	59.5	33.2
29	V	8.05	118.47	171.8	59.8	34.4	74	R	8.32	123.53	175.4	54.1	33.4
30	D	8.79	122.51	174.7	52.4	44.6	75	F	9.45	124.72	174.7	59.3	37.6
31	L	8.68	121.59	176.7	54.5	41.1	76	I	8.09	121.37	177.5	61.5	38.3
32	V	8.11	121.22	175.3	61.6	31.7	77	T	7.27	119.04	173.3	62.7	69.9
33	D	8.37	124.25	176.9	54.4	40.7	78	K	8.19	126.37	173.9	56.0	31.5
34	E	8.33	122.95	175.7	55.6	32.0	79	I	8.13	122.67	173.5	60.42	37.46
35	N	8.16	121.29	ND	56.8	38.9	80	W	8.01	129.87	173.9	53.8	29.7
36	F	ND	ND	175.7	57.5	40.3	81	H	10.56	131.08	ND	55.3	34.8
37	T	7.96	116.62	ND	61.5	69.1	82	P	ND	ND	176.3	64.7	31.2
38	E	ND	ND	176.0	54.2	29.7	83	N	11.27	117.37	ND	55.0	40.2
39	L	9.11	122.03	175.4	52.8	44.6	84	I	ND	ND	174.3	57.9	41.1
40	R	8.98	122.88	175.9	53.0	30.8	85	S	9.08	118.68	177.1	58.2	62.5
41	G	9.08	112.18	171.4	43.0	-	86	S	9.93	129.97	173.8	61.2	62.9
42	E	8.81	121.17	173.3	54.9	32.7	87	V	7.99	121.56	177.8	63.9	33.0
43	I	8.6	116.14	174.7	58.1	41.1	88	T	8.19	106.42	176.2	60.9	71.0
44	A	8.29	125.46	178.7	50.3	19.1	89	G	7.84	109.76	173.6	45.7	-
45	G	8.73	107.63	ND	43.5	-	90	A	7.73	121.87	176.3	52.2	18.2

Table A.2 (Continued)

Residue		HN	N	CO	CA	CB	Residue		HN	N	CO	CA	CB
91	I	8.71	119.43	175.5	59.8	41.3	136	Q	8.48	115.81	176.9	56.7	28.5
92	C	8.85	127.95	171.9	57.0	26.0	137	N	8.77	116.25	ND	50.8	38.2
93	L	7.48	126.03	176.0	53.9	44.2	138	P	ND	ND	176.6	64.7	30.9
94	D	9.29	130.61	179.8	58.1	42.5	139	E	8.55	117.77	178.6	58.7	27.7
95	I	8.51	117.32	173.2	63.7	37.2	140	M	7.53	121.01	180.2	57.6	32.3
96	L	7.30	113.34	176.5	53.0	40.1	141	F	9.06	123.71	176.2	61.2	37.6
97	K	7.92	123.11	175.7	55.8	31.5	142	K	8.39	120.68	178.6	59.9	31.0
98	D	8.59	119.69	176.5	55.2	39.9	143	Q	7.89	115.60	179.2	57.6	26.9
99	Q	7.73	115.35	174.3	53.9	27.0	144	T	8.63	120.65	174.9	67.6	68.5
100	W	7.21	121.66	ND	58.3	29.6	145	A	9	124.70	180.5	55.1	16.8
101	A	ND	ND	177.3	49.3	21.2	146	R	8.16	119.25	177.9	58.2	29.4
102	A	8.01	120.39	176.3	53.1	17.4	147	L	7.88	122.89	180.2	57.1	39.2
103	A	7.05	115.84	178.4	51.7	18.0	148	W	9.22	120.79	181.0	62.0	27.6
104	M	7.58	120.31	172.5	56.7	31.0	149	A	9.02	128.49	179.7	55.0	17.5
105	T	7.45	103.677	ND	62.5	72.5	150	H	8.62	120.79	176.2	57.4	28.0
106	L	ND	ND	178.1	57.5	41.5	151	V	8.72	116.87	177.7	65.1	31.4
107	R	8.44	117.15	176.9	59.9	28.7	152	Y	8.16	113.77	176.0	58.4	38.6
108	T	7.88	113.83	178.1	65.8	67.5	153	A	7.29	120.72	177.5	50.4	21.3
109	V	8.50	124.41	177.1	66.7	30.7	154	G	7.53	106.96	174.3	45.5	-
110	L	8.25	119.48	178.4	58.2	40.2	155	A	8.03	124.19	ND	50.6	17.1
111	L	8.41	117.69	177.9	57.1	39.9	156	P	ND	ND	175.9	64.0	31.4
112	S	8.41	118.39	175.8	61.4	62.7	157	V	7.73	117.88	177.9	61.3	32.6
113	L	8.28	126.21	176.9	54.4	40.9	158	S	7.47	117.43	173.5	55.9	64.2
114	Q	8.27	121.86	176.5	55.6	31.5	159	S	8.14	114.70	ND	54.6	62.5
115	A	8.21	122.60	177.8	52.7	17.9	160	P	ND	ND	178.2	64.0	34.1
116	L	8.01	117.09	ND	53.7	37.9	161	E	8.31	118.64	178.8	58.5	28.1
117	L	ND	ND	177.1	57.4	39.2	162	Y	7.43	119.48	177.9	57.3	35.1
118	A	7.25	117.61	176.3	51.8	18.4	163	T	7.90	114.73	176.1	66.3	67.2
119	A	7.89	125.79	179.6	50.9	18.1	164	K	7.84	121.36	178.4	56.6	30.8
120	A	8.20	122.99	176.2	51.3	18.1	165	K	7.24	118.05	178.2	59.7	32.6
121	E	9.00	118.88	ND	51.5	28.7	166	I	7.78	118.27	178.3	63.6	38.0
122	P	ND	ND	174.6	63.5	30.7	167	E	8.47	119.20	179.5	58.7	28.1
123	D	8.48	117.86	175.1	54.4	39.2	168	N	8.31	118.15	177.5	55.4	37.4
124	D	7.16	119.52	ND	51.1	39.8	169	L	7.48	119.76	180.7	57.3	41.6
125	P	ND	ND	176.8	62.3	32.1	170	C	8.90	120.20	178.3	63.1	26.2
126	Q	8.65	117.76	174.1	54.3	28.8	171	A	8.01	122.48	178.3	53.7	16.8
127	D	7.10	118.22	175.4	52.0	42.8	172	M	7.26	115.26	175.7	55.4	32.0
128	A	8.92	128.65	179.5	54.5	17.6	173	G	7.79	105.29	173.5	43.9	-
129	V	7.88	118.45	177.6	65.3	30.6	174	F	6.55	117.97	174.3	56.4	40.4
130	V	7.13	121.32	ND	64.84	30.83	175	D	8.76	121.91	175.8	53.9	42.7
131	A	ND	ND	178.1	54.8	17.6	176	R	8.67	125.73	177.2	60.0	29.5
132	N	8.17	115.01	176.7	55.7	37.3	177	N	8.12	115.26	176.3	56.0	36.9
133	Q	7.59	121.65	178.9	59.1	30.5	178	A	8.04	123.82	180.2	54.4	16.8
134	Y	8.53	117.80	176.5	60.9	37.9	179	V	8.60	120.26	176.7	66.1	30.8
135	K	7.65	113.75	178.4	58.3	32.4	180	I	8.16	120.26	177.6	66.2	36.7

Table A.2 (Continued)

Residue		HN	N	CO	CA	CB	Residue		HN	N	CO	CA	CB
181	V	8.16	122.71	177.9	67.0	30.8	191	E	8.75	122.79	179.2	59.8	28.2
182	A	8.43	124.85	178.3	55.0	17.7	192	T	8.13	114.05	178.1	64.8	67.8
183	L	8.27	115.37	ND	57.0	39.4	193	A	8.47	124.95	177.9	54.8	17.0
184	S	ND	ND	174.6	61.8	63.7	194	T	8.09	114.33	174.9	67.2	68.0
185	S	7.76	112.49	174.6	60.0	62.9	195	E	7.31	119.42	179.1	58.6	28.4
186	K	7.19	120.67	175.9	52.3	28.4	196	L	7.31	119.90	179.5	57.1	40.8
187	S	7.90	112.47	172.8	59.5	60.6	197	L	7.84	121.36	178.6	56.6	39.6
188	W	8.69	110.48	172.3	58.7	24.1	198	L	7.76	117.84	177.3	55.2	41.6
189	D	7.25	119.81	174.9	52.7	41.4	199	S	7.59	115.00	173.0	58.4	63.3
190	V	8.75	127.29	178.4	66.1	30.8	200	N	7.72	125.77	ND	54.3	39.9

*ND, Not Detected

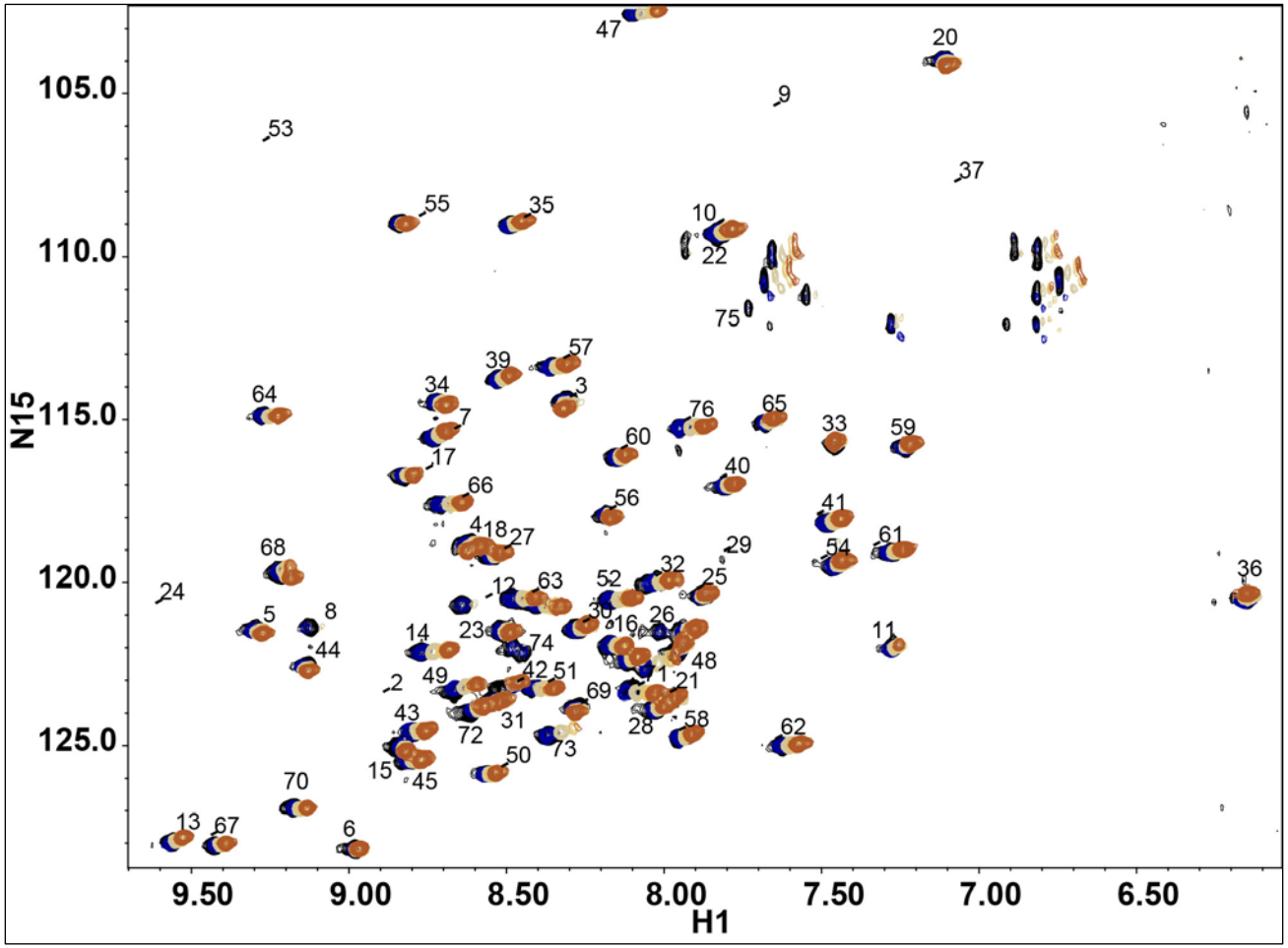

Figure A.1 Overlay of ^{1}H, ^{15}N-HSQC Spectra at 25ºC, 30ºC, 35ºC and 37ºC for Ubiquitin Titrated with E2-25K. [Black contours represent 25ºC with no E2-25K, blue contours represent 25ºC with E2-25K, light green contours represent 30ºC, light brown contours represent 35ºC, and brown contours represent 37ºC with E2-25K.]

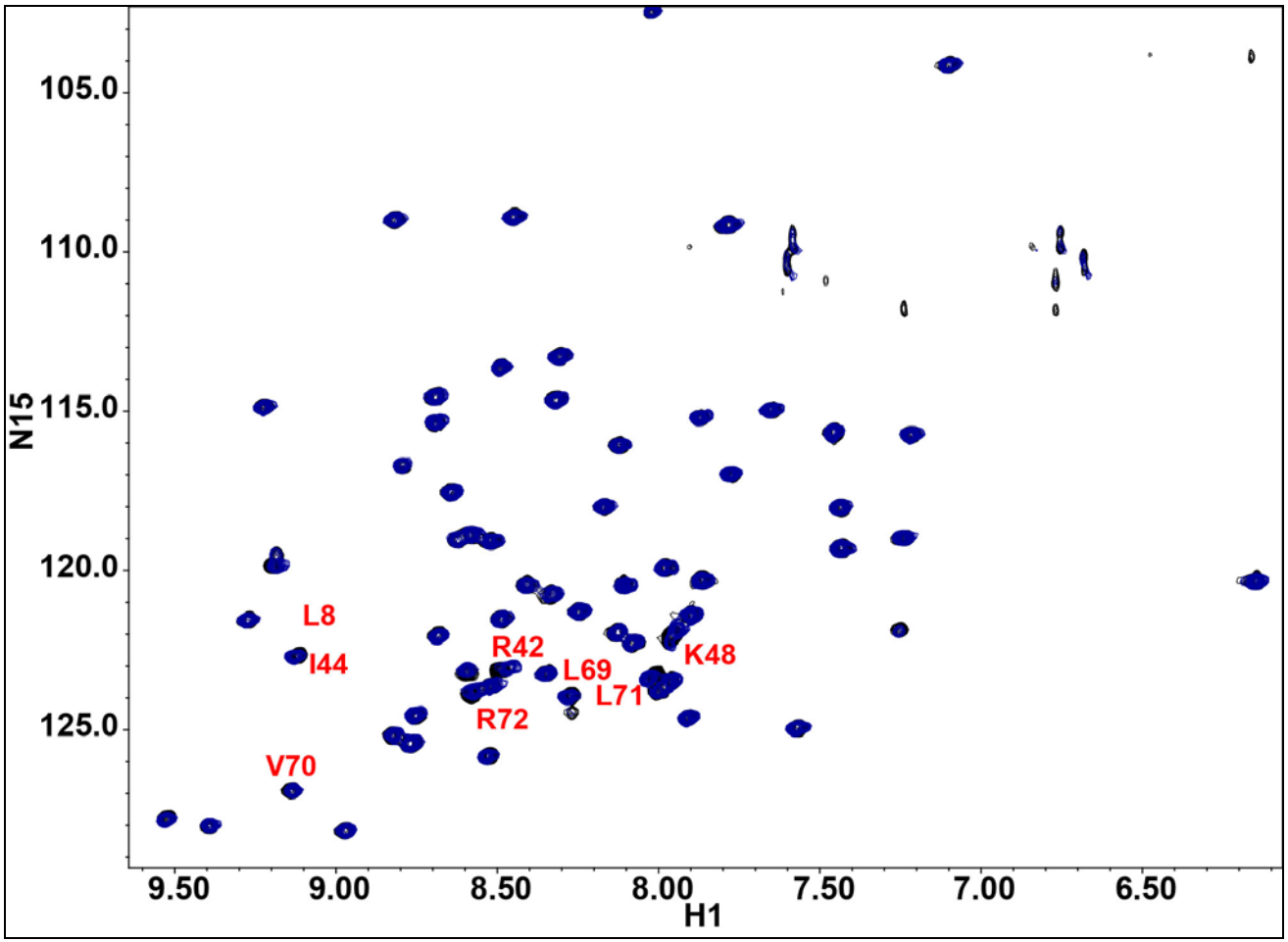

Figure A.2 Specific Interaction of Ubiquitin with E2-25K at 37°C. [Titration of ^{15}N-labeled Ub with unlabeled E2-25K was followed by solution NMR spectroscopy. Overlay of the ^{1}H-^{15}N HSQC spectra of the Ub where black contours represent 0 equivalents of E2-25K added. Blue contours represent 0.03 equivalents of E2-25K added.]

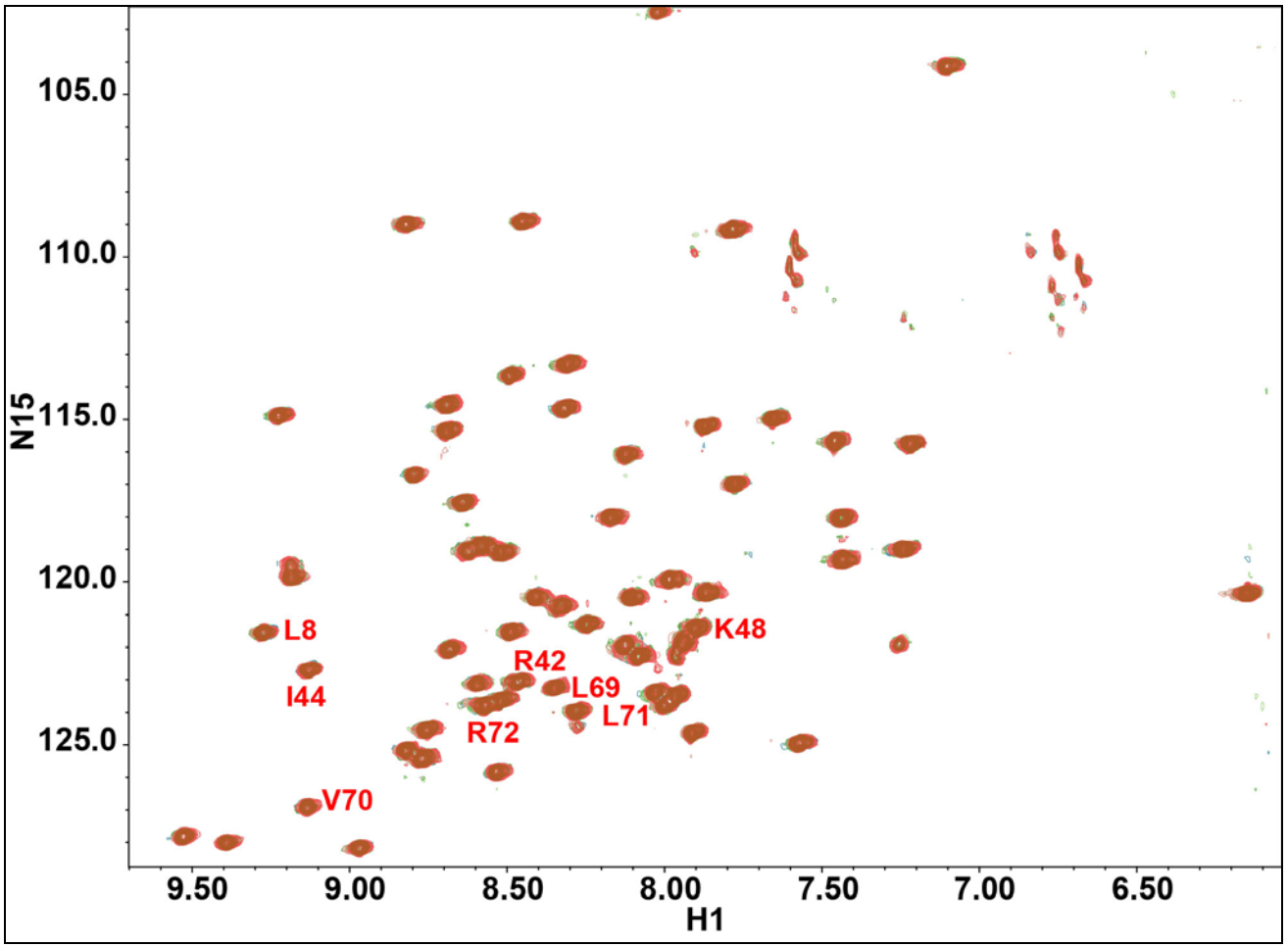

Figure A.3 Specific Interaction of Ubiquitin with E2-25K at 37°C after 15 Hours. [Titration of ^{15}N-labeled Ub with unlabeled E2-25K was followed by solution NMR spectroscopy. Overlay of the ^{1}H-^{15}N HSQC spectra of the Ub where teal contours represent Ub with E2-25K at initial time. Brown contours represent Ub with E2-25K after 15 hours.]

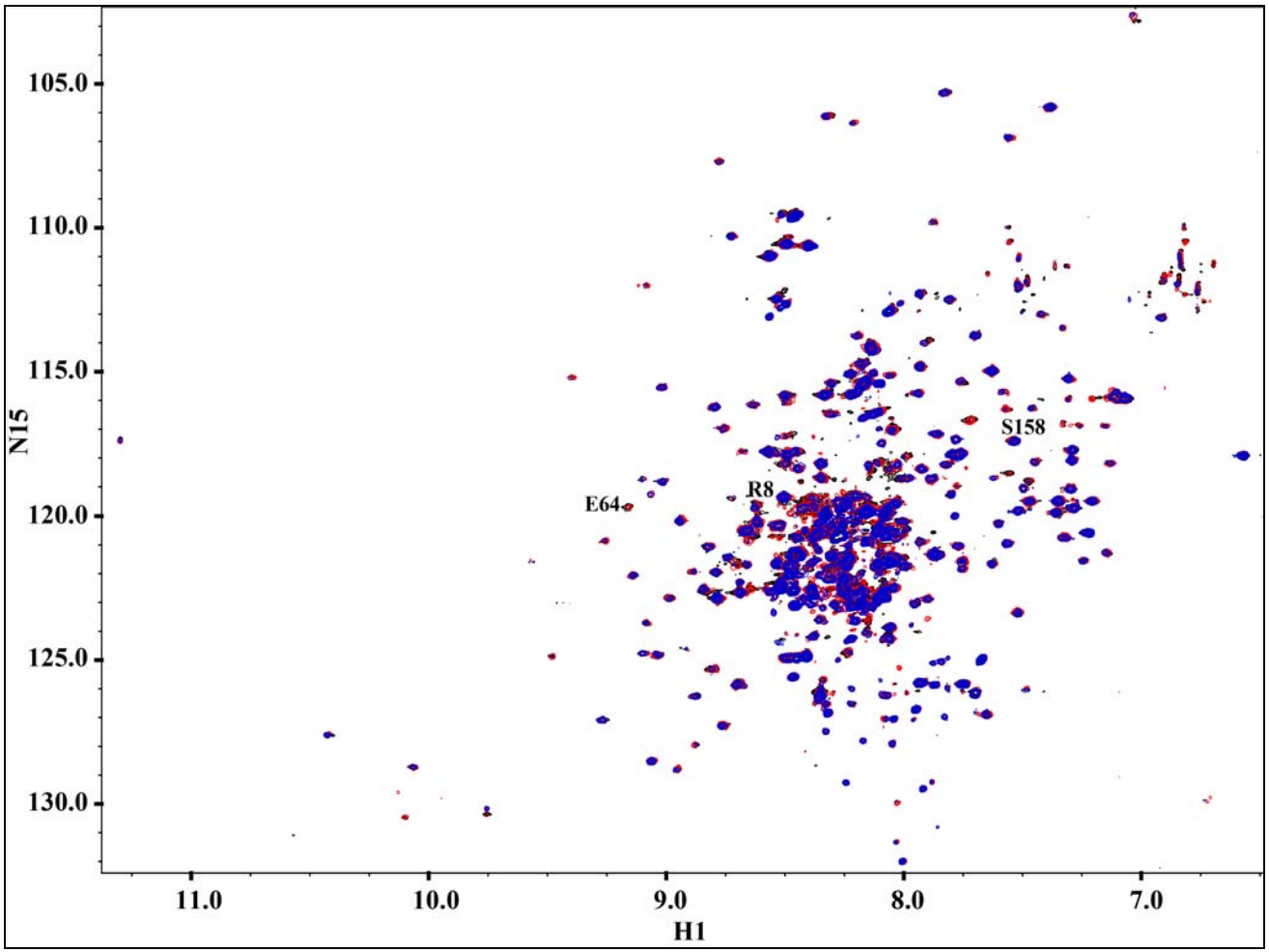

Figure A.4 Specific Interaction of E2-25K with RNF2. [Titration of ^{15}N-labeled E2-25K with unlabeled RNF2 was followed by solution NMR spectroscopy. Overlay of the ^{1}H-^{15}N HSQC spectra of the RNF2 where Black *contours* represent 0 equivalents, Red *contours* represent 0.07 equivalents, and Blue *contours* represent 0.14 equivalents of RNF2 added.]

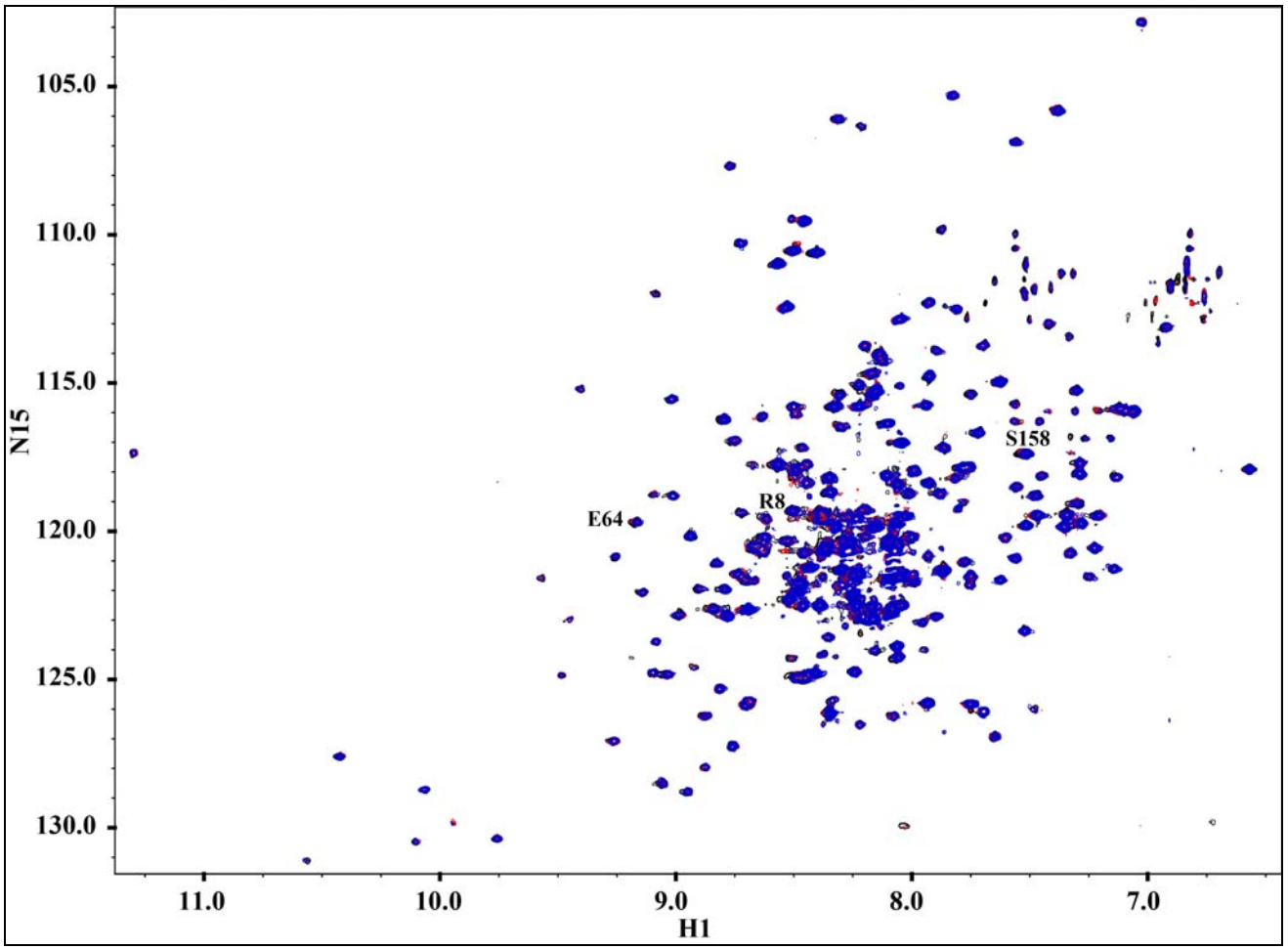

Figure A.5 Specific Interaction of E2-25K with MDM2. [Titration of ^{15}N-labeled E2-25K with unlabeled MDM2 was followed by solution NMR spectroscopy. Overlay of the ^{1}H-^{15}N HSQC spectra of the MDM2 where Black *contours* represent 0 equivalents, Red *contours* represent 0.08 equivalents, and Blue *contours* represent 0.21 equivalents of MDM2 added.]

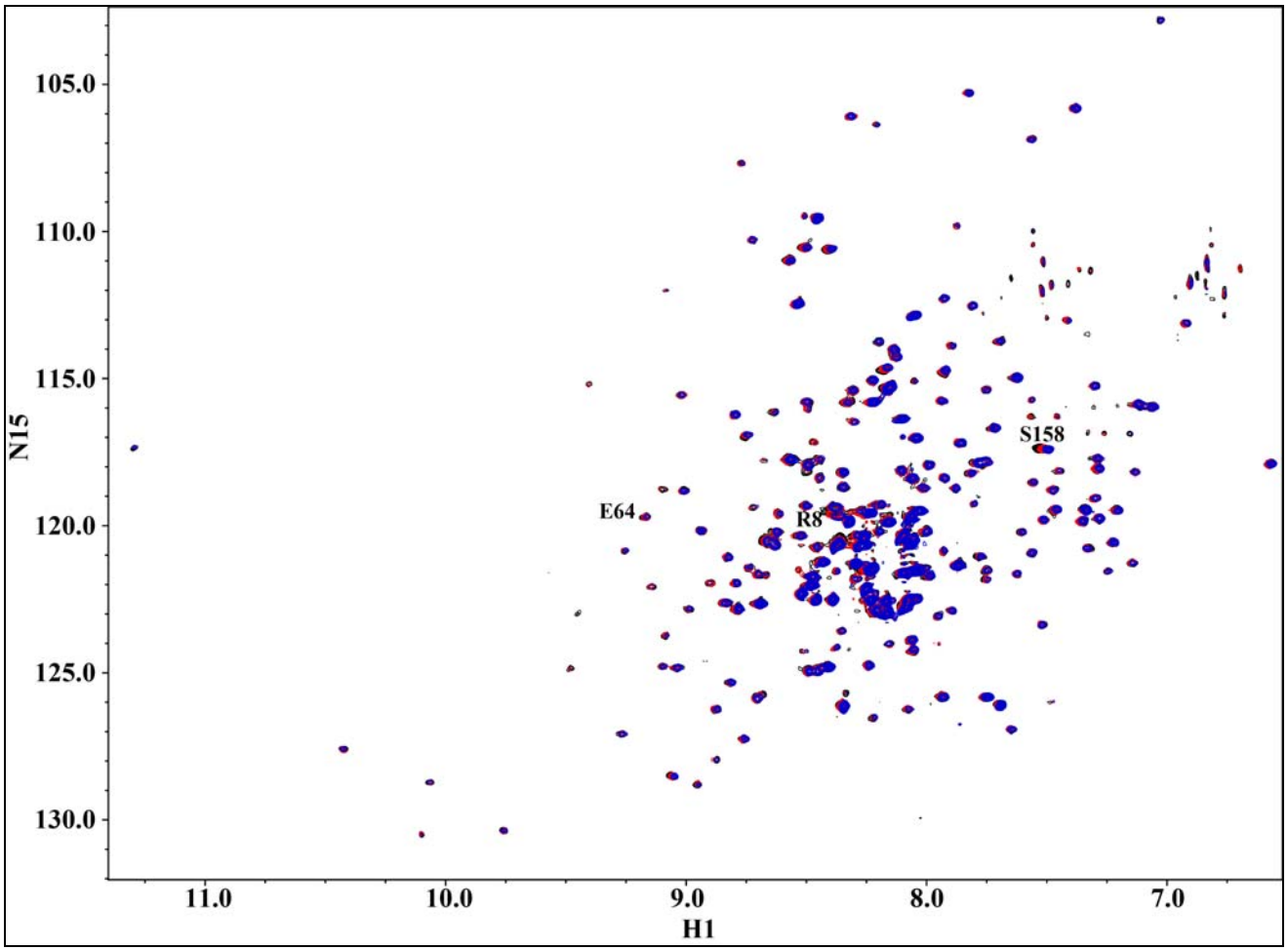

Figure A.6 Specific Interaction of E2-25K with APC11 RING Finger. [Titration of ^{15}N-labeled E2-25K with unlabeled APC11 was followed by solution NMR spectroscopy. Overlay of the ^{1}H-^{15}N HSQC spectra of the APC11 where Black *contours* represent 0 equivalents, Red *contours* represent 0.07 equivalents, and Blue *contours* represent 0.16 equivalents of APC11 added.]

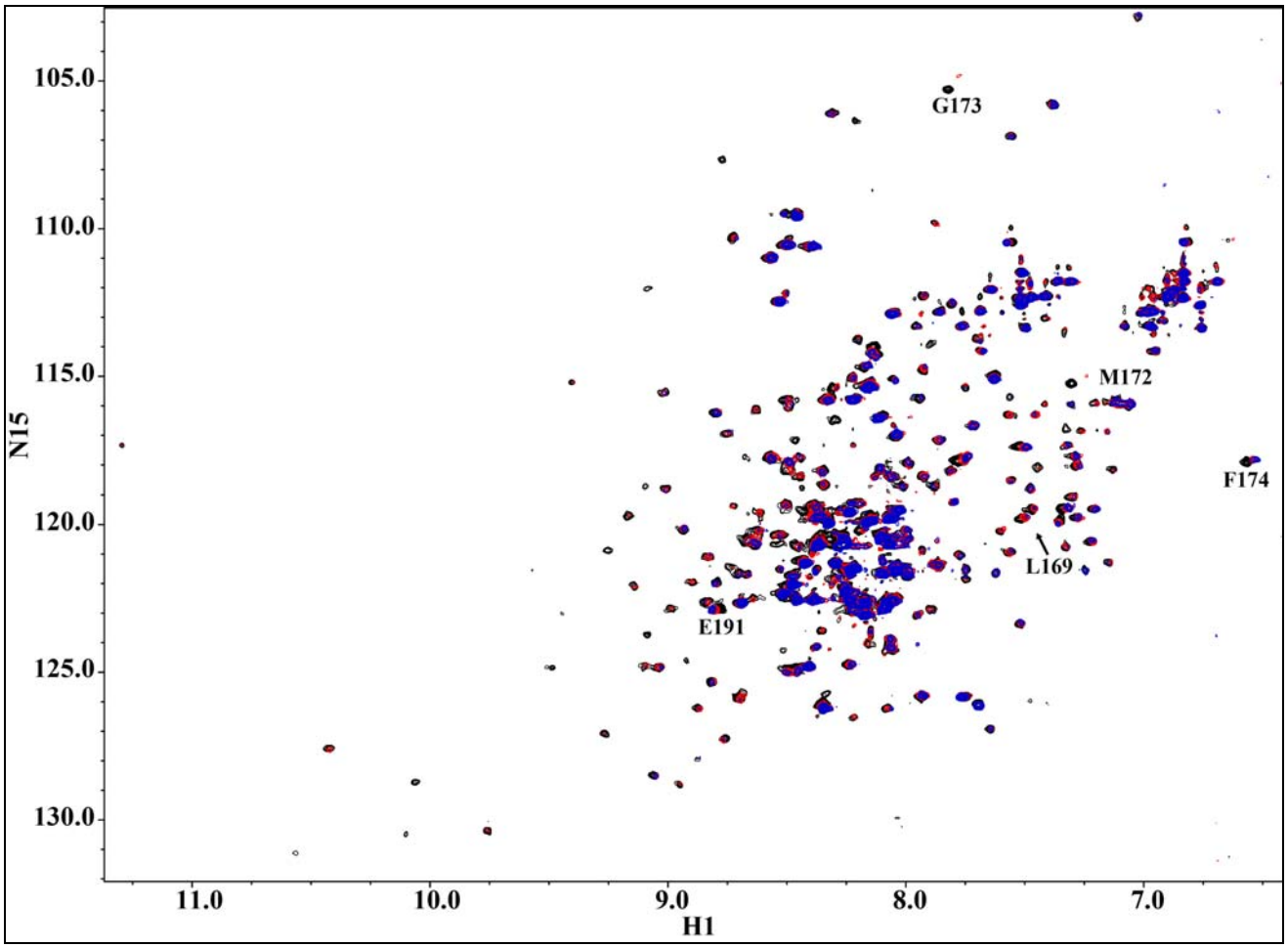

Figure A.7 Specific Interaction of E2-25K with Parkin Ubl Domain. [Titration of ^{15}N-labeled E2-25K with unlabeled Parkin was followed by solution NMR spectroscopy. Overlay of the ^{1}H-^{15}N HSQC spectra of the Parkin where Black *contours* represent 0 equivalents, Red *contours* represent 0.32 equivalents, and Blue *contours* represent 0.54 equivalents of Parkin added.]

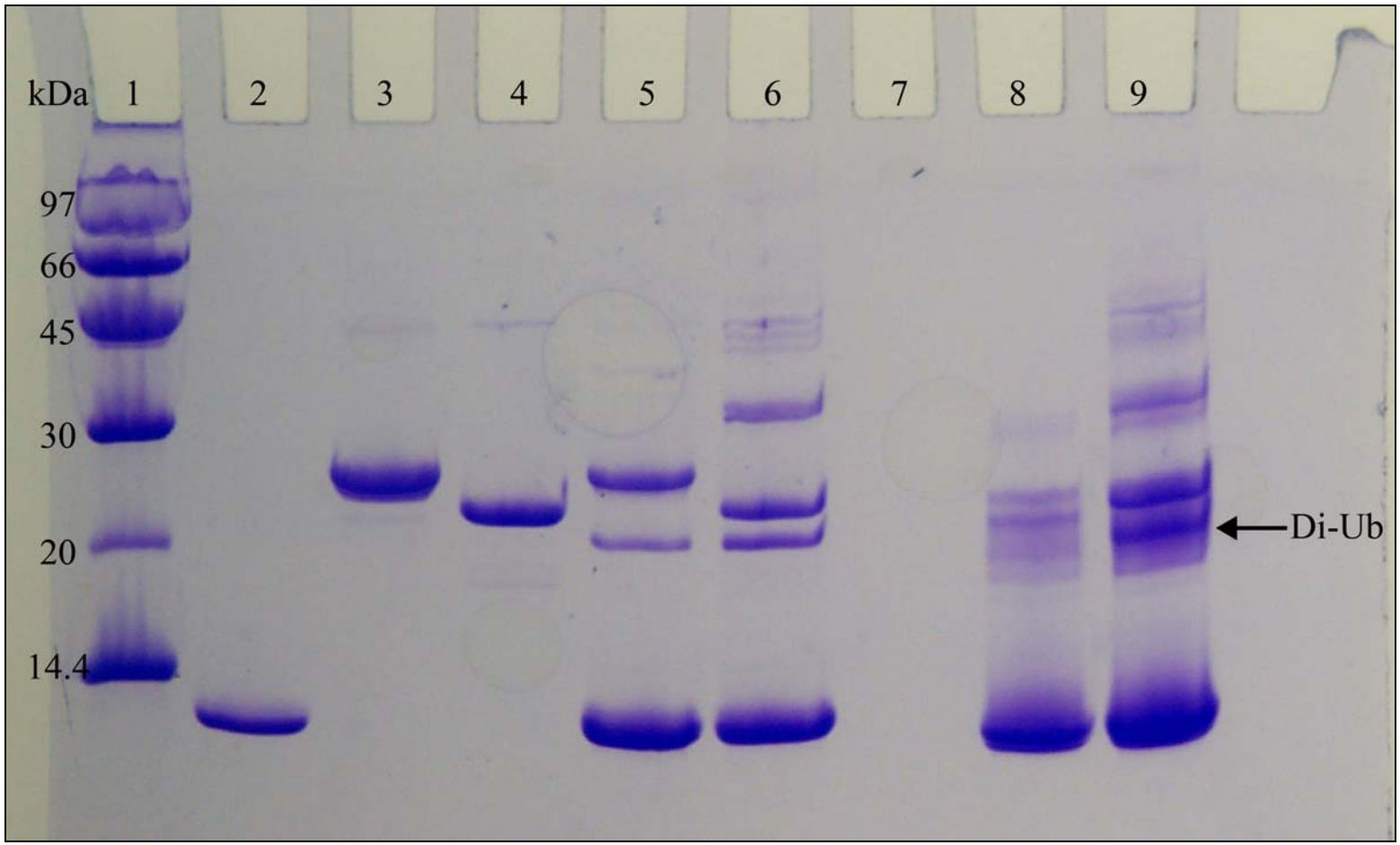

Figure A.8 E2-25K/UBC Polyubiquitin Chain Assay. [SDS page of Polyubiquitin Chain Assays. Lane 1 – LMW Marker, Lane 2 – Ub-K48C, Lane 3 – E2-25K, Lane 4 – E2-25K UBC Domain, Lane 5 – Assay with E2-25K and equimolar ratios of Ub-K48C and Ub-D77, Lane 6 – Assay with E2-25K UBC Domain and equimolar ratios of Ub-K48C and Ub-D77, Lane 7 – Empty, Lane 8 – Ub-K48C-K63C, Lane 9 – Assay with E2-25K UBC Domain and equimolar ratios of Ub-K48C-K63C and Ub-D77.]

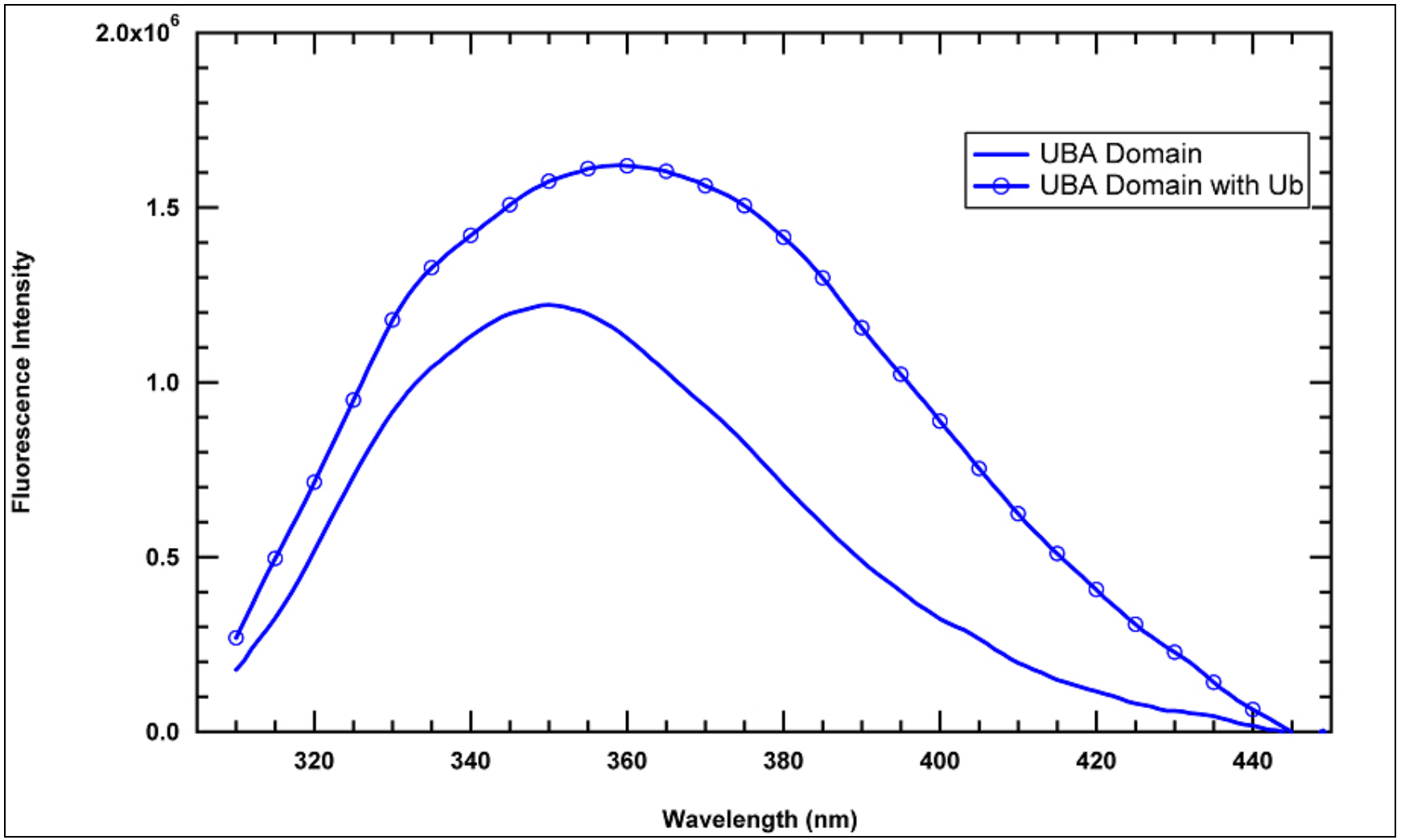

Figure A.9 Overlay of Tryptophan Fluorescence Spectra of the UBA Domain and UBA Domain with Ubiquitin. [The Trp maximum emission wavelength was 352 nm for the UBA domain and 355 nm for the UBA domain with Ub.]

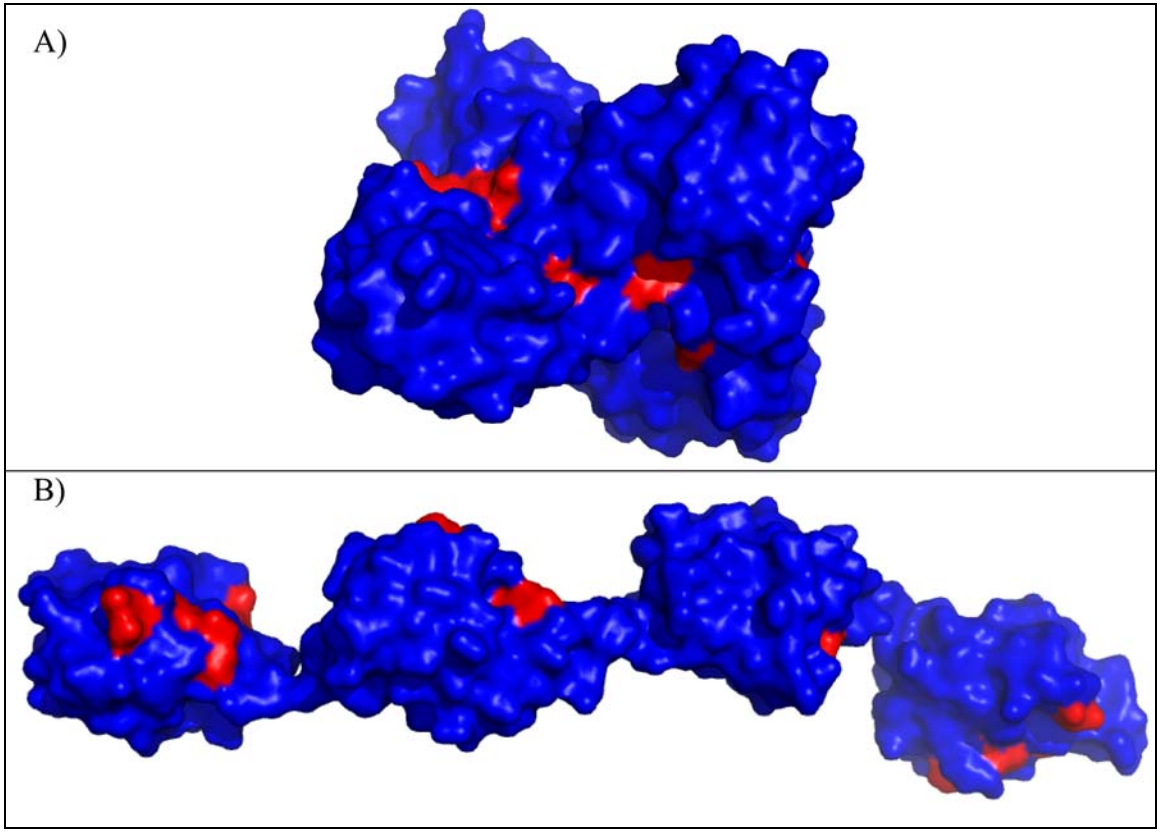

Figure A.10 Surface Representation of K48-linked and K63-linked Tetraubiquitin. [(*A*), surface representation of K48-linked tetraubiquitin where *red regions* indicate surface residues having a significant chemical shift change upon UBA domain binding (PDB code 2O6V). (*B*), surface representation of K63-linked tetraubiquitin where *red regions* indicate surface residues having a significant chemical shift change upon UBA domain binding (PDB code 3HM3).]

REFERENCES

[1] Shimura, H., N. Hattori, S. Kubo, Y. Mizuno, S. Asakawa, S. Minoshima, N. Shimizu, K. Iwai, T. Chiba, K. Tanaka, T. Suzuki: **Familial Parkinson disease gene product, parkin, is a ubiquitin-protein ligase.** *Nat Genet* 2000, **25**(3): 302-5.

[2] Scheffner, M., O. Staub: **HECT E3s and human disease.** *BMC Biochem* 2007, **8 Suppl 1**: S6.

[3] Cardozo, T., M. Pagano: **Wrenches in the works: drug discovery targeting the SCF ubiquitin ligase and APC/C complexes.** *BMC Biochem* 2007, **8 Suppl 1**: S9.

[4] Kalchman, M.A., R.K. Graham, G. Xia, H.B. Koide, J.G. Hodgson, K.C. Graham, Y.P. Goldberg, R.D. Gietz, C.M. Pickart, M.R. Hayden: **Huntingtin is ubiquitinated and interacts with a specific ubiquitin-conjugating enzyme.** *J Biol Chem* 1996, **271**(32): 19385-94.

[5] Song, S., Y.K. Jung: **Alzheimer's disease meets the ubiquitin-proteasome system.** *Trends Mol Med* 2004, **10**(11): 565-70.

[6] Ciechanover, A., P. Brundin: **The ubiquitin proteasome system in neurodegenerative diseases: Sometimes the chicken, sometimes the egg.** *Neuron* 2003, **40**(2): 427-46.

[7] Song, S., S.Y. Kim, Y.M. Hong, D.G. Jo, J.Y. Lee, S.M. Shim, C.W. Chung, S.J. Seo, Y.J. Yoo, J.Y. Koh, M.C. Lee, A.J. Yates, H. Ichijo, Y.K. Jung: **Essential role of E2-25K/Hip-2 in mediating amyloid-beta neurotoxicity.** *Mol Cell* 2003, **12**(3): 553-63.

[8] de Pril, R., D.F. Fischer, R.A. Roos, F.W. van Leeuwen: **Ubiquitin-conjugating enzyme E2-25K increases aggregate formation and cell death in polyglutamine diseases.** *Mol Cell Neurosci* 2007, **34**(1): 10-9.

[9] Outeiro, T.F., J. Tetzlaff: **Mechanisms of disease II: Cellular protein quality control.** *Semin Pediatr Neurol* 2007, **14**(1): 15-25.

[10] Hershko, A., A. Ciechanover: **The ubiquitin system.** *Annu Rev Biochem* 1998, **67**: 425-79.

[11] Passmore, L.A., D. Barford: **Getting into position: The catalytic mechanisms of protein ubiquitylation.** *Biochem J* 2004, **379**(Pt 3): 513-25.

[12] von Mikecz, A.: **The nuclear ubiquitin-proteasome system.** *J Cell Sci* 2006, **119**(Pt 10): 1977-84.

[13] Muratani, M., W.P. Tansey: **How the ubiquitin-proteasome system controls transcription.** *Nat Rev Mol Cell Biol* 2003, **4**(3): 192-201.

[14] Hicke, L., R. Dunn: **Regulation of membrane protein transport by ubiquitin and ubiquitin-binding proteins.** *Annu Rev Cell Dev Biol* 2003, **19**: 141-72.

[15] Jesenberger, V., S. Jentsch: **Deadly encounter: Ubiquitin meets apoptosis.** *Nat Rev Mol Cell Biol* 2002, **3**(2): 112-21.

[16] Kloetzel, P.M.: **Antigen processing by the proteasome.** *Nat Rev Mol Cell Biol* 2001, **2**(3): 179-87.

[17] Baboshina, O.V., A.L. Haas: **Novel multiubiquitin chain linkages catalyzed by the conjugating enzymes E2EPF and RAD6 are recognized by 26 S proteasome subunit 5**. *J Biol Chem* 1996, **271**(5): 2823-31.

[18] Okumura, F., S. Hatakeyama, M. Matsumoto, T. Kamura, K.I. Nakayama: **Functional regulation of FEZ1 by the U-box-type ubiquitin ligase E4B contributes to neuritogenesis**. *J Biol Chem* 2004, **279**(51): 53533-43.

[19] Vitte, A.L., S. Buchsbaum, P. Jalinot: **Modulation of HIV-1 Rev protein abundance and activity by polyubiquitination with unconventional Lys-33 branching**. *FEBS Lett* 2006, **580**(26): 6155-60.

[20] Peng, J., D. Schwartz, J.E. Elias, C.C. Thoreen, D. Cheng, G. Marsischky, J. Roelofs, D. Finley, S.P. Gygi: **A proteomics approach to understanding protein ubiquitination.** *Nat Biotechnol* 2003, **21**(8): 921-6.

[21] Russell, N.S., K.D. Wilkinson: **Identification of a novel 29-linked polyubiquitin binding protein, Ufd3, using polyubiquitin chain analogues**. *Biochemistry* 2004, **43**(16): 4844-54.

[22] Thrower, J.S., L. Hoffman, M. Rechsteiner, C.M. Pickart: **Recognition of the polyubiquitin proteolytic signal.** *Embo J* 2000, **19**(1): 94-102.

[23] Schnell, J.D., L. Hicke: **Non-traditional functions of ubiquitin and ubiquitin-binding proteins.** *J Biol Chem* 2003, **278**(38): 35857-60.

[24] Spence, J., S. Sadis, A.L. Haas, D. Finley: **A ubiquitin mutant with specific defects in DNA repair and multiubiquitination.** *Mol Cell Biol* 1995, **15**(3): 1265-73.

[25] Wang, C., L. Deng, M. Hong, G.R. Akkaraju, J. Inoue, Z.J. Chen: **TAK1 is a ubiquitin-dependent kinase of MKK and IKK**. *Nature* 2001, **412**(6844): 346-51.

[26] Soetens, O., J.O. De Craene, B. Andre: **Ubiquitin is required for sorting to the vacuole of the yeast general amino acid permease, Gap1**. *J Biol Chem* 2001, **276**(47): 43949-57.

[27] Haas, A.L., J.V. Warms, A. Hershko, I.A. Rose: **Ubiquitin-activating enzyme. Mechanism and role in protein-ubiquitin conjugation**. *J Biol Chem* 1982, **257**(5): 2543-8.

[28] Ciechanover, A.: **The ubiquitin-proteasome pathway: On protein death and cell life**. *Embo J* 1998, **17**(24): 7151-60.

[29] Jin, J., X. Li, S.P. Gygi, J.W. Harper: **Dual E1 activation systems for ubiquitin differentially regulate E2 enzyme charging.** *Nature* 2007, **447**(7148): 1135-8.

[30] Haas, A.L., I.A. Rose: **The mechanism of ubiquitin activating enzyme. A kinetic and equilibrium analysis**. *J Biol Chem* 1982, **257**(17): 10329-37.

[31] Dye, B.T., B.A. Schulman: **Structural mechanisms underlying posttranslational modification by ubiquitin-like proteins**. *Annu Rev Biophys Biomol Struct* 2007, **36**: 131-50.

[32] Merkley, N., K.R. Barber, G.S. Shaw: **Ubiquitin manipulation by an E2 conjugating enzyme using a novel covalent intermediate**. *J Biol Chem* 2005, **280**(36): 31732-8.

[33] Chen, Z., C.M. Pickart: **A 25-kilodalton ubiquitin carrier protein (E2) catalyzes multi-ubiquitin chain synthesis via lysine 48 of ubiquitin**. *J Biol Chem* 1990, **265**(35): 21835-42.

[34] Cyr, D.M., J. Hohfeld, C. Patterson: **Protein quality control: U-box-containing E3 ubiquitin ligases join the fold.** *Trends Biochem Sci* 2002, **27**(7): 368-75.

[35] Pickart, C.M., M.J. Eddins: **Ubiquitin: Structures, functions, mechanisms.** *Biochim Biophys Acta* 2004, **1695**(1-3): 55-72.

[36] Huang, D.T., A. Paydar, M. Zhuang, M.B. Waddell, J.M. Holton, B.A. Schulman: **Structural basis for recruitment of Ubc12 by an E2 binding domain in NEDD8's E1.** *Mol Cell* 2005, **17**(3): 341-50.

[37] Eletr, Z.M., D.T. Huang, D.M. Duda, B.A. Schulman, B. Kuhlman: **E2 conjugating enzymes must disengage from their E1 enzymes before E3-dependent ubiquitin and ubiquitin-like transfer.** *Nat Struct Mol Biol* 2005, **12**(10): 933-4.

[38] Hamilton, K.S., M.J. Ellison, K.R. Barber, R.S. Williams, J.T. Huzil, S. McKenna, C. Ptak, M. Glover, G.S. Shaw: **Structure of a conjugating enzyme-ubiquitin thiolester intermediate reveals a novel role for the ubiquitin tail.** *Structure* 2001, **9**(10): 897-904.

[39] Wu, P.Y., M. Hanlon, M. Eddins, C. Tsui, R.S. Rogers, J.P. Jensen, M.J. Matunis, A.M. Weissman, C. Wolberger, C.M. Pickart: **A conserved catalytic residue in the ubiquitin-conjugating enzyme family.** *Embo J* 2003, **22**(19): 5241-50.

[40] Eddins, M.J., C.M. Carlile, K.M. Gomez, C.M. Pickart, C. Wolberger: **Mms2-Ubc13 covalently bound to ubiquitin reveals the structural basis of linkage-specific polyubiquitin chain formation.** *Nat Struct Mol Biol* 2006, **13**(10): 915-20.

[41] Petroski, M.D., R.J. Deshaies: **Mechanism of lysine 48-linked ubiquitin-chain synthesis by the cullin-RING ubiquitin-ligase complex SCF-Cdc34.** *Cell* 2005, **123**(6): 1107-20.

[42] Verdecia, M.A., C.A. Joazeiro, N.J. Wells, J.L. Ferrer, M.E. Bowman, T. Hunter, J.P. Noel: **Conformational flexibility underlies ubiquitin ligation mediated by the WWP1 HECT domain E3 ligase.** *Mol Cell* 2003, **11**(1): 249-59.

[43] Wang, M., C.M. Pickart: **Different HECT domain ubiquitin ligases employ distinct mechanisms of polyubiquitin chain synthesis.** *Embo J* 2005, **24**(24): 4324-33.

[44] Deshaies, R.J., C.A. Joazeiro: **RING domain E3 ubiquitin ligases.** *Annu Rev Biochem* 2009, **78**: 399-434.

[45] Zheng, N., P. Wang, P.D. Jeffrey, N.P. Pavletich: **Structure of a c-Cbl-UbcH7 complex: RING domain function in ubiquitin-protein ligases.** *Cell* 2000, **102**(4): 533-9.

[46] Dominguez, C., A.M. Bonvin, G.S. Winkler, F.M. van Schaik, H.T. Timmers, R. Boelens: **Structural model of the UbcH5B/CNOT4 complex revealed by combining NMR, mutagenesis, and docking approaches.** *Structure* 2004, **12**(4): 633-44.

[47] Seol, J.H., R.M. Feldman, W. Zachariae, A. Shevchenko, C.C. Correll, S. Lyapina, Y. Chi, M. Galova, J. Claypool, S. Sandmeyer, K. Nasmyth, R.J. Deshaies, A. Shevchenko, R.J. Deshaies: **Cdc53/cullin and the essential Hrt1 RING-H2 subunit of SCF define a ubiquitin ligase module that activates the E2 enzyme Cdc34.** *Genes Dev* 1999, **13**(12): 1614-26.

[48] Poyurovsky, M.V., C. Priest, A. Kentsis, K.L. Borden, Z.Q. Pan, N. Pavletich, C. Prives: **The Mdm2 RING domain C-terminus is required for supramolecular assembly and ubiquitin ligase activity.** *Embo J* 2007, **26**(1): 90-101.

[49] van Leeuwen, F.W., D.P. de Kleijn, H.H. van den Hurk, A. Neubauer, M.A. Sonnemans, J.A. Sluijs, S. Koycu, R.D. Ramdjielal, A. Salehi, G.J. Martens, F.G. Grosveld, J. Peter, H. Burbach, E.M. Hol: **Frameshift mutants of beta amyloid precursor protein and ubiquitin-B in Alzheimer's and Down patients.** *Science* 1998, **279**(5348): 242-7.

[50] Pan, Z.Q., A. Kentsis, D.C. Dias, K. Yamoah, K. Wu: **Nedd8 on cullin: Building an expressway to protein destruction.** *Oncogene* 2004, **23**(11): 1985-97.

[51] Johnson, E.S.: **Protein modification by SUMO.** *Annu Rev Biochem* 2004, **73**: 355-82.

[52] Hartmann-Petersen, R., C. Gordon: **Integral UBL domain proteins: A family of proteasome interacting proteins.** *Semin Cell Dev Biol* 2004, **15**(2): 247-59.

[53] Walters, K.J., M.F. Kleijnen, A.M. Goh, G. Wagner, P.M. Howley: **Structural studies of the interaction between ubiquitin family proteins and proteasome subunit S5a.** *Biochemistry* 2002, **41**(6): 1767-77.

[54] Tanaka, K., T. Suzuki, N. Hattori, Y. Mizuno: **Ubiquitin, proteasome and parkin.** *Biochim Biophys Acta* 2004, **1695**(1-3): 235-47.

[55] Barnard, C. *Huntingtin Protein and Protein Aggregation*. 2002 [cited; Available from: http://hopes.stanford.edu.

[56] Hardy, J., D. Allsop: **Amyloid deposition as the central event in the aetiology of Alzheimer's disease.** *Trends Pharmacol Sci* 1991, **12**(10): 383-8.

[57] Hernandez, F., J. Avila: **Tauopathies.** *Cell Mol Life Sci* 2007, **64**(17): 2219-33.

[58] Davie, C.A.: **A review of Parkinson's disease.** *Br Med Bull* 2008, **86**: 109-27.

[59] Pichler, A., P. Knipscheer, E. Oberhofer, W.J. van Dijk, R. Korner, J.V. Olsen, S. Jentsch, F. Melchior, T.K. Sixma: **SUMO modification of the ubiquitin-conjugating enzyme E2-25K.** *Nat Struct Mol Biol* 2005, **12**(3): 264-9.

[60] Hughes, R.C., R.C. Wilson, J.W. Flatt, E.J. Meehan, J.D. Ng, P.D. Twigg, *PDB ID: 3e46; Crystal structure of ubiquitin-conjugating enzyme E2-25kDa (Huntington interacting protein 2) M172A mutant*. 2008.

[61] Merkley, N., G.S. Shaw: **Solution structure of the flexible class II ubiquitin-conjugating enzyme Ubc1 provides insights for polyubiquitin chain assembly.** *J Biol Chem* 2004, **279**(45): 47139-47.

[62] PDB ID: 3E46 Hughes, R.C., R.C. Wilson, J.W. Flatt, E.J. Meehan, J.D. Ng, P.D. Twigg, **Crystal structure of ubiquitin-conjugating enzyme E2-25kDa (Huntington interacting protein 2) M172A mutant.**

[63] Lee, S.J., J.Y. Choi, Y.M. Sung, H. Park, H. Rhim, S. Kang: **E3 ligase activity of RING finger proteins that interact with Hip-2, a human ubiquitin-conjugating enzyme.** *FEBS Lett* 2001, **503**(1): 61-4.

[64] Windheim, M., M. Peggie, P. Cohen: **Two different classes of E2 ubiquitin-conjugating enzymes are required for the mono-ubiquitination of proteins and elongation by polyubiquitin chains with a specific topology.** *Biochem J* 2008, **409**(3): 723-9.

[65] Rodrigo-Brenni, M.C., D.O. Morgan: **Sequential E2s drive polyubiquitin chain assembly on APC targets.** *Cell* 2007, **130**(1): 127-39.

[66] van Nocker, S., R.D. Vierstra: **Multiubiquitin chains linked through lysine 48 are abundant in vivo and are competent intermediates in the ubiquitin proteolytic pathway.** *J Biol Chem* 1993, **268**(33): 24766-73.

[67] Yao, T., R.E. Cohen: **Cyclization of polyubiquitin by the E2-25K ubiquitin conjugating enzyme.** *J Biol Chem* 2000, **275**(47): 36862-8.

[68] Song, S., H. Lee, T.I. Kam, M.L. Tai, J.Y. Lee, J.Y. Noh, S.M. Shim, S.J. Seo, Y.Y. Kong, T. Nakagawa, C.W. Chung, D.Y. Choi, H. Oubrahim, Y.K. Jung: **E2-25K/Hip-2 regulates caspase-12 in ER stress-mediated Abeta neurotoxicity.** *J Cell Biol* 2008, **182**(4): 675-84.

[69] Bae, Y., D. Choi, H. Rhim, S. Kang: **Hip2 interacts with cyclin B1 and promotes its degradation through the ubiquitin proteasome pathway.** *FEBS Lett*, **584**(22): 4505-10.

[70] Bae, Y., C.W. Kho, S.Y. Lee, H. Rhim, S. Kang: **Hip2 interacts with and destabilizes Smac/DIABLO.** *Biochem Biophys Res Commun*, **397**(4): 718-23.

[71] Saville, M.K., A. Sparks, D.P. Xirodimas, J. Wardrop, L.F. Stevenson, J.C. Bourdon, Y.L. Woods, D.P. Lane: **Regulation of p53 by the ubiquitin-conjugating enzymes UbcH5B/C in vivo.** *J Biol Chem* 2004, **279**(40): 42169-81.

[72] Flierman, D., C.S. Coleman, C.M. Pickart, T.A. Rapoport, V. Chau: **E2-25K mediates US11-triggered retro-translocation of MHC class I heavy chains in a permeabilized cell system.** *Proc Natl Acad Sci U S A* 2006, **103**(31): 11589-94.

[73] Kim, H.T., K.P. Kim, F. Lledias, A.F. Kisselev, K.M. Scaglione, D. Skowyra, S.P. Gygi, A.L. Goldberg: **Certain pairs of ubiquitin-conjugating enzymes (E2s) and ubiquitin-protein ligases (E3s) synthesize nondegradable forked ubiquitin chains containing all possible isopeptide linkages.** *J Biol Chem* 2007, **282**(24): 17375-86.

[74] Hakli, M., K.L. Lorick, A.M. Weissman, O.A. Janne, J.J. Palvimo: **Transcriptional coregulator SNURF (RNF4) possesses ubiquitin E3 ligase activity.** *FEBS Lett* 2004, **560**(1-3): 56-62.

[75] Hurley, J.H., S. Lee, G. Prag: **Ubiquitin-binding domains.** *Biochem J* 2006, **399**(3): 361-72.

[76] Hartmann-Petersen, R., C.A. Semple, C.P. Ponting, K.B. Hendil, C. Gordon: **UBA domain containing proteins in fission yeast.** *Int J Biochem Cell Biol* 2003, **35**(5): 629-36.

[77] Haldeman, M.T., G. Xia, E.M. Kasperek, C.M. Pickart: **Structure and function of ubiquitin conjugating enzyme E2-25K: The tail is a core-dependent activity element.** *Biochemistry* 1997, **36**(34): 10526-37.

[78] Wilson, R.C., R.C. Hughes, J.W. Flatt, E.J. Meehan, J.D. Ng, P.D. Twigg: **Structure of full-length ubiquitin-conjugating enzyme E2-25K (huntingtin-interacting protein 2).** *Acta Crystallogr Sect F Struct Biol Cryst Commun* 2009, **65**(Pt 5): 440-4.

[79] Mastrandrea, L.D., E.M. Kasperek, E.G. Niles, C.M. Pickart: **Core domain mutation (S86Y) selectively inactivates polyubiquitin chain synthesis catalyzed by E2-25K.** *Biochemistry* 1998, **37**(27): 9784-92.

[80] McKenna, S., L. Spyracopoulos, T. Moraes, L. Pastushok, C. Ptak, W. Xiao, M.J. Ellison: **Noncovalent interaction between ubiquitin and the human DNA repair protein Mms2 is required for Ubc13-mediated polyubiquitination.** *J Biol Chem* 2001, **276**(43): 40120-6.

[81] Li, W., D. Tu, A.T. Brunger, Y. Ye: **A ubiquitin ligase transfers preformed polyubiquitin chains from a conjugating enzyme to a substrate.** *Nature* 2007, **446**(7133): 333-7.

[82] Gazdoiu, S., K. Yamoah, K. Wu, C.R. Escalante, I. Tappin, V. Bermudez, A.K. Aggarwal, J. Hurwitz, Z.Q. Pan: **Proximity-induced activation of human Cdc34 through heterologous dimerization.** *Proc Natl Acad Sci U S A* 2005, **102**(42): 15053-8.

[83] Deng, L., C. Wang, E. Spencer, L. Yang, A. Braun, J. You, C. Slaughter, C. Pickart, Z.J. Chen: **Activation of the IkappaB kinase complex by TRAF6 requires a dimeric ubiquitin-conjugating enzyme complex and a unique polyubiquitin chain.** *Cell* 2000, **103**(2): 351-61.

[84] Raasi, S., R. Varadan, D. Fushman, C.M. Pickart: **Diverse polyubiquitin interaction properties of ubiquitin-associated domains.** *Nat Struct Mol Biol* 2005, **12**(8): 708-14.

[85] Lakowicz, J.R., **Principles of fluorescence spectroscopy.** 3rd ed. 2006, New York ; Berlin: Springer. xxvi, 954 p.

[86] Markley, J.L., A. Bax, Y. Arata, C.W. Hilbers, R. Kaptein, B.D. Sykes, P.E. Wright, K. Wuthrich: **Recommendations for the presentation of NMR structures of proteins and nucleic acids.** *J Mol Biol* 1998, **280**(5): 933-52.

[87] Delaglio, F., S. Grzesiek, G.W. Vuister, G. Zhu, J. Pfeifer, A. Bax: **NMRPipe: A multidimensional spectral processing system based on UNIX pipes.** *J Biomol NMR* 1995, **6**(3): 277-93.

[88] Johnson, B.A.: **Using NMRView to visualize and analyze the NMR spectra of macromolecules.** *Methods Mol Biol* 2004, **278**: 313-52.

[89] Ruckert, M., G. Otting: **Alignment of biological macromolecules in novel nonionic liquid crystalline media for NMR experiments.** *J. Am. Chem. Soc.* 2000, **122**(32): 7793-7797.

[90] Dosset, P., J.C. Hus, D. Marion, M. Blackledge: **A novel interactive tool for rigid-body modeling of multi-domain macromolecules using residual dipolar couplings.** *J Biomol NMR* 2001, **20**(3): 223-31.

[91] Piotrowski, J., R. Beal, L. Hoffman, K.D. Wilkinson, R.E. Cohen, C.M. Pickart: **Inhibition of the 26 S proteasome by polyubiquitin chains synthesized to have defined lengths.** *J Biol Chem* 1997, **272**(38): 23712-21.

[92] Ko, S., G.B. Kang, S.M. Song, J.G. Lee, D.Y. Shin, J.H. Yun, Y. Sheng, C. Cheong, Y.H. Jeon, Y.K. Jung, C.H. Arrowsmith, G.V. Avvakumov, S. Dhe-Paganon, Y.J. Yoo, S.H. Eom, W. Lee: **Structural basis of E2-25K/UBB+1 interaction leading to proteasome inhibition and neurotoxicity.** *J Biol Chem*, **285**(46): 36070-80.

[93] PDB ID: 1YLA Choe, J., G.V. Avvakumov, E.M. Newman, F. Mackenzie, I. Kozieradzki, A. Bochkarev, M. Sundstrom, C. Arrowsmith, A. Edwards, S. Dhe-paganon, (Structural Genomics Consortium), **Ubiquitin-conjugating enzyme E2-25 kDa (Huntington interacting protein 2)**

[94] Chen, J., J.B. Anderson, C. DeWeese-Scott, N.D. Fedorova, L.Y. Geer, S. He, D.I. Hurwitz, J.D. Jackson, A.R. Jacobs, C.J. Lanczycki, C.A. Liebert, C. Liu, T. Madej, A. Marchler-Bauer, G.H. Marchler, R. Mazumder, A.N. Nikolskaya, B.S. Rao, A.R. Panchenko, B.A. Shoemaker, V. Simonyan, J.S. Song, P.A. Thiessen, S. Vasudevan, Y. Wang, R.A. Yamashita, J.J. Yin, S.H. Bryant: **MMDB: Entrez's 3D-structure database.** *Nucleic Acids Res* 2003, **31**(1): 474-7.

[95] Otwinowski, Z., W. Minor, **Processing of X-ray diffraction data collected in oscillation mode, in Methods in Enzymology.** 1997, Academic Press. p. 307-326.

[96] Vagin, A., A. Teplyakov: **MOLREP: An Automated Program for Molecular Replacement.** *Journal of Applied Crystallography* 1997, **30**(6): 1022-1025.

[97] PDB ID: 3F92 Wilson, R.C., R.C. Hughes, J.W. Flatt, E.J. Meehan, J.D. Ng, P.D. Twigg: **Crystal structure of ubiquitin-conjugating enzyme E2-25kDa (Huntington Interacting Protein 2) M172A mutant crystallized at pH 8.5.**

[98] Murshudov, G.N., A.A. Vagin, E.J. Dodson: **Refinement of macromolecular structures by the maximum-likelihood method.** *Acta Crystallogr D Biol Crystallogr* 1997, **53**(Pt 3): 240-55.

[99] Emsley, P., K. Cowtan: **Coot: Model-building tools for molecular graphics.** *Acta Crystallogr D Biol Crystallogr* 2004, **60**(Pt 12 Pt 1): 2126-32.

[100] Perrakis, A., M. Harkiolaki, K.S. Wilson, V.S. Lamzin: **ARP/wARP and molecular replacement.** *Acta Crystallogr D Biol Crystallogr* 2001, **57**(Pt 10): 1445-50.

[101] Lovell, S.C., I.W. Davis, W.B. Arendall, 3rd, P.I. de Bakker, J.M. Word, M.G. Prisant, J.S. Richardson, D.C. Richardson: **Structure validation by Calpha geometry: phi, psi and Cbeta deviation.** *Proteins* 2003, **50**(3): 437-50.

[102] Hodgins, R., C. Gwozd, T. Arnason, M. Cummings, M.J. Ellison: **The tail of a ubiquitin-conjugating enzyme redirects multi-ubiquitin chain synthesis from the lysine 48-linked configuration to a novel nonlysine-linked form.** *J Biol Chem* 1996, **271**(46): 28766-71.

[103] Wilson, R.C., **Structural and functional characterization of the UBA domain of E2-25K/HIP2**, in *Chemistry*. 2007, University of Alabama in Huntsville: Huntsville, AL p. 65.

[104] Gasymov, O.K., B.J. Glasgow: **ANS fluorescence: Potential to augment the identification of the external binding sites of proteins.** *Biochim Biophys Acta* 2007, **1774**(3): 403-11.

[105] Varelas, X., C. Ptak, M.J. Ellison: **Cdc34 self-association is facilitated by ubiquitin thiolester formation and is required for its catalytic activity.** *Mol Cell Biol* 2003, **23**(15): 5388-400.

[106] Komander, D., F. Reyes-Turcu, J.D. Licchesi, P. Odenwaelder, K.D. Wilkinson, D. Barford: **Molecular discrimination of structurally equivalent Lys 63-linked and linear polyubiquitin chains.** *EMBO Rep* 2009, **10**(5): 466-73.

[107] Markley, J.L., A. Bax, Y. Arata, C.W. Hilbers, R. Kaptein, B.D. Sykes, P.E. Wright, K. Wuthrich: **Recommendations for the presentation of NMR structures of proteins and nucleic acids. IUPAC-IUBMB-IUPAB Inter-Union task group on the standardization of data bases of protein and nucleic acid structures determined by NMR spectroscopy.** *J Biomol NMR* 1998, **12**(1): 1-23.

[108] Muhandiram, D.R., L.E. Kay: **Gradient-enhanced triple-resonance three-dimensional NMR experiments with improved sensitivity.** *Journal of Magnetic Resonance, Series B* 1994, **103**(3): 203-216.

[109] BMRB ID: 17362 Wilson, R.C., S.P. Edmondson, P.D. Twigg: **Backbone assignments for E2-25K.**

[110] Wishart, D.S., B.D. Sykes: **The 13C chemical-shift index: a simple method for the identification of protein secondary structure using 13C chemical-shift data.** *J Biomol NMR* 1994, **4**(2): 171-80.

[111] Ottiger, M., A. Bax: **Bicelle-based liquid crystals for NMR-measurement of dipolar couplings at acidic and basic pH values.** *J Biomol NMR* 1999, **13**(2): 187-91.

[112] Hamilton, K.S., M.J. Ellison, G.S. Shaw: **Identification of the ubiquitin interfacial residues in a ubiquitin-E2 covalent complex.** *J Biomol NMR* 2000, **18**(4): 319-27.

[113] Shuker, S.B., P.J. Hajduk, R.P. Meadows, S.W. Fesik: **Discovering high-affinity ligands for proteins: SAR by NMR.** *Science* 1996, **274**(5292): 1531-4.

[114] Trempe, J.F., N.R. Brown, E.D. Lowe, C. Gordon, I.D. Campbell, M.E. Noble, J.A. Endicott: **Mechanism of Lys48-linked polyubiquitin chain recognition by the Mud1 UBA domain.** *Embo J* 2005, **24**(18): 3178-89.

[115] Swanson, K.A., L. Hicke, I. Radhakrishnan: **Structural basis for monoubiquitin recognition by the Ede1 UBA domain.** *J Mol Biol* 2006, **358**(3): 713-24.

[116] Zhang, D., S. Raasi, D. Fushman: **Affinity makes the difference: Nonselective interaction of the UBA domain of Ubiquilin-1 with monomeric ubiquitin and polyubiquitin chains.** *J Mol Biol* 2008, **377**(1): 162-80.

[117] Kay, L., P. Keifer, T. Saarinen: **Pure absorption gradient enhanced heteronuclear single quantum correlation spectroscopy with improved sensitivity.** *J. Am. Chem. Soc.* 1992, **114**(26): 10663-10665.

[118] BMRB ID: 17195 Wilson, R.C., P.D. Twigg: **Backbone assignments for the UBA domain of E2-25K.**

[119] Dominguez, C., R. Boelens, A.M. Bonvin: **HADDOCK: A protein-protein docking approach based on biochemical or biophysical information.** *J Am Chem Soc* 2003, **125**(7): 1731-7.

[120] Vijay-Kumar, S., C.E. Bugg, W.J. Cook: **Structure of ubiquitin refined at 1.8 A resolution.** *J Mol Biol* 1987, **194**(3): 531-44.

[121] Chang, Y.G., A.X. Song, Y.G. Gao, Y.H. Shi, X.J. Lin, X.T. Cao, D.H. Lin, H.Y. Hu: **Solution structure of the ubiquitin-associated domain of human BMSC-UbP and its complex with ubiquitin.** *Protein Sci* 2006, **15**(6): 1248-59.

[122] Mueller, T.D., J. Feigon: **Solution structures of UBA domains reveal a conserved hydrophobic surface for protein-protein interactions.** *J Mol Biol* 2002, **319**(5): 1243-55.

[123] Mueller, T.D., M. Kamionka, J. Feigon: **Specificity of the interaction between ubiquitin-associated domains and ubiquitin.** *J Biol Chem* 2004, **279**(12): 11926-36.
[124] Wilson, R.C., S.P. Edmondson, J.W. Flatt, K. Helms, P.D. Twigg: **The E2-25K ubiquitin-associated (UBA) domain aids in polyubiquitin chain synthesis and linkage specificity.** *Biochem Biophys Res Commun*.
[125] Fang, J., T. Chen, B. Chadwick, E. Li, Y. Zhang: **Ring1b-mediated H2A ubiquitination associates with inactive X chromosomes and is involved in initiation of X inactivation.** *J Biol Chem* 2004, **279**(51): 52812-5.
[126] Honda, R., H. Tanaka, H. Yasuda: **Oncoprotein MDM2 is a ubiquitin ligase E3 for tumor suppressor p53.** *FEBS Lett* 1997, **420**(1): 25-7.
[127] Leverson, J.D., C.A. Joazeiro, A.M. Page, H. Huang, P. Hieter, T. Hunter: **The APC11 RING-H2 finger mediates E2-dependent ubiquitination.** *Mol Biol Cell* 2000, **11**(7): 2315-25.
[128] Martinez-Noel, G., U. Muller, K. Harbers: **Identification of molecular determinants required for interaction of ubiquitin-conjugating enzymes and RING finger proteins.** *Eur J Biochem* 2001, **268**(22): 5912-9.
[129] Sasaki, T., M. Funakoshi, J.A. Endicott, H. Kobayashi: **Budding yeast Dsk2 protein forms a homodimer via its C-terminal UBA domain.** *Biochem Biophys Res Commun* 2005, **336**(2): 530-5.
[130] Kang, Y., R.A. Vossler, L.A. Diaz-Martinez, N.S. Winter, D.J. Clarke, K.J. Walters: **UBL/UBA ubiquitin receptor proteins bind a common tetraubiquitin chain.** *J Mol Biol* 2006, **356**(4): 1027-35.
[131] Withers-Ward, E.S., T.D. Mueller, I.S. Chen, J. Feigon: **Biochemical and structural analysis of the interaction between the UBA(2) domain of the DNA repair protein HHR23A and HIV-1 Vpr.** *Biochemistry* 2000, **39**(46): 14103-12.
[132] Yuan, X., P. Simpson, C. McKeown, H. Kondo, K. Uchiyama, R. Wallis, I. Dreveny, C. Keetch, X. Zhang, C. Robinson, P. Freemont, S. Matthews: **Structure, dynamics and interactions of p47, a major adaptor of the AAA ATPase, p97.** *Embo J* 2004, **23**(7): 1463-73.
[133] Chim, N., W.E. Gall, J. Xiao, M.P. Harris, T.R. Graham, A.M. Krezel: **Solution structure of the ubiquitin-binding domain in Swa2p from Saccharomyces cerevisiae.** *Proteins* 2004, **54**(4): 784-93.
[134] Ciani, B., R. Layfield, J.R. Cavey, P.W. Sheppard, M.S. Searle: **Structure of the ubiquitin-associated domain of p62 (SQSTM1) and implications for mutations that cause Paget's disease of bone.** *J Biol Chem* 2003, **278**(39): 37409-12.
[135] Dieckmann, T., E.S. Withers-Ward, M.A. Jarosinski, C.F. Liu, I.S. Chen, J. Feigon: **Structure of a human DNA repair protein UBA domain that interacts with HIV-1 Vpr.** *Nat Struct Biol* 1998, **5**(12): 1042-7.
[136] Scheffner, M., J.M. Huibregtse, P.M. Howley: **Identification of a human ubiquitin-conjugating enzyme that mediates the E6-AP-dependent ubiquitination of p53.** *Proc Natl Acad Sci U S A* 1994, **91**(19): 8797-801.

[137] Tolbert, B.S., S.G. Tajc, H. Webb, J. Snyder, J.E. Nielsen, B.L. Miller, R. Basavappa: **The active site cysteine of ubiquitin-conjugating enzymes has a significantly elevated pKa: Functional implications**. *Biochemistry* 2005, **44**(50): 16385-91.

[138] Weeks, S.D., K.C. Grasty, L. Hernandez-Cuebas, P.J. Loll: **Crystal structures of Lys-63-linked tri- and di-ubiquitin reveal a highly extended chain architecture.** *Proteins* 2009, **77**(4): 753-9.

[139] Eddins, M.J., R. Varadan, D. Fushman, C.M. Pickart, C. Wolberger: **Crystal structure and solution NMR studies of Lys48-linked tetraubiquitin at neutral pH**. *J Mol Biol* 2007, **367**(1): 204-11.

[140] Wilson, R.C., S.P. Edmondson, J.W. Flatt, K. Helms, P.D. Twigg: **The E2-25K ubiquitin-associated (UBA) domain aids in polyubiquitin chain synthesis and linkage specificity.** *Biochem Biophys Res Commun* 2011, **405**(4): 662-6.

[141] Kostic, M., T. Matt, M.A. Martinez-Yamout, H.J. Dyson, P.E. Wright: **Solution structure of the Hdm2 C2H2C4 RING, a domain critical for ubiquitination of p53.** *J Mol Biol* 2006, **363**(2): 433-50.